Comprehensive Design Review

Team 31: CU Boulder Baja SAE 2025-2026

November 13th, 2025

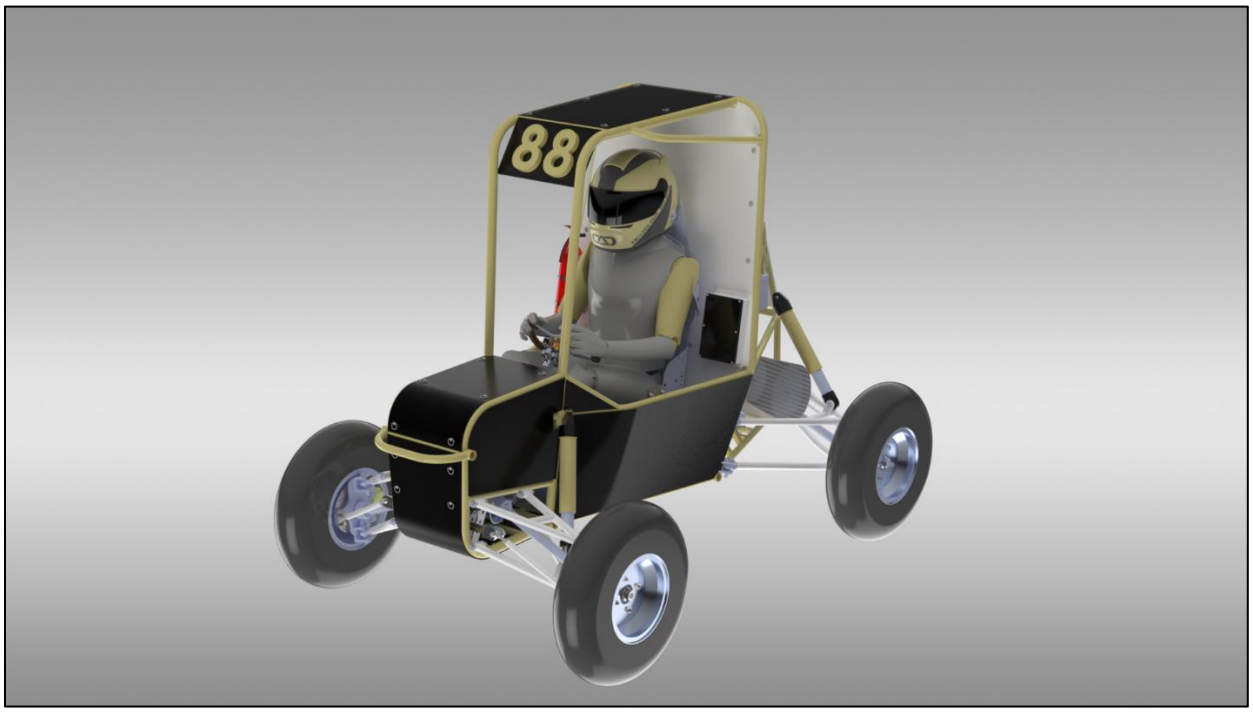

BOULDER BAJA

Paul M. Rady
Mechanical Engineering
UNIVERSITY OF COLORADO **BOULDER**

dc DESIGN CENTER COLORADO

Jim's Automotive
Jamsi online.com
Machine Shop, Inc.

Painter's Grinding

MONSTER ENERGY

Table of Contents:

1. Team Introduction and Background 13
1.1. Overview: 13
1.2. Timeline: 14
1.3. Finance Overview: 14
1.4. Overall Vehicle Goals: 16
1.4.1. System Level Goals: 17
1.4.1.1. Suspension 17
1.4.1.2. Controls 17
1.4.1.3. Drivetrain 17
1.4.1.4. Chassis 17
1.5. Full Car Specifications: 17
1.6. Full Car Renders: 18
2. Suspension 22
2.1. System Level Breakdown 22
2.1.1. Critical Rules 22
2.1.2. Front Suspension System 22
2.1.2.1 Front Suspension System CAD 22
2.1.3. Rear Suspension System 24
2.1.3.1 Rear Suspension System CAD 25
2.1.2 Kinematics 26
2.1.2.1 Front Suspension 26
2.1.2.2 Rear Suspension 28
2.2. Part Level Breakdown 29
2.2.1. Front Lower Control Arm – (FLCA) 29
2.2.1.1. Discussion of Design Reasoning – FLCA 29
2.2.1.2. FLCA CAD Design: 30
2.2.1.3. FLCA Critical Parts – Model Views and Discussion: 30
2.2.1.4. FLCA Analysis: 32
2.2.2. Front Upper Control Arm – (FUCA) 35
2.2.2.1. Discussion of Design Reasoning – FUCA 35
2.2.2.2. FUCA CAD Design: 35

2.2.2.3. FUCA & FLCA BOM: 36
2.2.2.4. FUCA Critical Parts – Model Views and Discussion: 37
2.2.2.5. FUCA Analysis: 38
2.2.3. Front Hub/Upright Assembly 39
2.2.3.1. Discussion of Design Reasoning – Front Hub 39
2.2.3.2. Front Hub CAD Design: 39
2.2.3.3. Front Hub BOM: 40
2.2.3.4. Front Hub Critical Parts – Model Views and Discussion: 41
2.2.3.5. Front Hub Analysis: 43
2.2.4. Rear Lower Control Arm – (RLCA) 54
2.2.4.1. Discussion of Design Reasoning – RLCA 54
2.2.4.2. RLCA CAD Design: 54
2.2.4.3. RLCA BOM: 55
2.2.4.4. RLCA Critical Parts – Model Views and Discussion: 55
2.2.4.5. RLCA Analysis 56
2.2.5. Rear Upper Control Arm – (RUCA) 58
2.2.5.1. Discussion of Design Reasoning – RUCA 58
2.2.5.2. RUCA CAD Design: 58
2.2.5.3. RUCA BOM: 59
2.2.5.4. RUCA Critical Parts – Model Views and Discussion: 59
2.2.5.5. RUCA Analysis: 60
2.2.6. Rear Toe Rod 65
2.2.6.1. Discussion of design Reasoning 65
2.2.6.2. Rear Toe Rod CAD Design 65
2.2.6.3. Rear Toe Rod BOM 65
2.2.6.4. Rear Toe Rod Analysis 66
2.2.7. Rear Hub/Upright Assembly 67
2.2.7.1. Discussion of Design Reasoning – Rear Hub 67
2.2.7.2. Rear Hub CAD Design: 67
2.2.7.3. Rear Hub BOM: 68
2.2.7.4. Rear Hub Critical Parts – Model Views and Discussion: 69
2.2.7.5. Rear Hub Analysis 71
2.2.7.6 Rear Bracket Analysis 75

3. Controls 78
3.1. System Level Breakdown 79
3.2. Part Level Breakdown 79
3.2.1. Steering Assembly 79
3.2.1.1. Discussion of Design Reasoning – Steering Assembly: 79
3.2.1.2. Steering Assembly Critical Rules: 80
3.2.1.3. Steering Assembly CAD Design: 81
3.2.1.4. Steering Assembly BOM: 82
3.2.1.5. Steering Assembly Critical Parts – Model Views and Discussion: 84
3.2.1.6. Steering Assembly Analysis: 85
3.2.2. Brake Pedal 88
3.2.2.1. Discussion of Design Reasoning – Brake Pedal: 88
3.2.2.2. Brake Pedal Critical Rules: 88
3.2.2.3. Brake Pedal CAD Design: 89
3.2.2.4. Brake Pedal BOM: 91
3.2.3. Throttle Pedal 97
3.2.3.1. Discussion of Design Reasoning – Throttle System/Pedal: 97
3.2.3.2. Throttle System/Pedal Critical Rules: 97
3.2.3.3. Throttle Pedal CAD Design: 97
3.2.3.4. Throttle Pedal BOM: 98
3.2.3.6. Throttle Pedal Analysis 100
3.2.4. Brake System 102
3.2.4.1. Brake System Critical Rules: 102
3.2.5. Seat Mounting 102
3.2.5.1. Discussion of Design - Seat Mounting: 102
3.2.5.2. Seat Mounting Critical Rules: 103
3.2.5.3. Seat Mounting CAD Design: 103
3.2.6. Harness Mounting 105
3.2.6.1. Discussion of Design - Harness Mounting: 105
3.2.6.2. Harness Mounting Critical Rules: 105
3.2.6.3. Harness Mounting CAD Design: 106
3.2.7. Gas Tank Assembly 108
3.2.7.1. Discussion of Design - Gas Tank: 108

3.2.7.2. Gas Tank Assembly Critical Rules: 108
3.2.7.3. Gas Tank CAD Design: 108
3.2.7.4. Gas Tank BOM: 109
4. Drivetrain 110
4.1. System Level Breakdown 111
4.2. Part Level Breakdown 112
4.2.1. Engine and CVT Assembly 112
4.2.1.1. CVT 112
4.2.1.2. CVT Cover (HROE and PPAE) 113
4.2.2 Transfer Case ("Franken-box") 115
4.2.2.1. Internal View of the Franken-Box 118
4.2.2.2. Problems with the current Franken box: 120
4.2.2.3. Franken-Box relevant stress analysis: 121
4.2.2.4. Bearings 125
4.2.2.5. Franken-Box Output Shaft 125
4.2.2.6. Shafts & Keys 126
4.2.2.6.1. Strength Calculations for Shaft and Keys 129
4.2.3. Differentials 131
4.2.5.1. Discussion of Selection Reasoning and CAD Model: 131
4.2.4. CV Axles 132
4.2.4.1. Discussion of Design Reasoning: 132
4.2.4.2. CV Axel CAD Model: 132
4.2.4.3. CV Analysis: 133
4.2.5. Driveshaft 134
4.2.5.1. Driveshaft CAD Model: 134
4.2.5.2. Drive Shaft BOM: 135
4.2.5.3. Drive Shaft Analysis: 136
4.2.5.4. Drive Shaft Critical Component: 138
4.2.5.5. HROE and PPAE Guards 141
4.2.5.6. HROE and PPAE BOM: 142
5. Chassis 143
5.2. System Level Breakdown 143
5.2.1. Design Choices 143

5.2.2. Critical Rules 144
5.2.3. Integration Overview 144
5.3. Part Level Breakdown 145
5.3.1. Frame Tubes 145
5.3.2. Body Panels and Numbers 146
5.3.3. Firewall and Splash Guard 147
5.3.4. Skid plates 148
5.3.5. Stress Analysis 150
5.3.6. Supporting Calculations 162
5.3.7. Bill of Materials 162
6. Electronics 163
6.2. Differential PCB 163
6.2.1.2. Discussion of Design Reasoning 163
6.3. Differential Switches 163
6.3.1.2. Discussion of Design Reasoning – Mounting 163
6.3.1.3. Powering the Switches 164
6.4. Brake Light 164
6.4.1.2. Discussion of Design Reasoning – Mounting, Signal, Part 164
6.4.1.3. Powering the Brake Light 164
6.5. Kill Switches 165
6.5.1.2. Discussion of Design Reasoning – Mounting 165
7. Appendix 166
7.2. Supplemental Hand Calculations and Code 166
7.2.1. Suspension Calculations 166
7.1.1.1 Front Suspension Calculations 166
7.1.1.2 Rear Suspension Calculations 168
7.2.2. Controls Calculations 177
7.2.2.2. Brake Force Calculations: 177
7.2.3. Drivetrain Calculations 179
7.2.3.2. Gearbox Calculations: 179

Figures Reference:

Figure 1: Team Photo 13
Figure 2: Full Assembly Isometric View 18
Figure 3: Full Assembly Left Side View 18
Figure 4: Full Assembly Right Side View 19
Figure 5: Full Assembly Front View 19
Figure 6: Full Assembly Rear View 20
Figure 7: Full Assembly Top View 21
Figure 8: Full Assembly Bottom View 21
Figure 9: Isometric view of the front suspension 22
Figure 10: Front Suspension at Ride Hight 23
Figure 11: Front Suspension at Full Droop 24
Figure 12: Rear Suspension at Ride Height 25
Figure 13: Real Suspension at Full Bump 26
Figure 14: Rear Suspension at Full Droop 26
Figure 15: Camber through travel for front suspension 27
Figure 16: Camber Change through Rear Suspension Travel 28
Figure 17: Toe Change through Rear Suspension Travel 29
Figure 18: Lower Control Arm Assembly 30
Figure 19: Lower Control Arm 30
Figure 20: Lower Control Arm Analysis 32
Figure 21: Lower Control Arm Shock Analysis 33
Figure 22: Load Distribution to Upper & Lower Control Arms 34
Figure 23: Upper Control Arm Assembly 35
Figure 24: Front Control Arms BOM 36
Figure 25: Front Upper Control Arm Analysis 38
Figure 26: Front Upright Assembly 39
Figure 27: Exploded View of the Front Upright 40
Figure 28: Driver Left Upright 41
Figure 29: Bracket Connecting the Upright and Control Arm 41
Figure 30: Upright brackets with hardware highlighting the upper and lower max of Heim travel 42
Figure 31: 2024-25 Upright FEA with frontal loading case experienced in testing this year 43
Figure 32: Results of Analysis in Figure 31 44
Figure 33: This year's Upright FEA with frontal loading derived from failure case modeled above 45
Figure 34: Results of Analysis in Figure 33 46
Figure 35: Front loading with max brake force 47
Figure 36: Results of Analysis in Figure 35 48
Figure 37: Upward Loading Case 49
Figure 38: Results of Analysis in Figure 37 50
Figure 39: Supplementary hand calculations from upward impact 51
Figure 40: Bearing failure calculations for Hiem bolts pulling out 52

Figure 41: Thread tear out calculations for the 1/4-20 hardware attaching the control arm brackets to the upright 53
Figure 42: Rear Lower Control Arm 54
Figure 43: RLCA Exploded View 55
Figure 44: RLCA Top View to show Geometry 55
Figure 45: Forward Impact on Rear Wheel 56
Figure 46: Side Impact on Rear Wheel 57
Figure 47: Rear Upper Control Arm 58
Figure 48: RUCA Exploded View 59
Figure 49: RUCA Geometry 59
Figure 50: Forward impact of rear upper control arm 60
Figure 51: Side impact on upper control arm 61
Figure 52: Maximum force of shock on upper control arm 62
Figure 53: Shock load distribution on middle A-arm member 63
Figure 54: Shock load distribution on A-arm side member 64
Figure 55: Rear tie rod exploded view 65
Figure 56: Side impact on rear tie rod 66
Figure 57: Rear upright Assembly 67
Figure 58: Rear upright exploded view 68
Figure 59: Rear Right Upright 69
Figure 60: Control Arm Bracket 70
Figure 61: Rear upright FEA 71
Figure 62: Results from Figure 61 72
Figure 63: Upward loading on rear upright 73
Figure 64: Results from Figure 63 74
Figure 65: Rear Upright Bracket Bending Calculations 75
Figure 66: Rear Upright Heim Bolt Tear out 76
Figure 67: Rear Upright Bracket Thread Tear Out Calculations 77
Figure 68: Controls Assembly Rear Isometric View 78
Figure 69: Controls Assembly Side View 78
Figure 70: Absolute Toe vs. Suspension Travel 80
Figure 71: Isometric View of Steering Assembly 81
Figure 72: Steering Assembly Exploded View 82
Figure 73: Upright Tie-Rod Mounting Bracket on Suspension Upright 84
Figure 74: Upright Tie-Rod Mounting Bracket Top View 84
Figure 75: Side View of Tie-Rod Heim in Full Bump Angle 84
Figure 76: Side View of Tie-Rod Heim in Full Droop Angle 84
Figure 77: Upright Tie-Rod Mounting Bracket Side View 84
Figure 78: Steering Shaft Torsion Calculations 85
Figure 79: Tie Rod Buckling Calculations 86
Figure 80: Steering Rod Insert Bending Calculations 87
Figure 81: Brake Pedal Assembly 89
Figure 82: Exploded Brake Pedal Assembly 90

Figure 83: Shared Base Pedal Assembly 92
Figure 84: Master Cylinder Mounting Tabs 92
Figure 85: Basic Pedal Assembly 450lbf Loading Analysis 93
Figure 86: FEA Results of 450lbf Loading Case on Pedal 94
Figure 87: FEA Result of 46lbf Loading Case on Pedal 95
Figure 88: FEA Results of the Master Cylinder Mounting Tabs under a 1100lbf load 96
Figure 89: Throttle Pedal Assembly 97
Figure 90: Exploded Throttle Pedal Assembly 98
Figure 91:Throttle Pedal Barrel Adjuster Plate 99
Figure 92: Throttle Pedal Barrel Adjuster Plate Mounted to Front Differential 100
Figure 93: Throttle Limiter Bolt 100
Figure 94: Analysis of Throttle Limiter Bolt Plate 101
Figure 95: Top View – Bottom and Rear Seat Mounting 103
Figure 96: Front View – Rear Seat Mounting 104
Figure 97: Isometric View – Bottom and Rear Seat Mounting 104
Figure 98: Isometric View of Harness Mounting 106
Figure 99: Front View of Harness Mounting 106
Figure 100: Top View of Harness Mounting 107
Figure 101: Gas Tank Assembly 108
Figure 102: Exploded Gas Tank Assembly 108
Figure 103: Full Drivetrain Left Side Isometric 110
Figure 104: Full Drivetrain Right Side Isometric 110
Figure 105 - Speed over time graph showing acceleration anomaly 112
Figure 106 – Top: CVTech CVT; Bottom: Gaged CVT 113
Figure 107: Full CVT Cover, HROE and PPAE 114
Figure 108: CVT Cover Exploded View 114
Figure 109: Isometric view of the Franken-Box, a single- 116
Figure 110: Exploded view of the Franken Box and BOM labels. 117
Figure 111: Cross section view of the spiral bevel gear mesh and supporting geometry. 119
Figure 112: Spiral Bevel Gear Stress Analysis 122
Figure 113: Analysis of Spiral Bevel Miter Gears Backlash Under Maximum Possible Torque 123
Figure 114: Analysis of Spiral Bevel Gear at Full Axial Load Against B1 124
Figure 115: Output shaft with press fit internal spline and roll pin holes between the output shaft and spline pattern. 126
Figure 116 – Equations used to solve for shaft diameter 126
Figure 117 - Estimated Minimum Shaft Diameters 127
Figure 118 – Equations for Average Shear and Bearing Stress for keys 127
Figure 119 – Transfer Case Input Shaft 127
Figure 120 - Key Stress Calculations Results 128
Figure 121 - Input shaft failure calculation 129
Figure 122 - Key failure calculation 130
Figure 123: CV Axle Assembly 132
Figure 124: Analysis of CVT Center Shaft in Torsion 133

Figure 125: Driveshaft CAD Model 134
Figure 126: Exploded Driveshaft Model 134
Figure 127: Driveshaft Torsional Failure Analysis 136
Figure 128: Driveshaft U-joint 138
Figure 129: Driveshaft U-joint Phasing Diagram 139
Figure 130: Graph of U-joint angle vs. RPM and Transmittable Torque 140
Figure 131: Driveshaft with HROE and PPAE Guards 141
Figure 132: Exploded Assembly of Driveshaft with HROE and PPAE Guards 141
Figure 133: Overall Chassis View 143
Figure 134: Seat Clearance Template, resting on 3D seat scan 144
Figure 135: 6-inch helmet bubble, 3-inch hand bubble 145
Figure 136: Tilted front suspension member removed other mounting bars for controls and PPAE 145
Figure 137: Chassis Schematic, separated by color 146
Figure 138: Panels, Numbers, and Plates 147
Figure 139: Red exhaust cone redirected out the left side, and drip tray out the back 148
Figure 140: Curved front nose, with thick skid plate (in red) 149
Figure 141: Rollover Load Case 150
Figure 142: Rollover FOS 151
Figure 143: End over end Loads 152
Figure 144: End over end FOS 153
Figure 145: Front Impact Loads 154
Figure 146: Front Impact FOS 155
Figure 147: Byron-Case Loads 156
Figure 148: Byron-Case FOS 157
Figure 149: Front Combined Loads 158
Figure 150: Front Combined FOS 159
Figure 151: Rear Combined Loads 160
Figure 152: Rear Combined FOS 161
Figure 153: Hand Calculations to Validate the Strength of Frame Material 162
Figure 154: Chassis Tubing BOM 162
Figure 155: Wiring Diagram 163
Figure 156: Brake Light and Diff Power Circuit 164
Figure 157: External Kill Switch Location 165
Figure 158: Driver Kill Switch Location 165
Figure 159: Spiral Bevel Gear Force Reference Directions 180
Figure 160: Spur Gear Force Reference Directions 181

Tables Reference:

Table 1: Project Timeline 14
Table 2: 2025-2026 Budget Projection 15
Table 3: Current Funds as of 11/10/25 15
Table 4: Anticipated Funds and Future Funding Paths 16
Table 5: Current In-kind Donations and Sponsored Discounts 16
Table 6: Anticipated In kind Donations and Sponsored Discounts 16
Table 7: Full Car Specifications 17
Table 8: Data for the CV Axle in Bump and Droop 27
Table 9: Data for the CV Axle in Bump and Droop 28
Table 10: Front Suspension BOM 36
Table 11: Full Upright BOM 40
Table 12: RLCA BOM 55
Table 13: RUCA BOM 59
Table 14: Rear Tie Rod BOM 65
Table 15: Rear Upright BOM 69
Table 16: Steering Assembly BOM 83
Table 17: Brake Pedal BOM 91
Table 18: Throttle Pedal BOM 99
Table 19: CVT Cover BOM 115
Table 20: Franken-Box BOM 118
Table 21: Bearing Numbers, Types, Loads, and L_{10} Values 125
Table 22: Differential BOM 131
Table 23: Driveshaft BOM 135
Table 24: Driveshaft HROE and PPAE BOM 142
Table 25: Comparison of chassis dimensions and weight 143
Table 26: Color-coded legend of tubing sizes 146
Table 27: Spiral Bevel Gear Force Calculations 180
Table 28: Spur Gear Force Calculations 181

1. Team Introduction and Background

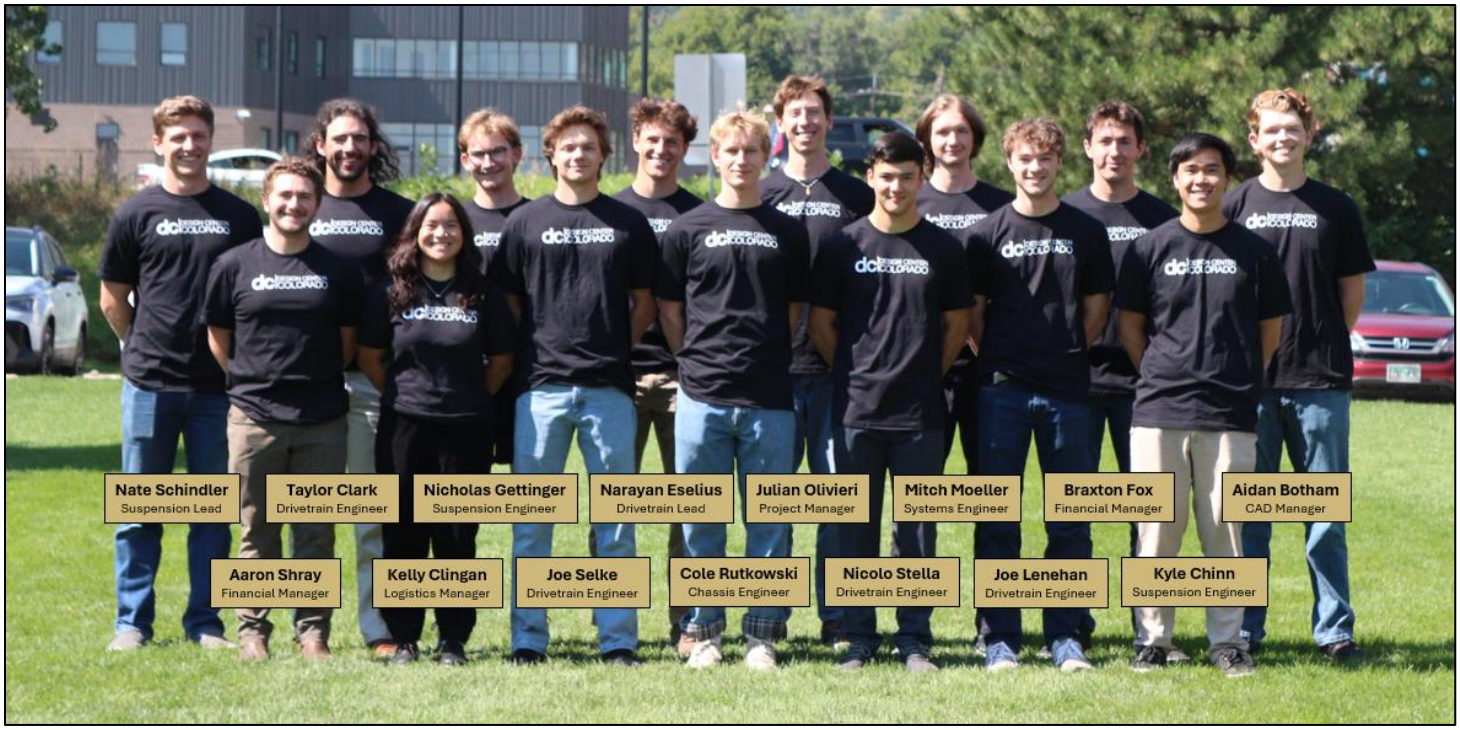

Figure 1: Team Photo

1.1. Overview:

Each year, the CU Boulder Baja Senior Design team participates in the Society of Automotive Engineers (SAE) Baja Collegiate Design Series, an international competition that challenges university students to design, build, and race a single-seat, off-road vehicle capable of withstanding rough terrain. The competition provides students with hands-on experience in engineering design, project management, and real-world problem solving, as teams work to create vehicles that balance performance, durability, and manufacturability. Baja SAE events are divided into static and dynamic categories. The static events include a detailed design review, cost analysis, and business presentation, while the dynamic events test the vehicle's performance through challenges such as acceleration, maneuverability, hill climb or sled pull, suspension and traction testing, and a four-hour endurance race. At CU Boulder, the project is structured across two semesters: the fall semester focuses on design, simulation, and analysis, while the spring semester emphasizes manufacturing, testing, and validation. This year's team aims to produce a highly competitive vehicle with optimized performance, durability, and handling—targeting a finish within the top 25 teams. The following report outlines the team's design goals, project milestones, budget and fundraising considerations, and designs for this year's competition vehicle.

1.2. Timeline:

Project Milestone	Tentative Dates	Notes
CDR	November 13th	About 90% of the car should not change after CDR
Manufacturing Review	December 5th	Last Day of Classes
First Major Parts Order	December 6th	Reading Day of Finals Week
Steel Order	December 6th	
SAE Business Presentation Report	December 13th	Can submit late for partial scoring
Start of Chassis	January 8th	First day back in the spring
Rolling Chassis	February 6th	Suspension and Chassis Need to be completed for rolling chassis
Roll Cage Documentation Package	February 16th	Required SAE Deliverable
Written Cost Reduction Report	February 20th	Required SAE Deliverable
Business Presentation	February	
Online Cost Prototype	March 20th	Required SAE Deliverable
Design Review Briefing	April 2nd	Required SAE Deliverable
Running Vehicle	April 10th	Mid-semester Reading Day
Testing	April 11th – April 25th	Testing Stops Before Final Exams
Competition in Oregon	5/7 - 5/10	

Table 1: Project Timeline

1.3. Finance Overview:

The finance team for the 2025-2026 team set several ambitious goals for the 2025-2026 season. Our first goal was to completely overhaul the team's existing sponsorship and outreach resources. This will polish portfolio to the business presentation event, which previous teams performed poorly on, and allow future teams to build on previous team's successes and connections. Our second goal was to protect our funding plan from unexpected cost increases like through expanding connections to sponsors contributing financially or via in-kind donation. Our third goal was to reconnect with previous sponsors, including single and multi-year supporters. Our final goal was to increase the amount of money left behind to rollover for next year's SAE Baja team.

Throughout the design cycle, our team has been cementing the sub-team costs from general concept to nearly developed reality. Table 2 shows the team's current estimates for their expected cost needs for the 2025-2026 season assuming no purchasing support or discounts from sponsors such as EMJ, SKF, or KHK. *Competition travel costs assume the rental of 2 vehicles, with $1000 gas for each vehicle.

Area	Expected Cost:
Front Suspension	$1300
Rear Suspension	$800
Controls	$400
Drivetrain	$2,150
Chassis	$3,000
Competition Registration	$1,850

Competition Housing	$2,500
Competition Travel	$4,000
Miscellaneous	$1,000
Total	$17,000

Table 2: 2025-2026 Budget Projection

As mentioned, the team pursued financial support for travel and manufacturing needs. Contacting family members for support yielded a number of donations. Additionally, we directed outreach to companies mentioned in previous sponsor pages and Colorado-based engineering companies. Through this, we secured $1,500 from Painter's Grinding. See Table 3 for the full list of financial contributions as of November 10th 2025.

Current Funds	
Source	**Contribution**
2024-2025 Rollover Funding	$~500
Individual Donations	$2,000
Design Center Colorado	$2,000
Painter's Grinding	$1,500
Taylor Clark Gallery	$1,000
Total	$7,000

Table 3: Current Funds as of 11/10/25

The team received pledged support the following sources summarized in Table 4. Additionally, we are exploring fundraising through volunteer programs such as ticket scanning for CU Athletics and SAE International's Learn Twice program. Finally, we are pursuing funding through sponsorship and grant proposals, including the Engineering Excellence Fund, the CEAS travel program, and the Gene Haas Foundation grant.

Anticipated Funding					
Pledged Funds		Pending Proposals	Volunteer Opportunities		
Jamsi Online	$2000	Engineering Excellence Fund (Spring Award)	$5,500	SAE International Learn Twice Program	$2500
Gates Belts	$2000+	CEAS Travel	$4,500	CU Athletics and Ticketing	$50/volunteer (Per CUEC Event) *
O'Reilly Auto	$350+	Gene Haas Foundation	$2,500	*Up to 27 CEUC Events Per Academic Year	
			CU Athletics and Ticketing	$100/Volunteer (Per Folsom Event) *	
			*Up to 6 Football Games Per Academic Year		
Total	$4,350+	Total	$ 11,500	Total	$2,500+

Total	$18,350

Table 4: Anticipated Funds and Future Funding Paths

As per the finance team's second goal, the team has focused on reaching out to companies for in kind support covering a wide base of materials and applications. Listed in table 5 is the teams abridged summary of their successful efforts to ascertain either discounted products or donated materials and fabrication support carried over from previous team's sponsors.

Current In-Kind Support		
Donor	Material/In Kind Donation	Estimated Value
Monster Energy	Soft Drinks, Pop Up Tent, Fridge	$1,500
Gates Belts	CVT belts	$100
Colorado Waterjet	50% discount	$500
A&A manufacturing	Donation of Catalogue Items	~

Table 5: Current In-kind Donations and Sponsored Discounts

In addition, the finance team has been in contact with a number of companies with which they are hopeful they can receive in kind support from, through either discounted materials or fabrication, although a defined relationship is still undetermined. An abridged list is provided in table 6.

Anticipated In-Kind Support		
Donor	Material/In Kind Donation	Estimated Value
O'Reilly Auto	Auto Parts/Tools	$250-$750
SKF bearings	Bearings	$500
KHK Gears	Catalogue Discount/Donation	$500
Michigan Science Inc.	Wheel Force Transducer	$2000
C&C Design and Fab	9310 Gear Stock	$1000
IZZE racing	Discounts on Sensors	$1000
Segger	Hardware/Software	~
AFCO industries	25% Discount on Products	~
Binsfeld Engineering	Torque sensors	~
Futek	Torque Sensors	~

Table 6: Anticipated In kind Donations and Sponsored Discounts

1.4. Overall Vehicle Goals:

- Complete endurance <u>without failure</u>
- Reduce weight by 10%
    - Reducing weight will increase acceleration, for a constant drivetrain power, and will enable us to place higher in endurance.
- Increase serviceability
    - Increased serviceability will allow for more rapid testing and modifying during our test phase throughout April which will also enable us to have a better performing vehicle.

1.4.1. System Level Goals:

1.4.1.1. Suspension

- Goal 1: Reduce body roll in cornering by 5%
  - Roll Center is 10.2-inch higher than last year which will reduce body roll
- Goal 2: Have zero set-in from suspension travel (shocks return the vehicle to designed ride height and have 0 roll at steady state)
  - Both front and rear shocks have progressive travel and are angled to prevent set in
- Goal3: Tilt the front suspension backwards to give some absorption of frontal impacts
  - Front suspension has a 10˚ tilt backward

1.4.1.2. Controls

- Make electronic controls accessible.
  - Differential switches have been moved to the steering wheel
- Create a lighter brake pedal with more travel.
  - Missed. Our pedal weight and travel are nearly identical to last years.
- Improve throttle pedal cable clamping reliability.
  - By using a motorcycle clutch cable, a barrel adjuster, and a mounting notch we gain more adjustability and reliability.

1.4.1.3. Drivetrain

- Complete endurance without drivetrain failure
- Increase acceleration by 10%
- Increase serviceability
  - Be able to remove all custom components in 10 minutes or less.
- Lower center of gravity of the drivetrain by 10% compared to last year

1.4.1.4. Chassis

- Reduce weight of chassis by 10%
  - Reducing the raw chassis weight will improve acceleration
- Shorten chassis by 6”
  - Improves turning radius and reduces weight
- Contain drivetrain components above floor members
  - Raises ground clearance in full bump

1.5. Full Car Specifications:

Height	Length	Width	Dry Weight (approx.)
64.5 in	82 in	54 in	496 lbs

Table 7: Full Car Specifications

1.6. Full Car Renders:

Figure 2: Full Assembly Isometric View

Figure 3: Full Assembly Left Side View

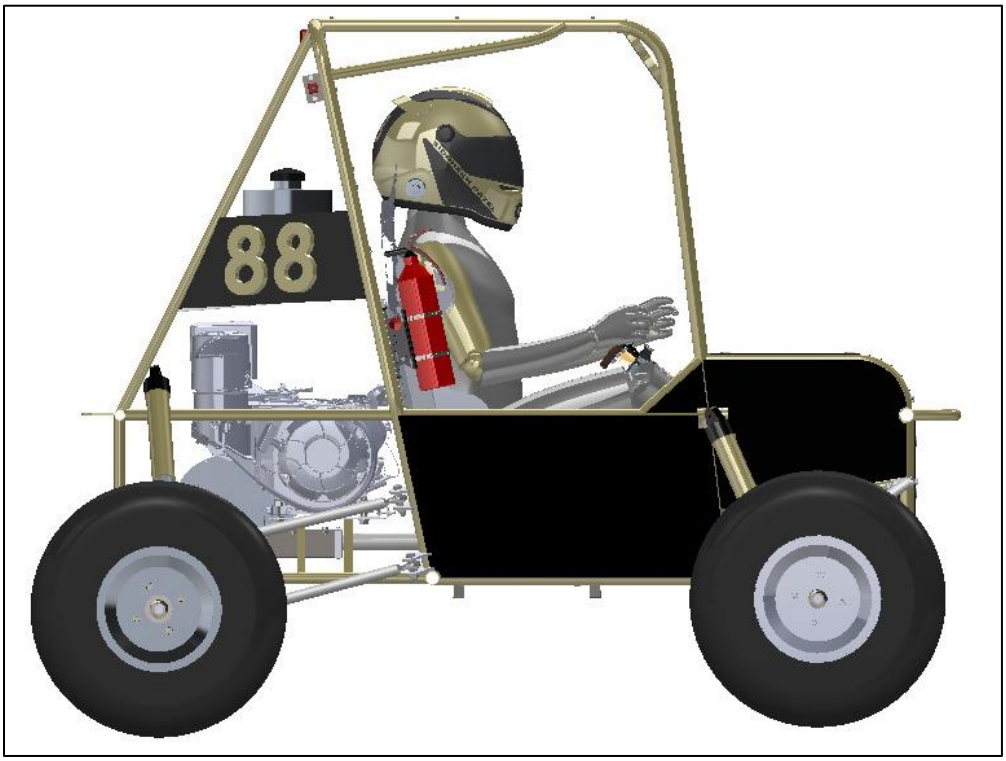

Figure 4: Full Assembly Right Side View

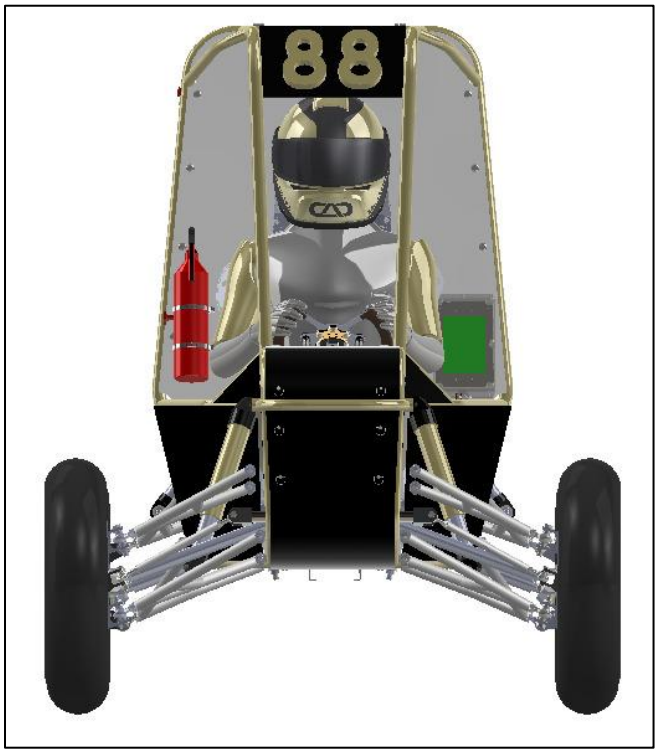

Figure 5: Full Assembly Front View

Figure 6: Full Assembly Rear View

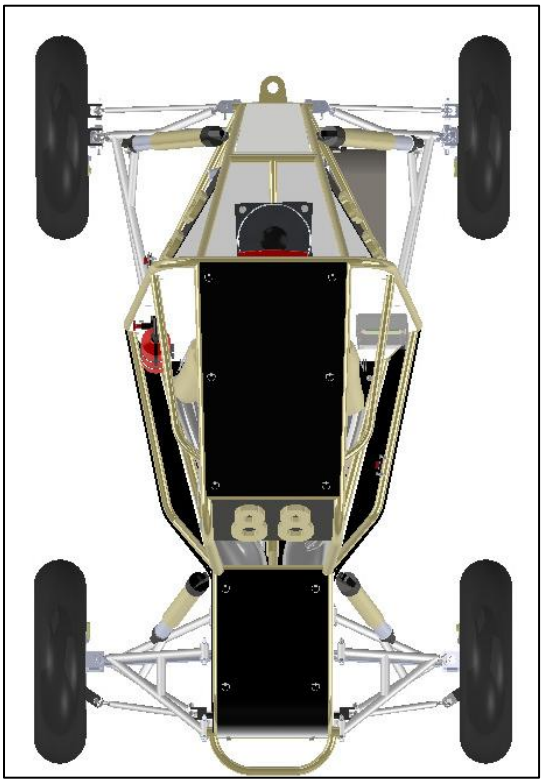

Figure 7: Full Assembly Top View

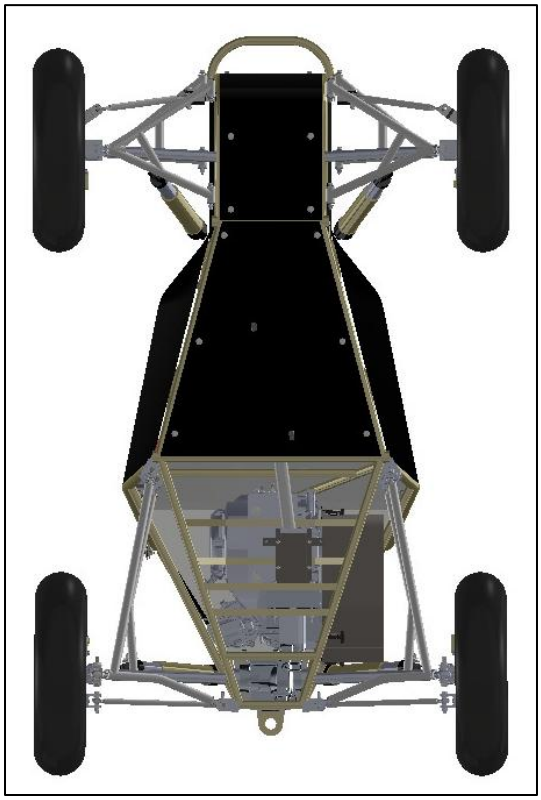

Figure 8: Full Assembly Bottom View

2. Suspension

2.1. System Level Breakdown

2.1.1. Critical Rules

- B.1.4.1 - Terrain Type
- B.1.4.2 - Clearance and Traction
- B.1.5.1.1 - Wheeled Vehicles
- B.1.5.2 - Four Wheel Drive/All-Wheel Drive
- B.1.6 – Limitations

2.1.2. Front Suspension System

Through testing we found that last year's car handling to be exceptional over bumps; however, during cornering there was a large amount of body roll and seemed to never fully return zero roll after the corner. Due to this, our main design goals for this year are to reduce body roll by at least 5% and always return the vehicle to the designed ride height and have 0 roll at steady state. To achieve these goals, we decided to shorten the distance between the roll center (RC) and the center of gravity (CG) by raising the RC. To achieve this, we centered our design around unparalleled arms that allow for the tuning of the vehicle's RC. Keeping the 6 inches in distance between the control arms on the chassis side, we were about to raise the RC to 10.2 inches from the ground using a 7-inch distance on the upright (4 above the center line of the wheel and 3 below). Compared to last year's RC of 0in we theorize that the decreased lever arm between the RC and CG will decrease the body roll by more than 5%. Furthermore, to prevent set-in body roll after the corner we have angled our shocks outward more, especially in the rear, to create a progressive suspension. Last year's car had close to vertical shocks, which led to an extremely linear compression ratio through travel. The progression of our new design will allow for more force from the shocks under compression to counteract the set-in. Finally, we have decided to title our suspension backwards 10 degrees, allowing for some absorption of frontal impacts.

2.1.2.1 Front Suspension System CAD

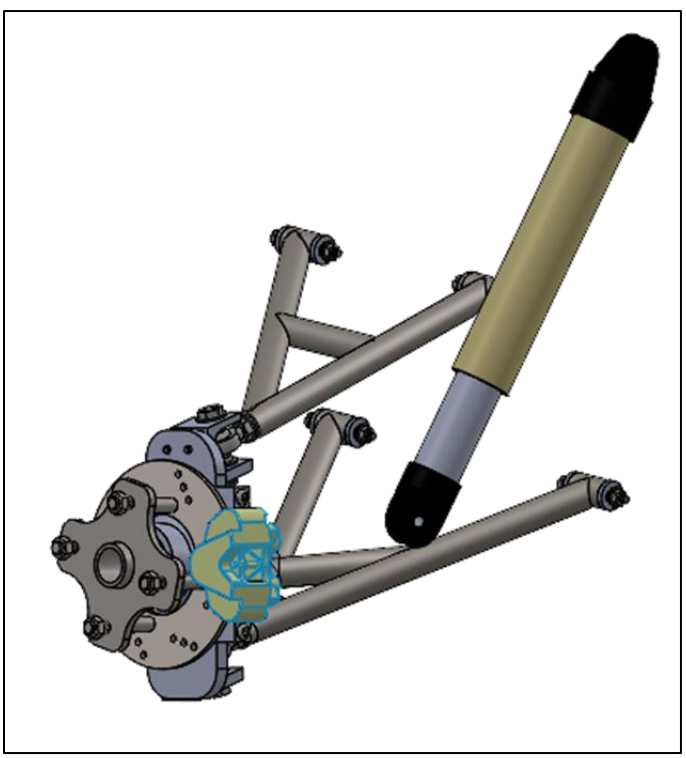

Figure 9: Isometric view of the front suspension

Figure 10: Front Suspension at Ride Hight

Figure 11: Front Suspension at Full Droop

Figure 12: Front Suspension at Full Bump

2.1.3. Rear Suspension System

The rear suspension system is a double wishbone A-arm style suspension based off a similar geometry model as the front system, and thus shares many of the same goals. It was designed around the constraints set by the use of a rear supported chassis and optimization of the drivetrain design. As a result of this, the mounting of the system to the chassis and clearance around drivetrain components, such as the CVT cover, proved to be the largest challenge we faced during our design iterations. The design currently incorporates hiem joints at both chassis and upright pickup points to compensate for differences in the axis of rotation between the two control arms, and the sharp angle that the front member of each control arm meets the chassis. Like the front, the arms are not parallel, with a distance of 6’’ between chassis pickup points, and a distance of 7’’ between upright pickup points. This rases the roll center and makes it closer to the center of gravity, decreasing body roll while turning. A main goal was to achieve 10 inches of travel, 4’’ down from ride height (One inch below the lowest chassis member) and 6’’ up.

2.1.3.1 Rear Suspension System CAD

Figure 12: Rear Suspension at Ride Height

Figure 14: Rear Suspension at Full Droop

Figure 13: Real Suspension at Full Bump

2.1.2 Kinematics

2.1.2.1 Front Suspension

This year, our main goal was to raise the roll center (RC) and close the distance between the driver's center of gravity and RC. To achieve this, we aimed to use non-parallel and unequal-length control arms. We began the design process in SolidWorks, using partially undefined 2D sketches with driven dimensions to explore different configurations. From this analysis, we determined an optimal geometry with a 7-inch vertical separation between the control arm mounting points on the upright and a 6-inch separation on the chassis. Using this same method, we also evaluated the arm length ratio, CV axle plunge, and CV axle angles.

After the Preliminary Design Review (PDR), we decided to experiment with a tilted front suspension layout. This addition complicated the kinematics, as the suspension motion now followed a fully three-dimensional path. As a result, SusProg was used to obtain the necessary suspension geometry data, which is summarized in Table and shown in Figure 15.

By implementing a tilted suspension, non-parallel arms, and unequal-length control arms, the RC height increased to 10.2 inches above the ground. Compared to last year's configuration—with a roll center of 0 inches, determined in SusProg due to the parallel arm layout—this represents a substantial improvement in roll resistance. Theoretically, if the RC were located at the vehicle's center of gravity (CG), there would be no body roll during cornering. By raising the RC, we reduce the effective lever arm between the RC and

the CG, thereby decreasing the moment that induces body roll. Consequently, a greater lateral force is required to generate the same amount of body roll.

LH and RH wheel	Drive Shaft Length	Plunge [in]	Inner CV Joint Angle	Outer CV Joint Angle
8 bump	16.5	-0.44	11.32	6.34
7.5 bump	16.5	-0.456	9.67	5.03
7 bump	16.5	-0.469	8.04	3.79
6.5 bump	16.5	-0.478	6.43	2.73
6 bump	16.5	-0.484	4.88	2.17
5.5 bump	16.5	-0.486	3.46	2.5
5 bump	16.5	-0.486	2.42	3.51
4.5 bump	16.5	-0.482	2.35	4.79
4 bump	16.5	-0.475	3.31	6.21
3.5 bump	16.5	-0.464	4.72	7.68
3 bump	16.5	-0.451	6.29	9.21
2.5 bump	16.5	-0.433	7.94	10.78
2 bump	16.5	-0.412	9.62	12.38
1.5 bump	16.5	-0.387	11.34	14.01
1 bump	16.5	-0.358	13.08	15.68
0.5 bump	16.5	-0.323	14.85	17.38
Static	16.5	-0.284	16.65	19.13
0.5 droop	16.5	-0.239	18.47	20.92
1 droop	16.5	-0.188	20.32	22.76
1.5 droop	16.5	-0.13	22.2	24.65
2 droop	16.5	-0.063	24.12	26.61
2.5 droop	16.5	0.014	26.09	28.64
3 droop	16.5	0.102	28.1	30.77
3.5 droop	16.5	0.205	30.18	33
4 droop	16.5	0.326	32.33	35.37

Table 8: Data for the CV Axle in Bump and Droop

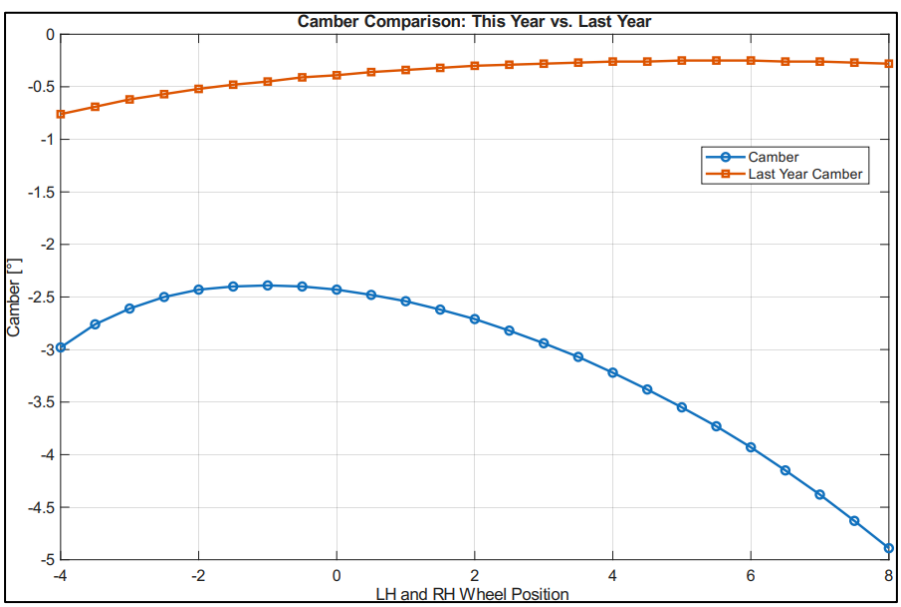

Figure 15: Camber through travel for front suspension

2.1.2.2 Rear Suspension

Similar to front suspension, the control arms of the rear suspension are not parallel to increase the roll center and decrease body roll. The length and pickup points of the toe arm were optimized to decrease the amount of toe change throughout wheel travel. Heims on the upright side of the control arms allow for camber adjustability.

LH and RH wheel	Drive Shaft Length	Plunge [in]	Inner CV Joint Angle	Outer CV Joint Angle
6 bump	17.03	-0.144	7.74	6.54
5.5 bump	17.03	-0.145	6.14	5.55
5 bump	17.03	-0.144	4.56	4.76
4.5 bump	17.03	-0.141	3.05	4.31
4 bump	17.03	-0.135	1.72	4.29
3.5 bump	17.03	-0.127	1.38	4.72
3 bump	17.03	-0.117	2.47	5.49
2.5 bump	17.03	-0.104	3.95	6.48
2 bump	17.03	-0.089	5.51	7.61
1.5 bump	17.03	-0.071	7.11	8.83
1 bump	17.03	-0.05	8.73	10.11
0.5 bump	17.03	-0.027	10.37	11.43
Static	17.03	0	12.02	12.79
0.5 droop	17.03	0.03	13.68	14.16
1 droop	17.03	0.063	15.36	15.56
1.5 droop	17.03	0.1	17.06	16.98
2 droop	17.03	0.141	18.77	18.41
2.5 droop	17.03	0.187	20.5	19.86
3 droop	17.03	0.238	22.26	21.32
3.5 droop	17.03	0.295	24.04	22.79
4 droop	17.03	0.358	25.85	24.28

Table 9: Data for the CV Axle in Bump and Droop

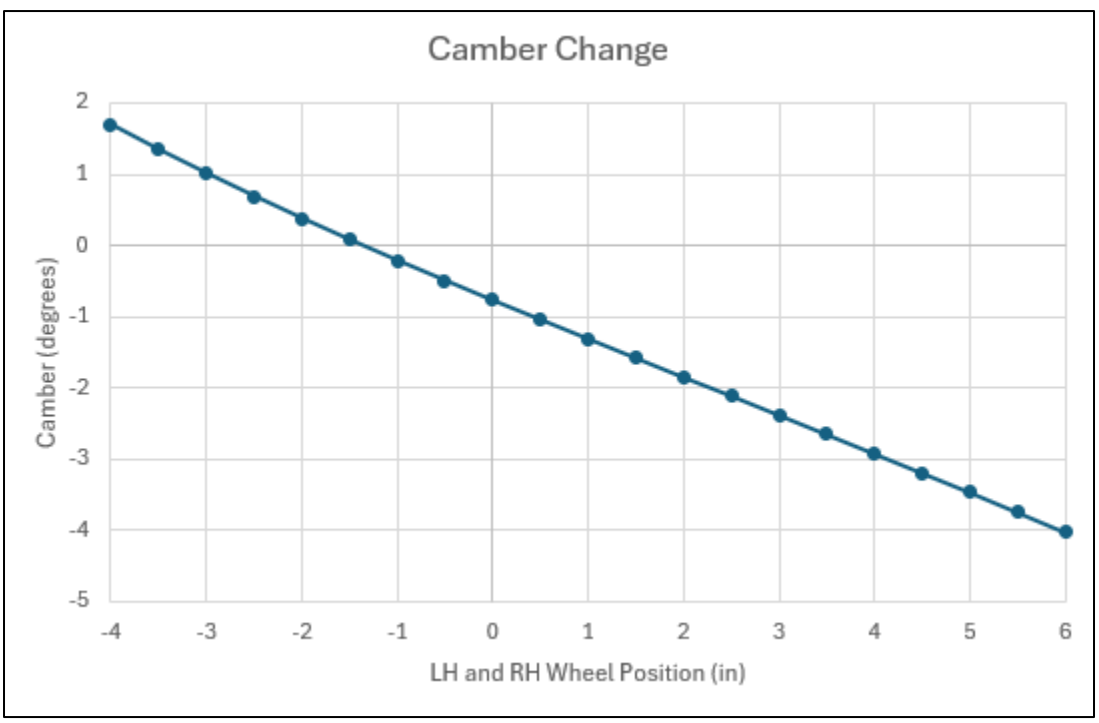

Figure 16: Camber Change through Rear Suspension Travel

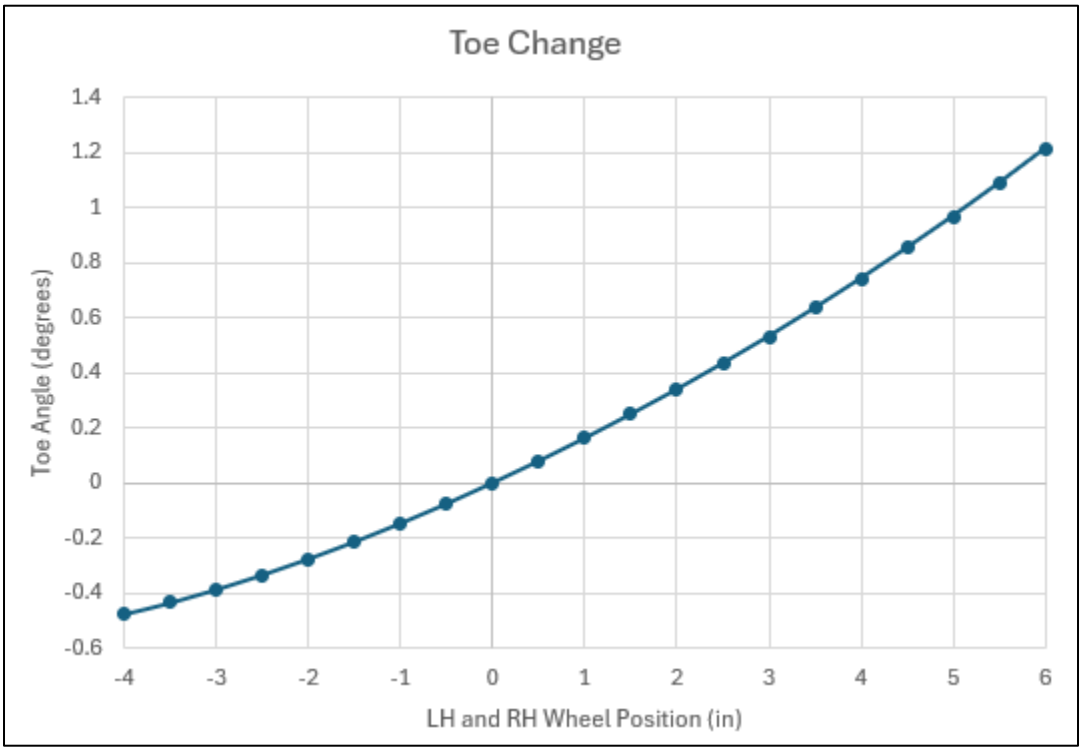

Figure 17: Toe Change through Rear Suspension Travel

2.2. Part Level Breakdown

2.2.1. Front Lower Control Arm – (FLCA)

2.2.1.1. Discussion of Design Reasoning – FLCA

We decided to continue using double wishbone suspension in the front. This year however the shock will be mounted to the lower control arm (FLC A) and as previously mentioned rake will be introduced tilting the suspension 10 degrees backward to help absorb frontal impacts. With the shock being mounted to the FLCA it was possible to make the front suspension lighter. This is because the arm that supports the shock needs to be stronger to withstand the induced bending moment by the shock, and because the lower is usually reenforced to withstand impacts by obstacles we were able to take advantage of the FLCA being more robust to begin with. The shock being mounted to the FLCA latter became a necessity as the chassis was changed to a rear supported as opposed to front supported the previous year. Due to this change, we lost higher up chassis mounting locations for the shock. Lowering the mounting location allowed us to mount to the toe box of the chassis without adding single use chassis members.

2.2.1.2. FLCA CAD Design:

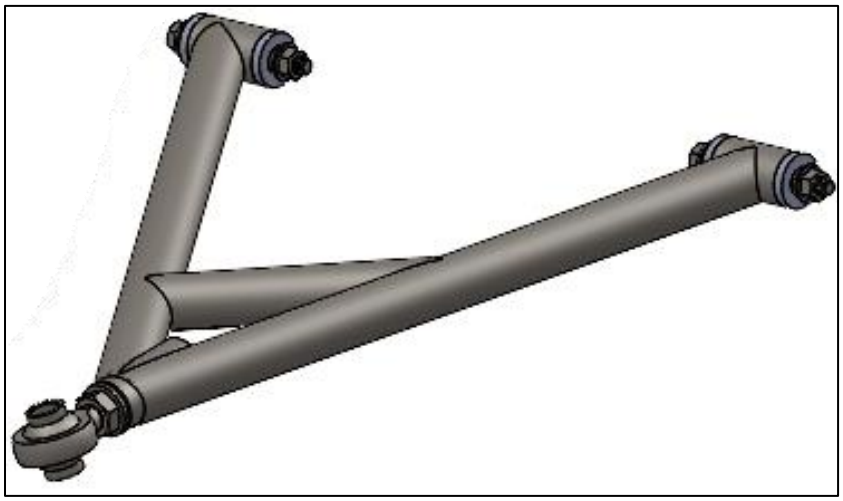

Figure 18: Lower Control Arm Assembly

For the lower arm we have chosen a traditional A arm with each long member consisting of a 1” OD x 0.095” wall. The crossmember is a 1’OD x 0.058” wall. The rod end is a ½-20 connected with a weld in bung. For chassis mounting we will be manufacturing our own bushings using Delrin AF.

2.2.1.3. FLCA Critical Parts – Model Views and Discussion:

Figure 19: Lower Control Arm

The Lower control arm was designed with a traditional A style with the crossmember to support the shock. At the end is a tube in between each arm to allow for easier copes and a strait tube to weld in a weld nut for the rod end. The bushings will be machined out of Delrin AF as it allows for custom lengths and minimal resistance.

2.2.1.4. FLCA Analysis:

Failure Condition: Frontal impact on the front of the wheel
Material: Alloy Steel 4130 1”OD x 0.093”Wall, Crossmember 1”OD x 0.058”Wall

Justification: when we experience frontal obstacles at speed, part of the force will be translated into the control arms.

Load Diagram:

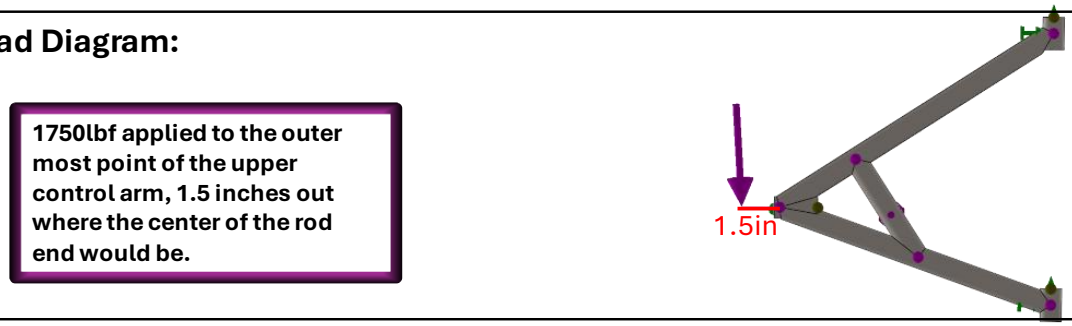

Constraints:

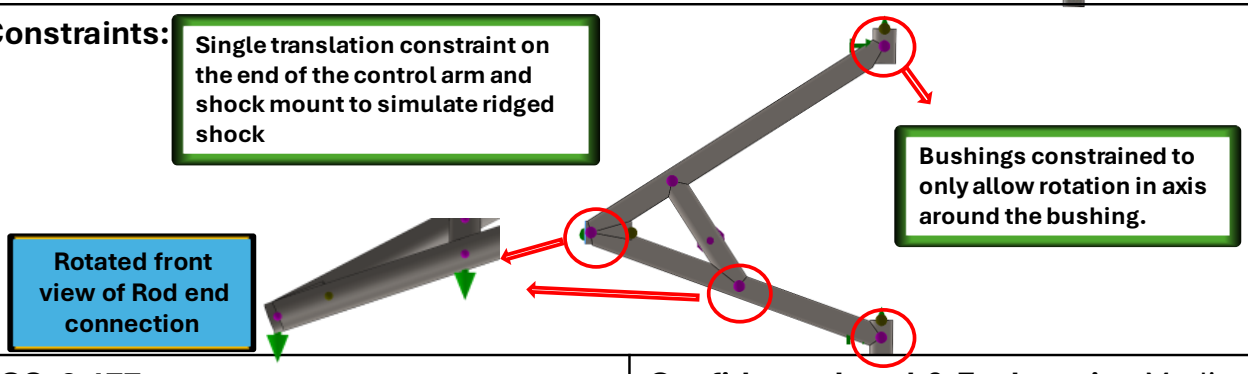

FOS: 2.177

Equations (If Applicable):

Confidence Level & Explanation: Medium, Using previous years numbers with 3000lbf frontal impact, they have never experienced failure.

Calculations and/or FEA:

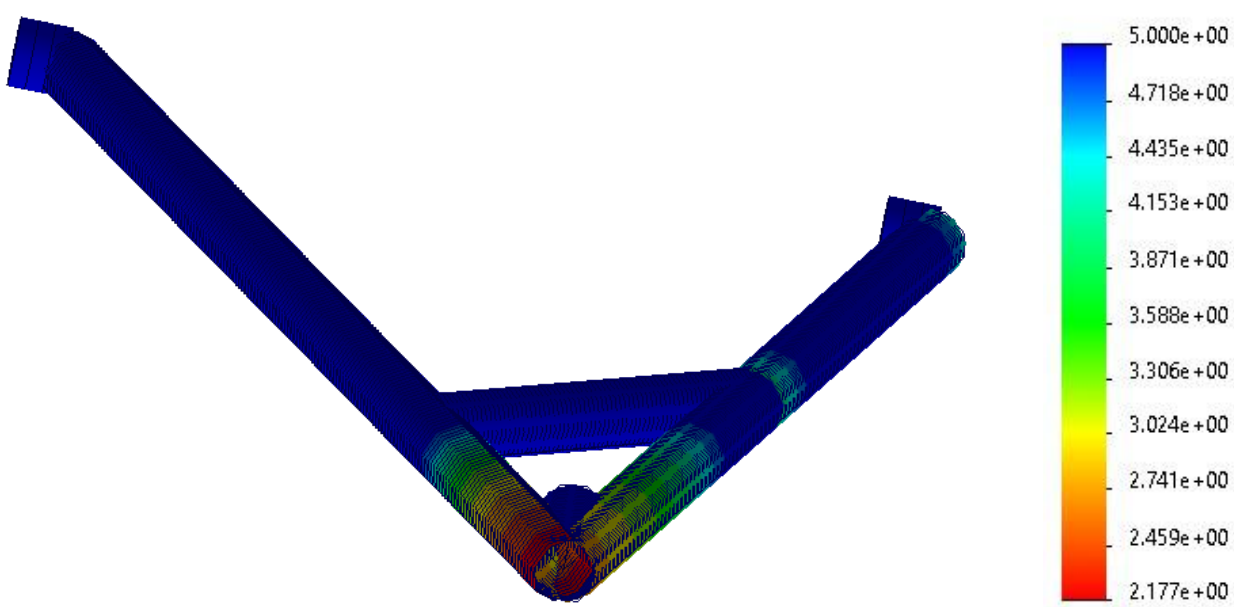

Figure 20: Lower Control Arm Analysis

Failure Condition: Arm failure due to shock loading
Material: Alloy Steel 4130 1”OD x 0.093”Wall, Crossmember 1”OD x 0.058”Wall

Justification: using data form Fox Shocks we have derived that the maximum force exerted by the shock is 1600lbf.

Load Diagram:

1600lbf is applied perpendicular to the arm on the crossmember

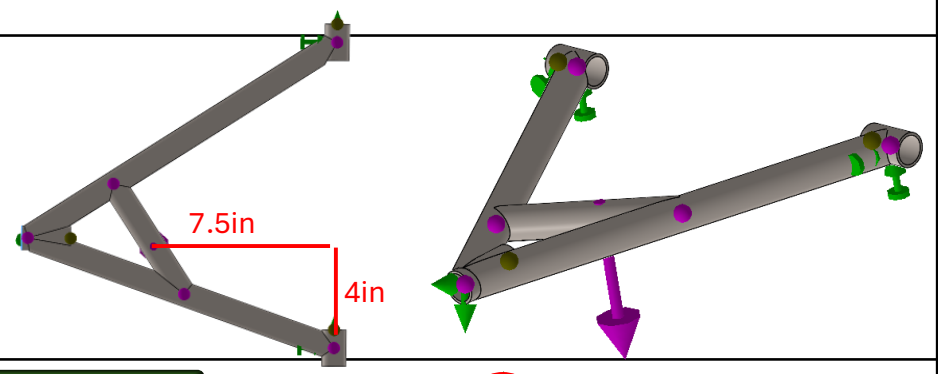

Constraints:

Single translation constraint on the end of the control arm to prevent rotation and simulate a ridged shock force translated through the upright.

Bushings constrained to only allow rotation in axis around the bushing.

Rotated front view of Rod end connection

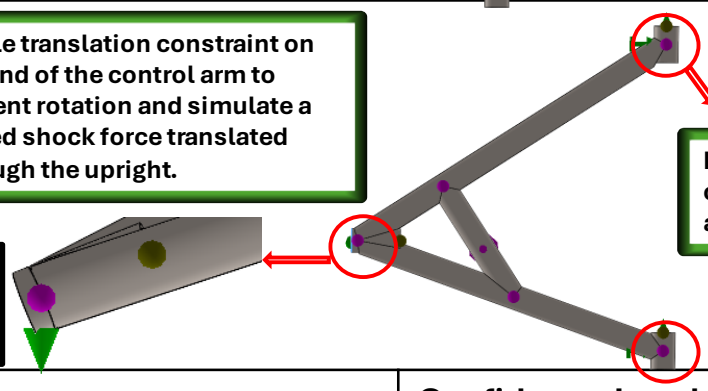

FOS: 1.641

Equations (If Applicable):

Confidence Level & Explanation: medium, Deriving the maximum force from FOX shocks data and previous years using the same value without failure.

Calculations and/or FEA:

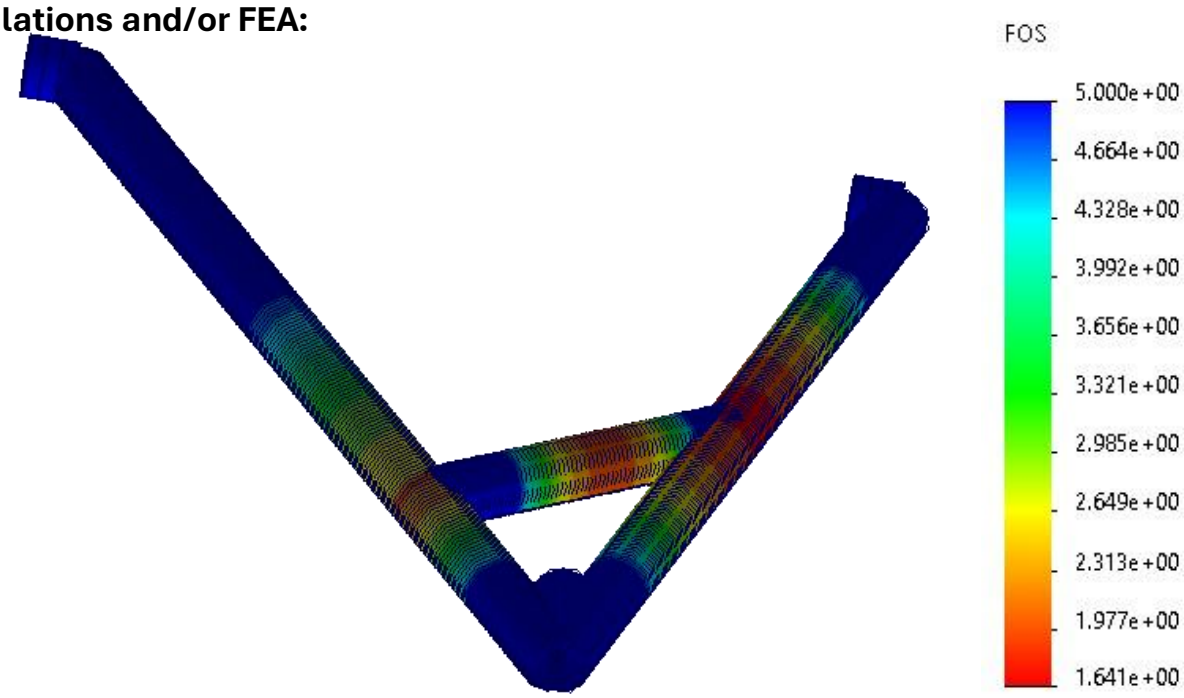

Figure 21: Lower Control Arm Shock Analysis

Failure Condition: Upright frontal load distribution to top and bottom control arms

Justification: with the hub not being centered between the upper and lower control arms the weight is not evenly distributed to each arm.

Load Diagram:

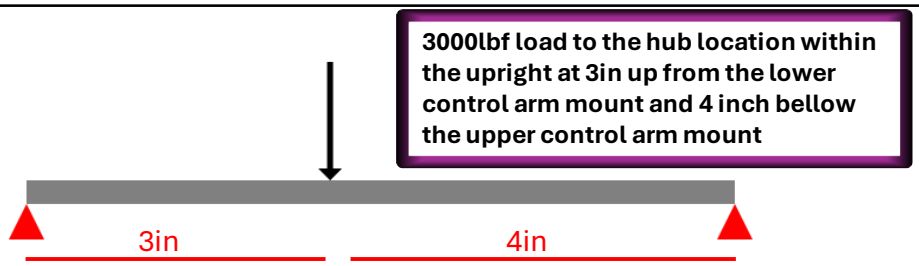

Constraints:

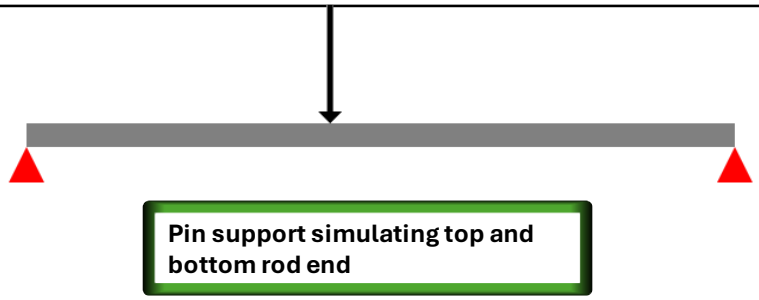

FOS: N/A

Equations (If Applicable):

Confidence Level & Explanation: Medium, Using previous years numbers with 3000lbf frontal impact, they have never experienced failure.

Calculations and/or FEA:

Shear Diagram

(Max +ve)Shear Load (lb): 1714.286,

Location (in): 0.000, 3.000

(Max -ve)Shear Load (lb): -1285.714,

Location (in): 3.000, 7.000

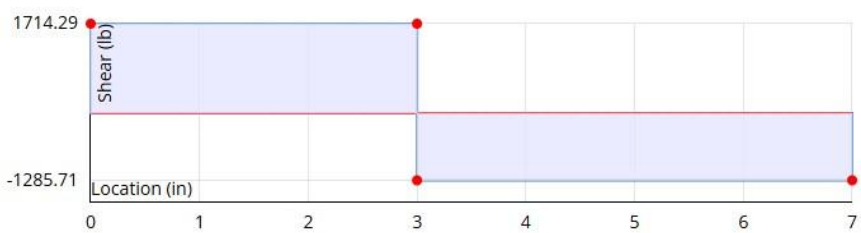

Moment Diagram

(Max +ve)Moment Load (lb-in): 5142.857,

Location (in): 3.000

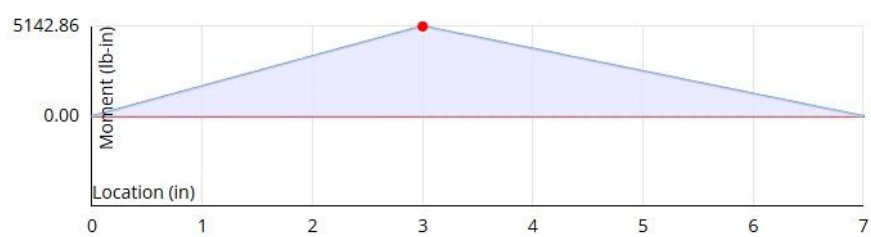

Figure 22: Load Distribution to Upper & Lower Control Arms

2.2.2. Front Upper Control Arm – (FUCA)

2.2.2.1. Discussion of Design Reasoning – FUCA

With the front lower control arm taking the load of the shock the front upper control arm could be made lighter as its loads were much less. In addition to not having the shock load the frontal impact load is not split evenly as shown in **Error! Reference source not found.**. This allowed us to use thin-walled steel tube having the arm be only 1.32 pounds.

2.2.2.2. FUCA CAD Design:

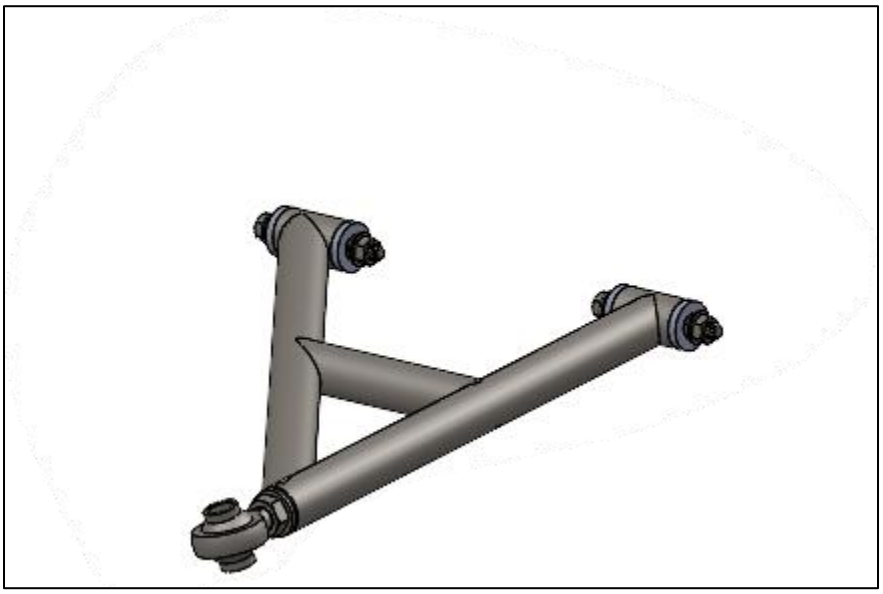

Figure 23: Upper Control Arm Assembly

With the upper control arm, the arms consist of alloy steel 4130 1” OD x 0.058 wall thickness. This was chosen due to the fact that it does not have to support the shock and that the more force is translated to the lower from frontal impacts. The top arm is also unlikely to experience and impacts with debris and obstacles as opposed to the bottoms.

2.2.2.3. FUCA & FLCA BOM:

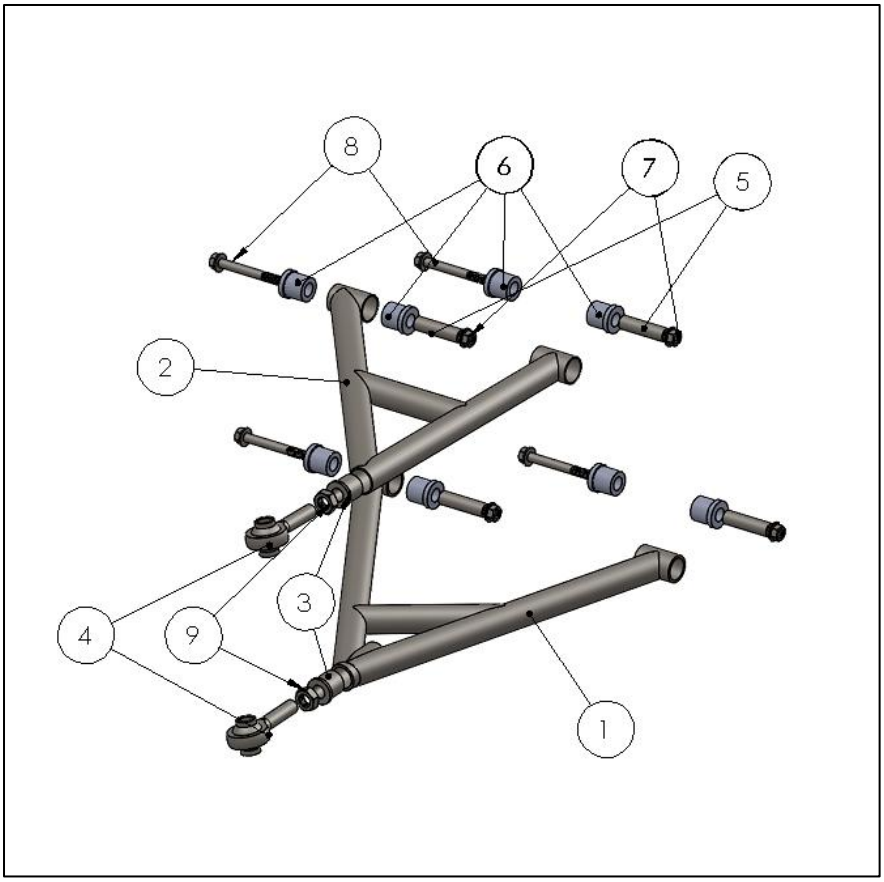

Figure 24: Front Control Arms BOM

BOM Part #	Description	Qty:	Source (Hyperlink to Part)	Cost:	Weight/1Pc [lbs]
1	LCA (6ft 1” OD x 0.58”)	1	EMJ	$N/A	
2	UCA (6ft 1” OD x 0.95)	1	EMJ	$N/A	
3	Weld Nuts	2	McMaster	$8.42	
4	½”-20 Rod End	2	McMaster	$21.55	
5	Bushing inner sleeve	2	Metalsdepot	$8.40	
6	Delrin AF Stock	2	McMaster	$33.89	
7	5/16”-18 Nut	4	McMaster	$13.80	
8	5/16”-18 Bolt	4	McMaster	$16.49	
9	½”-20 Nut	2	McMaster	$7.53	
Total				$280.74	

Table 10: Front Suspension BOM

2.2.2.4. FUCA Critical Parts – Model Views and Discussion:

The upper control arm was designed with a traditional A style with a crossmember. At the end is a tube in between each arm to allow for easier copes and a strait tube to weld in a weld nut for the rod end. The bushings will be machined out of Delrin AF as it allows for custom lengths and minimal resistance.

2.2.2.5. FUCA Analysis:

Failure Condition: Frontal impact on the front of the wheel
Material: Alloy Steel 4130 1”OD x 0.058”Wall

Justification: when we experience frontal obstacles at speed, part of the force will be translated into the control arms.

Load Diagram:

1350lbf applied to the outer most point of the upper control arm, 1.5 inches out where the center of the rod end would be.

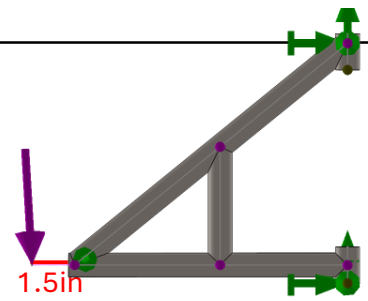

Constraints:

Single translation constraint on the end of the control arm to prevent rotation and simulate a ridged shock force translated through the upright

Rotated front view of Rod end connection

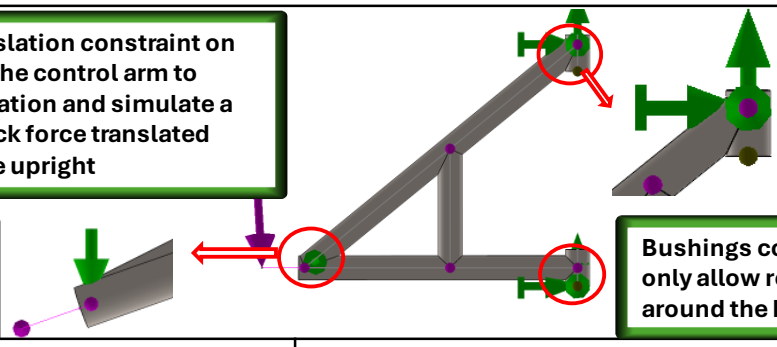

Bushings constrained to only allow rotation in axis around the bushing.

FOS: 1.921

Equations (If Applicable):

Confidence Level & Explanation: Medium, Using previous years numbers with 3000lbf frontal impact, they have never experienced failure.

Calculations and/or FEA:

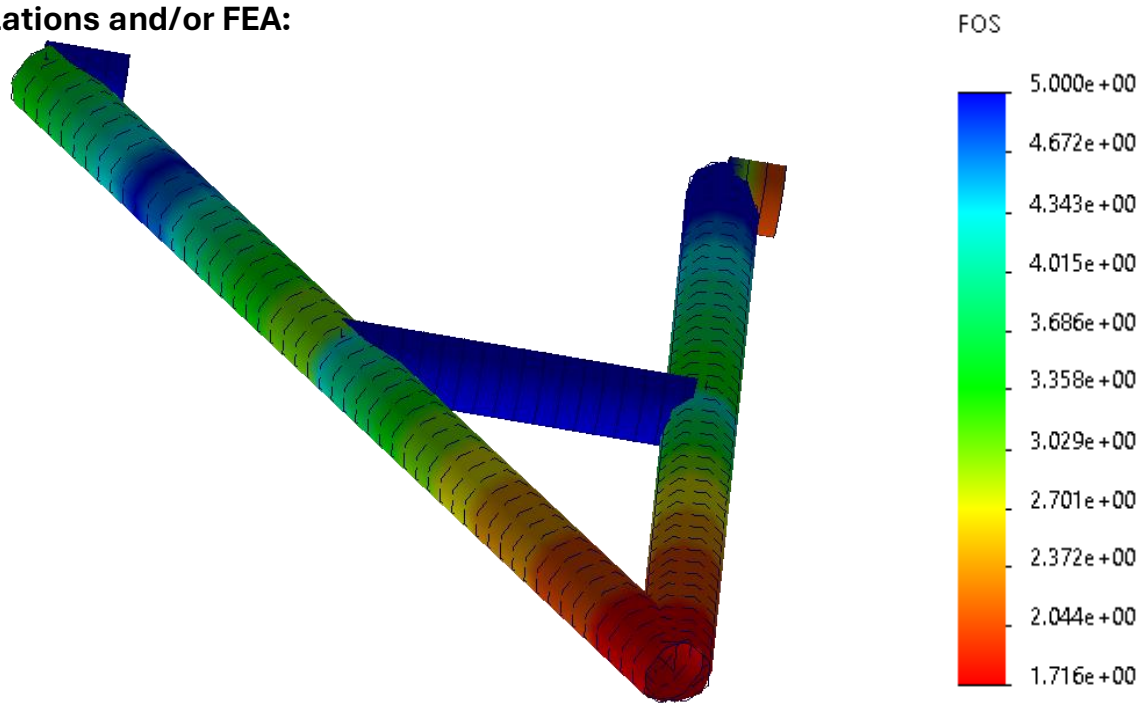

Figure 25: Front Upper Control Arm Analysis

2.2.3. Front Hub/Upright Assembly

2.2.3.1. Discussion of Design Reasoning – Front Hub

In designing our Front Hub Assembly, fitting the upright within the wheel well was our largest constraint. To achieve the desired non-parallel arm geometry, it was necessary to increase the height of the upright, resulting in a total height of 9-inches, which just fits within the 9.75-inch diameter wheel. However, this required the brackets to be designed to avoid interference with both the rim and the tire. Initially, the brackets were designed to be flat, as the rod ends listed on McMaster-Carr were specified to allow 65° of angular freedom—sufficient for full suspension travel. However, after modeling the rod ends as two-part assemblies in SolidWorks to allow realistic articulation, we discovered that they actually provide only about 55° of freedom. This realization required us to revert to a design similar to last year's.

2.2.3.2. Front Hub CAD Design:

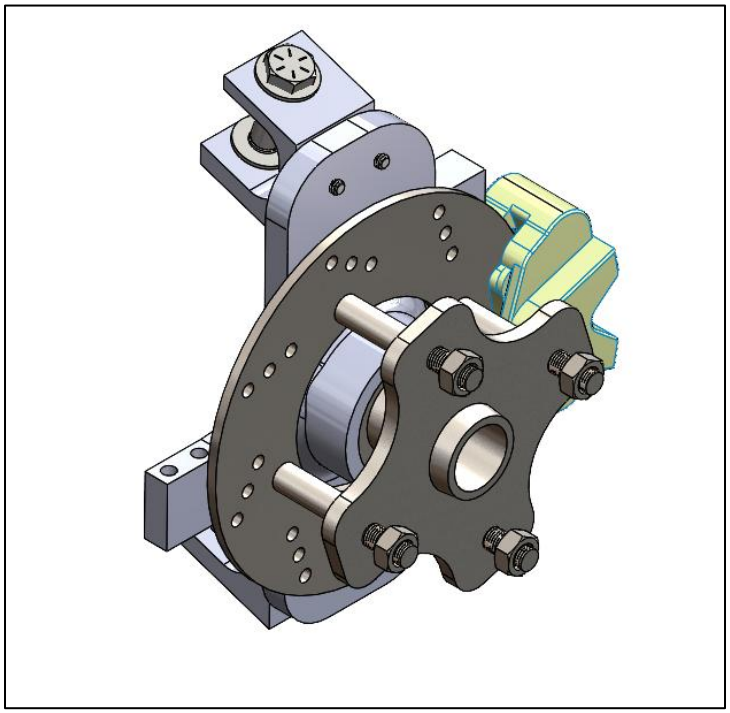

Figure 26: Front Upright Assembly

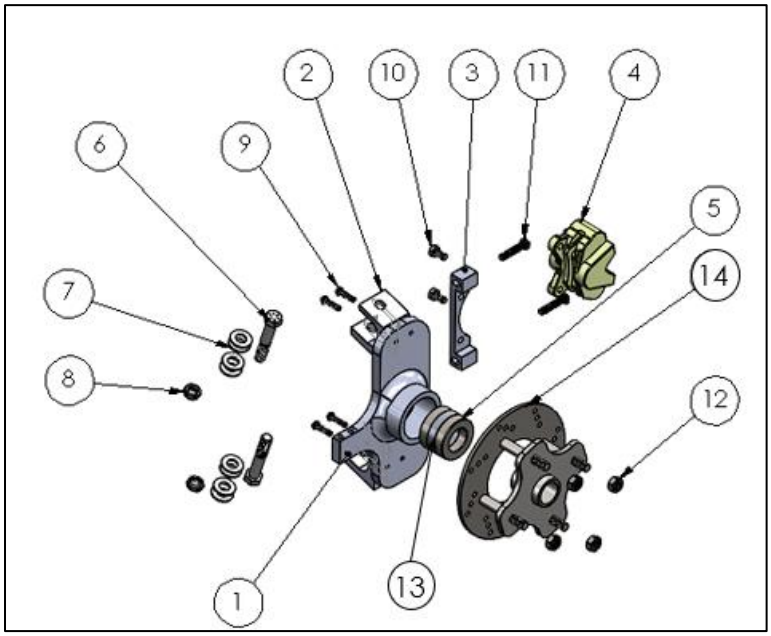

Figure 27: Exploded View of the Front Upright

2.2.3.3. Front Hub BOM:

BOM Part #	Description	Qty:	Source (Hyperlink to Part)	Cost:	Weight/1Pc [lbs]
1	Upright	1	(Stock) In Hand	N/A	1.59
2	Control Arm Bracket	2	(Stock) McMaster-Carr	$36.67	0.21
3	Brake Bracket	1	In Hand	N/A	0.15
4	Willwood Brake	1	In Hand	N/A	
5	Bearing	2	qualitybearingsonline.com	$23.73	0.26
6	½-20 rod end Bolt	2	McMaster-Carr	$11.65 per 50	
7	½ washer	8	McMaster-Carr	$7.12 per 10	
8	½-20 low profile lock nut	2	McMaster-Carr	$11.53 per 50	
9	1/4-20 upright bolt	4	McMaster-Carr	$11.65 for 50	
10	M8 x 1.25 mm, 20 mm long for brake calipers	2	In Hand	N/A	
11	M8 x 1.25 mm Thread, 35 mm long for brake bracket	2	In Hand	N/A	
12	10mm 1.25 lung nuts	4	McMaster-Carr	$14.51 per 50	
13	Bearing Spacer	1	(Stock) McMaster-Carr	$37.04 per 4	0.37
14	Hub Break Assembly	1	(Stock) In Hand	N/A	4.4
Total:				$137.85	7

Table 11: Full Upright BOM

2.2.3.4. Front Hub Critical Parts – Model Views and Discussion:

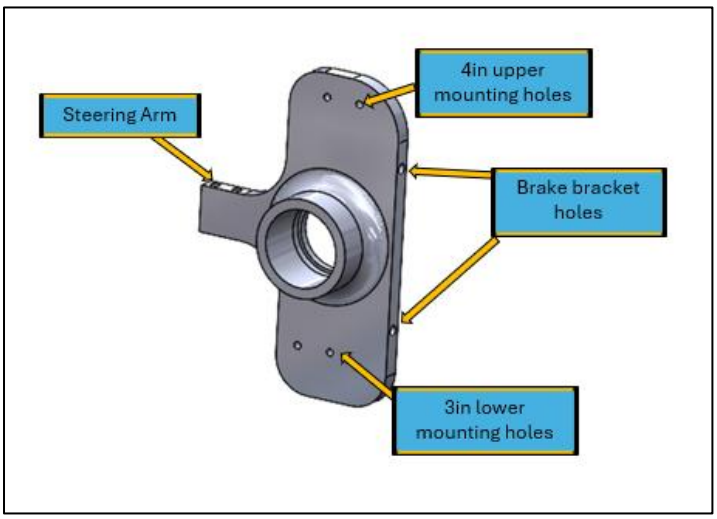

Figure 28: Driver Left Upright

The component shown in Figure 28 is the upright. This is a modified version of last year's design, updated to better meet our goals while improving manufacturability and structural strength. The most significant change is the increased height. Additionally, the bearing housing was redesigned to be machined in a single fixture rather than the two setups required last year. This change will require a spacer to be added between the bearings.

During testing at the beginning of this school year, the car experienced a large frontal impact on the front right tire. During this collision, the steering arm experienced plastic deformation of 0.075 inches. Finite Element Analysis (FEA) was used to back-calculate the failure load case, which was determined to be approximately 400 lbf, as shown in the analysis below. From this failure analysis, we used FEA on this year's upright design and made several small improvements to strengthen it under similar loading conditions. These improvements included increasing the upright thickness to 0.590 inches, which is the maximum allowable for our stock material. In addition, the bolts connecting the steering arm to the upright were reduced to size 10-32 to increase the amount of material in that region. This component is made from 6061-T6 aluminum, chosen for its balance of strength, low weight, and ease of machining.

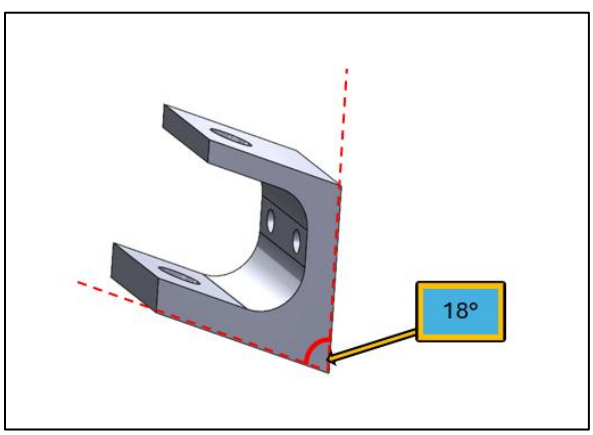

Figure 29: Bracket Connecting the Upright and Control Arm

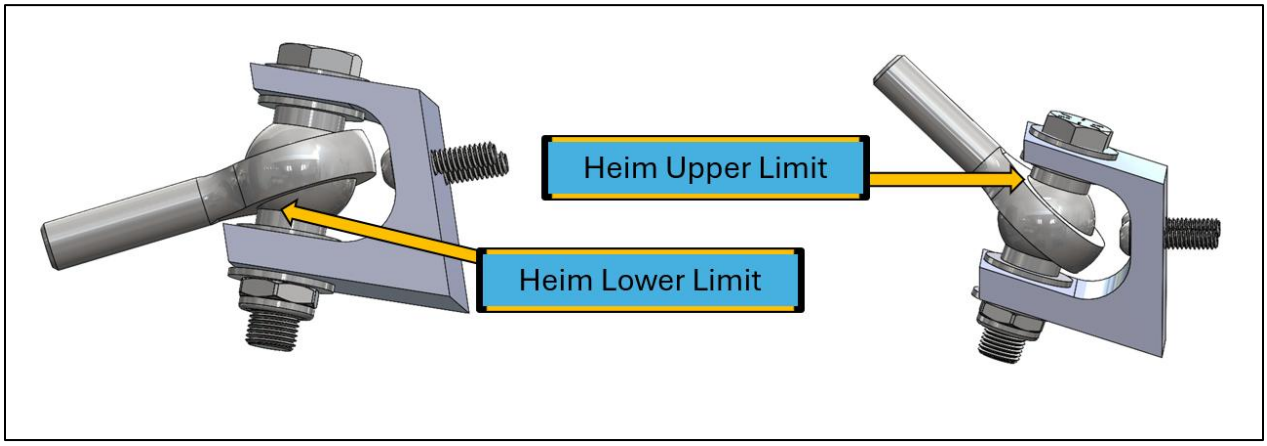

Figure 30: Upright brackets with hardware highlighting the upper and lower max of Heim travel

The component shown in Figure 30 is the bracket connecting the upright to the control arms. This bracket is tilted upward to allow for full suspension travel without binding the Heim joint, which is limited to 55°, as mentioned above. Upon discovering this limitation, our initial thought was to reuse last year's brackets; however, due to their size, packaging within the wheel rim was not possible.

We also experimented with designing a single-shear bracket and considered mounting the Heim directly to the upright while creating a welded bracket to attach to the control arm. Ultimately, the solution we implemented is a modified and improved version of last year's bracket. To accommodate the smaller Heim's and fit within the wheel well, the bracket was reduced in size. Additionally, we removed the flats from last year's design to improve work holding during machining.

One of our main improvements was strengthening the bracket by increasing the thickness of the lower section to 3/8 inch while keeping the upper section at 1/4 inch due to clearance constraints with the CV axle boot. Although no structural issues were observed with last year's brackets, the additional aluminum mass is negligible, so the decision was made to thicken the bracket. The bracket is made from 6061-T6 aluminum to maintain strength while minimizing weight.

The bolt connecting the Heim to the bracket, shown in **Error! Reference source not found.**, is a stock bolt from McMaster-Carr. Due to clearance issues with the CV axle boot and the limited bolt lengths available, the bolt will need to be shortened. This limitation also informed our decision to use a low-profile lock nut.

2.2.3.5. Front Hub Analysis:

2.2.3.5.1 Last Year Analysis

Failure Condition: Frontal impact on the outermost point of the front of 1 front tire stopping the vehicle.

Justification: We experienced a crash on our first testing day which resulted in this loading case and a plastic deformation 0.075 thou originating in the aluminum right after the tie rod bracket ended.

Load Diagram:

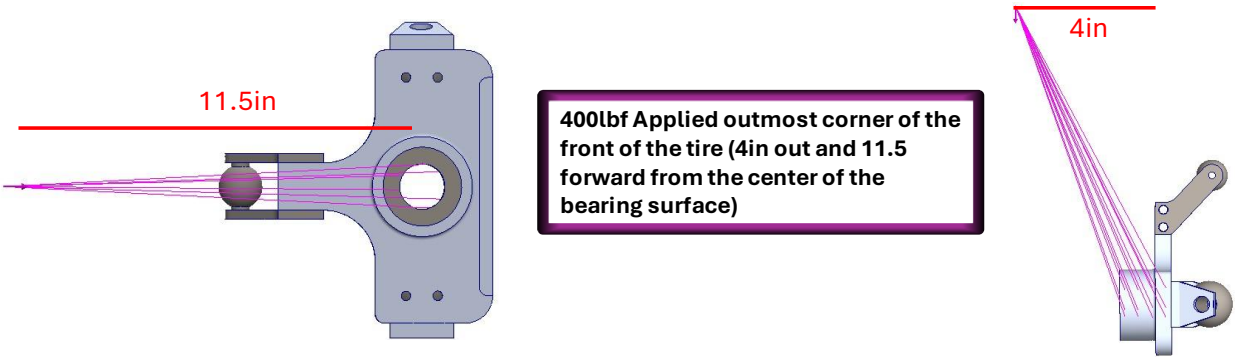

Constraints:

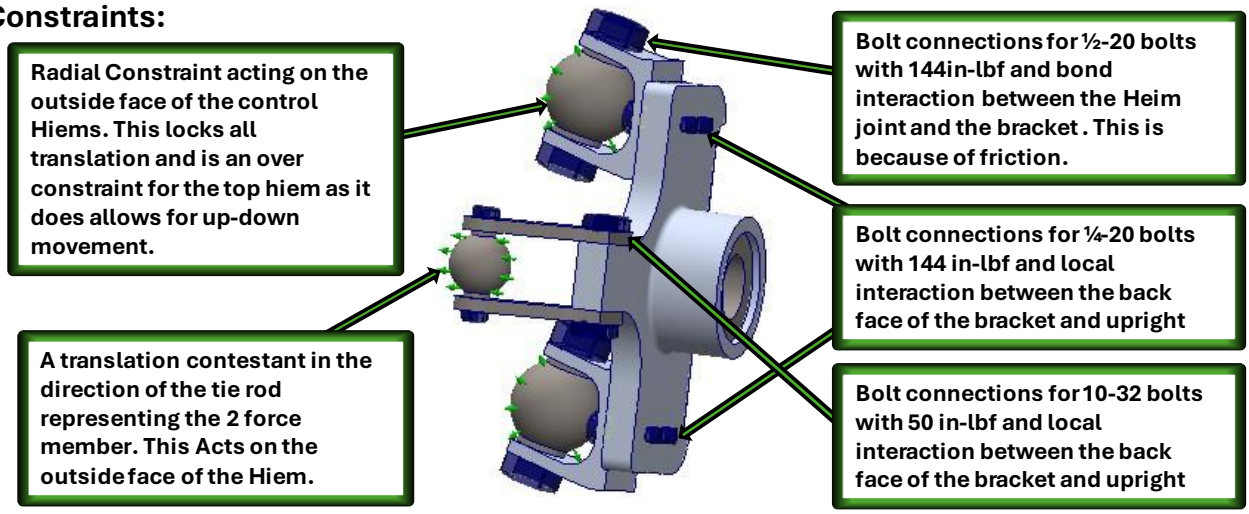

FOS: .8

Equations (If Applicable):

Confidence Level & Explanation: Medium: Due to SolidWorks limitations on Boundary conditions this model is over defined. For a front impact there is Little to no upward forces therefore this is an "OK" fix. Also Due to the 24-25 upright not failing at the base of the bearing housing, seen in the FEA, this model is close but not perfect.

Figure 31: 2024-25 Upright FEA with frontal loading case experienced in testing this year

Calculations and/or FEA:

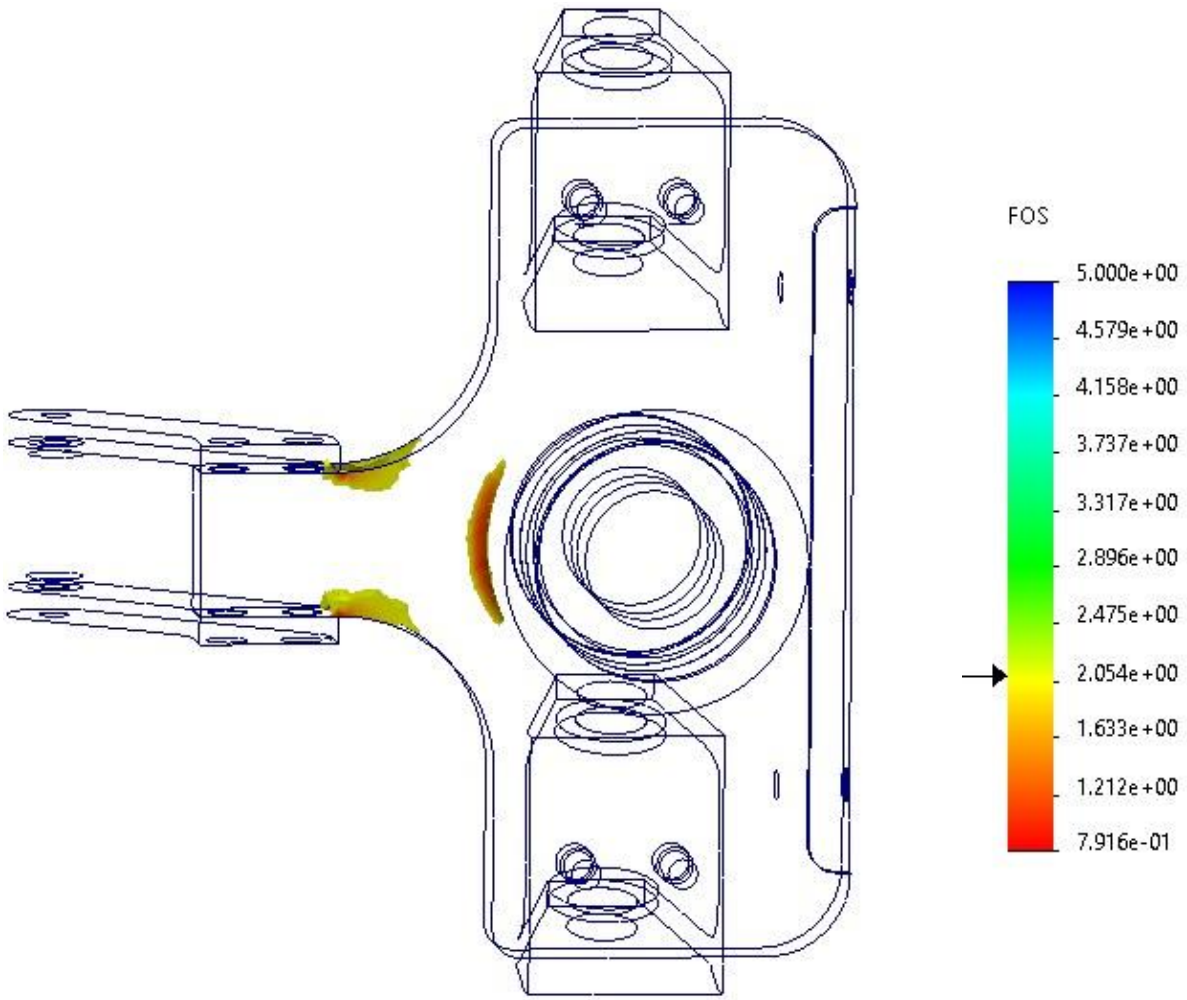

Figure 32: Results of Analysis in Figure 31

2.2.3.5.2 This Year Analysis

Failure Condition: Frontal impact on the outermost point of the front of 1 front tire stopping the vehicle.

Justification: Due to the failure of last years upright the same loading case was assumed on this year model

Load Diagram:

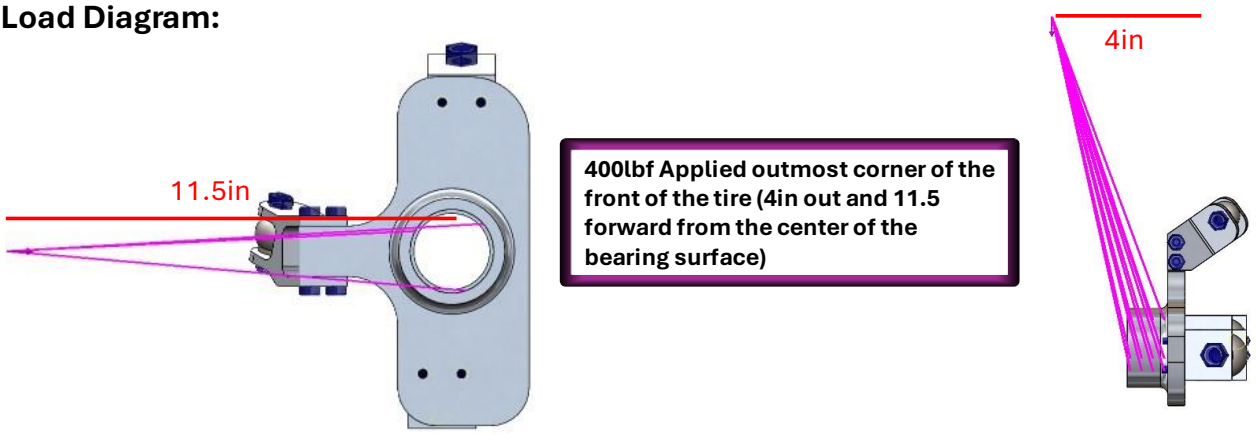

Constraints:

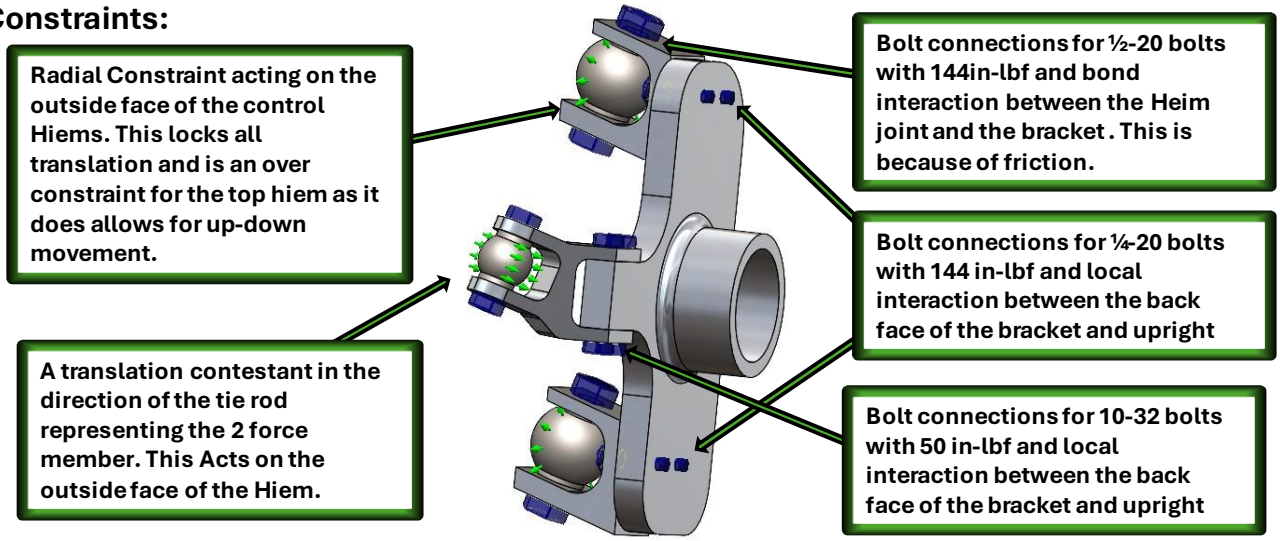

FOS: 2.05

Equations (If Applicable):

Confidence Level & Explanation: Medium: Numbers are gathered from previous FEA but lack supporting test data for loading force.

Figure 33: This year's Upright FEA with frontal loading derived from failure case modeled above

Calculations and/or FEA:

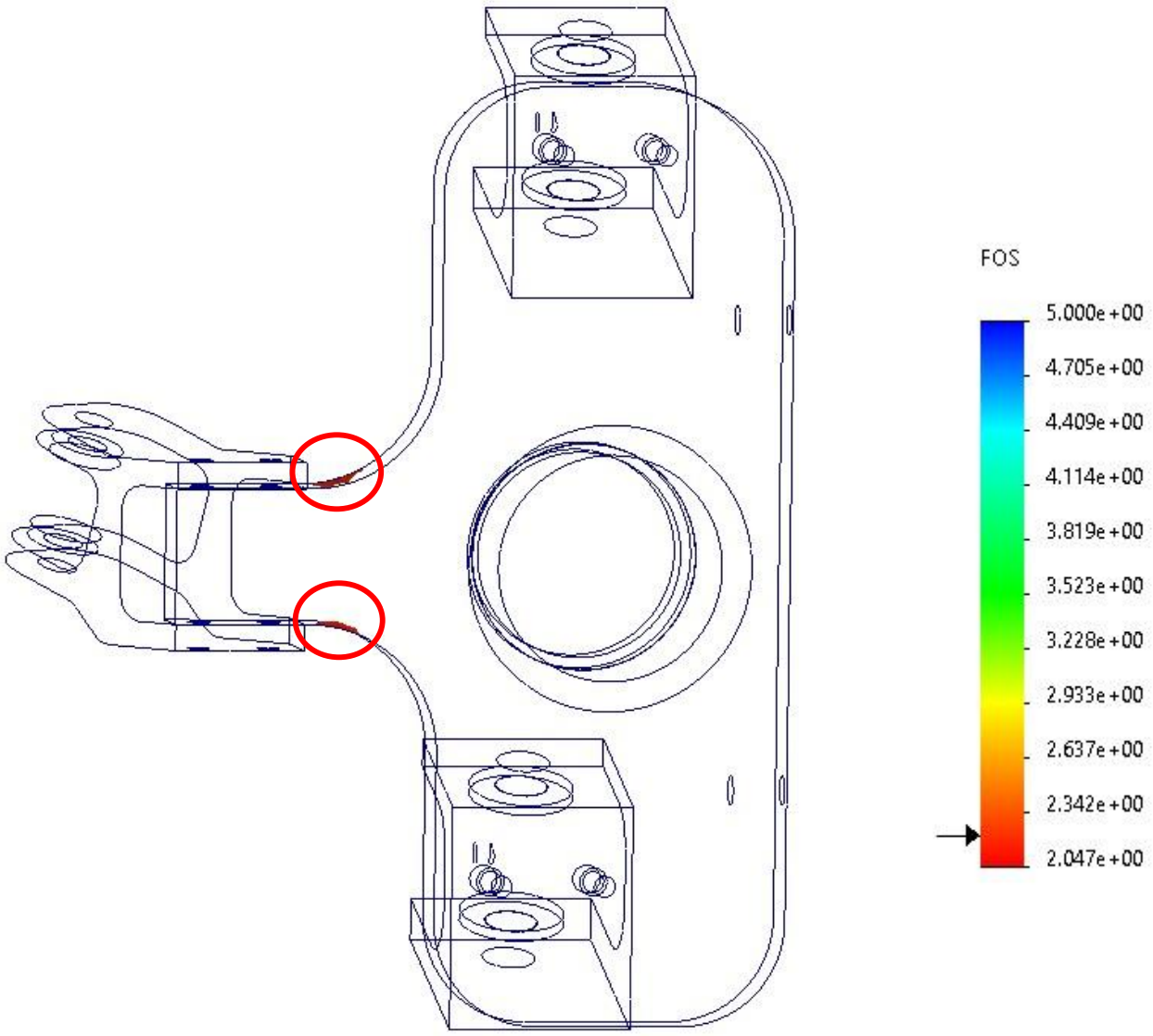

Figure 34: Results of Analysis in Figure 33

Failure Condition: Frontal impact on the outermost point of the front of 1 front tire stopping the vehicle with added braking .
Material: 6061 -T6 Aluminum upright (0.59" thick) and brackets (0.25" thick top and back with 0.375" thick bottom), Heim ball joints are 4130 Chromoly only input for BC's.

Justification: Frontal loading case derived from pervious FEA With the added condition of make braking torque.

Load Diagram:

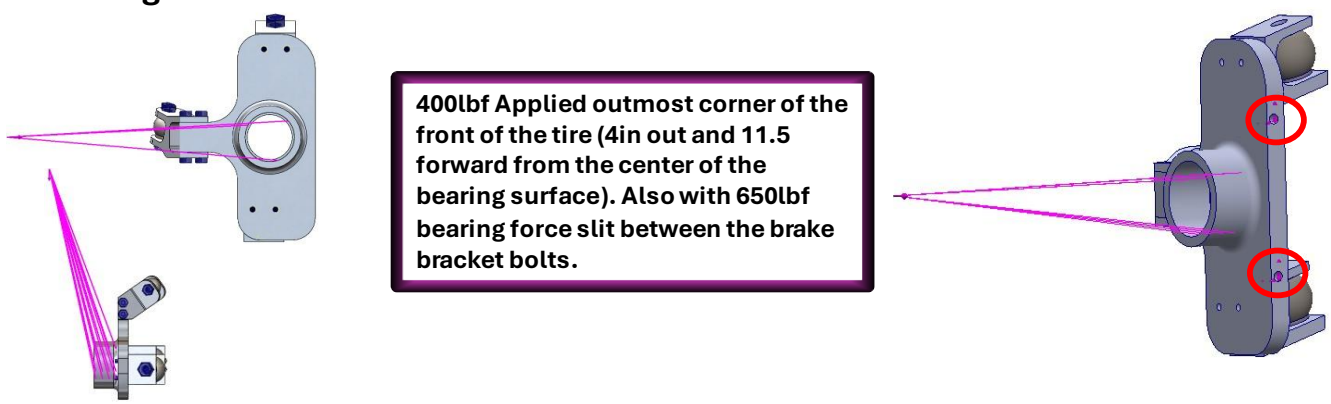

Constraints:

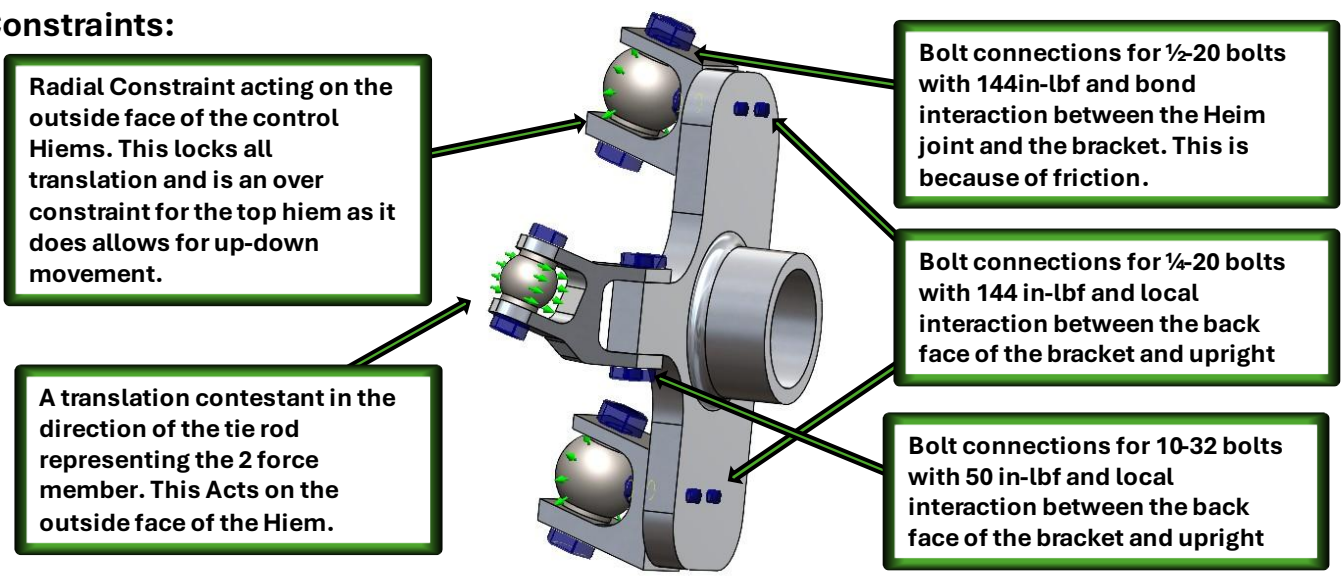

FOS: 2.1

Equations (If Applicable):

Confidence Level & Explanation: Medium: Numbers are gathered from previous FEA but lack supporting test data for loading force. Brake calculations are derived from max braking torque described in controls section 3.2.4.

Figure 35: Front loading with max brake force

Calculations and/or FEA:

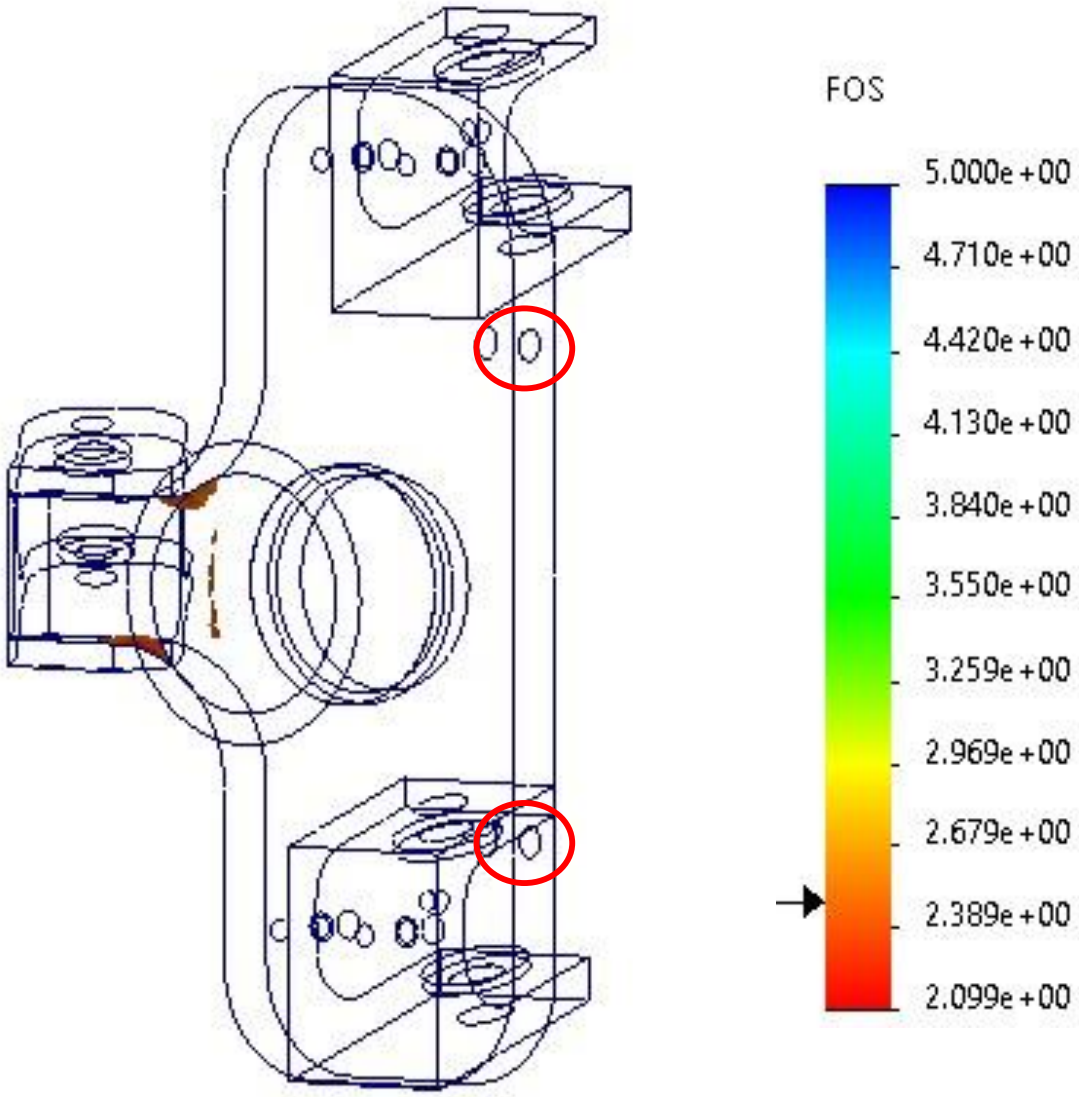

Figure 36: Results of Analysis in Figure 35

Failure Condition: Approximately a 2G load (1000ibf) loaded on the outmost corner of the bottom of the tire.
Material: 6061-T6 Aluminum upright (0.59" thick) and brackets (0.25" thick top and back with 0.375" thick bottom), Heim ball joints are 4130 Chromoly only input for BC's.

Justification: This is a worse case loading if the vehicle where to landed a jump on one wheel of the front wheels.

Load Diagram:

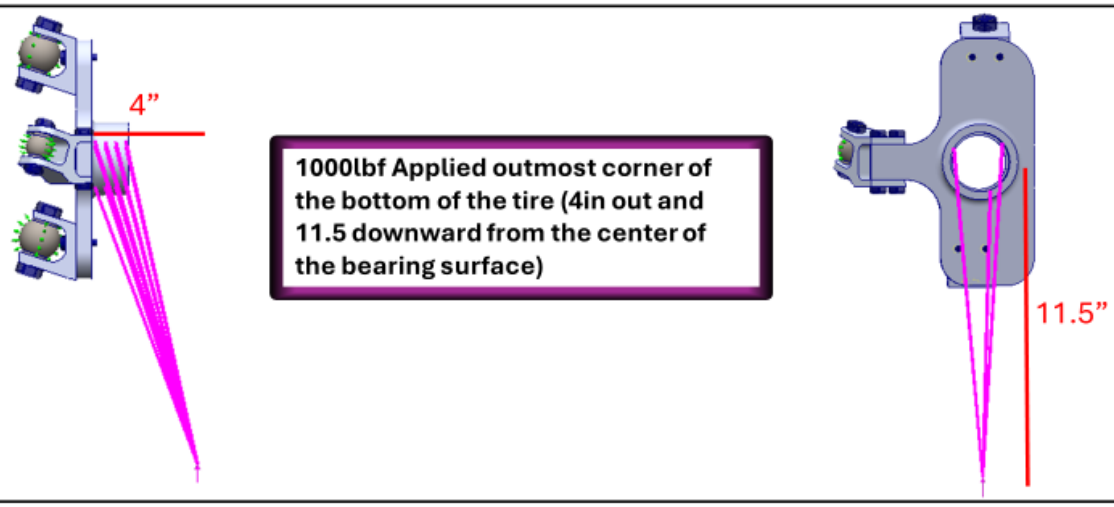

Constraints:

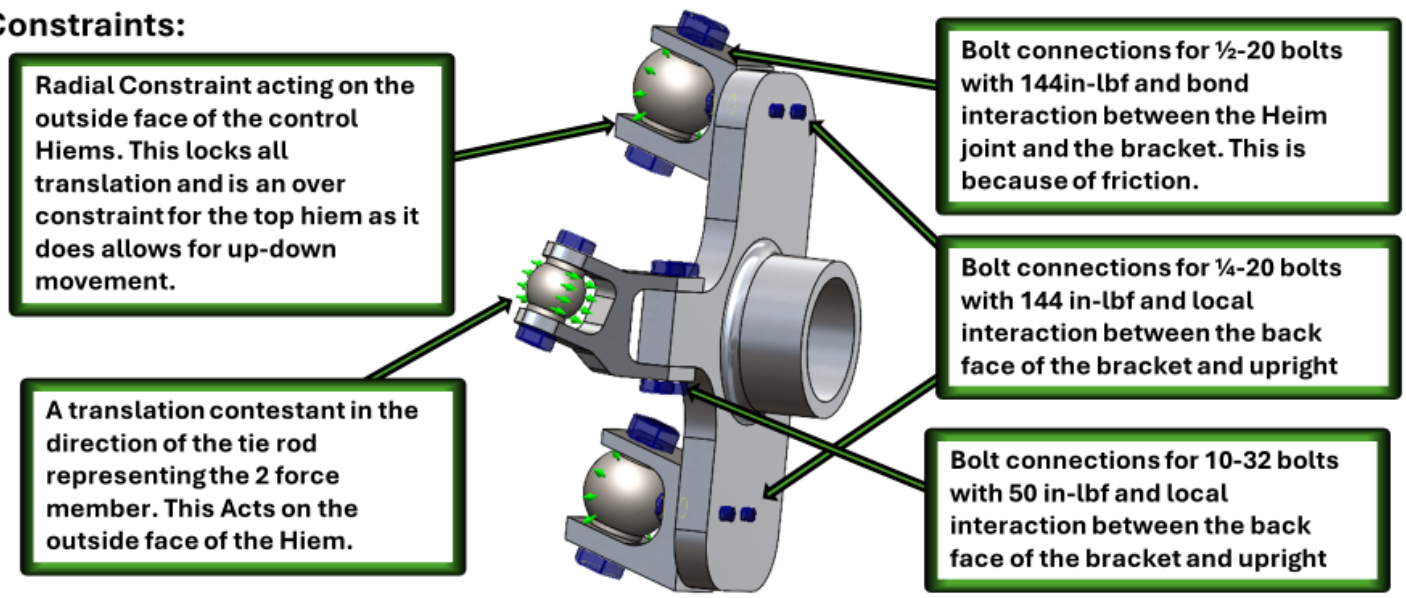

FOS: 1.5

Equations (If Applicable):

Confidence Level & Explanation: Low: Loads are not well known. Also Due to SolidWorks limitations the model is over defined in the top Hiem explained above.

Figure 37: Upward Loading Case

Calculations and/or FEA:

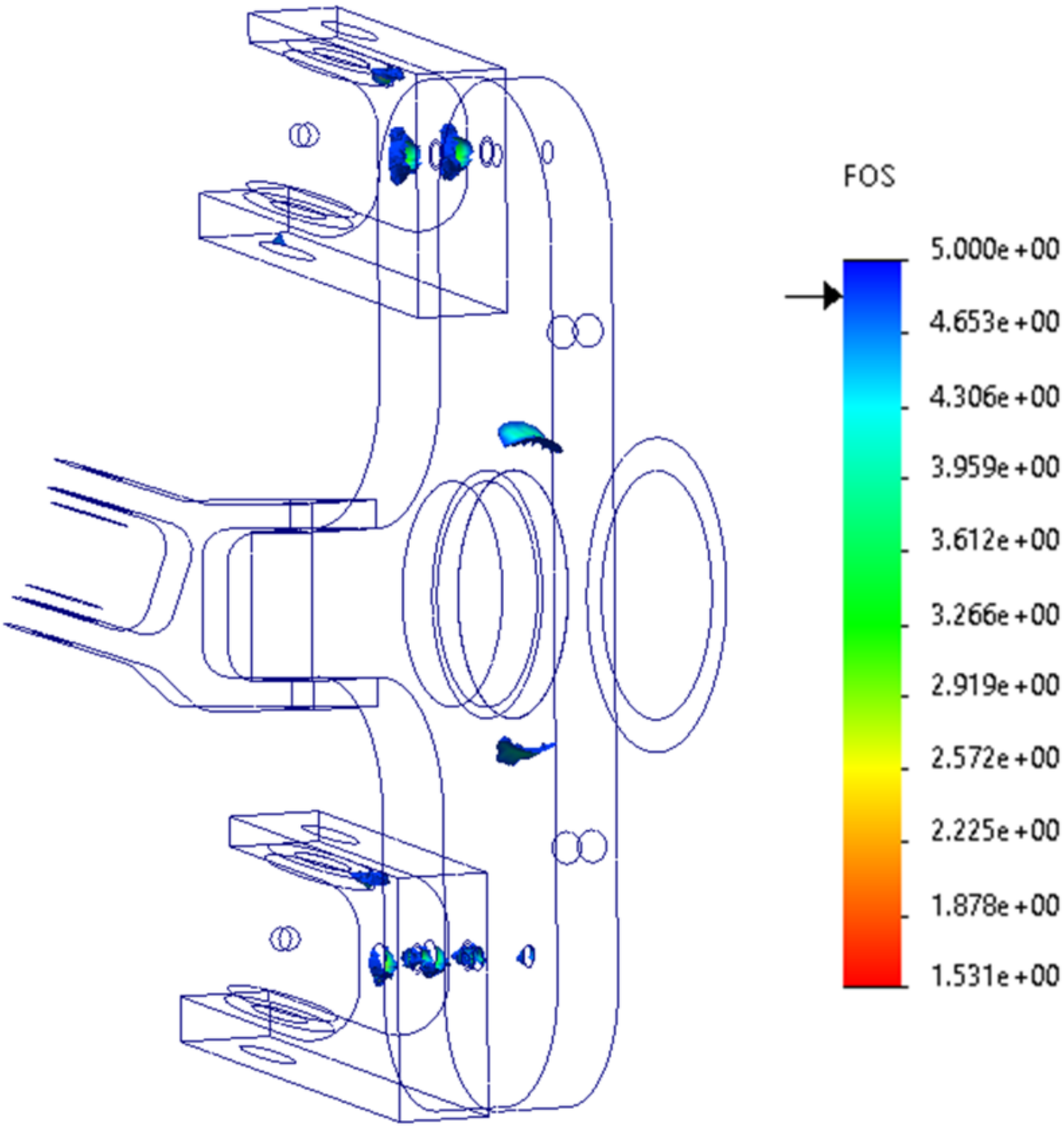

Figure 38: Results of Analysis in Figure 37

Failure Condition : Max force of shock acting on control arm translating to the bracket.
Material: 6061-T6 Aluminum (0.25" thick top and back with 0.375" thick bottom).

Justification: Compression loading from a jump or large bump acting on the bracket

Load Diagram:

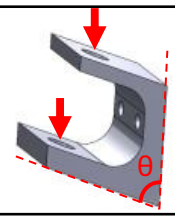

680lbf total downward perpendicular on the two the bracket arms. This was derived from a max force of the shock at 1600lbf

Constraints:

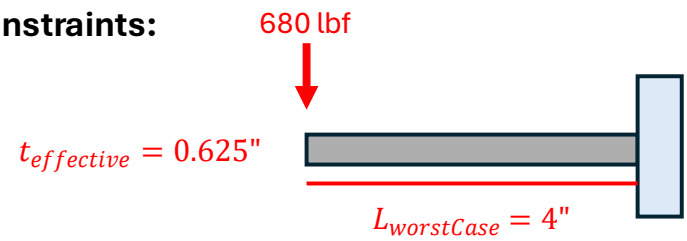

Simple beam calculation assume worse case length, force, and no filet.

FOS: 5

Equations (If Applicable):

$$F_{\text{bracket}} = \frac{F_{\text{shock}}\, L_{\text{shock}}\, \cos(\theta)}{L_{\text{arm}}}$$

$$M = F_{\text{bracket}} \cdot L$$

$$I = \frac{bh^3}{12}$$

$$\sigma_b = \frac{Mc}{I}$$

$$FS = \frac{\sigma_y}{\sigma_b}$$

Confidence Level & Explanation : Low: Pervious years have done testing of max force the chock can out put but they very from 1000lbf to 1600lbf

Calculations and/or FEA:

```
--- Aluminum Bracket Calculations ---
Moment of Inertia (I):        0.035604 in^4
Applied Moment:               1125.25 lb·in
Bending Stress:               9876.44 psi
Safety Factor (Bending):      3.54
```

Figure 39: Supplementary hand calculations from upward impact

Failure Condition: a 3000lbf force split equally between both control arm brackets
Material: 6061 -T6 Aluminum (0.25” thick top and back with 0.375” thick bottom).

Justification: A Frontal impact translated directly to the bracket or side impact causing a moment on the upright and translated to the bracket.

Load Diagram:

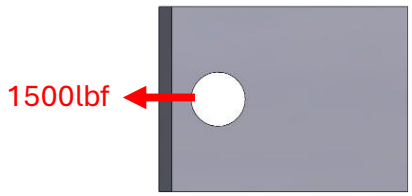

3000lbf total load in the worst case direction

Constraints:

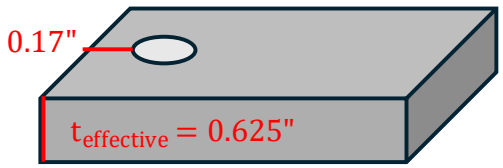

Combine Bracket thicken using the worsted case distance from edge

FOS: 5

Equations (If Applicable):

$$F = \frac{F_{\text{total}}}{n_{\text{brackets}}}$$

$$\sigma_{\text{tear}} = \frac{F}{A}$$

$$FS_{\text{tear}} = \frac{\sigma_y}{\sigma_{\text{tear}}}$$

Confidence Level & Explanation Low: Pervious years have done testing of max force the chock can out put but they very from 1000lbf to 1600lbf

Calculations and/or FEA:

```
--- Aluminum Bracket Calculations ---
Tear-Out Area:                0.2125 in^2
Force per Bracket Side:       1500.00 lb
Tear-Out Stress:              7058.82 psi
Safety Factor (Tear-Out):     4.96
```

Figure 40: Bearing failure calculations for Hiem bolts pulling out

Failure Condition : a 3000lbf force split equally between both control arm brackets
Material: 6061 -T6 Aluminum (0.59”).

Justification: A Frontal impact translated directly to the bracket or side impact causing a moment on the upright and translated to the bracket.

Load Diagram:

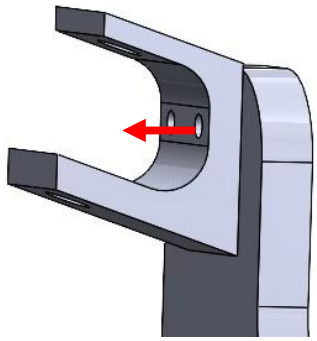

No force is applied in this direction instead we am calculating make strength of thread pull out

Constraints:

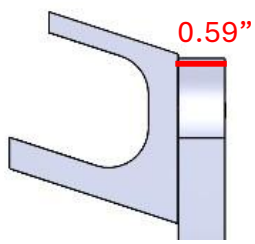

The upright which is what we are threading into is assumed to be ridged and 0.59in thick.

FOS: N/A

Equations (If Applicable):

$$A_{\text{shear}} = \pi D_{\text{avg}} L_{\text{eng}}$$

$$F_{\text{tear-out}} = \tau_{\text{allow}} \times A_{\text{shear}}$$

Confidence Level & Explanation : High: All values of material and their strengths are well know and tested throughout industry.

Calculations and/or FEA:

```
THREAD TEAR-OUT CALCULATION RESULTS:
------------------------------------
Bolt Size:          1/4"-20 UNF
Major Diameter:     0.2500 in
Minor Diameter:     0.1887 in
Engagement Length:  0.590 in
Average Diameter:   0.2193 in
Shear Area:         0.4066 in^2
Tear-Out Strength:  9758 lb
```

Figure 41: Thread tear out calculations for the 1/4-20 hardware attaching the control arm brackets to the upright

2.2.4. Rear Lower Control Arm – (RLCA)

2.2.4.1. Discussion of Design Reasoning – RLCA

The RLCA was designed with two tubing members joined by a single welded connection, we chose 4130 1” OD X 0.083 Wall tubing to maintain strength under impacts with the terrain below given the track setup and rocky conditions at SAE Oregon, in addition to our loading cases. Our loading cases were primarily based on the reuse and revalidation of the previous year’s loading cases since their RLCA did not fail during competition, despite extreme load conditions due to a forward rollover and impact from the rear of the tire from ground impact. The arm was designed to meet the roll hoop and rear most member of the chassis, while maintaining adequate clearance of drivetrain components such as the CVT cover.

2.2.4.2. RLCA CAD Design:

Figure 42: Rear Lower Control Arm

2.2.4.3. RLCA BOM:

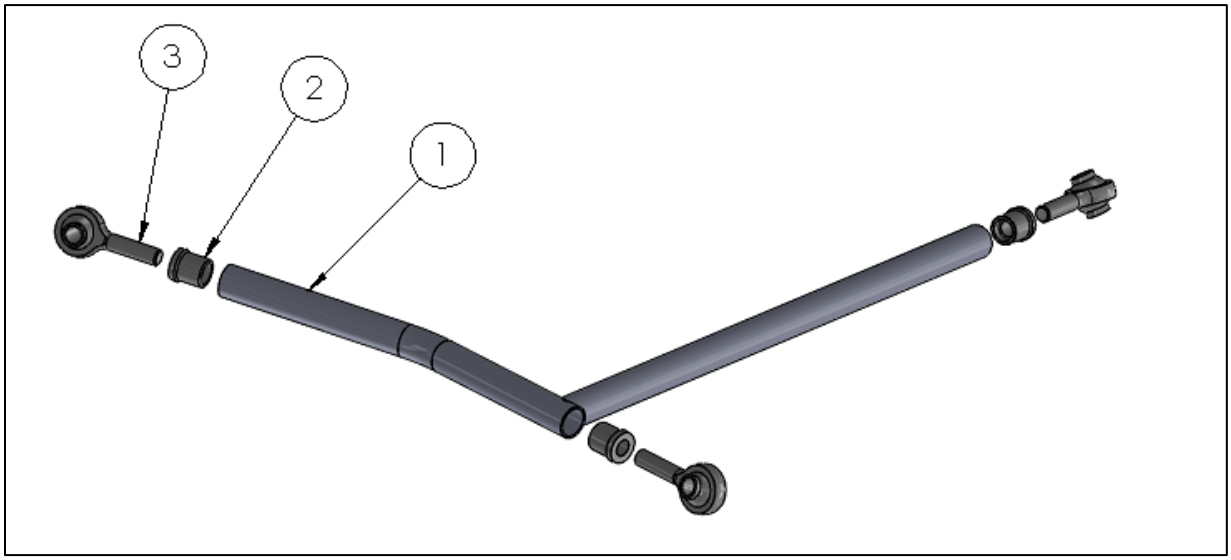

Figure 43: RLCA Exploded View

BOM Part #	Description	Qty:	Source (Hyperlink to Part)	Cost/1pc:	Weight/1Pc [lbs]
1	Lower control arm	1			2.17
2	Weld Nuts	3	McMaster	8.42	
3	½”-20 Rod End	3	McMaster	21.55	
Total				49.81	2.17

Table 12: RLCA BOM

2.2.4.4. RLCA Critical Parts – Model Views and Discussion:

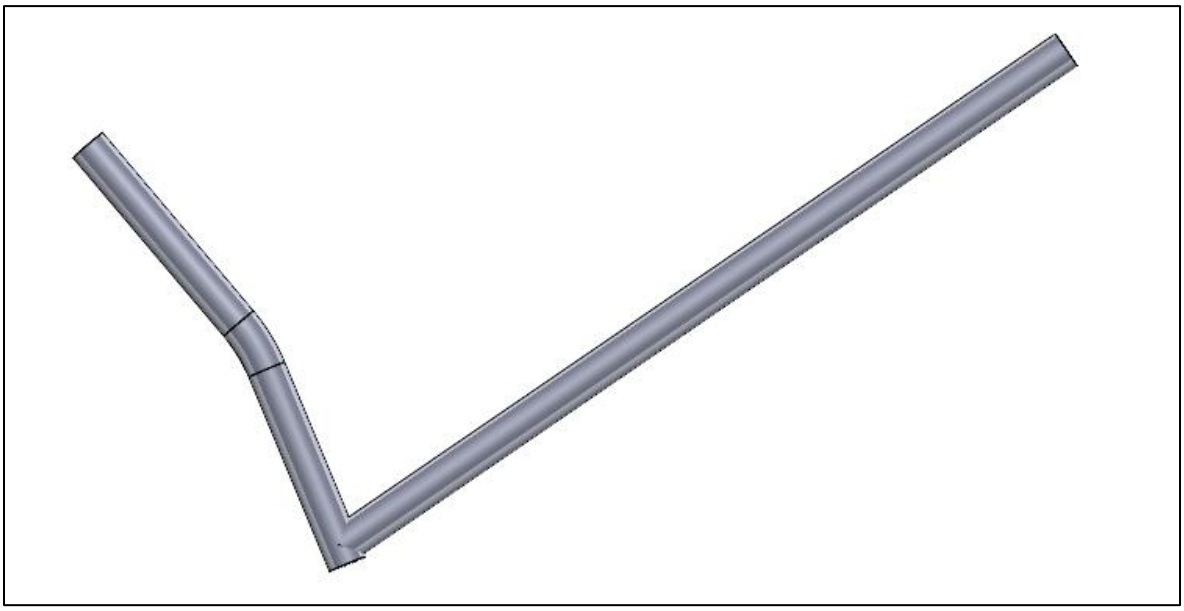

Figure 44: RLCA Top View to show Geometry

The lower arm is 4130 Steel with 1’’ OD and 0.083 wall thickness. The back member has a 4.5’’ radius bend allowing the Heim to be parallel with the faces of the upright brackets at ride height.

2.2.4.5. RLCA Analysis

Failure Condition: Front impact on the front of the rear wheel (Lower Control Arm)
Material: Alloy Steel 4130 1'' OD 0.083 Wall

Justification: When we impact frontal obstacles at speed, part of the force will be translated into the control arms.

Load Diagram:

1750lbf applied to the outer most point of the upper control arm, 1.5 inches out where the center of the rod end would be.

Constraints:

Single translation constraint on the end of the control arm to prevent rotation and simulate a ridged shock force translated through the upright

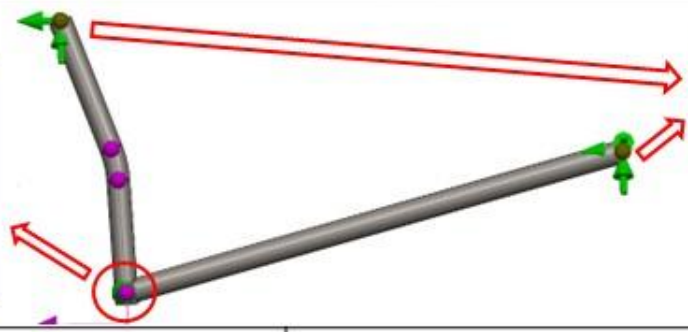

Heims constrained to only allow rotation

FOS: 1.7

Equations (If Applicable):

Confidence Level & Explanation:
Medium: Using a 3000 lbf impact, with 1750 lbf translating into lower arm, there is no failure but lack of testing data.

Calculations and/or FEA:

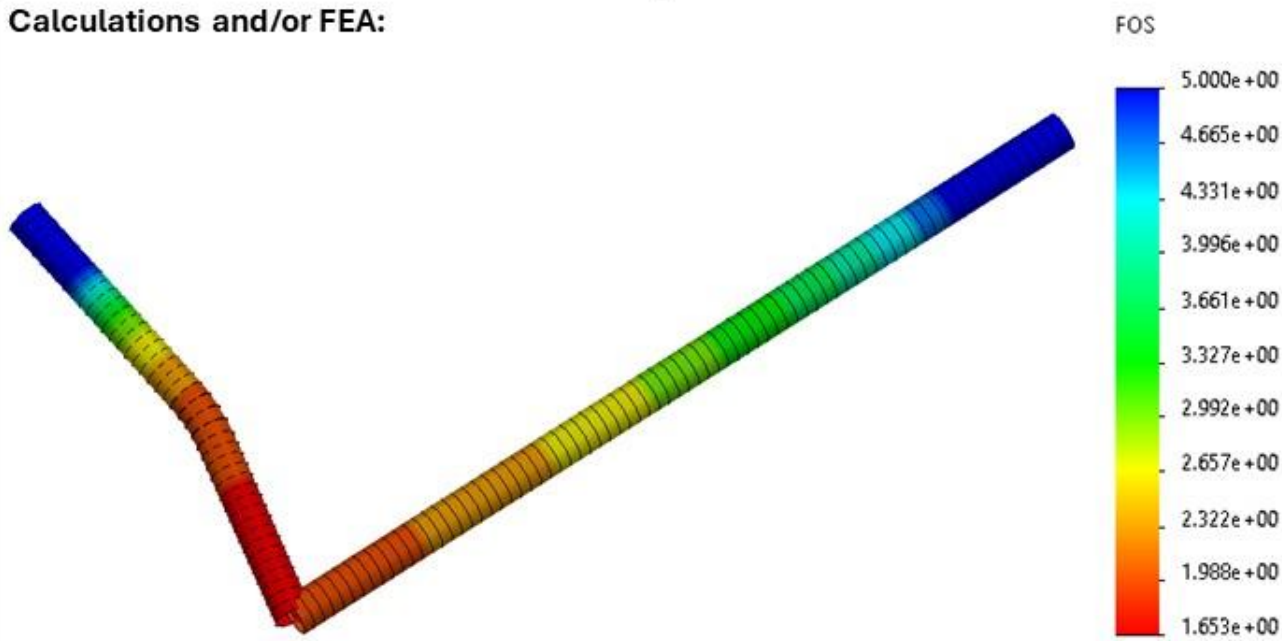

Figure 45: Forward Impact on Rear Wheel

Failure Condition: Side impact on the front of the rear wheel (Lower Control Arm)
Material: Alloy Steel 4130 1'' OD 0.083 Wall

Justification: The control arm will experience a force if the tire experiences an impact from the side.

Load Diagram:

1750lbf applied to the outer most point of the upper control arm, 1.5 inches out where the center of the rod end would be.

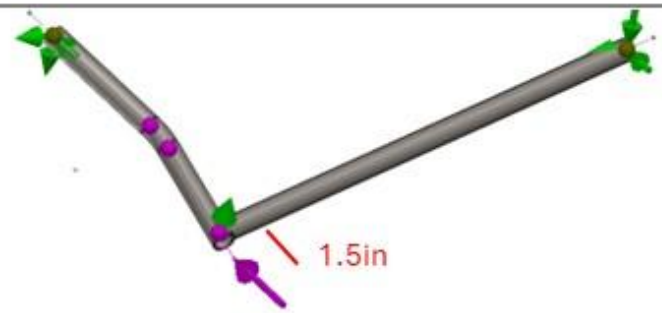

Constraints:

Single translation constraint on the end of the control arm to prevent rotation and simulate a ridged shock force translated through the upright

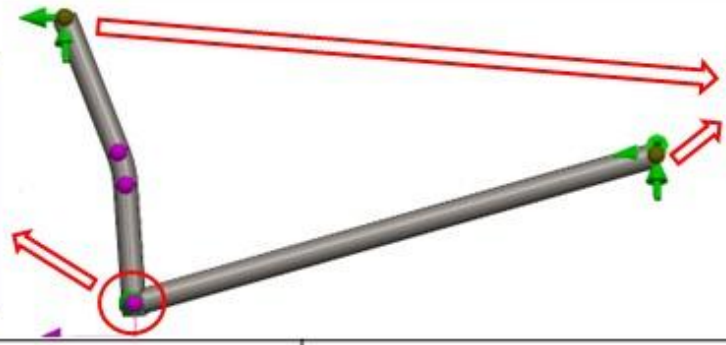

Heims constrained to only allow rotation

FOS: 1.7

Equations (If Applicable):

Confidence Level & Explanation:
Medium: Using a 3000 lbf impact, with 1750 lbf translating into lower arm, there is no failure but lack of testing data.

Calculations and/or FEA:

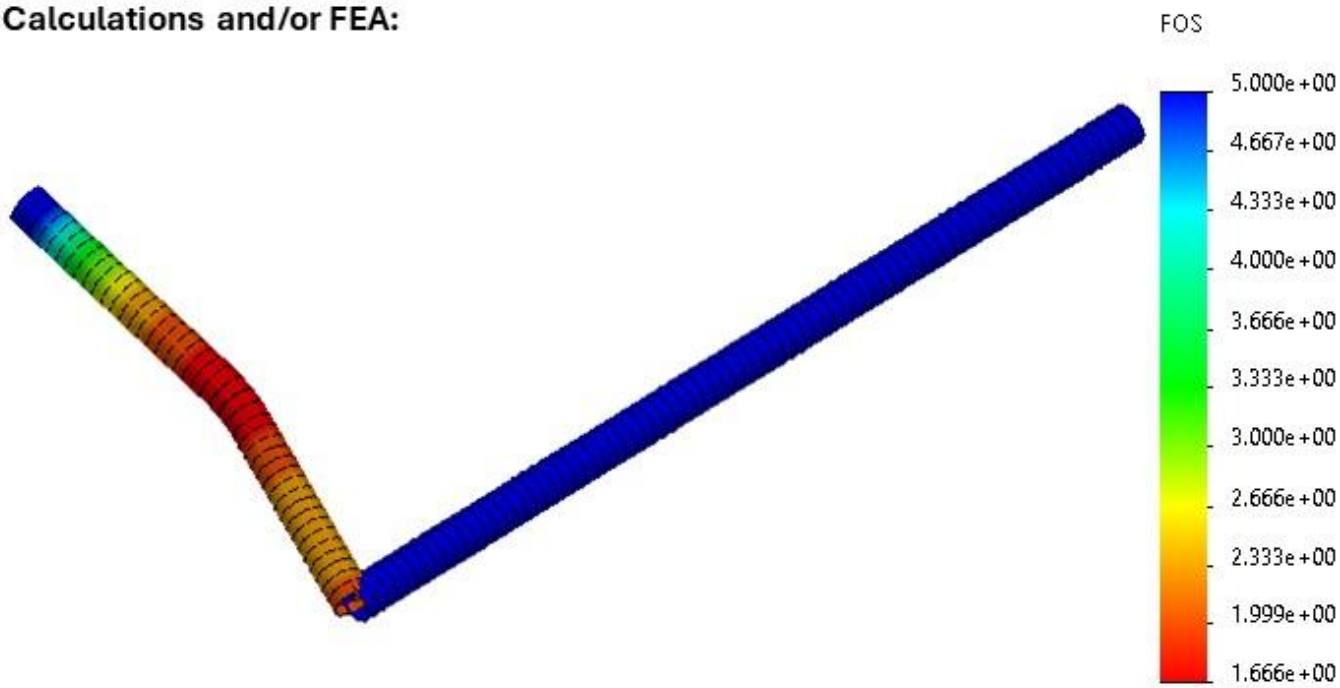

Figure 46: Side Impact on Rear Wheel

2.2.5. Rear Upper Control Arm – (RUCA)

2.2.5.1. Discussion of Design Reasoning – RUCA

For the RUCA, we chose 4130 Steel with 1'' OD. The back and cross members are 0.083'' wall thickness, and the forward member is 0.065 wall thickness. This maintains strength and resilience under maximum shock loads in addition to protection from other forces such as a forward impact from the wheel. The RUCA, pictured below, shows the 3 component members joined by welding, with tube nuts and hiem joints at all ends. The suspension tabs are 3/16 inch thick.

2.2.5.2. RUCA CAD Design:

Figure 47: Rear Upper Control Arm

2.2.5.3. RUCA BOM:

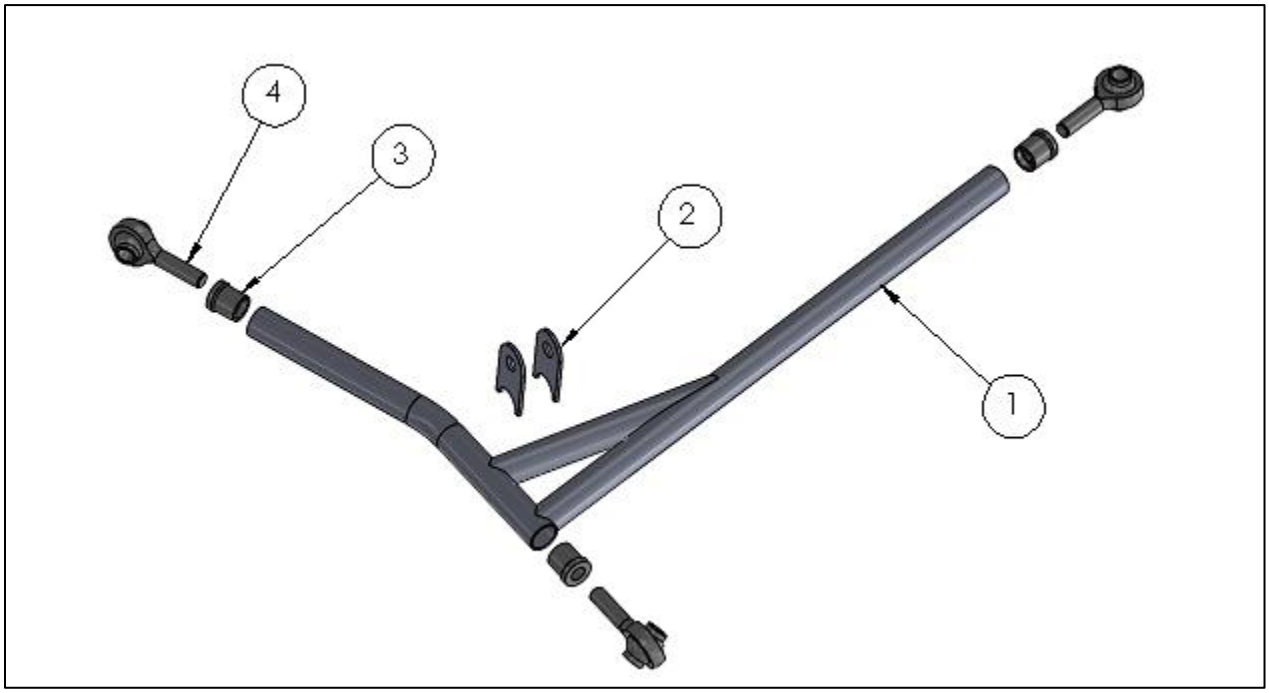

Figure 48: RUCA Exploded View

BOM Part #	Description	Qty:	Source (Hyperlink to Part)	Cost:	Weight/1Pc [lbs]
1	Upper control arm	1			1.9
2	Weld Nuts	3	McMaster	8.42	
3	½”-20 Rod End	3	McMaster	21.55	
4	Shock brackets	2			
				49.81	1.9

Table 13: RUCA BOM

2.2.5.4. RUCA Critical Parts – Model Views and Discussion:

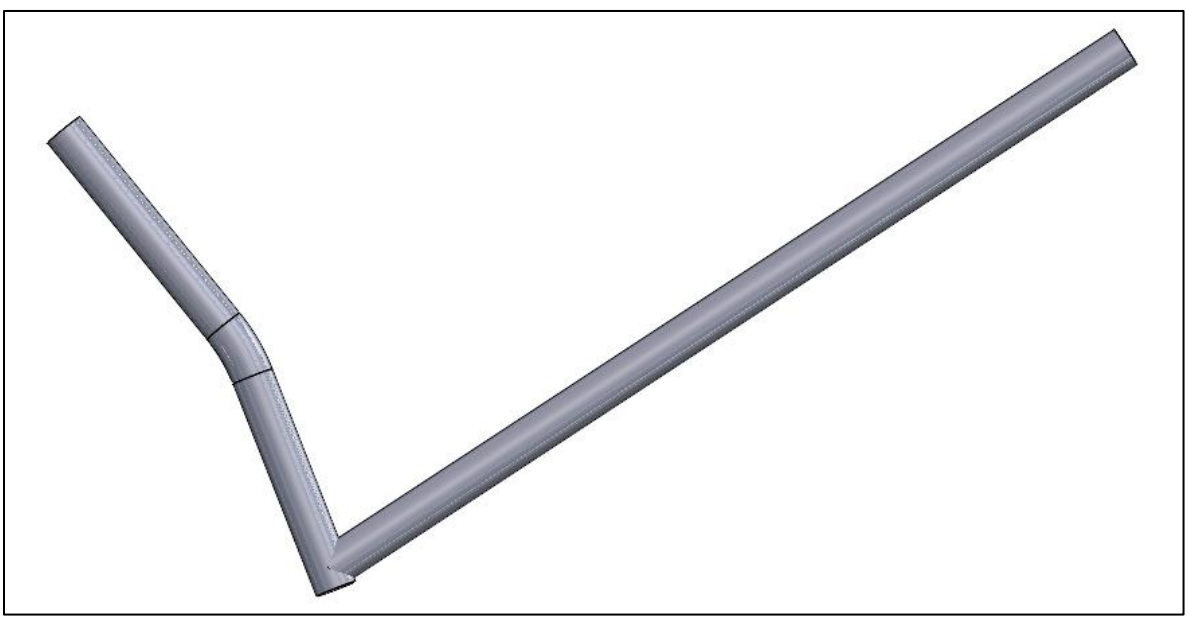

Figure 49: RUCA Geometry

2.2.5.5. RUCA Analysis:

Failure Condition: Front impact on the front of the rear wheel (Upper Control Arm)
Material: Alloy Steel 4130 1'' OD, forward member 0.065 Wall, rear and cross member 0.093'' OD

Justification: When we experience frontal obstacles at speed, part of the force will be translated into the control arms.

Load Diagram:

1350lbf applied to the outer most point of the upper control arm, 1.5 inches out where the center of the rod end would be.

Constraints:

Single translation constraint on the end of the control arm to prevent rotation and simulate a ridged shock force translated through the upright

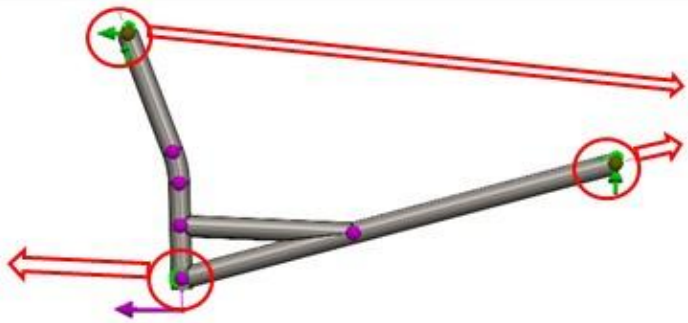

Heims constrained to only allow rotation

FOS: 2.3

Equations (If Applicable):

Confidence Level & Explanation:
Medium: Using a 3000 lbf impact, with 1350 lbf translating into lower arm, there is no failure but there is no testing data.

Calculations and/or FEA:

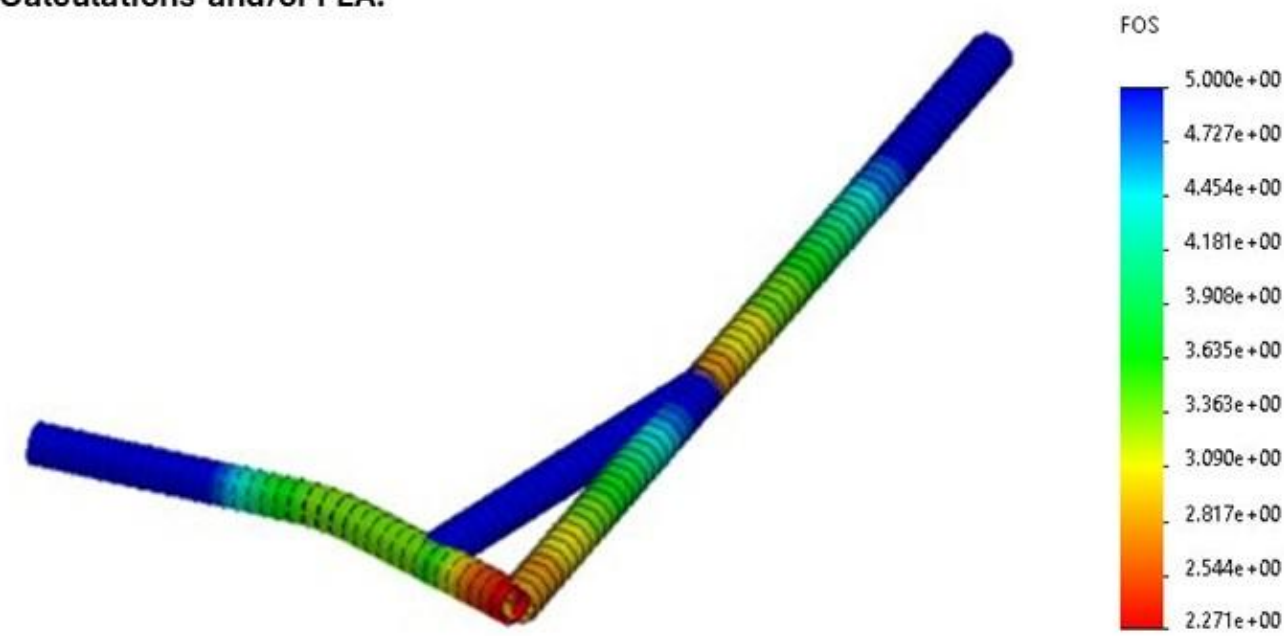

Figure 50: Forward impact of rear upper control arm

Failure Condition: Side impact on the center of the rear wheel (Upper Control Arm)
Material: Alloy Steel 4130 1'' OD, forward member 0.065 Wall, rear and cross member 0.093'' OD

Justification: The control arm will experience a force if the tire experiences an impact from the side.

Load Diagram:

1350lbf applied to the outer most point of the upper control arm, 1.5 inches out where the center of the rod end would be.

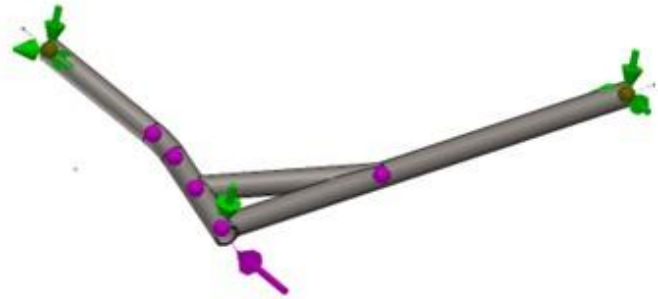

Constraints:

Single translation constraint on the end of the control arm to prevent rotation and simulate a ridged shock force translated through the upright

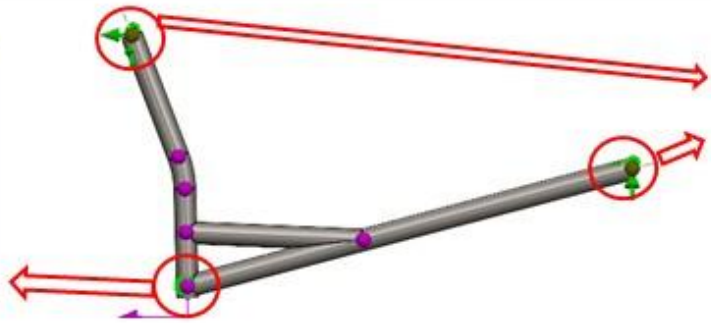

Heims constrained to only allow rotation

FOS: 13

Equations (If Applicable):

Confidence Level & Explanation:
Medium: Using a 3000 lbf impact, with 1350 lbf translating into lower arm, there is no failure but there is no testing data.

Calculations and/or FEA:

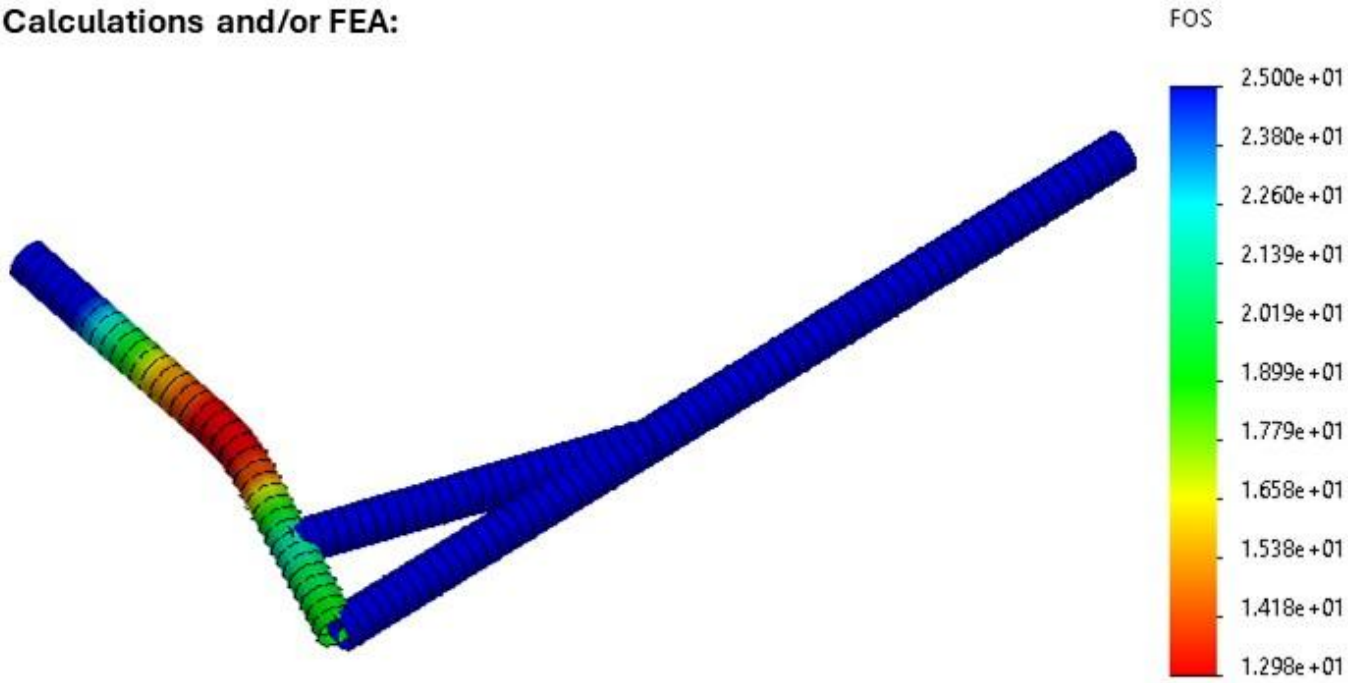

Figure 51: Side impact on upper control arm

Failure Condition: Maximum shock force on upper rear control arm
Material: Alloy Steel 4130 1'' OD, forward member 0.065 Wall, rear and cross member 0.093'' OD

Justification: At maximum compression, the shock experts a 1600 lbf force downwards on the upper control arm

Load Diagram:

1600 lbf applied to the shock mount point on the upper control arm cross member.

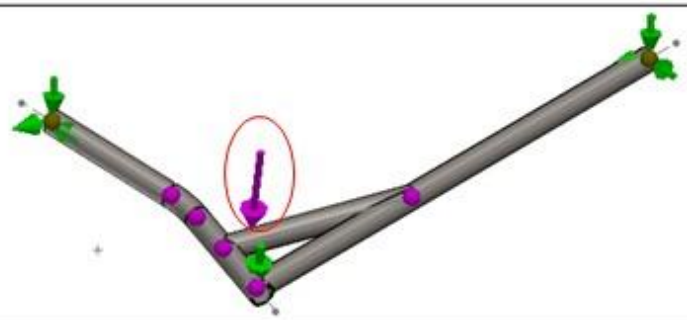

Constraints:

Single translation constraint on the end of the control arm to prevent rotation and simulate a ridged shock force translated through the upright

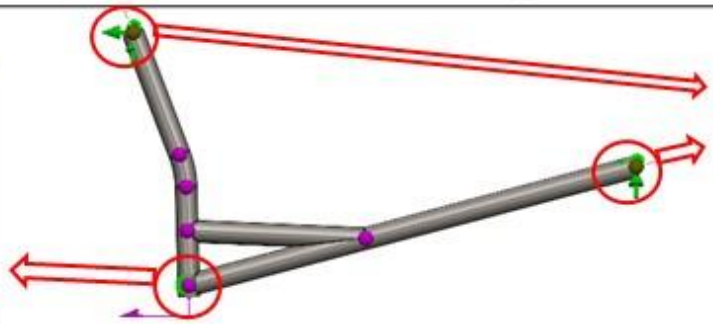

Heims constrained to only allow rotation

FOS: 1.2

Equations (If Applicable):

Confidence Level & Explanation:
Medium: Maximum force from FOX shock data was derived and has been used in previous years without failure.

Calculations and/or FEA:

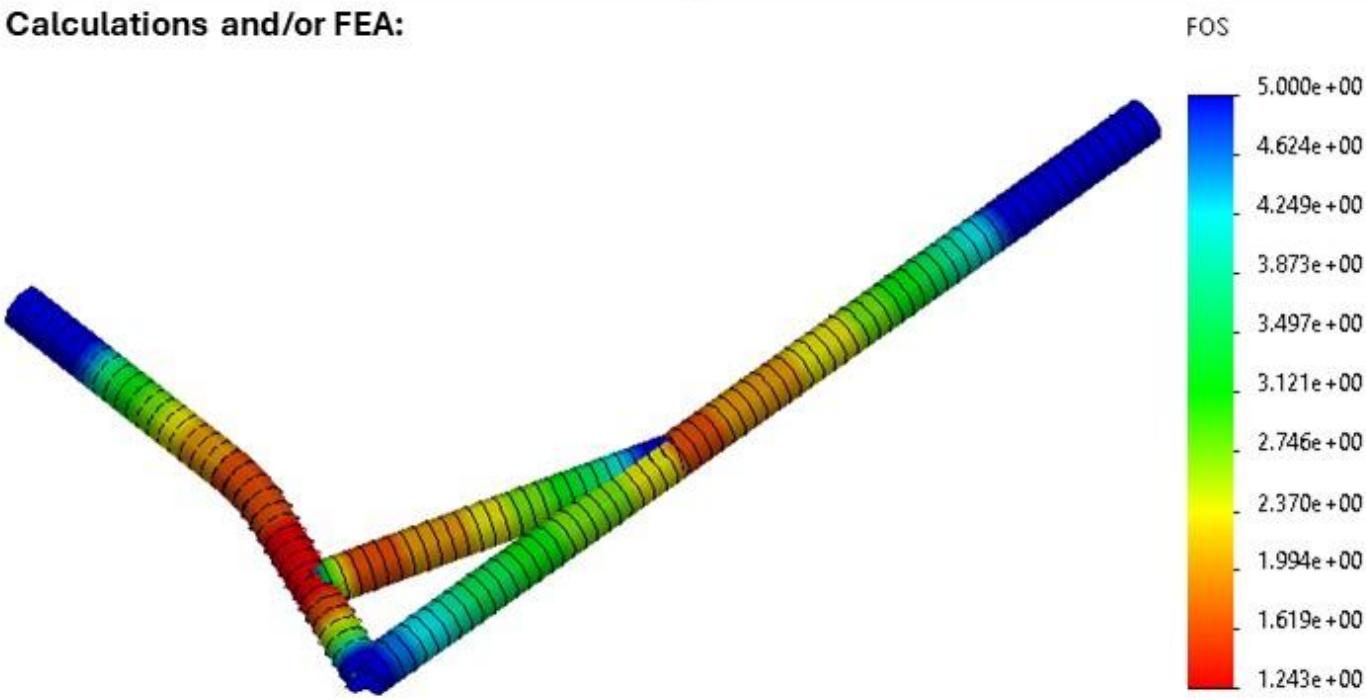

Figure 52: Maximum force of shock on upper control arm

Failure Condition: 1600lbf load at shock mount (side to side beam)

Justification: The shock is not equidistant between the chassis and upright.

Load Diagram:

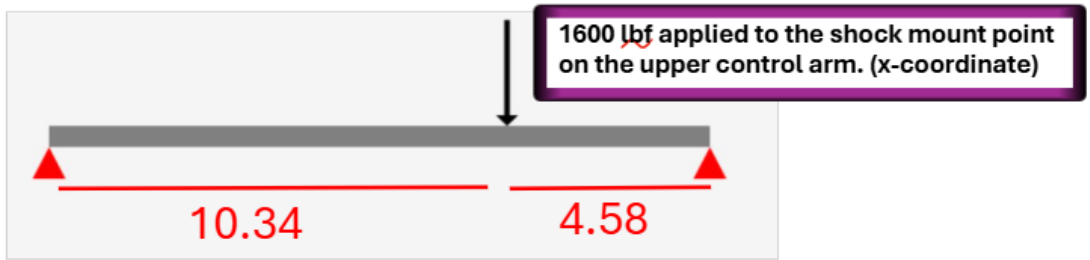

Constraints:

FOS:

Equations (If Applicable):

Confidence Level & Explanation: Medium,

Our single dimension beam approximation shows that the rear structural member from peak shock force

Calculations and/or FEA:

Reactions

Location: 0 (in), Force Reaction = -491.1528 (lb)

Location: 14.92 (in), Force Reaction = -1108.8472 (lb)

Shear Diagram

(Max +ve)Shear Load (lb): 491.153,

Location (in): 0.000, 10.340

(Max -ve)Shear Load (lb): -1108.847,

Moment Diagram

(Max +ve)Moment Load (lb-in): 5078.520,

Location (in): 10.340

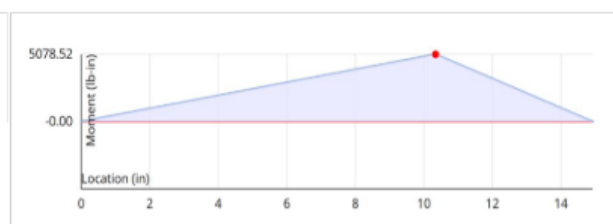

Figure 53: Shock load distribution on middle A-arm member

Failure Condition: 1600lbf load at shock mount (front to back beam)

Justification: With the mounting point of the shock being closer to the rear of the A-arm instead of the front, the load will be distributed unequally.

Load Diagram:

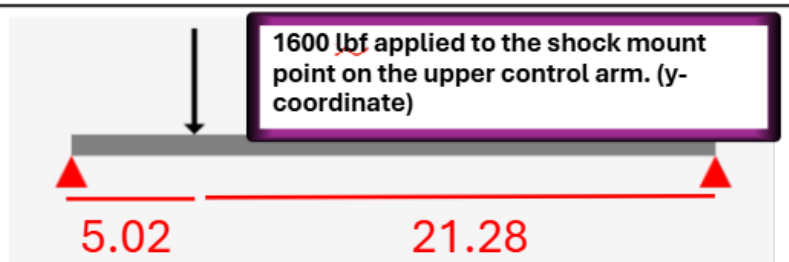

Constraints:

FOS:

Equations (If Applicable):

Confidence Level & Explanation: Medium, Our single dimension beam approximation shows that the rear structural member will take a majority of the load from peak shock force

Calculations and/or FEA:

Reactions

Location: 0 (in), Force Reaction = -1294.6008 (lb)

Location: 26.3 (in), Force Reaction = -305.3992 (lb)

Shear Diagram

(Max +ve)Shear Load (lb): 1294.60

Location (in): 0.000, 5.020

(Max -ve)Shear Load (lb): -305.399,

Location (in): 5.020, 26.300

Moment Diagram

(Max +ve)Moment Load (lb-in): 6498.896,

Location (in): 5.020

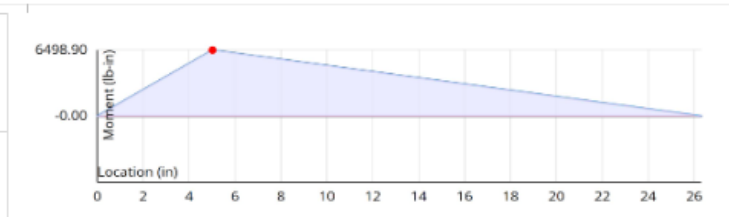

Figure 54: Shock load distribution on A-arm side member

2.2.6. Rear Toe Rod

2.2.6.1. Discussion of design Reasoning

The toe rod is 6063-T6 aluminum with 0.63'' OD and 0.13 wall thickness. The length of the tubing member is 13''. The ideal distance between the center of the two Heim's for optimized toe change throughout travel is 15.25''. The assembly has one right hand threaded locknut and Heim and one lefthand locknut and Heim to allow for easy length adjustability. The ideal chassis pickup point for the toe arm is 3.3'' up from the center of the lowest chassis member.

2.2.6.2. Rear Toe Rod CAD Design

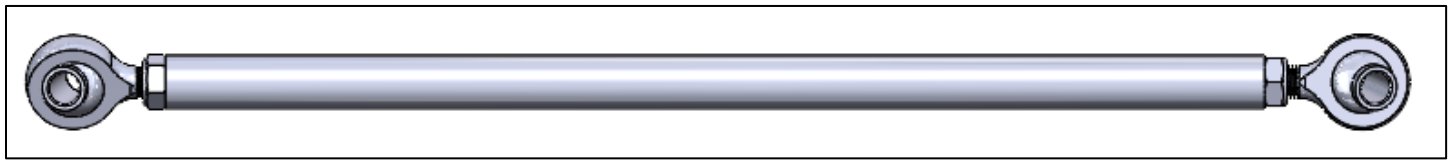

Figure 55: Rear tie rod

2.2.6.3. Rear Toe Rod BOM

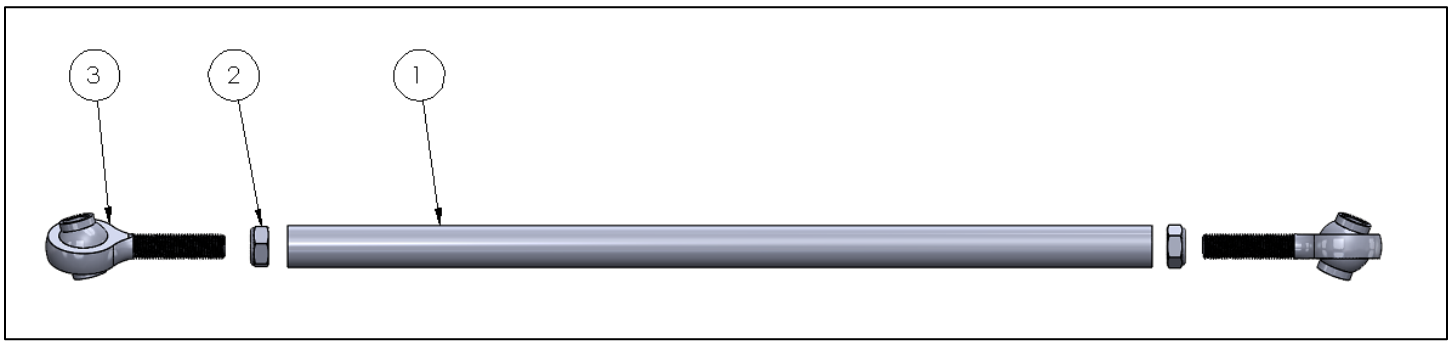

Figure 55: Rear tie rod exploded view

BOM Part #	Description	Qty:	Source (Hyperlink to Part)	Cost:	Weight/1Pc [lbs]
1	Toe arm rod	1			0.25
2	Locknuts (1 RH, 1 LH)	2	McMaster	12.94 (50 pack)	
3	3/8"-24 Rod End (1 RH, 1 LH)	2	McMaster	21.55	
Total				56.04	0.25

Table 14: Rear Tie Rod BOM

2.2.6.4. Rear Toe Rod Analysis

Failure Condition: Side impact or collision from an opposing vehicle, causing buckling in the toe rod.

Justification: Aluminum 6061 15'' long tie rod experiencing side impact of 2000lbf

Load Diagram:

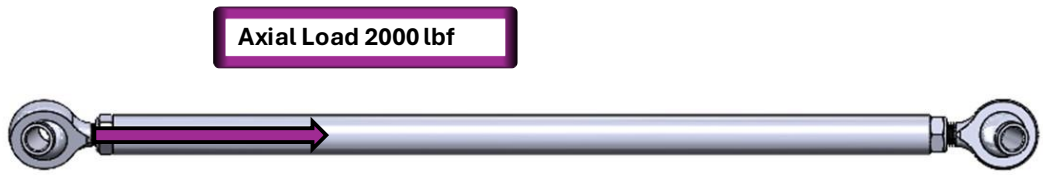

Constraints:

FOS: 1.991

Equations:

$$I = \frac{\pi}{64}\left(D_{\text{outer}}^4 - D_{\text{inner}}^4\right)$$

$$r = \sqrt{\frac{I}{A}}$$

$$R_s = \frac{L}{r}$$

$$R_{\text{trans}} = \sqrt{\frac{2\pi^2 E}{K^2 S_y}}$$

$$\sigma_{\text{buckling}} = \frac{\pi^2 E}{(K R_s)^2}$$

$$F_{\text{buckling}} = \sigma_{\text{buckling}} A$$

$$\text{FOS} = \frac{F_{\text{buckling}}}{F_{\text{max}}}$$

Confidence Level & Explanation:
Medium: The tie rod material and expected load values areknown from previous years

Calculations and/or FEA:

$$E = 1.001 \times 10^7 \ [\text{lbf/in}^2]$$
$$S_y = 19{,}943 \ [\text{lbf/in}^2]$$
$$\sigma_{\text{buckling}} = 19{,}499 \ [\text{lbf/in}^2]$$
$$F_{\text{buckling}} = \boxed{3{,}982 \ [\text{lbf}]}$$
$$F_{\text{max}} = 2{,}000 \ [\text{lbf}]$$
$$\text{FOS} = \boxed{1.991}$$

Figure 56: Side impact on rear tie rod

2.2.7. Rear Hub/Upright Assembly

2.2.7.1. Discussion of Design Reasoning – Rear Hub

The rear upright was designed with a similar geometry as the front upright. The upright is 8'' tall and 5.75'' wide, fitting within the constraints of the wheel hub. The upper bracket mount point is 4'' up from the hub and the lower bracket mount point is 3'' down from the hub.

2.2.7.2. Rear Hub CAD Design:

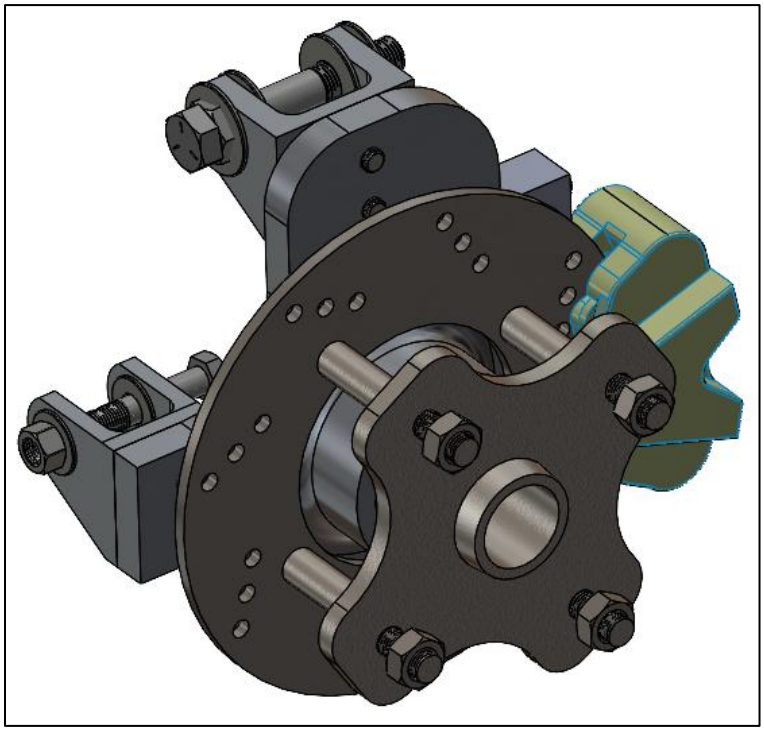

Figure 57: Rear upright Assembly

2.2.7.3. Rear Hub BOM:

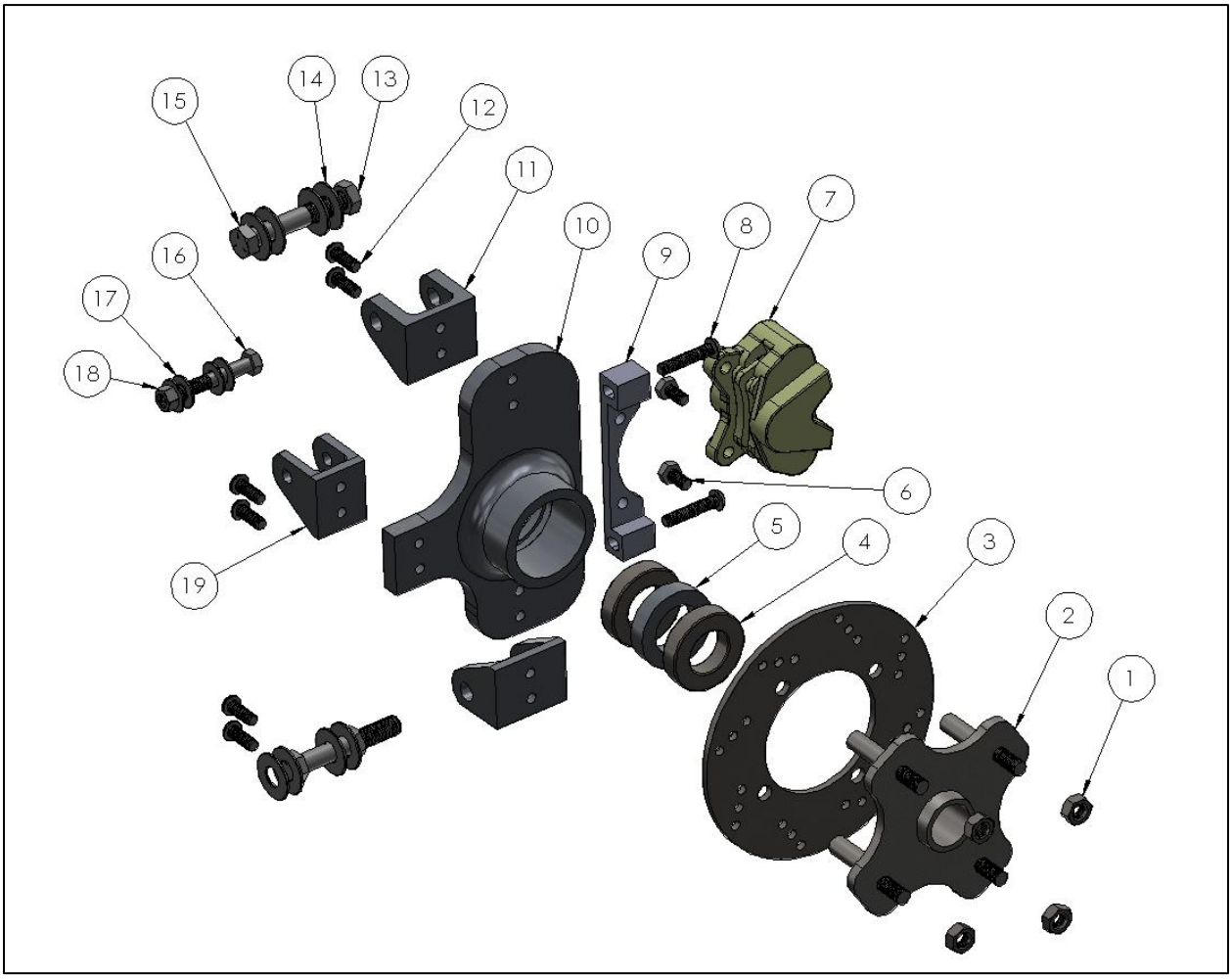

Figure 58: Rear upright exploded view

BOM Part #	Description	Qty:	Source (Hyperlink to Part)	Cost:	Weight/1Pc [lbs]
1	10mm 1.25 lung nuts	4	McMaster-Carr	$14.51 per 50	
2	Brake hub	1	(Stock) In Hand	N/A	4.4
3	Brake rotor	1	(Stock) In Hand	N/A	
4	Bearing	2	qualitybearingsonline.com	$23.73	0.26
5	Bearing Spacer	1	(Stock) McMaster-Carr	$37.04 per 4	0.37
6	M8 x 1.25 mm, 20 mm long for brake calipers	2	In Hand	N/A	
7	Willwood Brake	1	In Hand	N/A	
8	M8 x 1.25 mm Thread, 35 mm long for brake bracket	2	In Hand	N/A	
9	Brake Bracket	1	(Stock) McMaster-Carr	$12.05	0.15
10	Upright	1	(Stock) In Hand	N/A	1.64
11	Control Arm Bracket	2	(Stock) McMaster-Carr	$36.67	0.23
12	1/4-20 upright bolt	4	McMaster-Carr	$11.65	

				for 50	
13	½-20 low profile lock nut	2	McMaster-Carr	$11.53 per 50	
14	½ washer	8	McMaster-Carr	$7.12 per 10	
15	½-20 rod end Bolt (3’’)	2	McMaster-Carr	$14.12 per 50	
16	3/8-24 low profile lock nut	1	McMaster-Carr	$12.94 per 50	
17	3/8 washer	4	McMaster-Carr	$6.15 per 100	
18	3/8-24 upright bolt	4	McMaster-Carr	$12.36 for 10	
19	Toe Arm Bracket	1	(Stock) McMaster-Carr	$36.67	0.16
Total				$192.45	7.2

Table 15: Rear Upright BOM

2.2.7.4. Rear Hub Critical Parts – Model Views and Discussion:

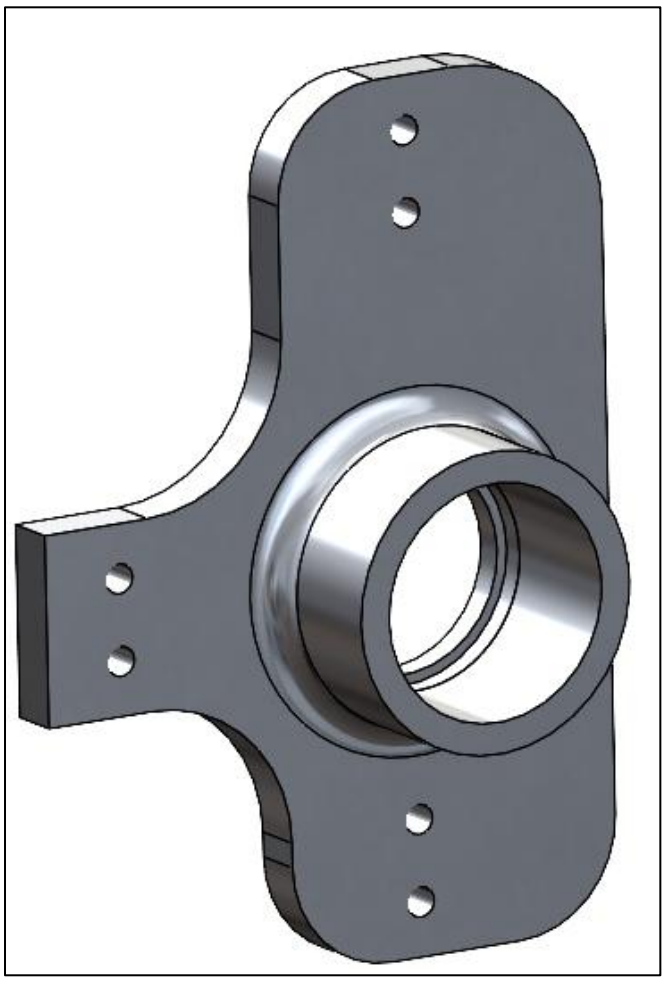

Figure 59: Rear Right Upright

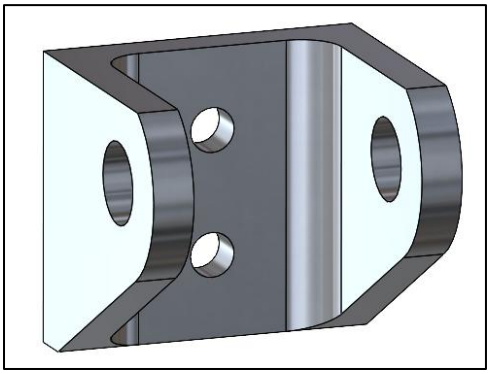

Figure 60: Control Arm Bracket

The control arm and toe arm brackets have a thickness on all faces of 0.25’’. Supporting calculations for bolt tear out and bracket bending are in section 2.2.7.6.

2.2.7.5. Rear Hub Analysis

Failure Condition: Frontal impact on the outermost point of the front of 1 front tire stopping the vehicle.
Material: 6061-T6 Aluminum upright (0.5" thick) and brackets (0.25" thick), Heim ball joints are 4130 Chromoly only input for boundary condition simulations

Justification:
This is the upright experiencing approximately a 2g load from hitting an obstacle head on.

Load Diagram:

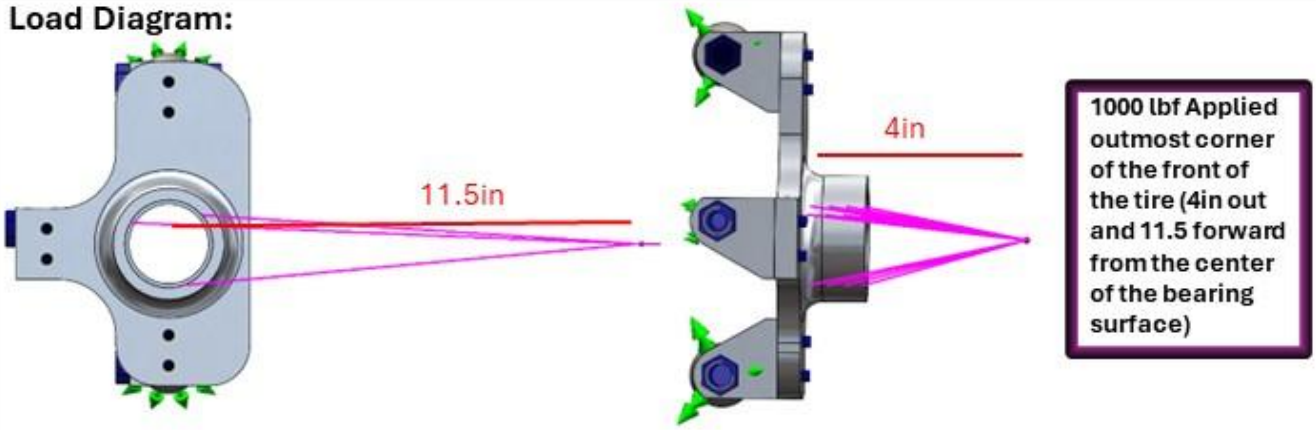

Constraints:

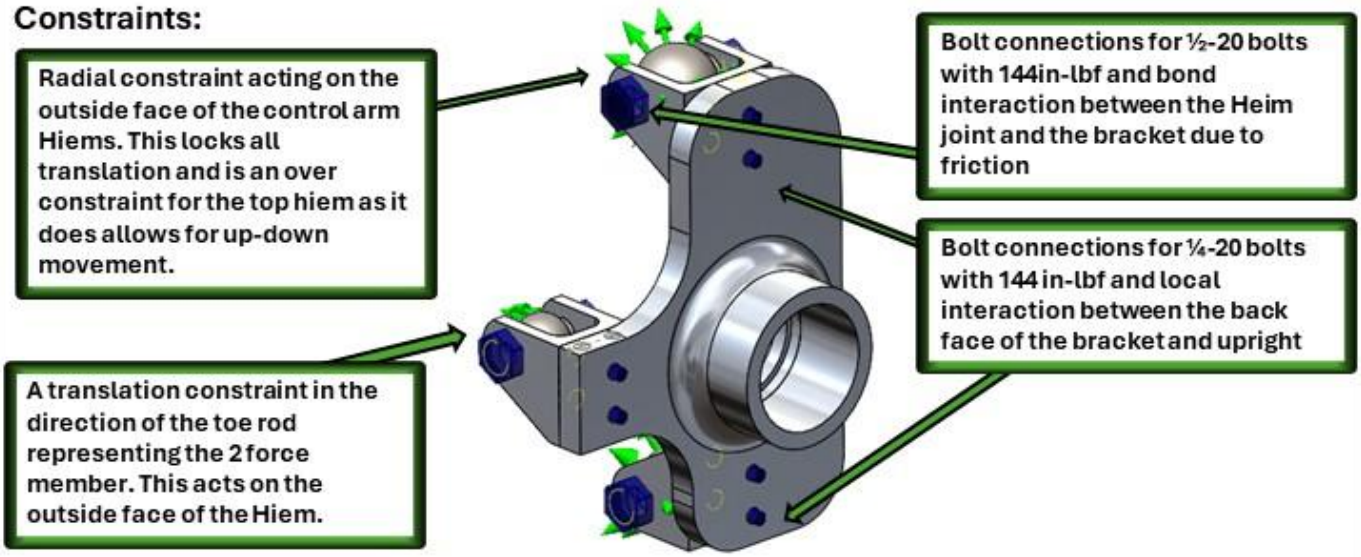

FOS: 0.52

Equations (If Applicable):

Confidence Level & Explanation: Low: Numbers are gathered from previous FEA but lack supporting test data for loading force. Heims are over constrained so results are not completely accurate. Failure occurs at brackets and results were disproven with tear out, bearing, and shear stress hand calculations.

Figure 61: Rear upright FEA

Calculations and/or FEA:

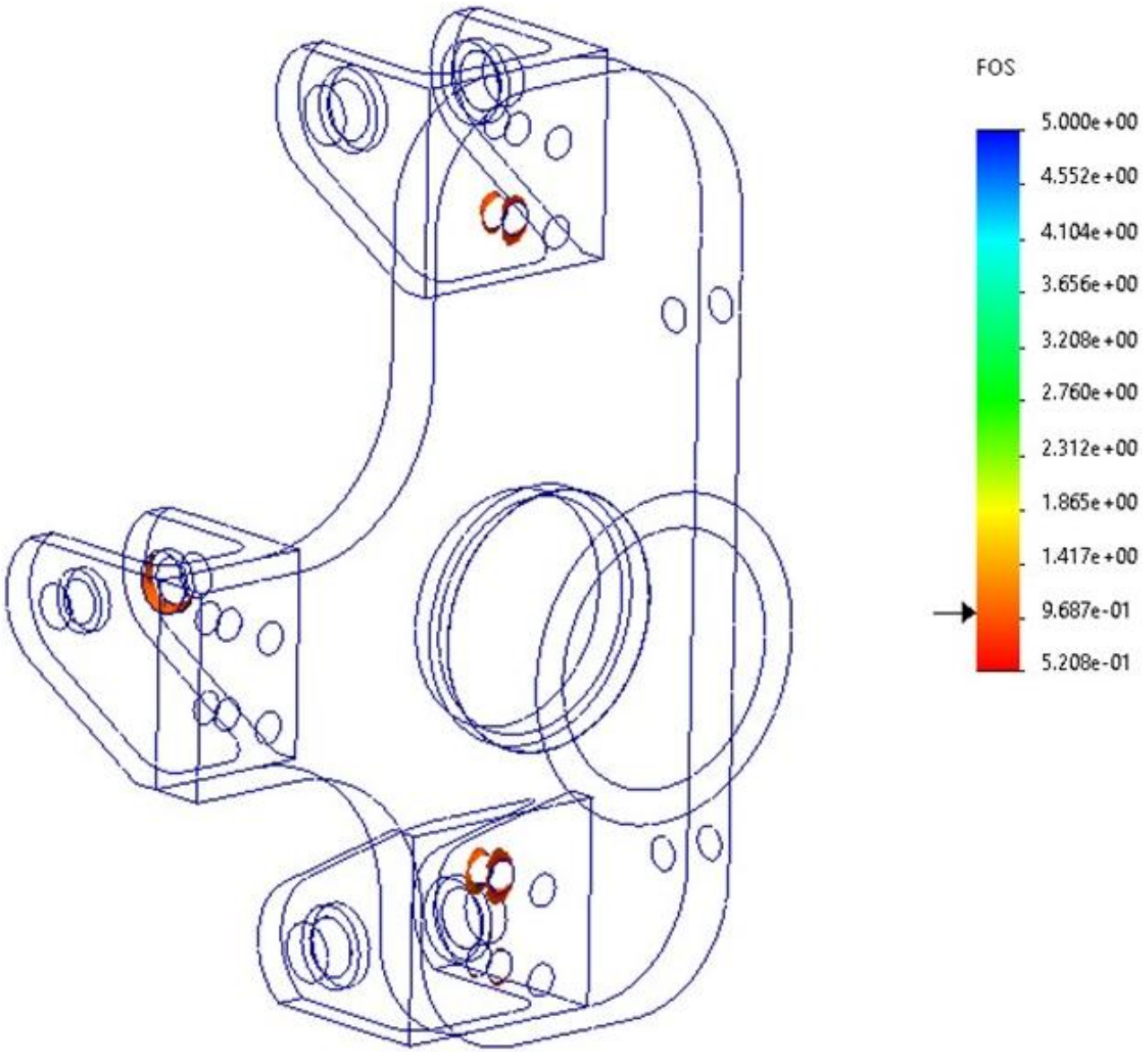

Figure 62: Results from Figure 61

Failure Condition: Landing a jump on the outside bottom of one wheel under approximately a 2G load.
Material: 6061-T6 Aluminum upright (0.5" thick) and brackets (0.25" thick), Heim ball joints are 4130 Chromoly only input for boundary condition simulations

Justification: This is a worse case loading if the vehicle where to landed a jump on one wheel of the front wheels.

Load Diagram:

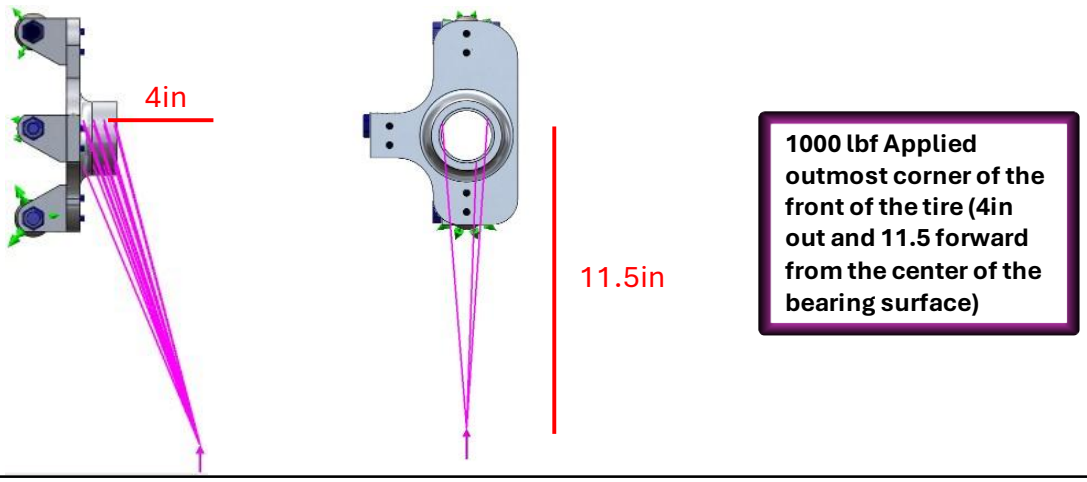

Constraints:

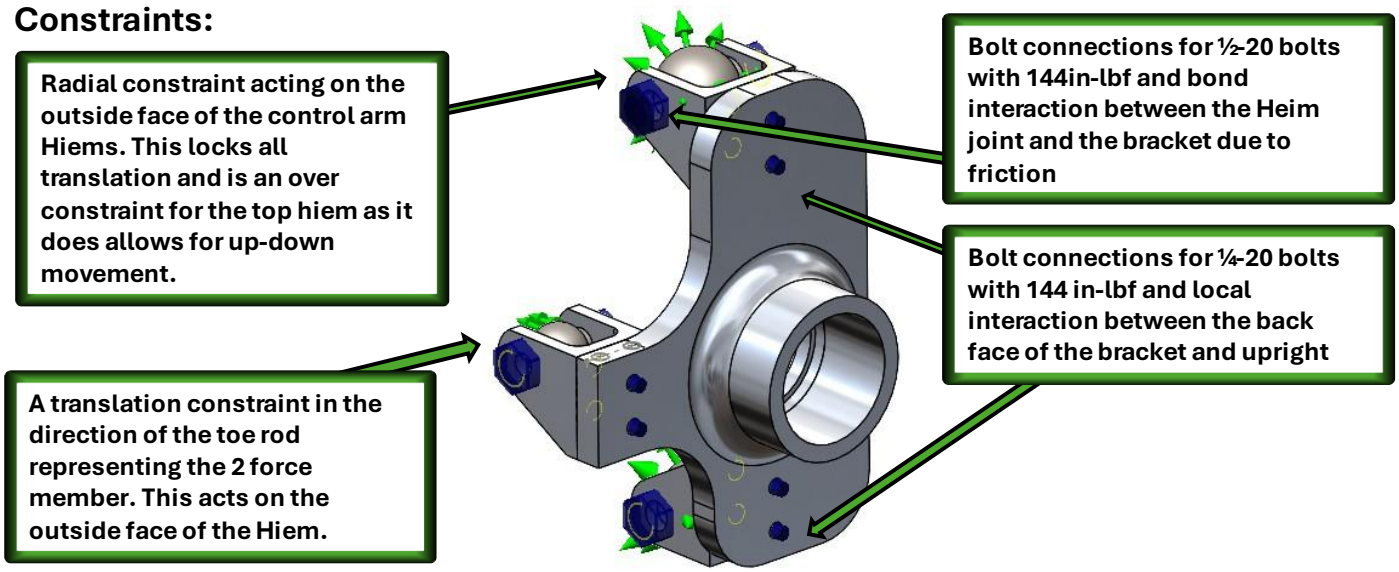

FOS: 1.0

Equations (If Applicable):

Confidence Level & Explanation:
Low: Loads are not well known. Due to SolidWorks limitations the model is over defined in the top Hiem explained above.

Figure 63: Upward loading on rear upright

Calculations and/or FEA:

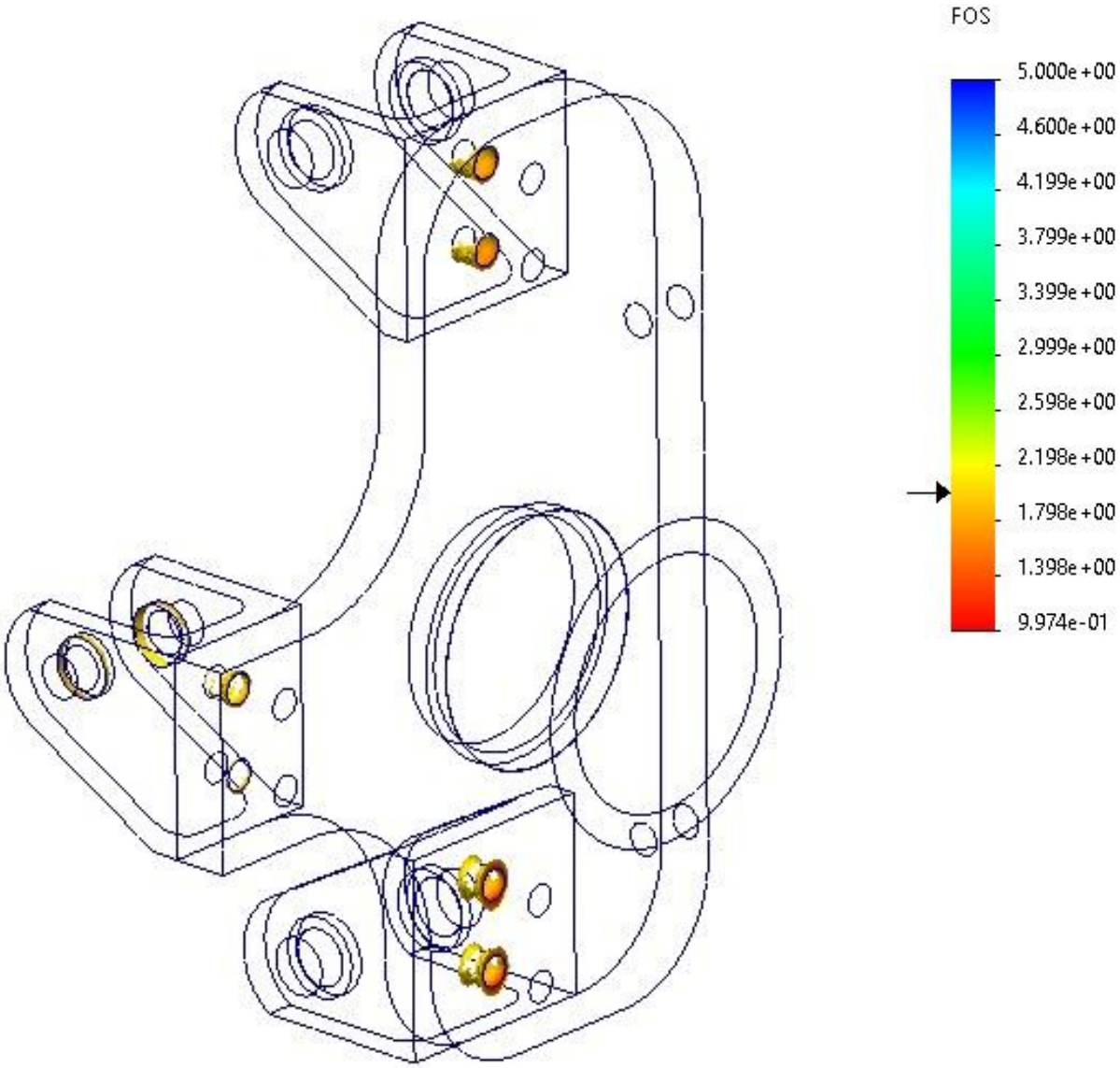

Figure 64: Results from Figure 63

2.2.7.6 Rear Bracket Analysis

Failure Condition: bending of the bracket due to a frontail impact of 3000lbf

Justification: Last year experience serial crashes and cloisons therefore calculating worse-case scenario of a side impact which would create a moment and attempt to pull the bolt out of the bracket

Load Diagram:

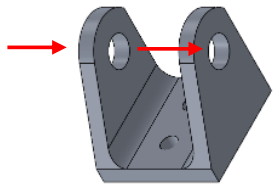

3000 lbf split between top and bottom brackets resulting in 1500lbf per bracket

Constraints:

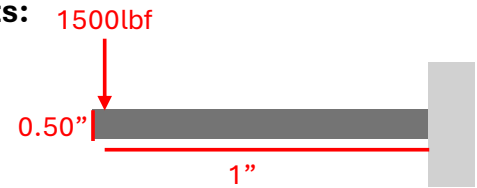

Simplified to a combine thickness of both bracket arms with worst case distance to edge.

FOS:

Equations (If Applicable):

$$I = \frac{bh^3}{12}$$

$$\sigma = \frac{Mc}{I}$$

$$FS_{\text{bend}} = \frac{\sigma_{\text{allow}}}{\sigma}$$

Confidence Level & Explanation: Low: Loads are not well known for this loading case. This loading case is backed out from a 20mph impulse lasting 0.15s with a car and rider combine weight of 700lbf

Calculations and/or FEA:

```
--- Aluminum Bracket Calculations ---
Moment of Inertia (I):        0.018229 in^4
Applied Moment:               1500.00 lb·in
Bending Stress:               20571.43 psi
Safety Factor (Bending):      1.70
```

Figure 65: Rear Upright Bracket Bending Calculations

Failure Condition: bolt tear out due to side impact of the wheel creating a pulling on the bracket of 2000lbf

Justification: Last year experience serial crashes and cloisons therefore calculating worse-case scenario of a side impact which would create a moment and attempt to pull the bolt out of the bracket

Load Diagram:

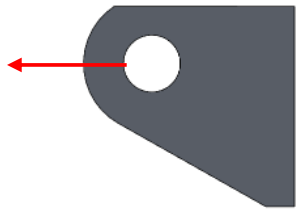

1200lbf applied to the Heim bolt which translate to a 1600lbf of the shock

Constraints:

Simplified to a combine thickness of both bracket arms with worst case distance to edge

FOS:

Equations (If Applicable):

$$F_{\text{bracket}} = F_{\text{shock}} \frac{L_{\text{shock}}}{L_{\text{arm}}}$$

$$\sigma = \frac{F_{\text{bracket}}}{A}$$

$$FS_{\text{tear}} = \frac{\sigma_{allow}}{\sigma}$$

Confidence Level & Explanation: Low: Loads are not well known for this loading case.

Calculations and/or FEA:

```
--- Aluminum Bracket Calculations ---
Tear-Out Area:                0.1250 in^2
Force on Bracket:             1166.01 lb
Tear-Out Stress:              9328.10 psi
Safety Factor (Tear-Out):     3.75
```

Figure 66: Rear Upright Heim Bolt Tear out

Failure Condition: bolt tear out due to side impact of the wheel creating a pulling on the bracket of 2000lbf

Justification: Last year experience serial crashes and cloisons therefore calculating worse-case scenario of a side impact which would create a moment and attempt to pull the bolt out of the bracket

Load Diagram:

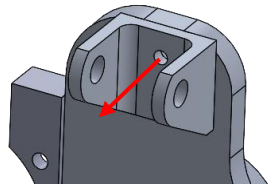

2000lbf applied to the Heim bolt which translate to roughly a 1250lbf impact to the bottom side of the tire

Constraints:

Simplified to a combine thickness of both bracket arms with worst case distance to edge

FOS:

Equations (If Applicable):

$$F_{\text{wheel}} = 1500\,\frac{L_{bt}}{L_{bw}}$$

$$\sigma = \frac{F}{A}$$

$$FS_{\text{tear}} = \frac{\sigma_{allow}}{\sigma}$$

Confidence Level & Explanation: Low: Loads are not well known for this loading case. Pervious years have done

Calculations and/or FEA:

```
--- Aluminum Bracket Calculations ---
Tear-Out Area:                0.5250 in^2
Force per Bracket Side:       2000.00 lb
Force on Bottom Wheel:       1235.29 lb
Tear-Out Stress:              3809.52 psi
Safety Factor (Tear-Out):     9.19
```

Figure 67: Rear Upright Bracket Thread Tear Out Calculations

3. Controls

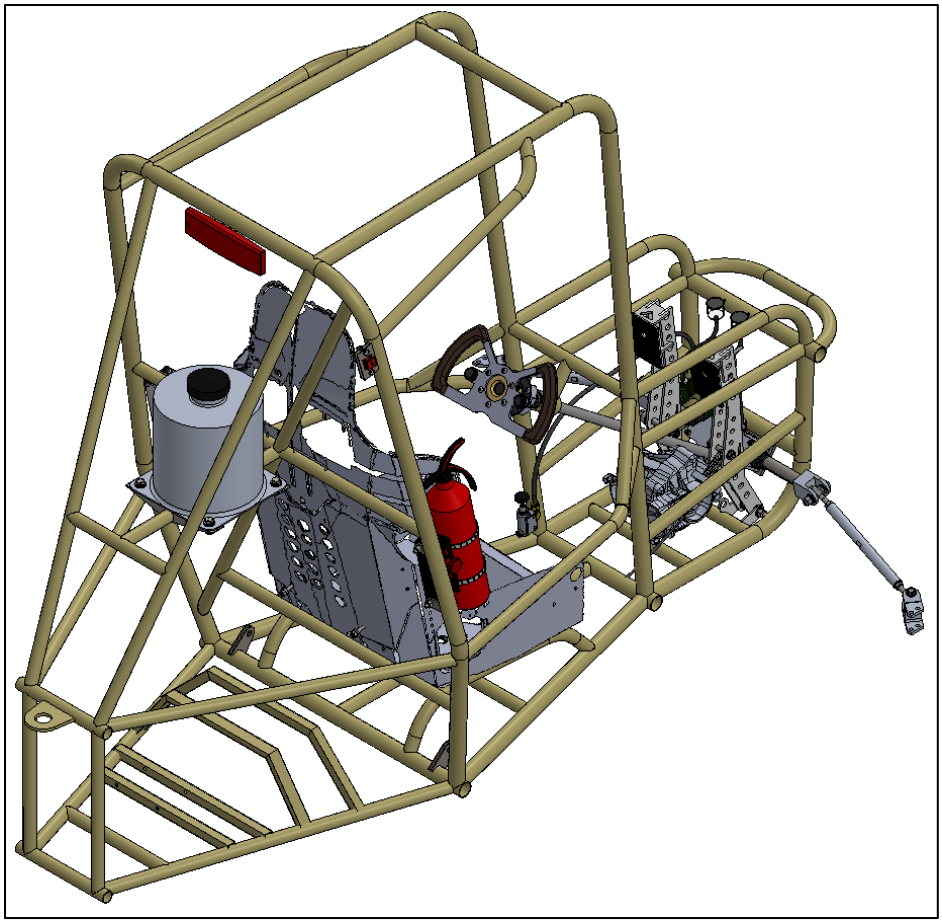

Figure 68: Controls Assembly Rear Isometric View

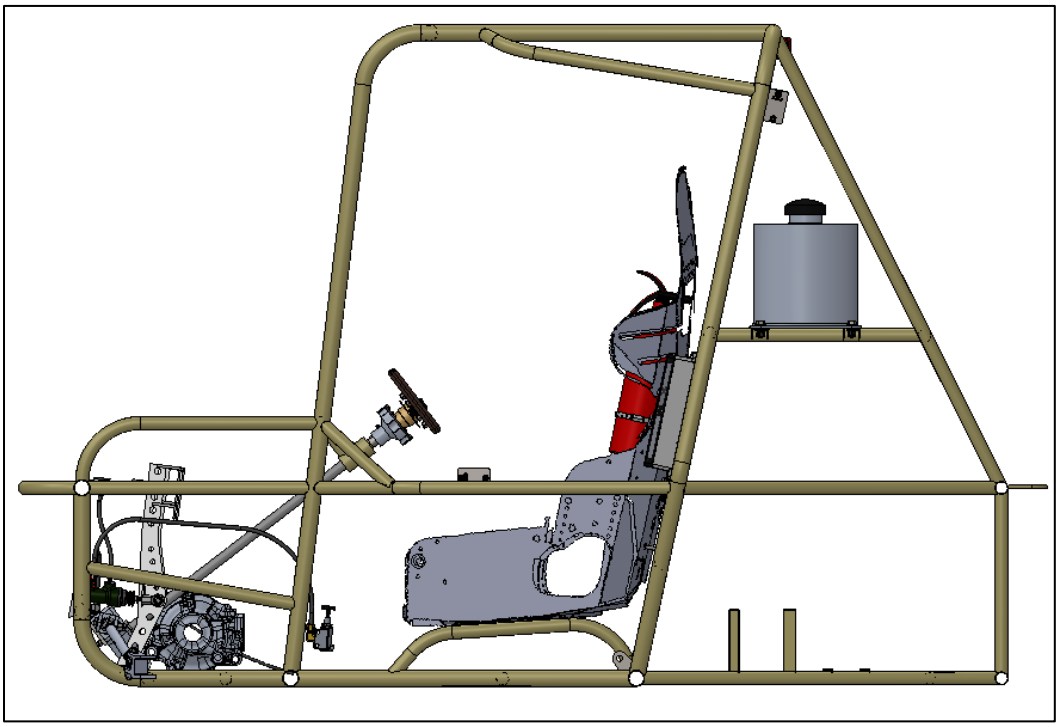

Figure 69: Controls Assembly Side View

3.1. System Level Breakdown

The controls system of the car incorporates seat mounting, seat, steering, and braking and throttle control. The full control assembly in Figure 69 & Figure 68, above, weighs approximately 42lbs, excluding only about 10% of the overall hardware, and the new cost to us this year will be roughly $320. Controls prioritized improving driver experience and decreasing complexity. We were able to improve pedal feel, save weight and decrease complexity in the steering assembly by getting rid of the U-joint in the steering column, and make the differential switches more accessible by mounting them to the steering wheel. Also, with redesigned seat mounting, we were able to mount our 18º seat-back seat at an angle to make the back match our 12º firewall angle.

3.2. Part Level Breakdown

3.2.1. Steering Assembly

3.2.1.1. Discussion of Design Reasoning – Steering Assembly:

Our goals for the steering assembly this year were to reduce weight and complexity, increase steering angle, and maintain driver comfort and ease. After testing in the beginning of the year, we decided that the steering felt comfortable, and responsive. Due to our positive takeaways from testing, we decided to reuse the steering rack from last year, and a similar steering wheel design. The largest difference in the steering assembly this year, compared to last year's, is that we were able to eliminate the U-joint in our steering column. We achieved this by mounting the steering assembly as far forwards as it can possibly go in the chassis which lets us angle the entire assembly back towards the driver, while still providing ample clearance above the front differential. Eliminating the U-joint saves roughly 2lbs and makes the assembling process easier. It should also have the added benefit of reducing slight sinusoidal steering output to a linear input, caused by the unphased single U-joint. Along with the elimination of the U-Joint, we also decided to target weight savings by using a hollow steering column, opposed to last year's solid column. This change results in another pound saved from the assembly. Last year's steering assembly was roughly 17 lbs while ours is approximately 13.2 lbs. The last notable change in the steering assembly is the component that attaches the tie-rod to the suspension uprights. Maintaining steering throughout the full range of suspension travel proved to be a difficult technical challenge; the articulation of the suspension, combined with steering angle, puts the Heim joint on the tie-rods at extreme angles and caused them to bind with the mounting bracket. To avoid this issue, we designed a bracket to mount to the upright that pre-angles the Heim joint to account for the uneven amounts of bump and droop in suspension (see Figures 75 & 76 below). The bracket is also spaced wide enough that heim can fully articulate through the full range of suspension travel without binding on the edge of the bracket (see Figure 75 & Figure 76 below). The bracket is also angled away from the upright to ensure that through the full steering range, and suspension travel, the wheel can never over-center (see Figure 74 below). The steering was also designed to have minimal bump steer. Figure 70 below shows the toe change through suspension travel as calculated via SusProg. The maximum toe in in full droop is 1.95˚ and the maximum toe out in bump is .2˚, with a static toe-in angle of 1.74˚.

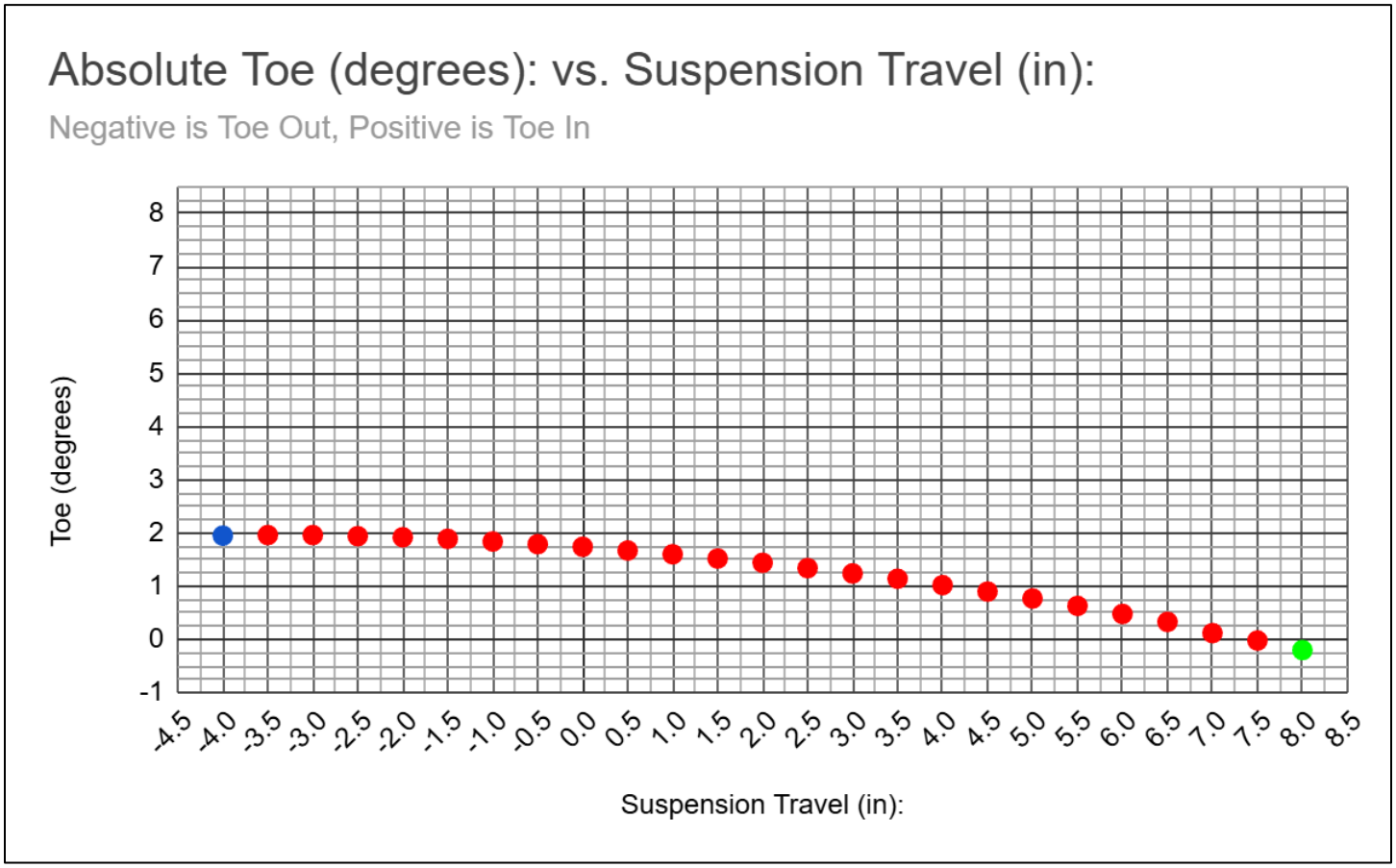

Figure 70: Absolute Toe vs. Suspension Travel

3.2.1.2. <u>Steering Assembly Critical Rules:</u>

- B.8.2 – Cockpit Egress
- B.8.7.1 – Linkages

Steering is largely unregulated in the Baja SAE 2026 Rules.

3.2.1.3. Steering Assembly CAD Design:

Figure 71: Isometric View of Steering Assembly

3.2.1.4. Steering Assembly BOM:

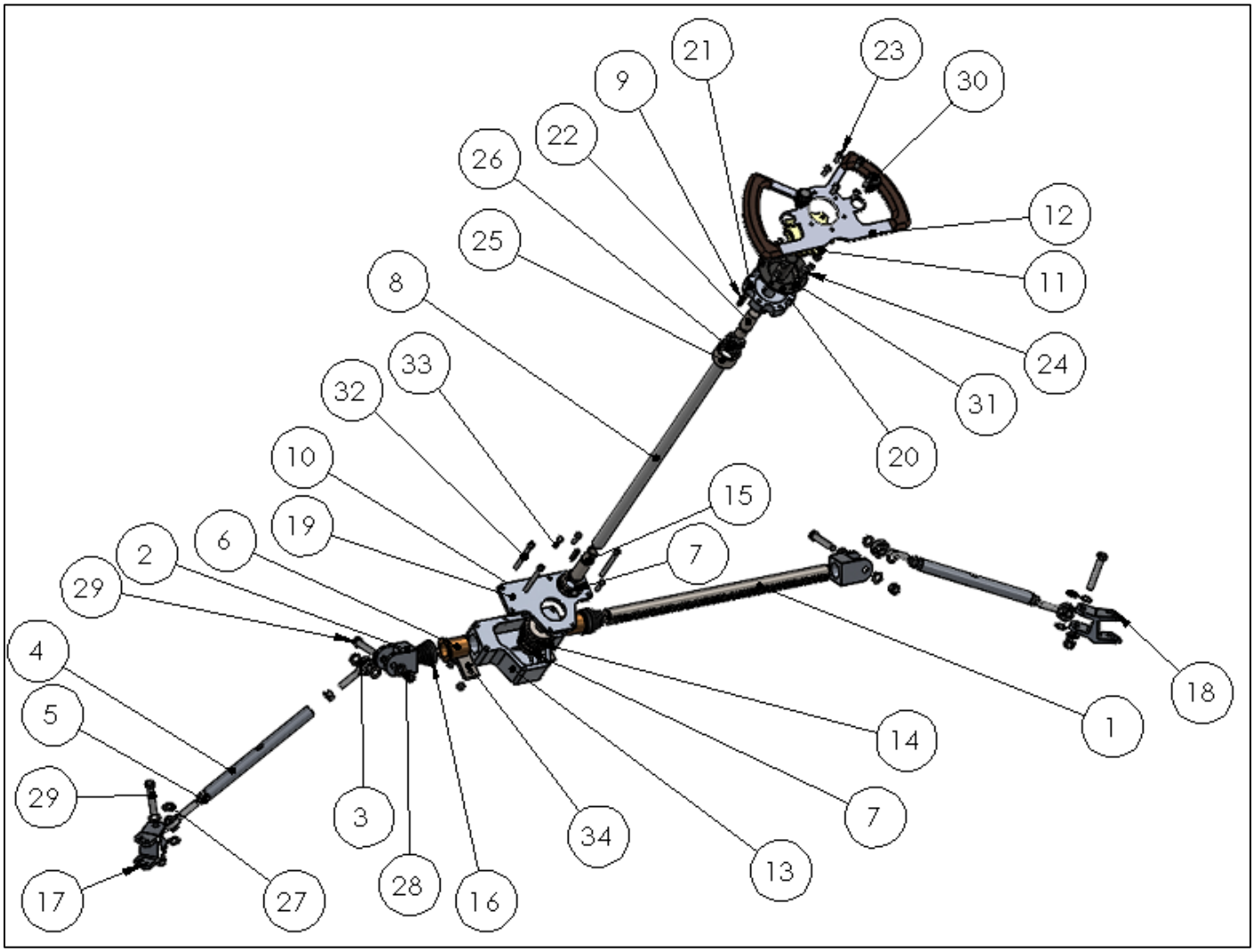

Figure 72: Steering Assembly Exploded View

BOM Part #	Description	Qty:	Source (Hyperlink to Part)	Cost:	Weight/1Pc [lbs]
1	Steering Rack	1	Stock On Hand	N/A	
2	Steering Rack Knuckle	2	Stock On Hand	N/A	
3	Super Swivel Ball Joint	4	McMaster-Carr	$13.74	
4	Tie Rod	2	Stock On Hand	N/A	
5	Steel Serrated Flange Locknut	4	McMaster-Carr	$15.87 per 100	
6	Embedded Sleeve Bearing	2	McMaster-Carr	$11.60	
7	¾” Ball Bearing	2	McMaster-Carr	$27.17	
8	Steering Column	1	Stock On Hand	0	
9	3/16” Key	2	Stock On Hand	0	
10	3/8” x ¼” – 20 Set Screw	2	McMaster-Carr	$11.74 per 50	
11	Steering Wheel Quick Release	1	Stock On Hand	N/A	

12	Steering wheel	1	Stock On Hand	N/A	~13.18 lbs (Measured in SolidWorks)
13	Steering Rack Housing	1	Stock On Hand	N/A	
14	Pinion Gear	1	Stock On Hand	N/A	
15	Steering Rod Insert	1	Stock On Hand	N/A	
16	Steering Rack Boot	2	Stock On Hand	N/A	
17	Tie Rod Upright Adapter	1	Stock On Hand	N/A	
18	Tie Rod Upright Adapter	1	Stock On Hand	N/A	
19	Steering Rack Cover	1	Stock On Hand	N/A	
20	Quick Release Coupler	1	Stock On Hand	N/A	
21	Steering Column Adapter	1	Stock On Hand	N/A	
22	Steering Rod Inserts	1	Stock On Hand	N/A	
23	¾” x ¼” – 20 Stainless Steel Button Head Screw	6	McMaster-Carr	8.31 per 50	
24	¼”-20 Nylon Lock Nut	10	McMaster-Carr	4.76 per 25	
25	Steering Column Support Tube	1	Stock On Hand	N/A	
26	¾” Swivel Joint	1	McMaster-Carr	$61.18	
27	18-8 Stainless Steel Washer	16	McMaster-Carr	$9.69 per 50	
28	3/8” -24 Nylon Lock Nut	4	McMaster-Carr	$4.68 per 20	
29	Grade 8 2.5” x 3/8” -24 Bolt	4	McMaster-Carr	$6.10	
30	Rocker Switch	2	McMaster-Carr	$7.83	
31	¾” x ¼” – 20 Stainless Steel Button Head Screw	6	McMaster-Carr	$8.31 per 50	
32	2.75” x ¼” – 20 Socket Head Screw	4	McMaster-Carr	$22.49 per 25	
33	¾” x ¼” – 20 Socket Head Screw	4	McMaster-Carr	11.38 per 50	
34	Steering Rack Mounting Plate	1	On Stock	N/A	
Total				$224.85	

Table 16: Steering Assembly BOM

3.2.1.5. Steering Assembly Critical Parts – Model Views and Discussion:

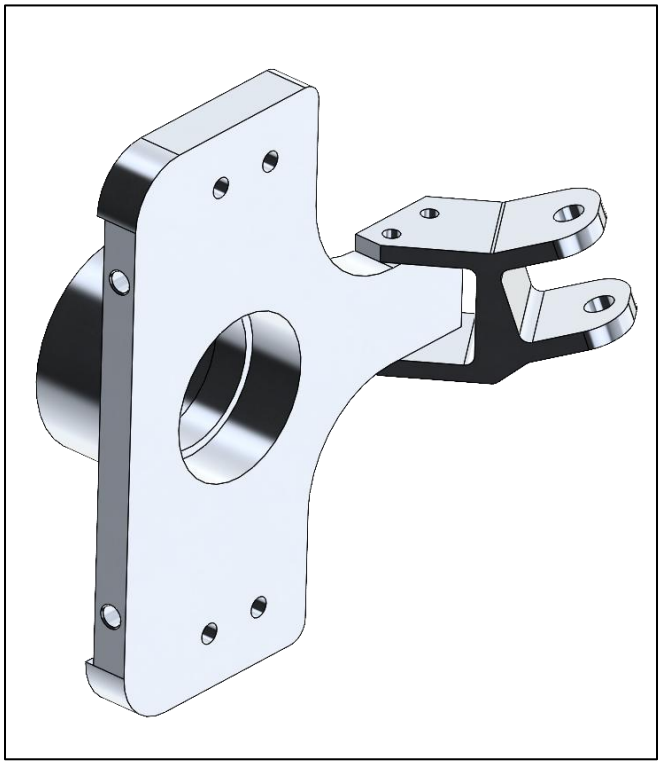

Figure 73: Upright Tie-Rod Mounting Bracket on Suspension Upright

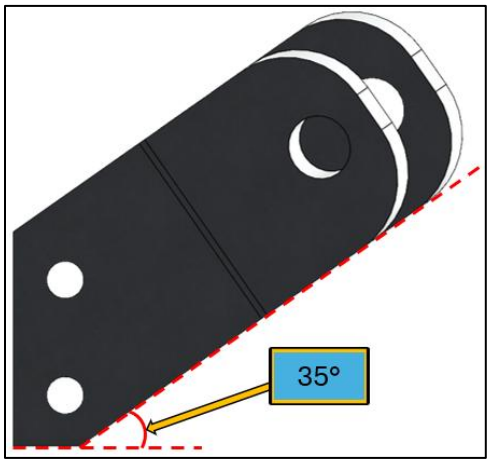

Figure 74: Upright Tie-Rod Mounting Bracket Top View

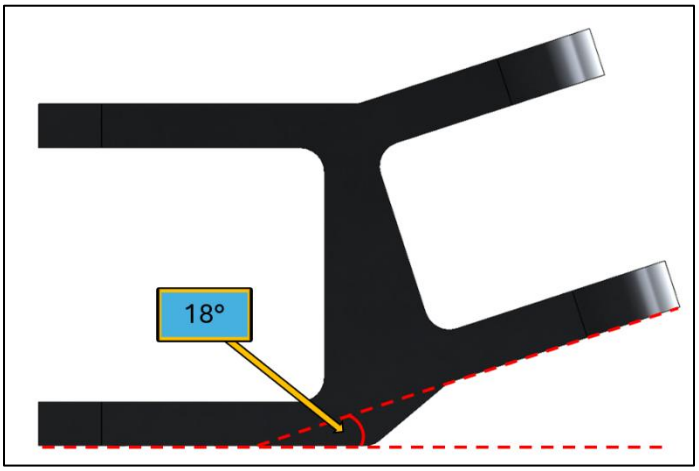

Figure 77: Upright Tie-Rod Mounting Bracket Side View

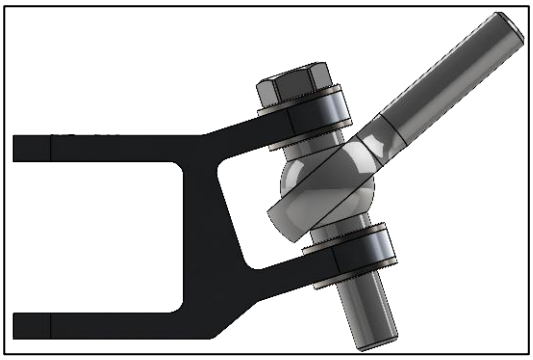

Figure 76: Side View of Tie-Rod Heim in Full Droop Angle

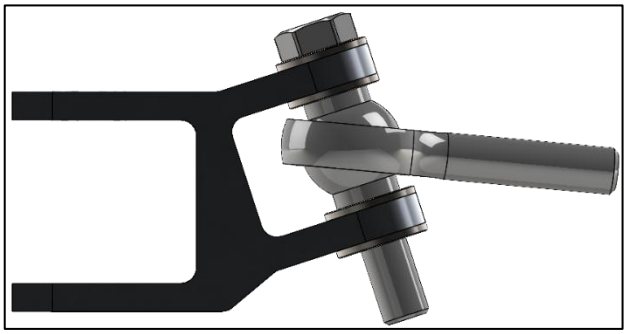

Figure 75: Side View of Tie-Rod Heim in Full Bump Angle

3.2.1.6. Steering Assembly Analysis:

The following figures (see below) demonstrate the load diagrams, constraints, and calculations for key components of the steering assembly. As suggested from the calculations, the steering shaft has a FOS of 1.88 from torsion, the tie rod has a FOS of 1.15 from buckling, and the steering rod insert has a FOS of 10.84 from bending.

Failure Condition: The driver hits an obstacle or an obstruction, and the steering wheel jerks out of the driver's hands.

Justification: The applied torque value of 100 Nm comes from a study conducted by an FSAE Chief Design Judge to evaluate minimum driver applied forces for SAE competition. Therefore, it is reasonable to use this as a baseline for the design of our steering assembly.

Load Diagram:

Constraints:

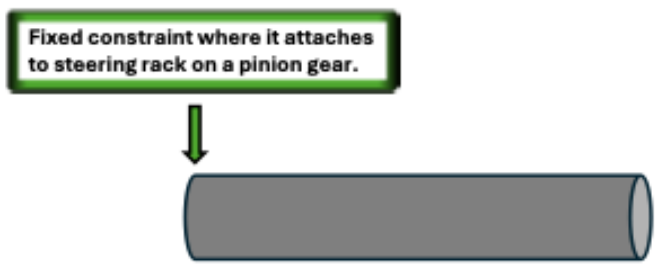

FOS: 1.88

Equations (If Applicable): See Below

Confidence Level & Explanation: Medium -High since applied torque is from FSAE Study. Steering column material properties are known.

Calculations and/or FEA:

Torque (in lbf)	applied torque	885.0745792
OD (in)	outer diameter	0.75
Thickness (in)	wall thickness	0.035
Shear Strength (ksi)	4130 tube	62
ID (in)	OD - 2*t	0.68
c (in)	OD/2	0.375
J (in^4)	polar moment	0.010071994
Shear Stress (ksi)	T*c/(J/1000)	32.953054
Modulus of Rigidity (GPa)	Found on MatWeb	80
Length (in)	Length of shaft from CAD	25
Angle of Twist (degrees)	TL/GJ	10.84815893
FOS	Shear strength/shear stress	1.881464462

Figure 78: Steering Shaft Torsion Calculations

Failure Condition: Side impact or collision from an opposing vehicle, causing buckling in the tie rod.

Justification: The calculated axial load of 5,000 lbf is significantly higher than a realistic side impact load of 2,000 lbf at competition. Therefore, with a FOS of 1.15 with an axial load of 5,000 lbf on an Aluminum 6061 tie rod, this suggests that the realistic impact of 2,000 lbf will not cause our tie rod to fail.

Load Diagram:

Constraints:

FOS: 1.15

Equations (If Applicable): See Below

Confidence Level & Explanation: Medium-High since the tie rod material and expected load values are known.

Calculations and/or FEA:

Input/Output	Equations	Calculation
OD (in)	outer diameter	0.75
Thickness (in)	wall thickness	0.19
E (ksi)	Young's Modulus	9993.1
I (in^4)	area moment of inertia	0.014611579
P (lbf)	Applied axial compressive load	5000
A (in^2)	Cross sectional area	0.334265458
L (in)	Unsupported length	15.8
FOS		1.154550534

Figure 79: Tie Rod Buckling Calculations

Failure Condition: Frontal impact from a collision with an opposing car or obstacle, where the driver pulls down on the steering wheel to brace themselves.

Justification: The applied lateral force of 660 N comes from a study conducted by an FSAE Chief Design Judge to evaluate minimum driver applied forces for SAE competition. Thus, it is reasonable to use this as a baseline for the design of the steering assembly.

Load Diagram:

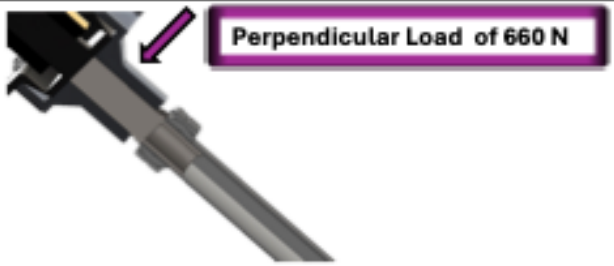

Constraints:

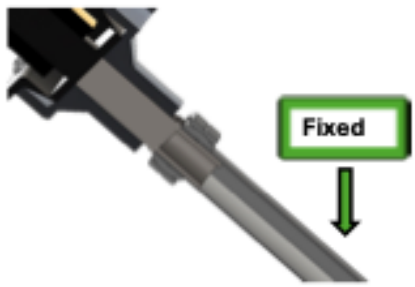

FOS: 10.84

Equations (If Applicable): See Below

Confidence Level & Explanation: Medium since the expected perpendicular load and length of the shaft are known.

Calculations and/or FEA:

Input/Output	Notes	Calculations
Force (lbf)	perpendicular load	148.374
Length (in)	distance of shaft (assuming key is gone)	1.625
OD (in)	outer diameter	0.75
Thickness (in)	wall thickness	0.048
Yield Strength (ksi)	4130 tube	63.1
ID (in)	OD - 2*t	0
Moment (in lbf)	F*L	241.10775
y	OD/2	0.375
I (in^4)	area moment of inertia	0.015531555
Stress (ksi)	M*y/(I/1000) to get ksi	5.821400592
FOS	yield/stress	10.8393159

Figure 80: Steering Rod Insert Bending Calculations

3.2.2. Brake Pedal

3.2.2.1. Discussion of Design Reasoning – Brake Pedal:

The brake pedal was designed for comfort throughout the 4-hour endurance race. To achieve this, we made the pedal pushing surface along the same horizontal plane as the driver's hips. The pedal ratio is 2.45:1, which means we get 2.45 times more travel in our pedal than our master cylinders compress, also giving us an amplified braking force. The brake pedal ratio is lower than last year's 3:1, but our calculations support that we will still have no issue in locking all four brakes under normal driving conditions. The biggest constraint for both of our pedals was packaging them into the new 10" shorter frame, and subsequently shorter toe-box. Hanging pedals, like used on last year's car, are beneficial for ergonomics and pedal ratio but they take up more space in the top of the toe box, and require their own lateral frame member to mount to, which we found to not be more beneficial than mounting them to the floor and sacrificing a slight amount of pedal ratio. Last year's brake pedal assembly was ≈ 4lbs (measured in person), excluding the weight of the two frame members that were added exclusively for pedals. This year our brake pedal weighs 4.02lbs (measured via CAD). Both weights are recorded without hardware.

3.2.2.2. Brake Pedal Critical Rules:

- B.7.1. – Brake System
- B.7.1.1 – Brake Pedal
- B.7.1.2 – Independent Circuits
- B.7.1.5 – Brake Lines

3.2.2.3. Brake Pedal CAD Design:

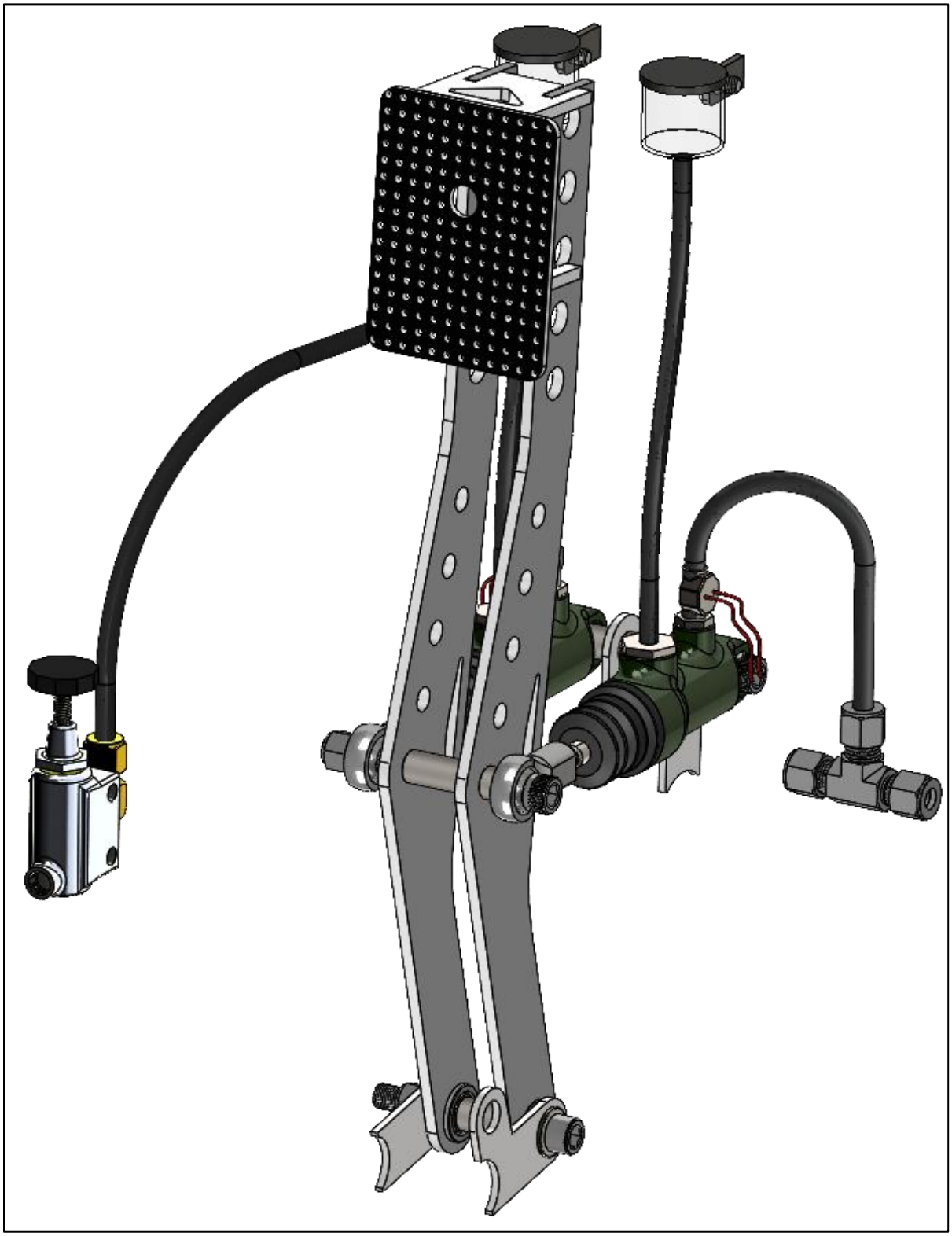

Figure 81: Brake Pedal Assembly

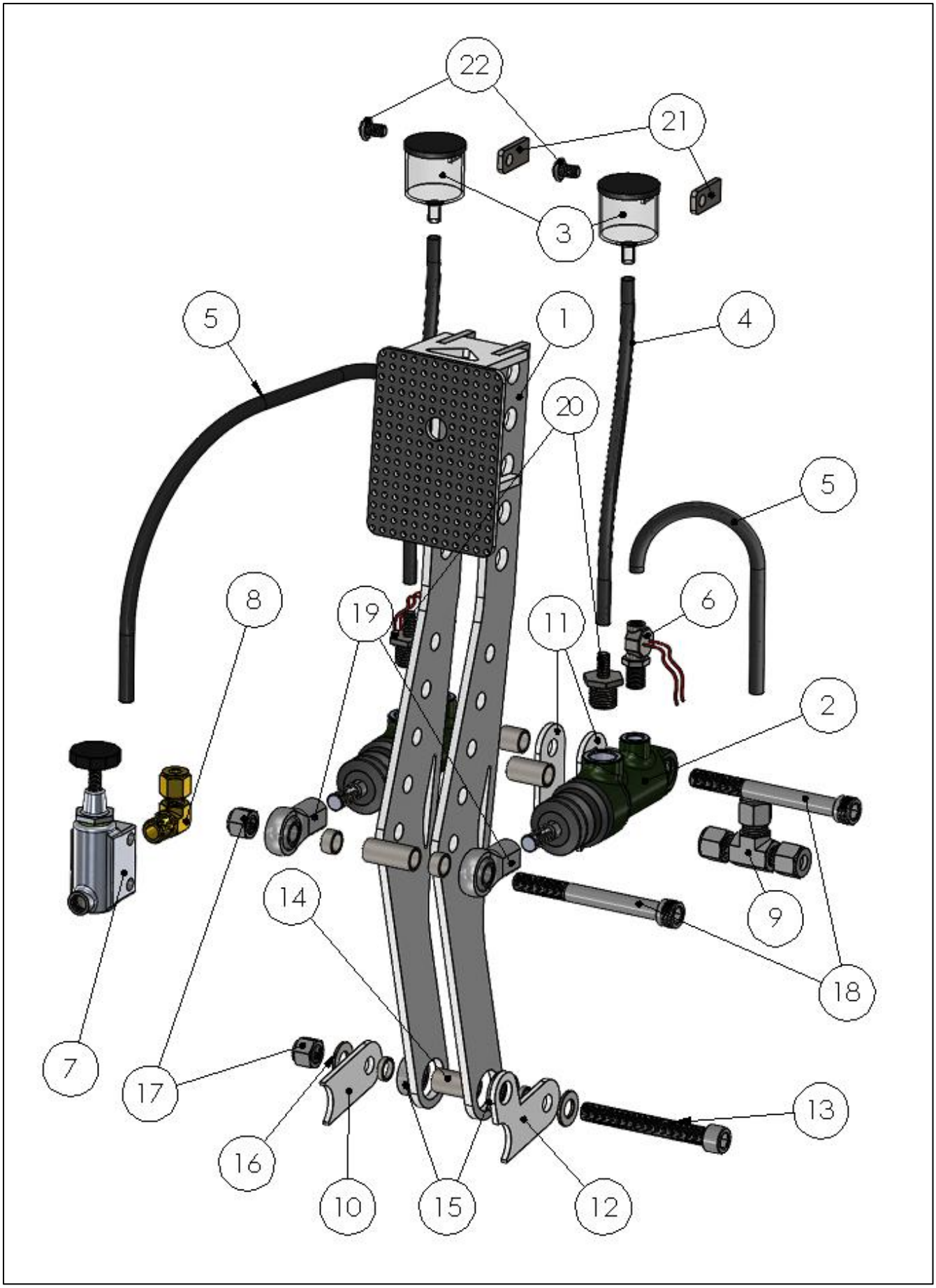

Figure 82: Exploded Brake Pedal Assembly

3.2.2.4. Brake Pedal BOM:

BOM Part #	Description	Qty:	Source (Hyperlink to Part)	Cost:	Weight/1Pc [lbs]
1	Basic Pedal Assembly	1	On Hand (Stock)	N/A	~4.5 (Measured in SolidWorks)
2	Master Cylinder	2	On Hand	N/A	
3	Brake Fluid Reservoir	2	On Hand	N/A	
4	16" Reservoir Tubing	1	On Hand	N/A	
5	23" Steel Threaded Brake Line	1	On Hand	N/A	
6	Braking Pressure Sensor	2	On Hand	N/A	
7	Proportioning Valve	1	On Hand	N/A	
8	Proportioning Valve Fitting	1	McMaster-Carr	$14.60	
9	Yor-Lok Fitting	1	On Hand	N/A	
10	Throttle Mounting Tab	1	On Hand (Stock)	N/A	
11	MC Mounting Bracket	2	On Hand (Stock)	N/A	
12	Throttle/Diff Mounting Tab	1	On Hand (Stock)	N/A	
13	3” x 3/8"-24 Hex Head Bolt	1	McMaster-Carr	$20.05 per 5	
14	6" Pedal Arm Spacer	1	McMaster-Carr	$16.71 per ft	
15	Pedal Arm Bearing	2	McMaster-Carr	$7.12	
16	18-8 Stainless Steel Washer	2	McMaster-Carr	$9.69 per 50	
17	Grade 8, 3/8"-24 Nylon-Insert Lock Nut	3	McMaster-Carr	$4.68 per 20	
18	3.5" x 3/8"-24 Socket Head Screw	2	McMaster-Carr	$12.66 per 5	
19	3/8"-24 Ball Joint Rod End	2	McMaster-Carr	$4.40	
20	Reservoir Hose Fitting	2	On Hand	N/A	
21	Reservoir Mounting Tab	2	On Hand (Stock)	N/A	
22	3/8" x 1/4"-20 18-8 Pan Head Screw	2	McMaster-Carr	$9.24 per 50	
Total				$64.88	

Table 17: Brake Pedal BOM

3.2.2.5. Brake Pedal Critical Parts – Model Views and Discussion:

The pedal assembly shown in Figure 83 below, is shared between the brake pedal and throttle pedal. Per rule B.7.1.1, the brake pedal must withstand a 450lbf load as the result of a crash/frontal impact. As such, this long pedal was designed for the worst-case scenario. The tabs that support the master cylinders on the frame, Figure 84, also need to be able to sustain the worst-case scenario load, which is 1100 lbs because of the lever arm of the pedal. The results of this study, shown in Figure 88, show a factor of safety on the tabs of roughly 9, before the welds rip.

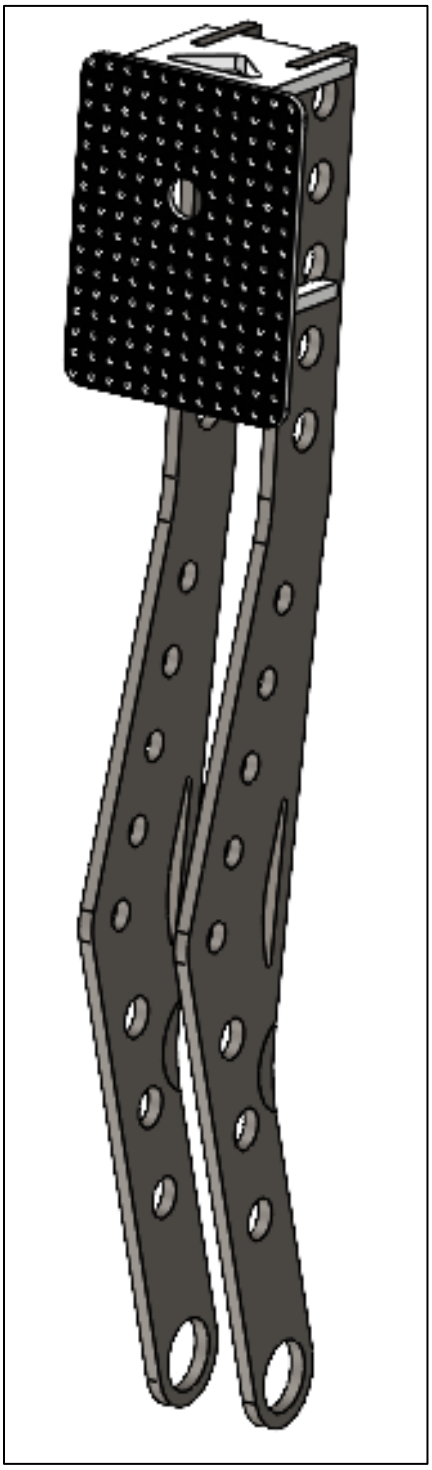

Figure 83: Shared Base Pedal Assembly

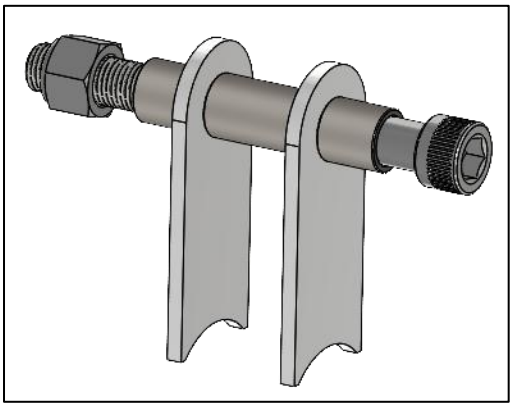

Figure 84: Master Cylinder Mounting Tabs

3.2.2.6. Brake Pedal Analysis:

Failure Condition: Frontal impact/Crash where driver's full momentum is transferred into the pedals resulting in a 450lbf load on the pedal arms with locked out master cylinders.

Justification: Baja SAE Ruleset requires that the brake pedal be able to sustain a 450lbf loading condition in the case of a crash or frontal impact. In this condition, you would fully lock out the brake master cylinders and they would act as a rigid fulcrum transmitting load throughout the top and bottom of the pedal arms.

Load Diagram:

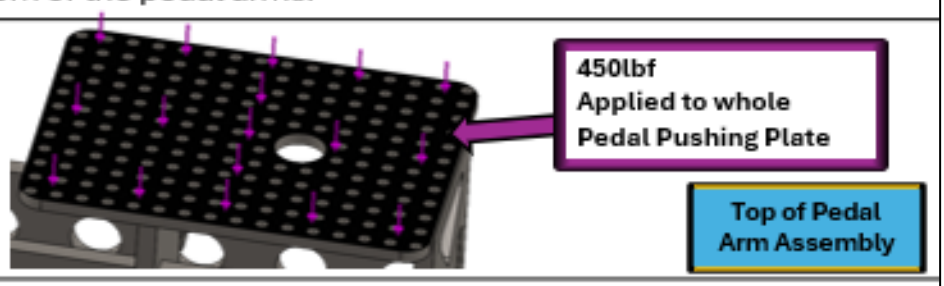

Constraints:

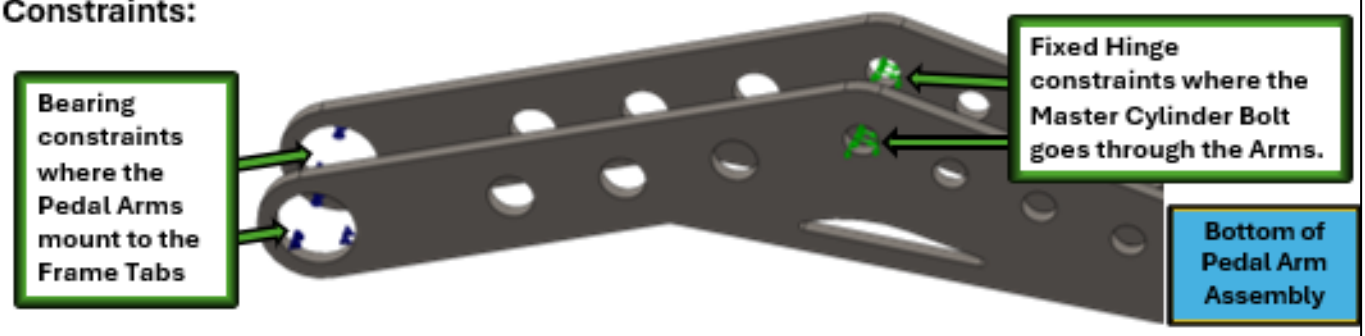

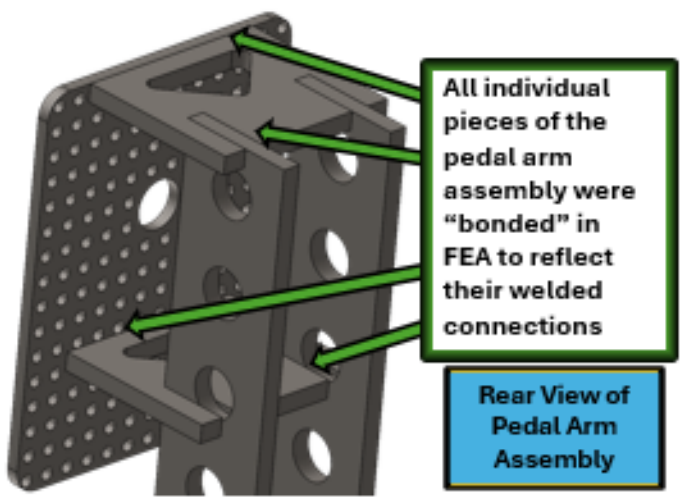

FOS: 1.138

Equations (If Applicable):

Confidence Level & Explanation: Medium-Low Confidence because the loading application is defined in the rules but the constraints available in SolidWorks FEA do not perfectly represent the fixturing of the part.

Figure 85: Basic Pedal Assembly 450lbf Loading Analysis

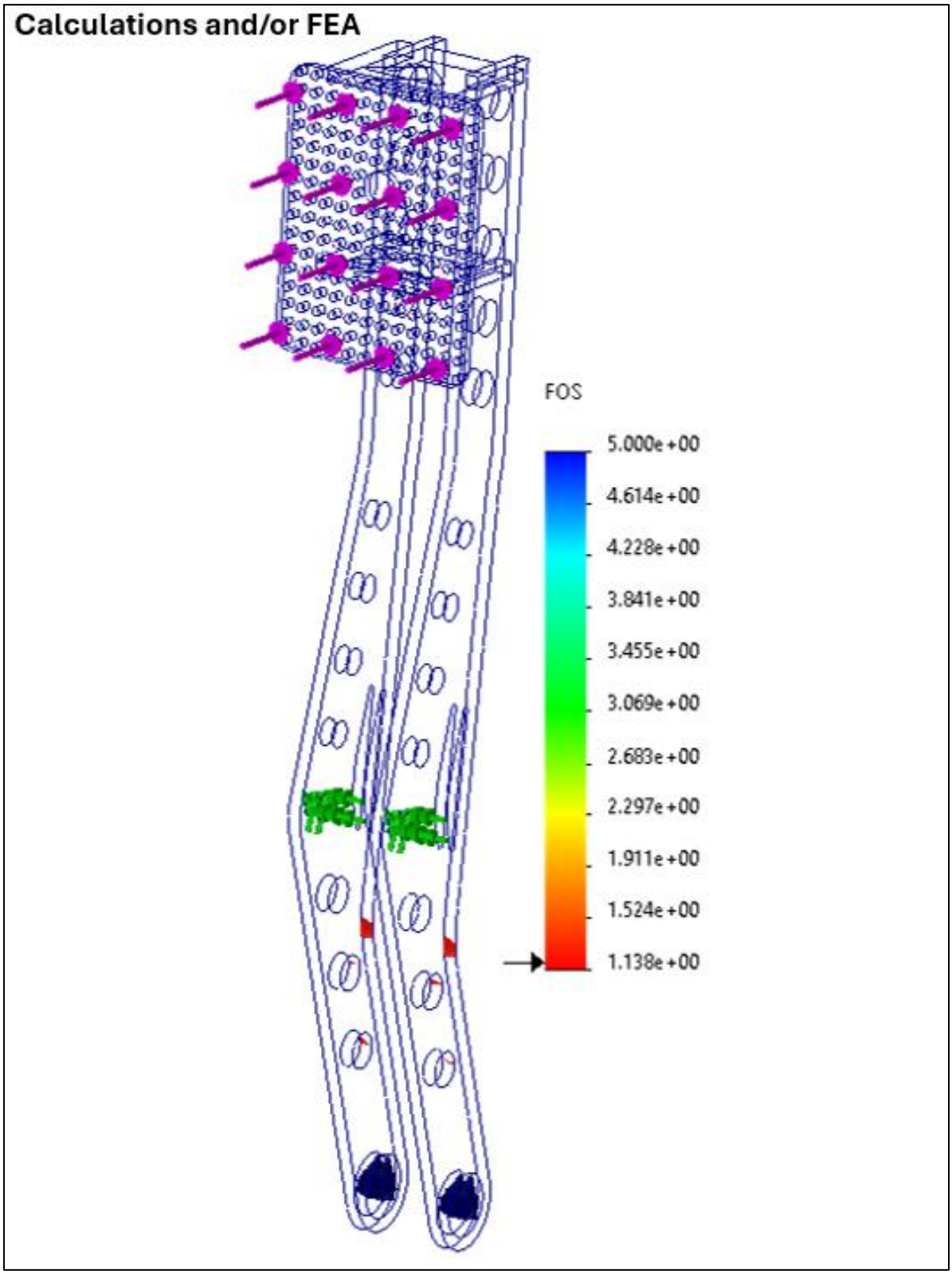

Figure 86: FEA Results of 450lbf Loading Case on Pedal

Calculations and/or FEA

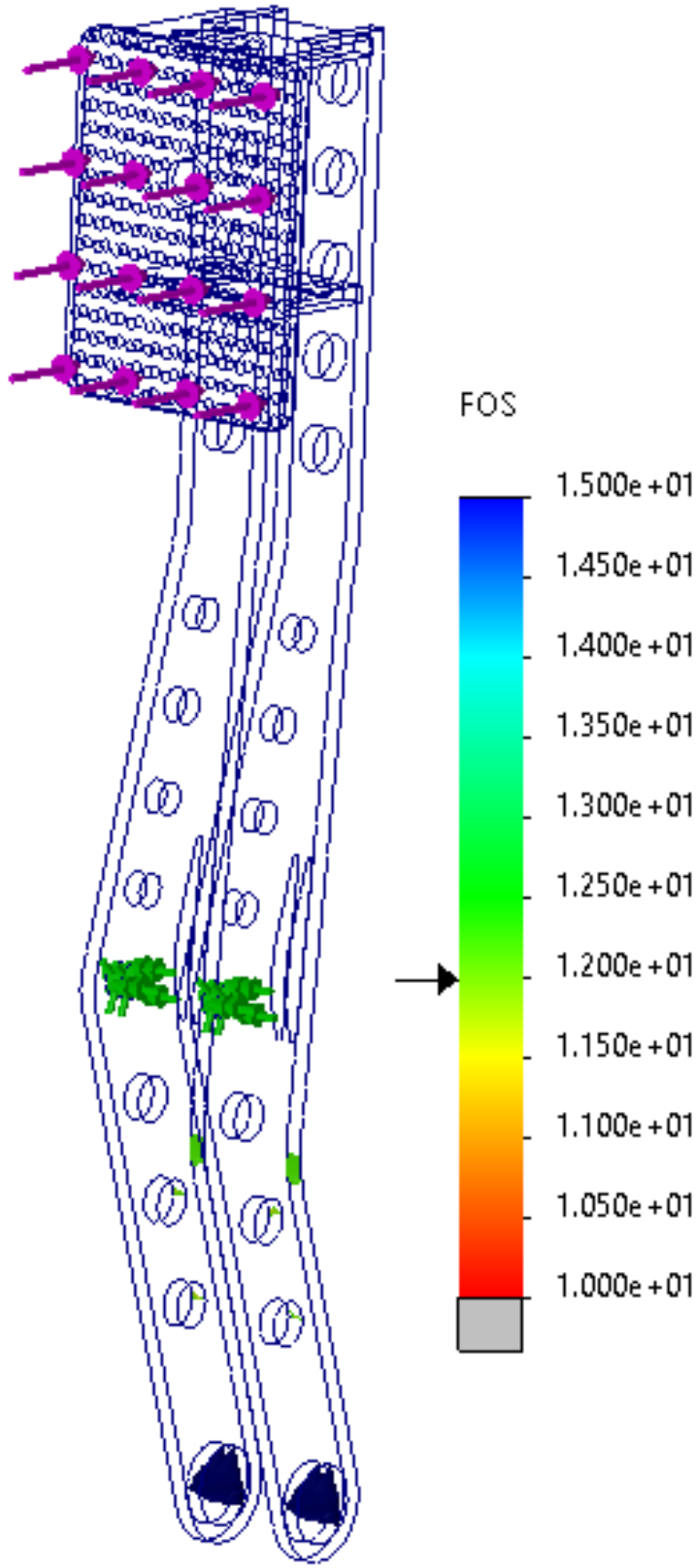

Figure 87: FEA Result of 46lbf Loading Case on Pedal

Calculations and/or FEA

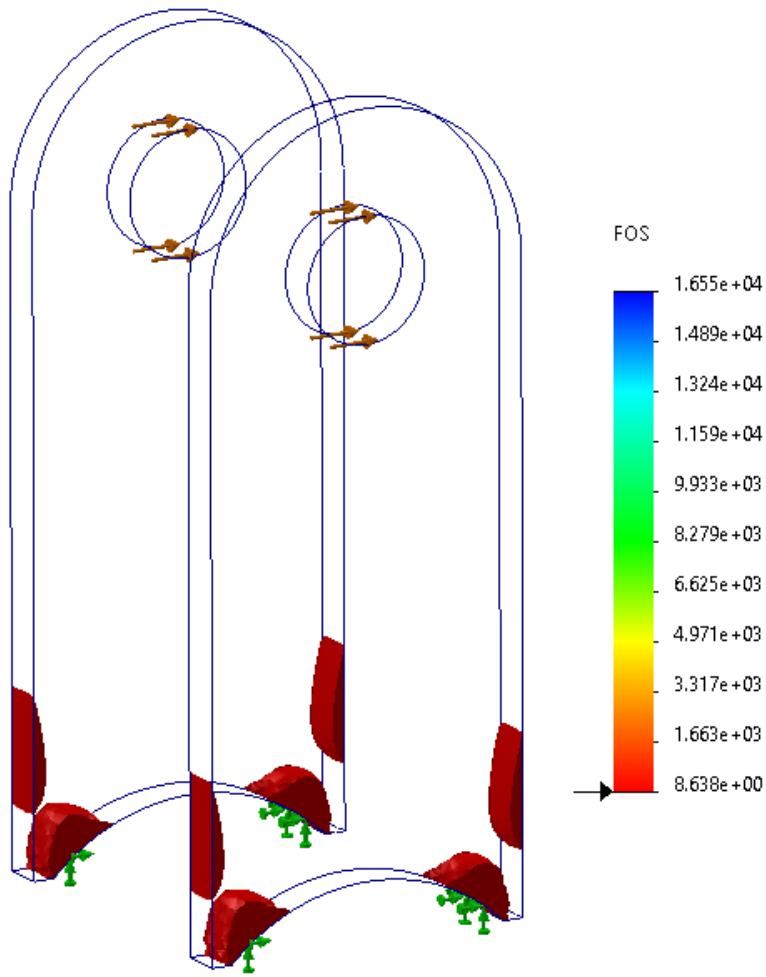

Figure 88: FEA Results of the Master Cylinder Mounting Tabs under a 1100lbf load

3.2.3. Throttle Pedal

3.2.3.1. Discussion of Design Reasoning – Throttle System/Pedal:

The throttle pedal was designed for comfort, reliability, and durability. On last year's car, the throttle pedal had only 1.5" of travel from 0-100% throttle. This made it feel very on-or-off so the driver didn't have much modularity. To improve the feel of the throttle, we increased the push-pull ratio (the cable attachment point compared to the location of the application of force, both relative to the fulcrum). Last year, the ratio was a direct 1:1 because the throttle cable attached at the same location that you apply force to the pedal. This year, with a long, floor-mounted-pedal, we are able to achieve a push-pull ratio of 2.41:1 which means our pedal will travel 3.615" from 0-100% throttle. Additionally, last year's pedals had an issue with cable slippage, resulting in a dramatic decrease in speed. This year's design aimed to fix that issue by securing the cable in a different fixture; instead of clamping the cable between nuts and washers, like last year, we will be using the lead head on the throttle cable (a motorcycle clutch cable) as a hard stop, and putting it in a tube. Our adjustability will then come from a barrel adjuster, mounted to the same plate that the throttle return spring will be mounted on. This cable securing configuration gives us high confidence in throttle performance over time because it doesn't rely on any mechanical fasteners to secure it.

3.2.3.2. Throttle System/Pedal Critical Rules:

- B.7.2 - Throttle System
- B.7.2.1 - Pedal
- B.7.2.2 - Pedal Stop
- B.7.2.3 - Throttle Cable
- B.7.2.4 – Fail Safe

3.2.3.3. Throttle Pedal CAD Design:

Shown in Figure 89 to the right.

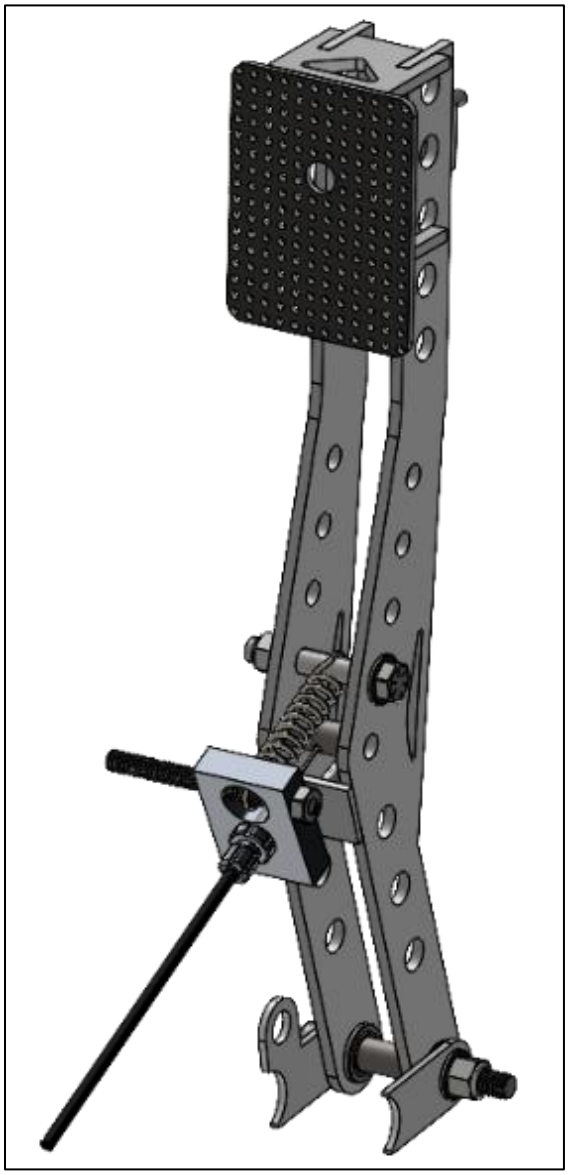

Figure 89: Throttle Pedal Assembly

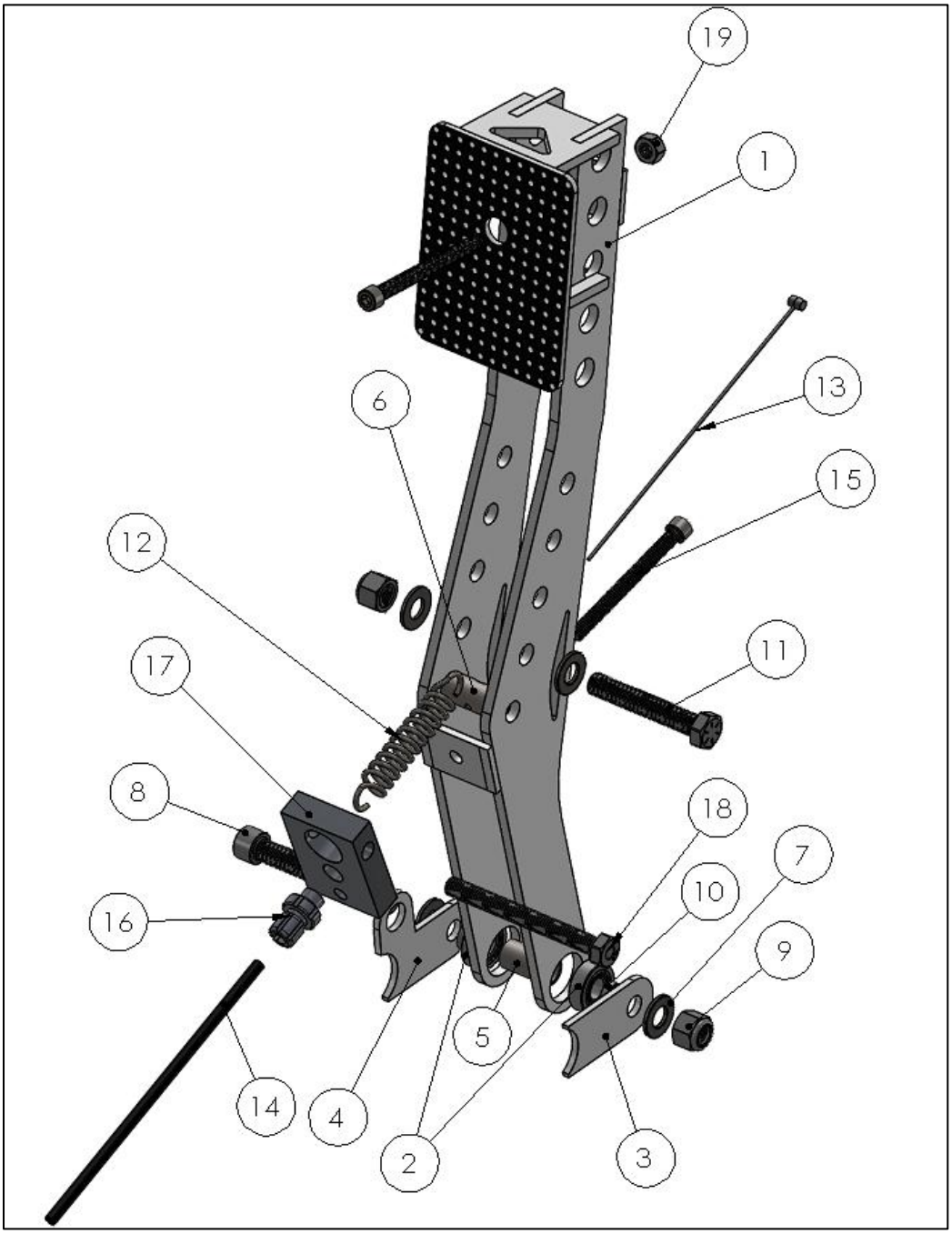

Figure 90: Exploded Throttle Pedal Assembly

3.2.3.4. Throttle Pedal BOM:

BOM Part #	Description	Qty:	Source (Hyperlink to Part)	Cost:	Weight/1Pc [lbs]
1	Basic Pedal Assembly	1	(Stock) In Hand	0	
2	Pedal Arm Bearings	2	Mcmaster-Carr	7.12	
3	Throttle mounting tab	1	(Stock) In Hand	0	
4	Throttle/Diff mounting tab	1	(Stock) In Hand	0	
5	Inner Bearing Spacer	1	(Stock) In Hand	0	
6	Pedal Arm Spacer	1	(Stock) In Hand	0	

7	18-8 Stainless Steel Washer	4	McMaster-Carr	$9.69 per 50	~ 3.5lbs
8	3” x 3/8-24 Hex Head Bolt	1	McMaster-Carr	$20.05 per 5	
9	Grade 8, 3/8-24 Nylon-Insert Lock Nut	2	McMaster-Carr	4.68 per 20	
10	Outer Bearing Spacer	2	(Stock) In Hand	0	
11	2”x 3/8-24 Zinc Plated Hex Head Bolt	1	McMaster-Carr	$5.97	
12	Tempered Steel Spring	1	McMaster-Carr	$3.67	
13	Throttle Cable	1	Donated	0	
14	Throttle Cable Housing	1	(Stock)	0	
15	2 ¾’ x ¼”-20 Hex Head Bolt	1	McMaster-Carr	$22.49 per 25	
16	Barrel Adjuster	1	Donated	0	
17	Barrel Adjuster Plate	1	(Stock) In Hand	0	
18	Bolt	1	McMaster-Carr	$13.11 per 10	
19	Throttle Limiter Nut	1	On Hand	0	
Total:				$23.41	

Table 18: Throttle Pedal BOM

3.2.3.5. Throttle Pedal Critical Parts – Model Views and Discussion:

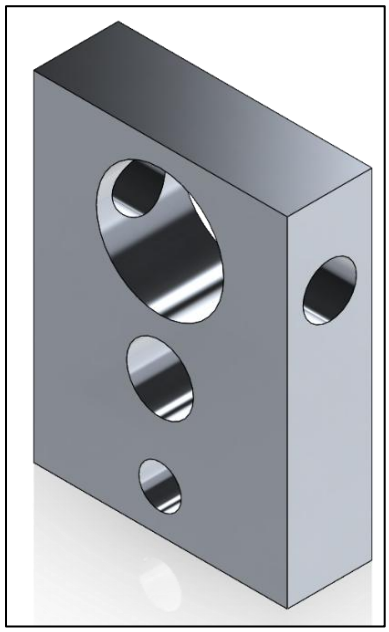

Figure 91:Throttle Pedal Barrel Adjuster Plate

The component in Figure 91, above, is the Barrel Adjusted Plate. Due to the packaging complexities with having our pedals mounted to the floor, we had to get creative with where we mount the stop for our cable housing. This plate is our solution; it mounts to the front differential to secure the housing in place, and our throttle pedal tensioning spring mounts to the bolt that secures this part to the differential. Finally, this part also acts as a “stop” for the pedal to back up again, ensuring that the spring won’t pull the pedal too far back towards the driver. See Figure 92 below which shows all of the functions and

mounting of this part. This piece will be made of 6061 T6 Aluminum because we want it to be light, easy to machine, and it's not a critical load bearing part.

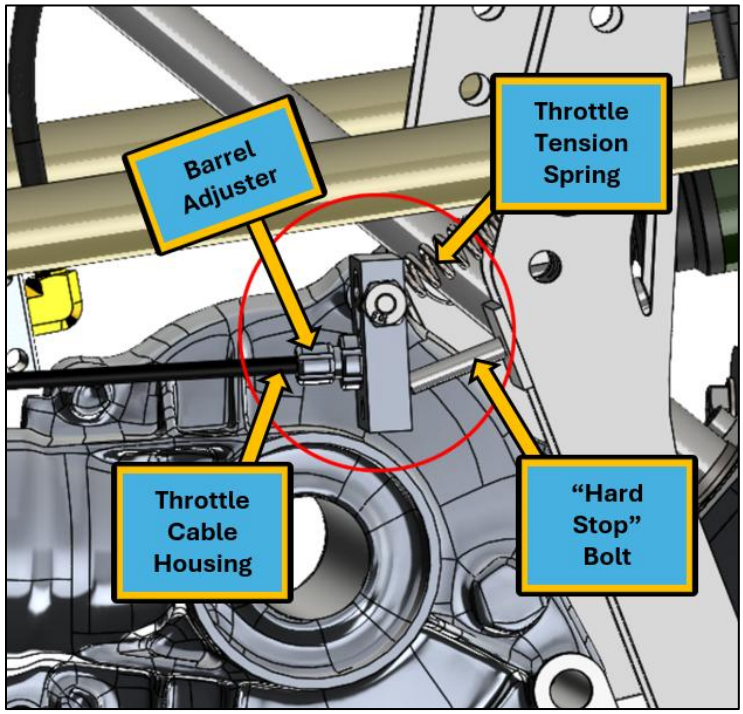

Figure 92: Throttle Pedal Barrel Adjuster Plate Mounted to Front Differential

3.2.3.6. Throttle Pedal Analysis

The throttle pedal assembly has the same core pedal as the brake assembly, as labeled in Figure 90, part 1. This part has been analyzed to ensure, with high confidence, that it can withstand the worst theoretical applied load, 450lbs. However, the throttle pedal will never have the same stress concentration as the brake pedal because there are not master cylinders mounted to the pedal that constrain its movement and create a reaction force. Instead, the reaction force, under worst case scenario conditions, is a 450lb load applied to the pedal and into the throttle limiting bolt on the backside of the pedal (see figure 93 below).

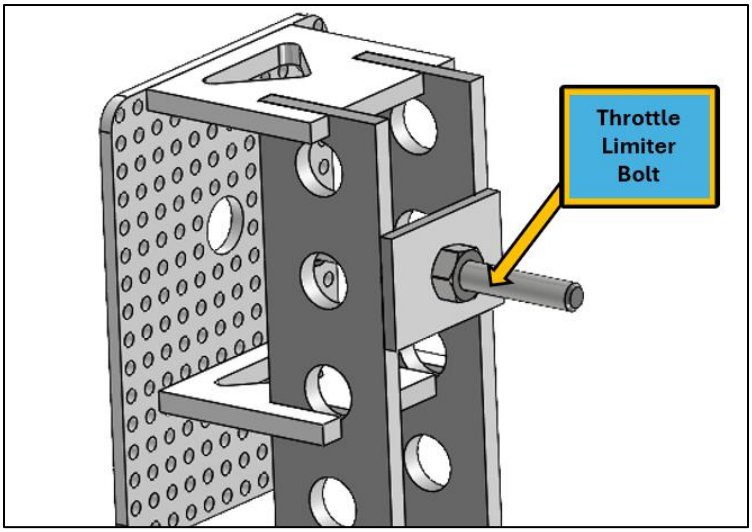

Figure 93: Throttle Limiter Bolt

Failure Condition: Frontal impact/Crash where driver's full momentum is transferred into the pedals resulting in a 450lbf load on the Throttle Limiter Bolt Plate.

Justification: Baja SAE Ruleset requires that the brake pedal be able to sustain a 450lbf loading condition in the case of a crash or frontal impact. Therefore, it is a safe to assume that the throttle pedal should be able to sustain the same force, for worst case scenario.

Load Diagram:

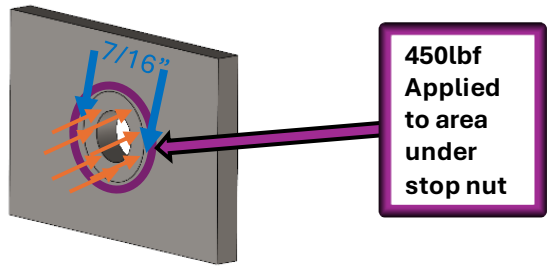

Constraints:

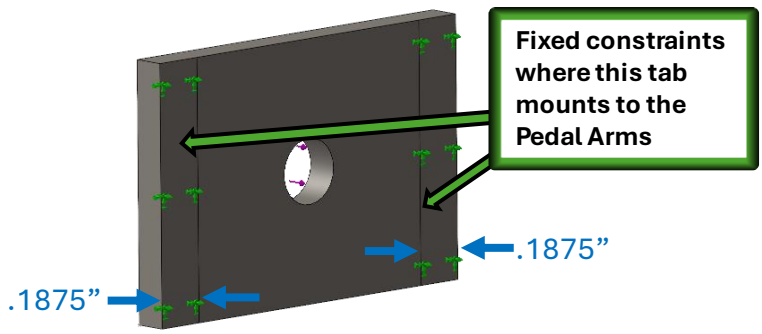

FOS: 0.73

Equations (If Applicable):

Confidence Level & Explanation: High. The loading force for this part is well known and the mesh/fixturing is simple.

Calculations and/or FEA:

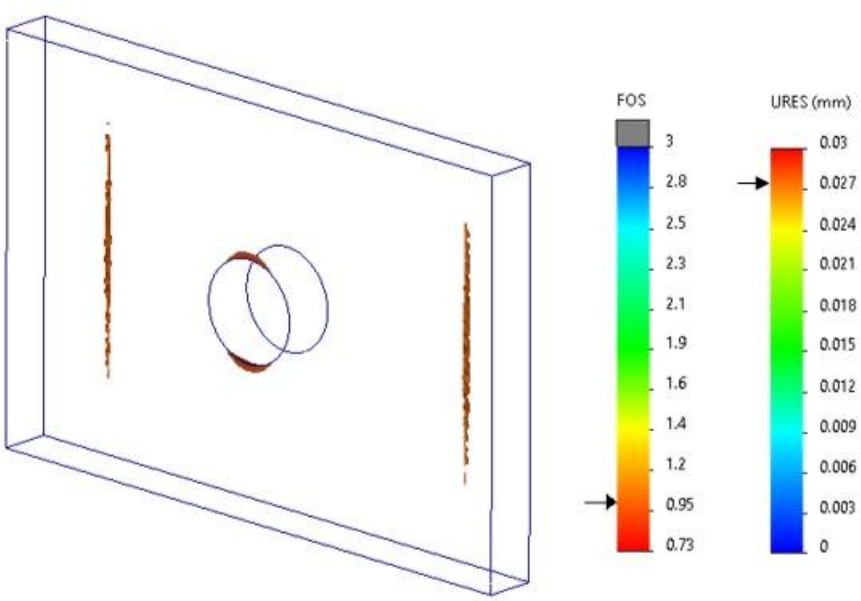

Figure 94: Analysis of Throttle Limiter Bolt Plate

3.2.4. Brake System

The brake system consists of four Wilwood PS1 calipers actuated via two Tilton 78 Series 5/8" Bore Master Cylinders, connected with 3/16" Hard Lines and an inline Wilwood Brake Proportioning Valve to the rear brake calipers. We are using an outboard braking system with hubs and rotors off of a Yamaha Grizzly. As required, the brake pedal withstands 450 lbs, but we only need to apply 120 lbs to the pedal to lock up all 4 wheels (See Brake pedal calculations in the Appendix). We will be using steel braided lines to ensure proper braking capabilities with repeatable behavior over the four-hour endurance race. Each master will have their own independent reservoir, which will be attached directly to the frame by mounting tabs. There are two pressure sensors located in the lines to illuminate the brake light.

3.2.4.1. Brake System Critical Rules:

- B.7.1.1 – Brake System
- B.7.1.2 – Independent Circuits
- B.7.1.3 – Brake Location
- B.7.1.4 – Cutting Brakes
- B.7.1.5 – Brake Lines
- B.7.2.1 - Pedal

3.2.5. Seat Mounting

3.2.5.1. Discussion of Design - Seat Mounting:

The seat mounting consists of four bottom and two rear seat tabs (see three Figures below). The bottom seat tabs have a width of 0.78 in and a height of 1 in. to the hole. Whereas, the rear tabs have a width of 1 in and a height of 1 in. to the hole. Both meet the dimensions as set in Rule: B.12.2.1 - Dimensions. The rear and bottom seat tabs are 6.5 inches apart, which directly satisfies Rule B.4.5.3 – Seat Mounting Points, which specifies that the minimum distance between the tabs must be at least 6 inches. With all tabs, we will use a 1 in. long ¼"-20 hex screw and respective steel nut, also within the rules. To mount the tabs on the two angled faces that are adjacent to the center panel of the seat (each are 0.2 degrees from the flush middle portion), our seat will require 0.17 mm of spacers which is within the 13 mm spacer maximum as set in Rule B.4.5.3 – Seat Mounting Points.

Originally, we had wanted to simplify the design by using two lateral members (like the member that contains the anti-submarine belt braces) across the chassis. However, due to the drive shaft height, this was not feasible as the lateral members had to be significantly higher, when there was a simpler solution. Similar to last year's design, we elected for two vertical members for our bottom seat mounting. However, this year, with two tabs on each member, this allows us to eliminate an extraneous lateral member in the chassis and lower our total number of bottom seat tabs from 6 to 4. In addition, our rear seat tabs are located 5 in. from the bottom of the vehicle, which is ideal given that the bottom of the seat is the flushest with the firewall (as the seat gradually separates from the firewall as the height increases).

Both the rear and bottom seat tabs are critical to ensure that the vehicle passes technical inspection and the driver is safe during competition. The overall front height of the seat is at 4.34 in from the bottom of the vehicle, which is more than 0.5 in lower than last year's car as the front seat height was 4.75 in. Thus, this allows the driver to have a lower center of gravity, making it easier for maneuverability.

3.2.5.2. Seat Mounting Critical Rules:

- B.4.5.1 – Seat Construction
- B.4.5.2 – Seat Design
- B.4.5.3 – Seat Mounting Points
- B.12.2.1 – Dimensions

3.2.5.3. Seat Mounting CAD Design:

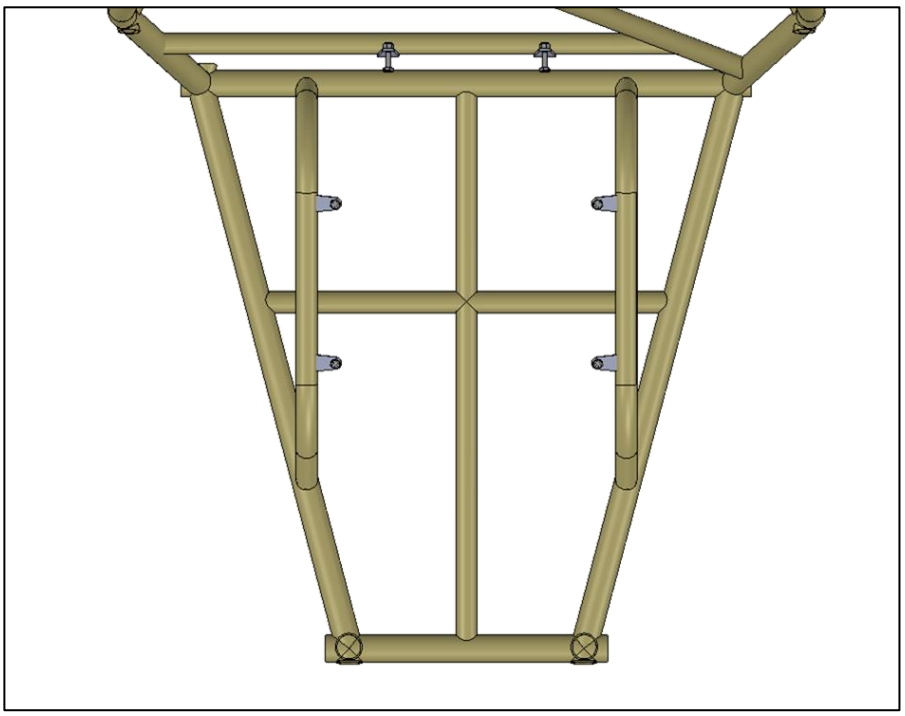

Figure 95: Top View – Bottom and Rear Seat Mounting

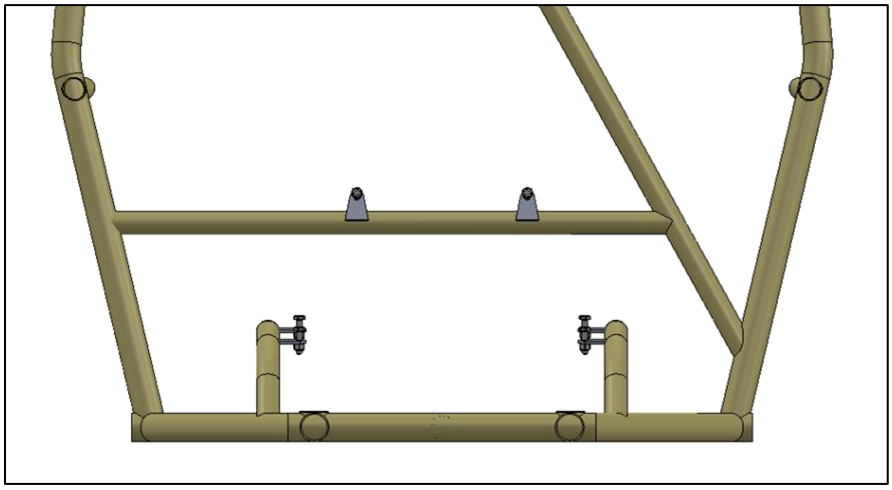

Figure 96: Front View – Rear Seat Mounting

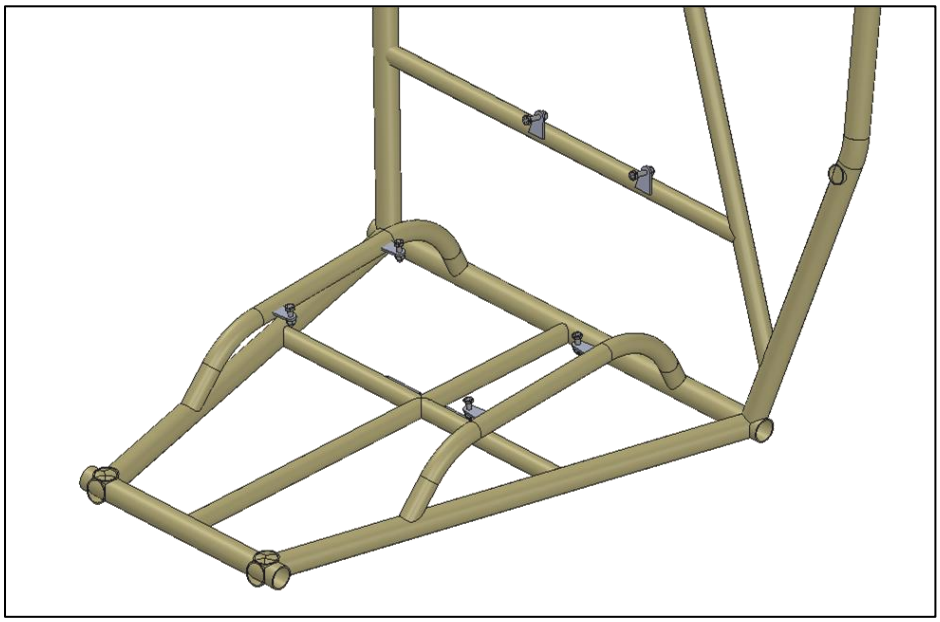

Figure 97: Isometric View – Bottom and Rear Seat Mounting

3.2.6. Harness Mounting

3.2.6.1. Discussion of Design - Harness Mounting:

The harness system uses the L&L 6-Point P&D Harness. The lap belt tabs (see below in Figure 100) are angled at 50 degrees from the horizontal, addressing the 45 to 80-degree requirement as set in Rule B.4.2.5.1. Thus, the harness goes directly through the cut-outs on the side of the Kirkey Series 65 Seat and fulfills the angle requirement.

Because this design uses a 6-point harness, there will be two anti-submarine belts, one on each side of the member that supports the drive-shaft. These must be positioned such that they fall behind the chest line of the driver yet far enough forward that they are redirected at less than a 30-degree angle, as required by Rule B.4.2.6.2 and Rule B.4.2.6.4. The chest line falls approximately at the front of the cut-out in the seat for the anti-submarine belts, so the member that supports the anti-submarine belts is positioned slightly behind the center of this cut-out to allow both of these rules to be satisfied with the greatest margin.

The shoulder belts will be supported using a lateral member that is 27 in from the bottom of the chassis. The positioning of this member fulfills the requirement from Rule B.4.2.4.1, which specifies that the shoulder belts must be between 0 to 4 inches below the driver's shoulders; it is set such that it is level with the shoulders of the team's shortest member, which allows it to be compliant for all team members. As shown in Figure 99, the shoulder belt braces will be spaced by 7.5 in from center to center, fulfilling the 6 to 9 in spacing requirement set by Rule B.4.2.4.2.

3.2.6.2. Harness Mounting Critical Rules:

- B.4.2.4 - Shoulder Belts
- B.4.2.5 - Lap Belts
- B.4.2.6 - Anti-Submarine Belts
- B.12.2 - Required Attachment Tabs

3.2.6.3. Harness Mounting CAD Design:

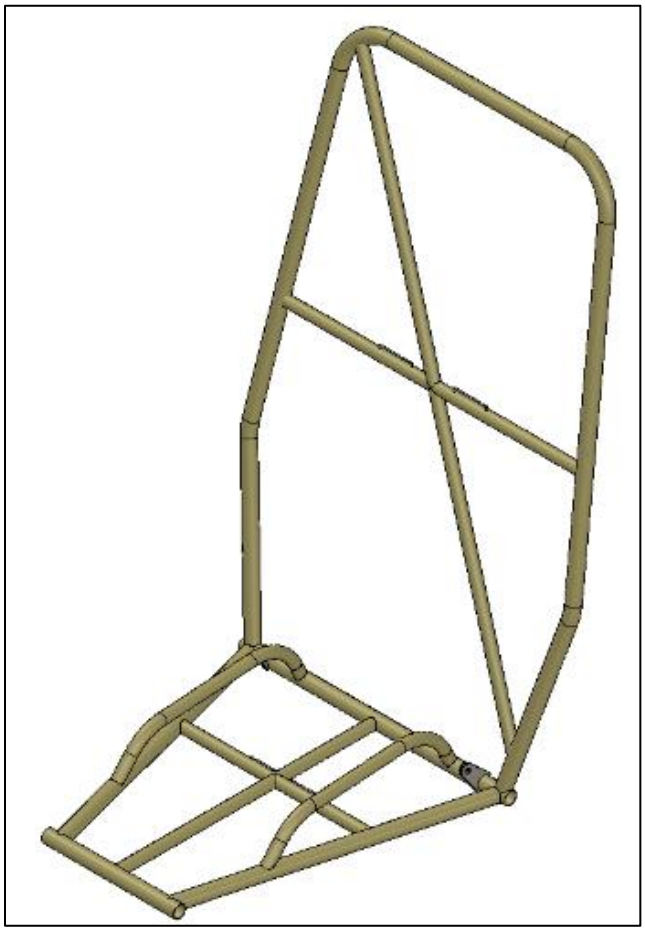

Figure 98: Isometric View of Harness Mounting

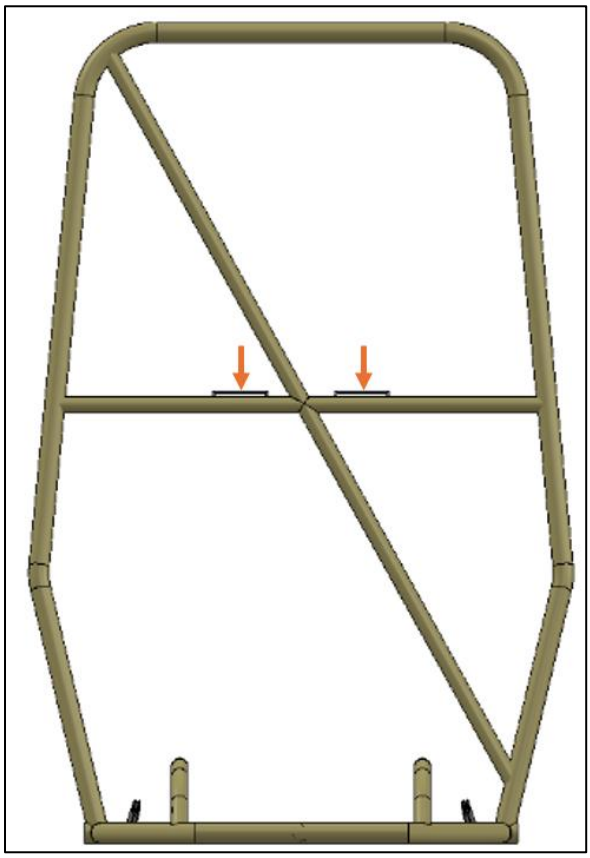

Figure 99: Front View of Harness Mounting

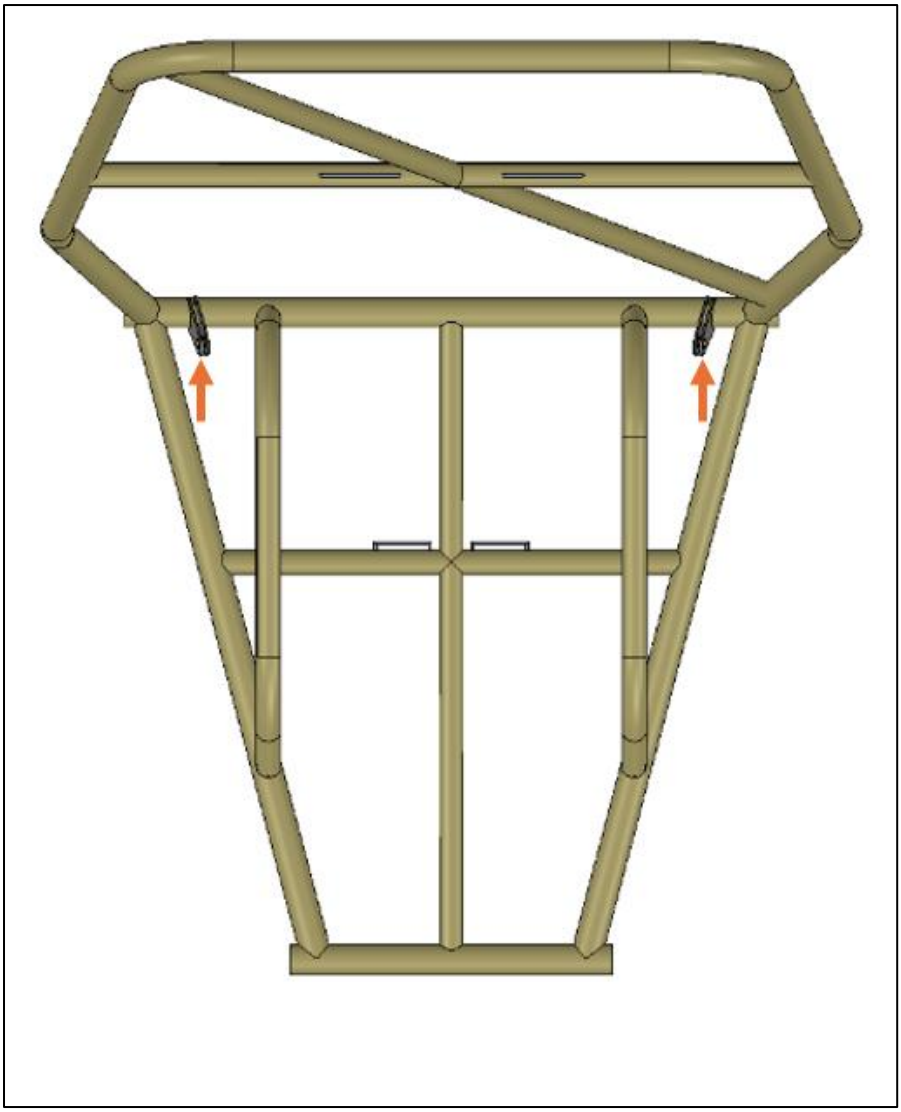

Figure 100: Top View of Harness Mounting

3.2.7. Gas Tank Assembly

3.2.7.1. Discussion of Design - Gas Tank:

The gas tank assembly is nearly identical to last year because it is heavily regulated by the rules. The only difference in the gas tank assembly this year is the length of the brackets. We have a .5” of extra length in the bracket to give ourselves a hefty tolerance during technical inspection at competition.

3.2.7.2. Gas Tank Assembly Critical Rules:

- B.6.3 – Location
- B.6.4 – Fuel Cap
- B.6.5 – Fuel Tank
- B.6.5.1 - Mounting

3.2.7.3. Gas Tank CAD Design:

Figure 101: Gas Tank Assembly

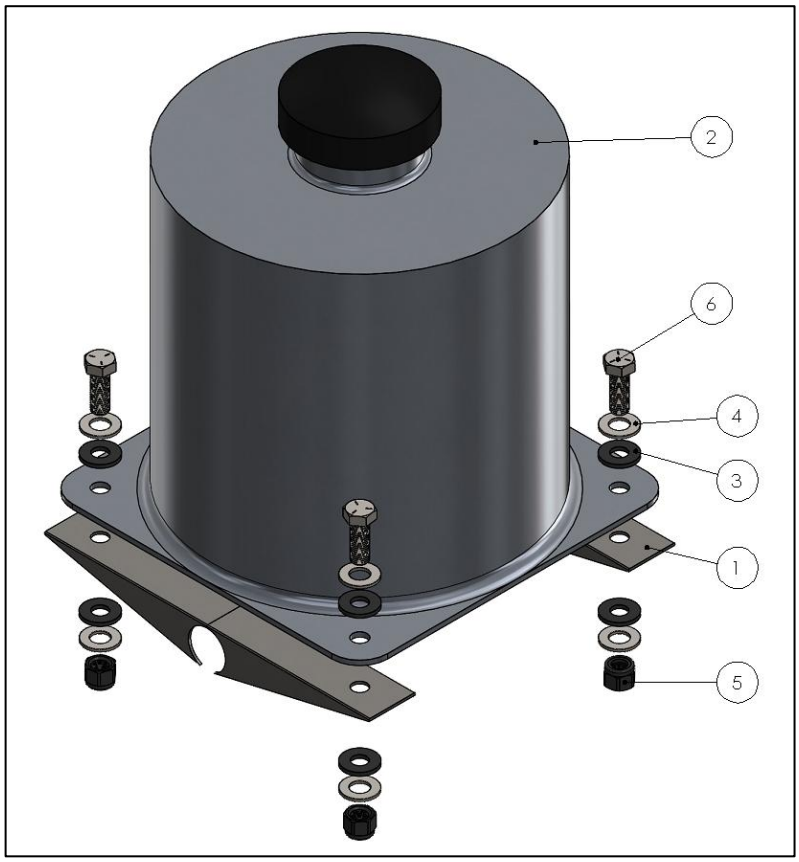

Figure 102: Exploded Gas Tank Assembly

3.2.7.4. Gas Tank BOM:

BOM Part #	Description	Qty:	Source (Hyperlink to Part)	Cost:	Weight/1Pc [lbs]
1	Mounting Brackets (Stock)	4	On-hand	N/A	0.18
2	Fuel Tank and Cap	1	On-hand	N/A	4.6
3	3/8” Santoprene Washer	8	McMaster-Carr	$13.97 per 50	~
4	3/8" Zinc Washer	8	McMaster-Carr	$9.97 per 50	~
5	3/8"-24 Nylon Locknut	4	McMaster-Carr	$13.71 per 100	~
6	3/8”-24 Grade 5 Hex Head Bolt	4	McMaster-Carr	$15.02 per 50	~
Total:				$5.58	4.78

4. Drivetrain

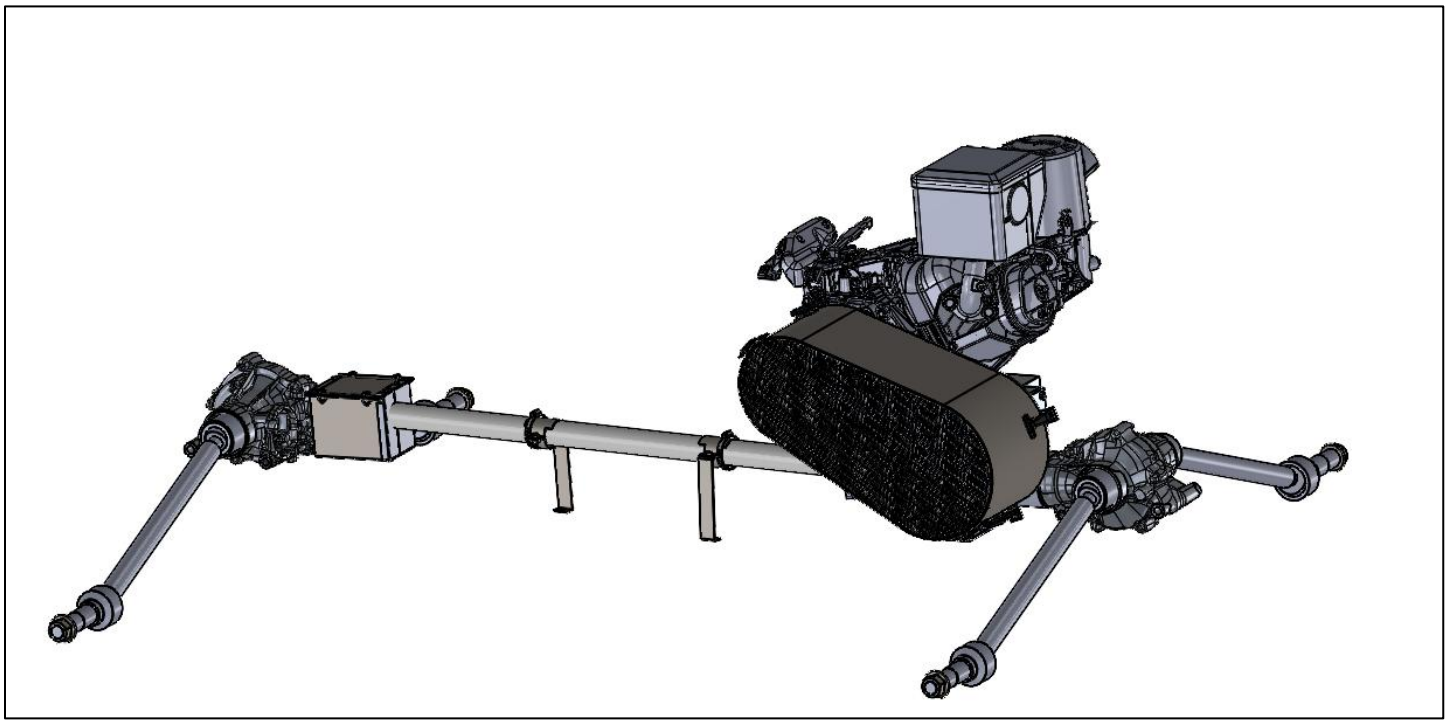

Figure 103: Full Drivetrain Left Side Isometric

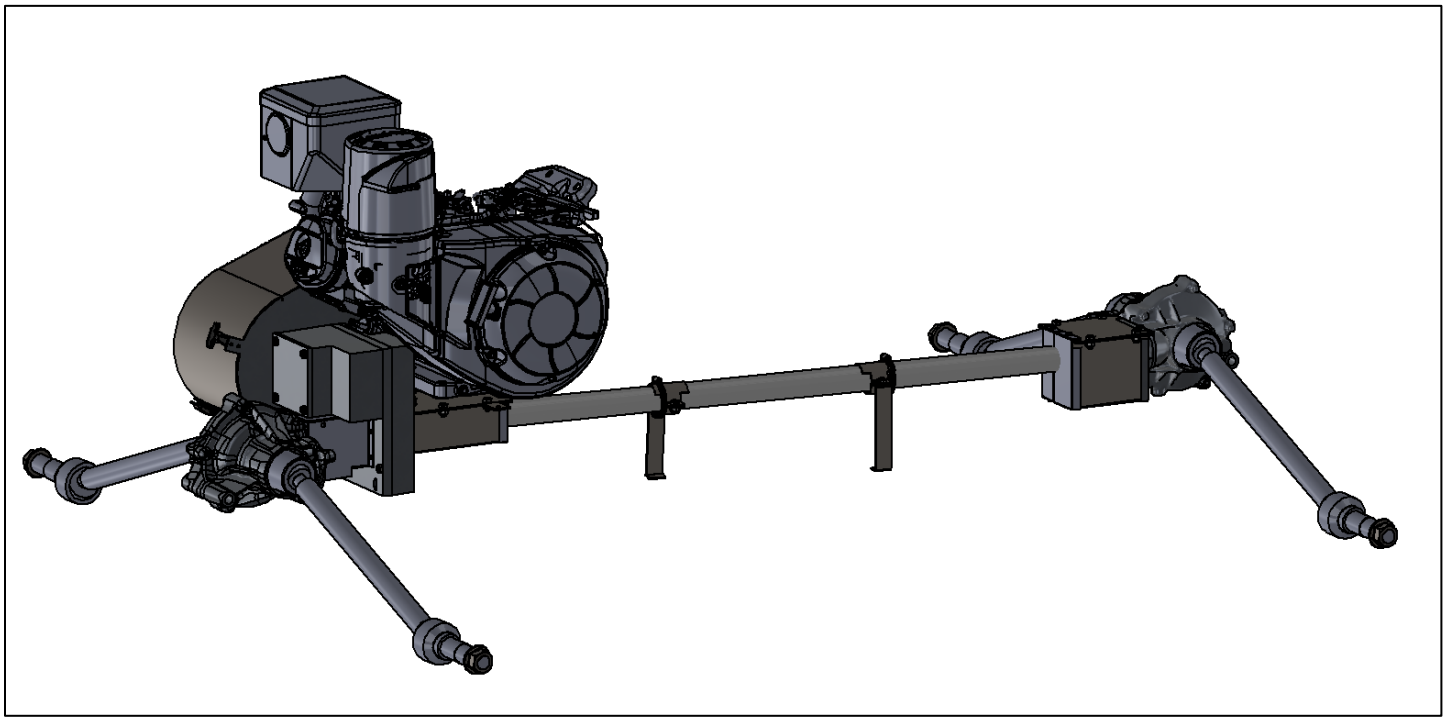

Figure 104: Full Drivetrain Right Side Isometric

4.1. System Level Breakdown

Our drivetrain transfers power from the rules specified Kohler CH440 engine to our Gaged Engineering GX9 CVT, post CVT we have a 90° reduction gearbox that powers both of our Yamaha Grizzly 350 differentials. The driveshaft runs from the reduction gearbox in the rear to the front differential, and each differential powers two CV axles which drives all four wheels. After previously exploring an offset driveshaft, we landed on this assembly to better align with our design goals. This year we are looking to complete the endurance race without a drivetrain failure, increase acceleration by 10% over last year's car, be able to remove custom components in under 10 minutes, and lower the center of gravity 10% compared to last year. The decision to remove some complexity and custom components that came with an offset driveshaft was made to improve reliability concerns and decrease the risk of endurance failure. Additionally, this will greatly help our efficiency, which together with our CVT selection and chosen final drive should increase our initial acceleration. While we lost significant capabilities to lower the center of gravity in placing the driveshaft under the seat, we still managed to lower the seat and engine. The overall weight without the engine or CVT is estimated at 95 pounds from the CAD, which is below last years measured 105lb weight. The cost is currently anticipated to be around $2200.

4.2. Part Level Breakdown

4.2.1. Engine and CVT Assembly

4.2.1.1. CVT

This year, we chose to use the Gaged CVT instead of the CVTech. Our reasoning behind this was that we wanted to meaningfully take advantage of its tuning flexibility, as given our MOTEC data from our previous track day, there are significant gains that could be made since we were able to determine that the acceleration curves of the vehicle were identical even with a significant weight difference, along with our primary CVT not holding our engine RPM at the peak power curve. It also has other advantages, namely a smaller profile on the secondary caliper and expansion in the same direction as the primary, allowing us more room to adjust the fit with the cover and members. Lastly, the Gaged CVT has a higher torque curve (from 0.43-3.0 to 0.9-3.9), allowing us to have a less significant reduction in our transfer case which saves space and money.

Figure 105 - Speed over time graph showing acceleration anomaly

Figure 106 – Top: CVTech CVT; Bottom: Gaged CVT

4.2.1.2. CVT Cover (HROE and PPAE)

The main rules specifications on drivetrain, outside of the engine, are in regard to safety covers for rotating components. The CVT requires a Hazardous Release of Energy (HROE) guard to dissipate any parts or debris that may come off the clutches. Additionally, there is a requirement to protect against Pinch Points and Entanglement (PPAE), guards must be added to prevent fingers or clothing from reaching the clutches in the directions perpendicular to their radial plane. The strict material and clearance specifications have made these guards much more of a hassle than anticipated in the past. Last year's CVT cover was difficult to remove, put on, and adjust. There were also issues at competition with last minute modifications needing to be made. While the initial plan was to have a one-piece loop for the HROE guard, other vehicle constraints have led us to pursue a two-piece loop, top and bottom half. This gives us the ability to remove the cover vertically from the clutches, or the option to remove the top half and still access the CVT. For rules compliance, manufacturability, and integration with the PPAE expanded metal on the front of the cover, 16-gauge mild steel was chosen for the HROE loop. To give our latching mechanisms better adjustability we have incorporated rubber and spring-loaded draw latches. We anticipate these will overcome the lack of precision from the given manufacturing capabilities, mitigating issues in securing the cover. Lastly, we have given ourselves a buffer with material choice and clearance in an effort to avoid issues at competition, and we have also submitted a rules clarification to better understand the constraints. The back plate is of HROE compliant aluminum, and more than the specified 0.5 inches away from the clutches. The back plate has slots for the engine mounting and slightly radial slots on the transfer case mounts to allow for tensioning of the belt.

4.2.1.2.1. <u>CVT Cover Critical Rules:</u>

- B.9.1 Powertrain Guard Function
- B.9.2 Hazardous Release of Energy (HROE)
- B.9.3 Pinch Points and Entanglement (PPAE)

4.2.1.2.2. <u>CVT Cover Cad Model:</u>

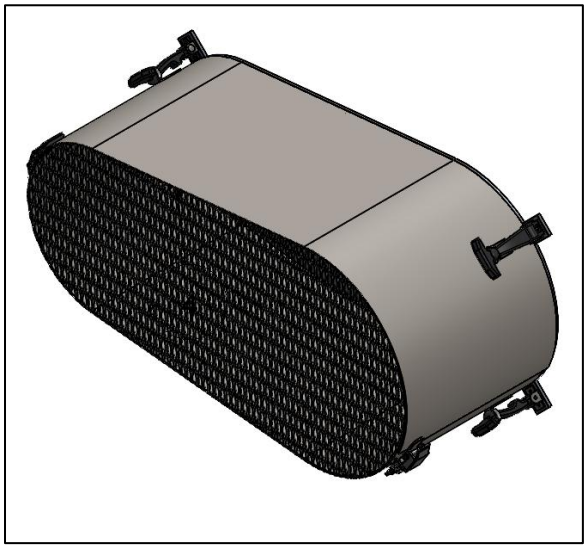

Figure 107: Full CVT Cover, HROE and PPAE

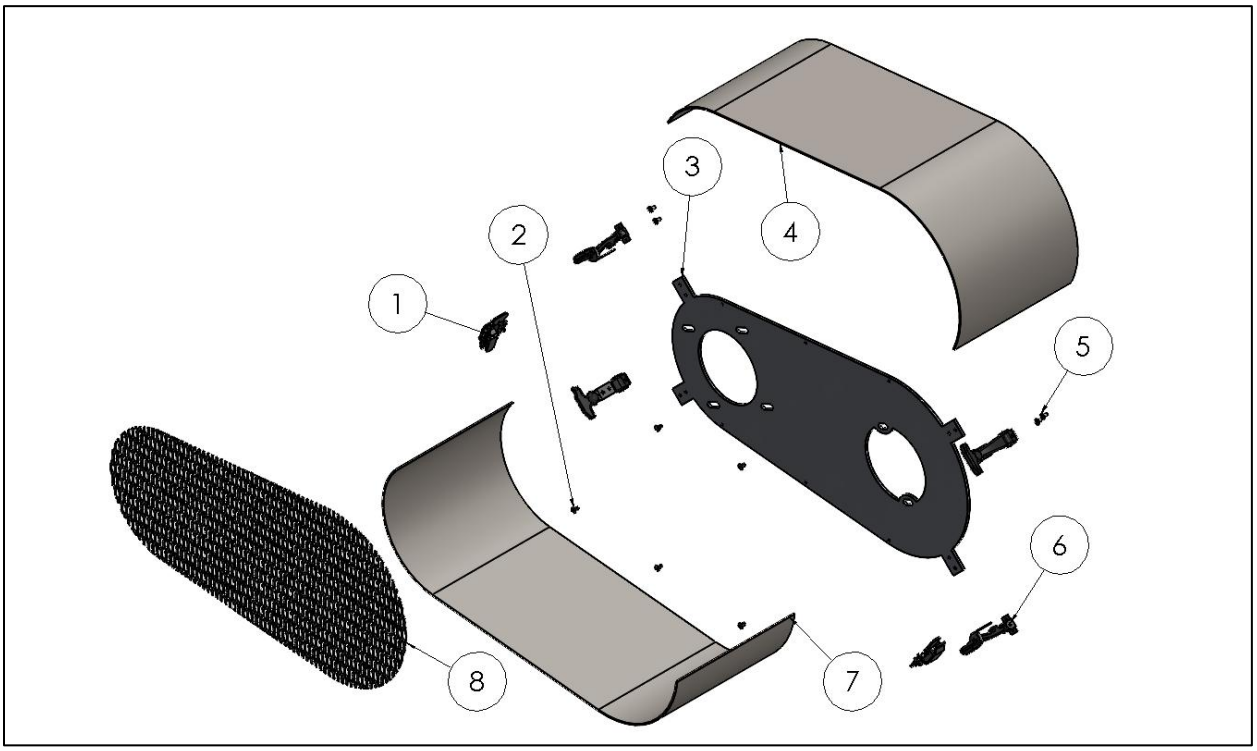

Figure 108: CVT Cover Exploded View

4.2.1.2.3. CVT Cover BOM:

BOM Part #	Description	Qty:	Source (Hyperlink to Part)	Cost:	Weight/1Pc [lbs]
1	Tight-Hold Draw Latch	2	McMaster Carr	$5.93	0.06
2	Flat Head Screws	6	McMaster Carr	$5.27	~
3	Back Plate	1	Metal Supermarkets	$55.56	1.29
4	HROE Top Half	1	Online Metals	$12.50	2.75
5	Rivets	8	McMaster Carr	$10.52	~
6	Rubber Draw Latch	4	McMaster Carr	$8.78	0.05
7	HROE Bottom Half	1	Online Metals	$12.50	2.85
8	Expanded Sheet Metal	1	McMaster Carr	$27.77	0.1
Total				275	

Table 19: CVT Cover BOM

4.2.2 Transfer Case ("Franken-box")

Primarily, the Franken-Box was designed for reliability throughout the four-hour endurance race. It accomplishes this by reducing the system complexity of the drivetrain, allowing for easier integration into the car with less dependency on an ideal assembly. The spur gears inside the box have a gear ratio of 2.44:1 which changes the final drive past the CVT to 9:1. Compared to last year's final drive of 11:1, the reduced gear ratio will increase the acceleration of the car improving performance in both the endurance race and the acceleration event. The Franken-Box utilizes a CNC'd clamshell design not only for ease of assembly and serviceability, but also to support the mesh of multiple different gear types within the box. To lower the COG, the engine was lowered by roughly 1.5 inches compared to last year. The Franken box accomplishes this by changing the height between the CVT and the driveshaft, where the input to the Franken Box is higher than the output based on the size of the spur gears used. The engine can then be lowered down to the height of the driveshaft HROE without the secondary of the CVT sticking out of the bottom of the frame. This geometry change supports the serviceability of the drivetrain system as well, moving the CVT Cover into a location much easier to access. Other advantages between the Franken-Box and the CVT include the support for the CVT secondary. Because the Franken-Box is mounted to the CVT cover backplate, no external geometry from the Franken-Box (such as the "snout" on last year's car) is necessary. Regarding mounting, the Franken-Box has adjustability is built into the mounting geometry, meaning that alignment issues become much more manageable during assembly. This is especially important, as the output shaft of the Franken-Box connects directly to the rear differential without a U-joint or similar feature. Since critical components are grouped in the Franken-Box, managing the alignment of this component sets up the rest of the drivetrain to function properly. The CVT and Driveshaft location relative to the frame are directly influenced by the location of the Franken-Box on the frame.

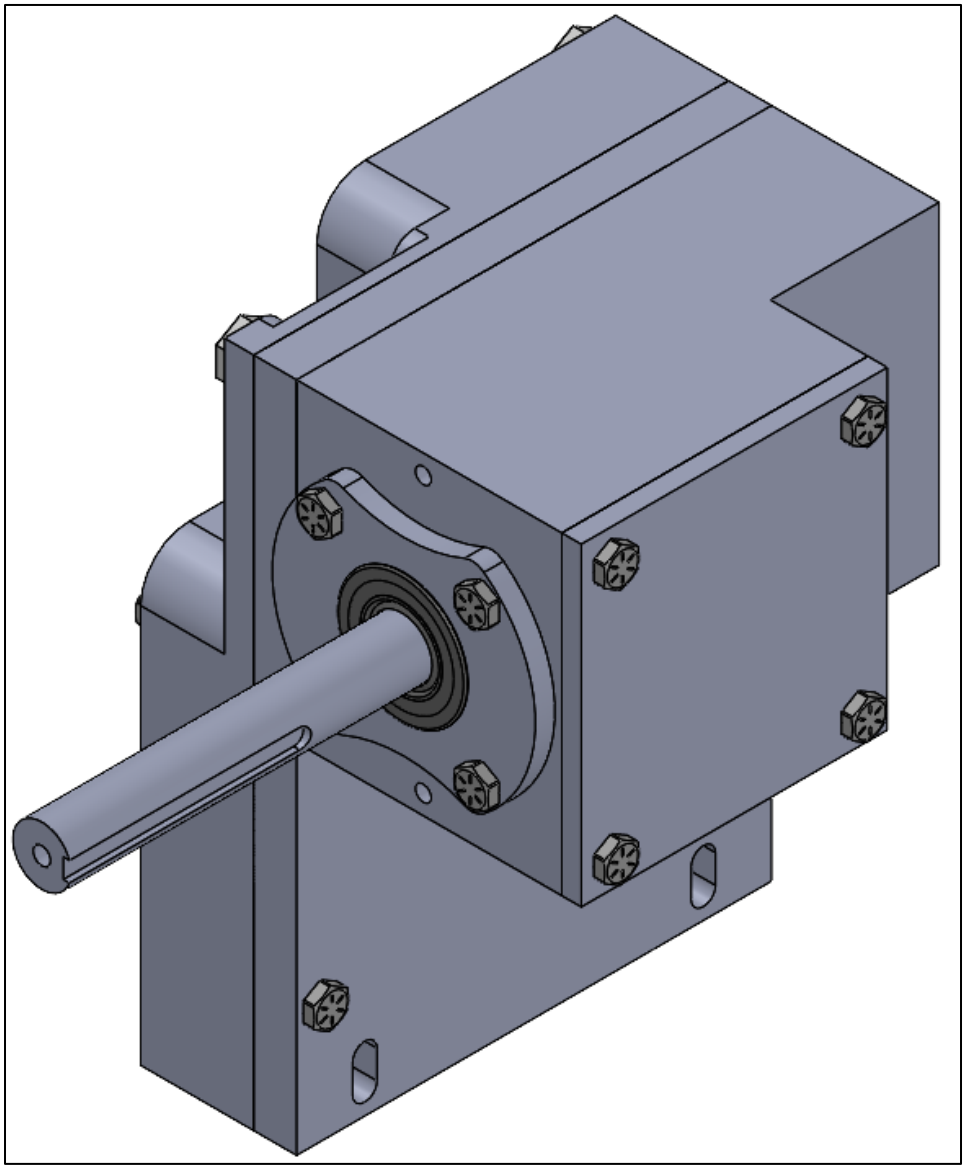

Figure 109: Isometric view of the Franken-Box, a single-stage reduction ninety-degree power transfer gearbox.

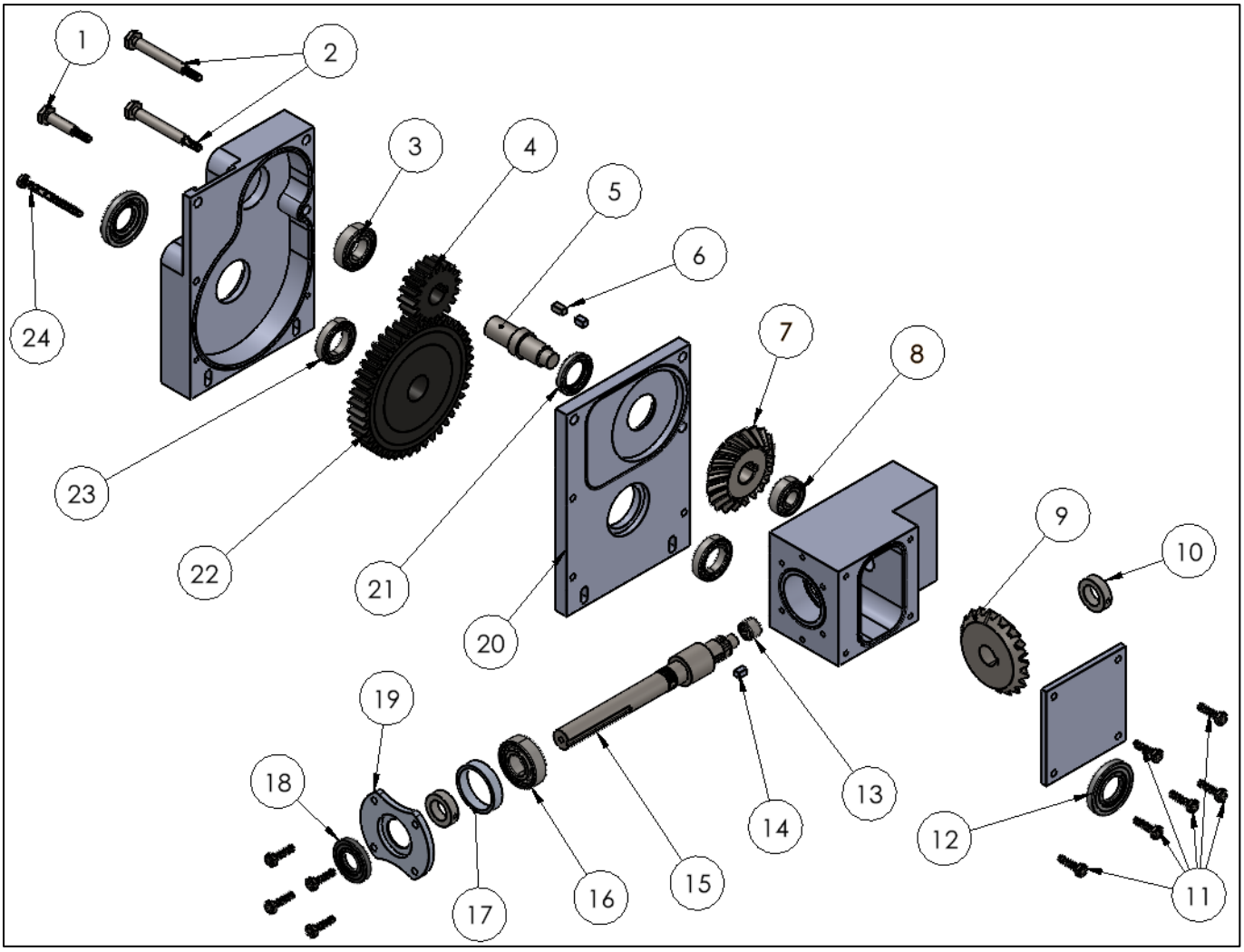

Figure 110: Exploded view of the Franken Box and BOM labels.

Figures 109 and 110 above show the current iteration of the Franken-Box, a gearbox containing a single stage reduction in the form of two spur gears and a ninety-degree power transfer accomplished with a set of spiral bevel miter gears. Table 20 represents the BOM associated with the Franken-Box.

BOM Part #	Description	Qty:	Source (Hyperlink to Part)	Cost:	Weight/1Pc [lbs]
1	3/8 X 1-5/16", ¼-20 thread Shoulder Bolt	1	McMaster-Carr	$7.13	0.06
2	3/8 X 2-1/2", ¼-20 thread Shoulder Bolt	2	McMaster-Carr	$14.52	0.1
3	6004 Deep Groove Ball Bearing	1	SKF	$51.74	0.115
4	SS3-18	1	KHK	$46.35	0.62
5	Pinion Shaft	1	Online metals	$30.08	0.41
6	12mm X 7mm X 7mm Key	1	McMaster-Carr	$6.25	0.01
7	MMS4-20L	1	KHK	$146.91	1.07
8	6202Deep Groove Ball Bearing	1	SKF	$29.26	0.096
9	MMS4-20R	1	KHK	$146.91	1.07

10	SKF 20mm X 32mm X 9mm Lockring	2	One on hand, other from SKF	$159.17	0.07
11	¼-20 X 1" Grade 8 Hex Head Bolt	1	McMaster-Carr	$17.24	0.02
12	25X52X7 HMSA10 RG	2	SKF	$9.85	0.04
13	HK1212 Needle Roller Bearing	1	SKF	$19.97	0.022
14	10mm X 7mm X 7mm Key	1	McMaster-Carr stock listed above	0	0.01
15	Input shaft	1	Online Metal stock listed above	0	1.21
16	6204 Deep Groove Ball Bearing	1	SKF	$26.61	0.225
17	Input Bearing Spacer	1	Metals Depot	$8.33	0.03
18	19X42X6 HMSA10 RG	1	SKF	$9.85	0.04
19	Input Flange Plate	1	Online Metals	$25.83	0.14
20	Clamshell Case	1	Metals Depot,	$43.76	9.78
21	25X40X5 HMSA10 RG	1	SKF	$9.00	0.04
22	SS3-44	1	KHK	$173.03	4.32
23	61905 Deep Groove Ball Bearing	2	SKF	$156.30	0.091
24	¼-20 X 2.75" Grade 8 Hex Head Bolt	1	McMaster - Carr	$13.32	0.04
-	0.002" shims	22	McMaster	$2.93	0.005
-	Hose Fitting	2	McMaster	$4.86	-
-	Drain Plug	2	McMaster	$1.95	-
-	ATV Bellow	2	Polaris	$15.99	-
-	SAE 80W-90 Gear Oil	-	On Hand	0	
-	Rubber rod	1	Amazon	$7.99	-
Total				1610	

Table 20: Franken-Box BOM

4.2.2.1. Internal View of the Franken-Box

The Exploded view in Figure 110 above shows all critical components of the Franken-Box but does not provide a clear image of the internal assembly of the gearbox. Particularly, the spiral bevel miter gears whose mesh requires additional design and features to keep aligned. Figure 111 below shows a color-divided section view of the Franken-Box for the miter gear mesh.

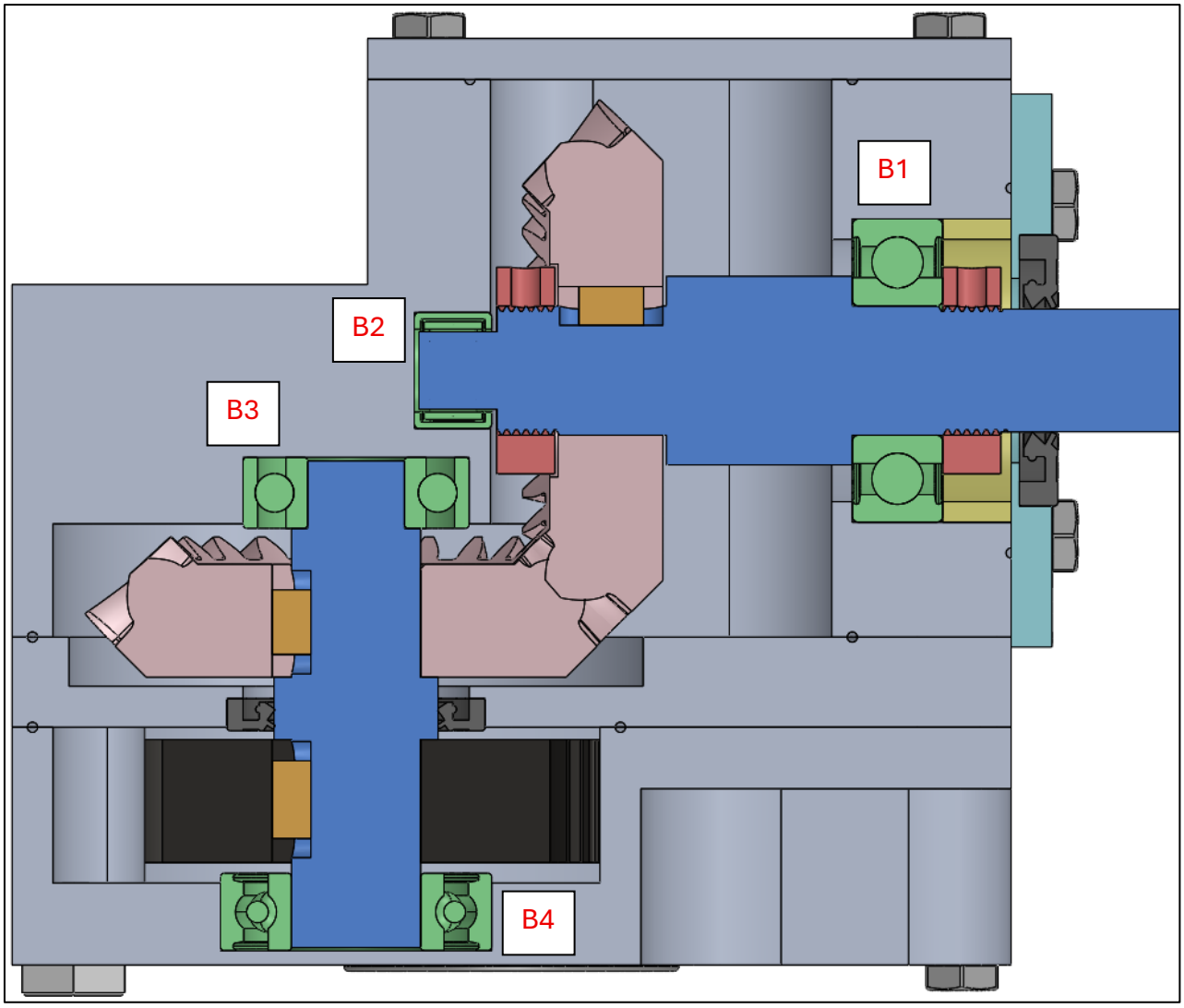

Figure 111: Cross section view of the spiral bevel gear mesh and supporting geometry.

Blue is for shafts, yellow for spacers, green for bearings, red for lockrings, orange for keys, brown for shaft seals, magenta for spiral gears, cyan for the flange plate supporting B1, and black for spur gears. B1, B2, B3, and B4 refer to the bearings inside the case, used heron out for brevity. On the input shaft, shown exiting the box on the right side of Figure 111, there are two lockrings to keep compression on the shaft. This prevents the spiral gears from moving once in mesh. Although not shown, shims between the lockring, input shaft step, and the input spiral gear control the axial backlash of the input spiral gear. To control the axial backlash on the pinion shaft spiral gear, a similar method of spacers will be used between the pinion shaft step, B3, and the pinion shaft spiral gear. To account for the axial load of the spiral bevel gears, we selected a right-hand spiral for the input shaft gear and a left-hand spiral for the pinion shaft gear. This places the axial loads on B1 and B4 respectively, which don't have as tight space constraints as B2 and B3. Keeping both the spur gear and the spiral gears lubricated means separating the compartments between each gear set, done using a shaft seal.

4.2.2.2. Problems with the current Franken box:

The version of the Franken box displayed in this report shows the thought process behind many of the critical components, however, there are still additional features and geometry changes required to make the Franken box both functional and fully rules compliant. The following contains a list of problems and their description.

- Lockring size on the input shaft.
    - Currently, the lockring has an ID of 20mm, and to keep compression on B1, has to press against the inner race of B1. The threads on the input shaft currently recess into the input shaft, meaning the lockring doesn't fit on the input shaft without modification. The current plan is to modify the ID of the lockring just slightly to fit over the input shaft.

- B1 shaft press fits over threads.
    - On the input shaft, B1 will need to be press fit over the lockring threads, which will certainly deform them. The current plan is to change the ID of B1 to be larger than the threads and step up the shaft after the threads.

- Round rubber gasket cord grove geometry
    - The geometry of the round rubber gasket cord groves in the clamshell case doesn't put compression on the gasket material. This means a seal isn't created and the gasket material isn't necessary. The plan is to consult relevant standards for O-ring groove depth.

- Spacer lengths and locations on the pinion shaft
    - There aren't spacers in the franken box right now, and they are necessary to control the spacing of the spiral and spur gears on the shaft. They also prevent the shaft from moving axially and rubbing against housing. Relevant spacers will most likely be sourced from McMaster-Carr or machined if unique geometry is needed.

- Interference between Shoulder bolt and the engine oil fill port.
    - The head of the shoulder bolt on the spur side of the clamshell case interferes with the engine fill port when the engine is moved back to tension the CVT belt. Changing the thickness of clamshell case where the shoulder bolt head currently rests on will solve this issue.

- Tensioning the CVT belt
    - The Franken-Box is very close to the engine, and as such, the engine can only move back a small amount before interfering with the Franken-Box. This is an issue, as getting the CVT on the engine and Franken-Box means the belt needs to be tensioned as the CVT is put on the engine and input shafts. As of right now, we do not have a reliable solution for this issue. Gaining some movement out of the engine by changing the Franken-Box geometry on the spur case may be possible.

- Determining gear lubricant
    - As of right now, there isn't a specific gear lubricant sourced for the Franken-Box. We have looked at information regarding fluid lubricant, and determined splash lubrication is sufficient for the gears. The current plan is to determine an ideal viscosity of lubricant and confirm the properties of the sourced lubricant match our application.

- Adding an expansion chamber
    - As of right now, there isn't any expansion chamber or fill port geometry integrated into the Franken-Box. We have sourced both of these components, and they are on the BOM, but they still need to be added. One consideration is that multiple fill and drain ports are required. According to rule B.9.4, the isolated compartments of the Franken-Box will need to have an appropriately sized expansion chamber connected to them.

4.2.2.3. Franken-Box relevant stress analysis:

The most important part of the Franken-Box is making sure that the gears inside don't fail. According to AGMA standards, the spiral gears have a safety factor of 2.5 and the spur gears have a safety factor of nearly 4. Both safety factors were determined using the Lewis Bending stress equation, which approximates the gear teeth as cantilevered beams and applies factors to account for geometry and the variety of conditions the gear is under. Other important failure modes to check are the tear out of the threads by shear, and the tear out of the wall due to bearing axial forces.

Failure Condition: Engine at peak torque while the front wheels are just off the ground and the Gage CVT is at its minimum gear ratio.

Justification: If this occurs, then the Spiral gears will experience the maximum realistic torque possible. Making sure the gears survive this will increase reliability

Load Diagram:
Ref: KHK Gear Forces Reference

Tangential, radial, and axial forces generated by the mesh of the spiral bevel gears.

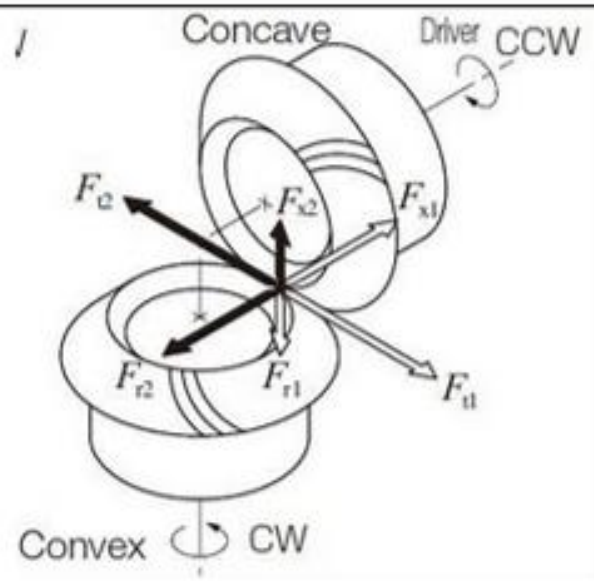

FOS: 1.45

Equations (If Applicable):

$$\sigma_F = F_{tm}\frac{Y_F Y_\varepsilon Y_\beta Y_C}{0.85\cos\beta_m mb}\frac{R_e}{R_e - 0.5b}\left(\frac{K_M K_V K_O}{K_L K_{FX}}\right)K_R$$

Confidence Level & Explanation

Medium confidence level. Accurate equations for torque loading and comparison to last years car.

Calculations and/or FEA:

```
Safey factor under JGMA standards:

    1.45


Last years safety factor under JGMA standards:

    1.01


Safety factor under last years conditions (AGMA standard):

    2.57


Last years safety factor under last years conditions (AGMA standard):

    2.34
```

Figure 112: Spiral Bevel Gear Stress Analysis

Failure Condition: Full axial force from spiral bevel miter gears on B1, supported by the bearing flange plate

Justification: If the engine is at peak torque, and the front wheels are just off the ground, and the CVT is at the minimum gear ratio, the gears would experience the maximum possible realistic torque, placing the maximum axial force on the bearing plate

Load Diagram:

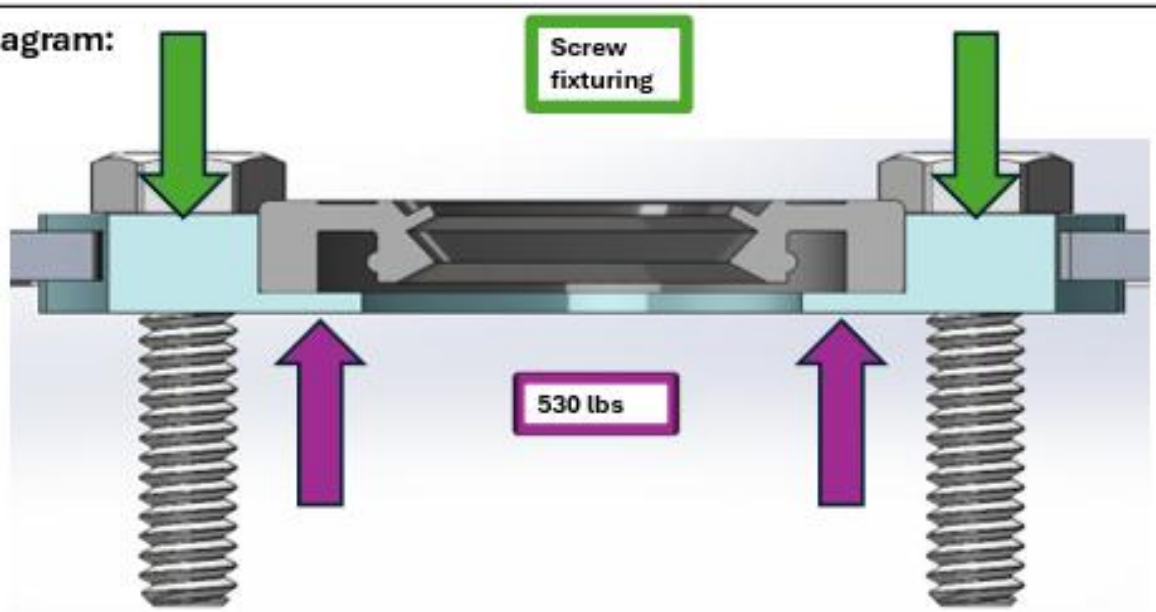

FOS: 14.7

Equations (If Applicable):

$$\tau = \frac{F}{A}$$

Confidence Level & Explanation

Medium confidence. Shear tear out calculation for the plate thickness.

Calculations and/or FEA:

```
%% Tearout stress on the bearing bore step
% Aluminum shear yield strength
SY_al = 30000; %psi

A_shear_mid = pi*42*0.05/25.4;
F_shear_mid = 530; %lbs

S_shear_mid = F_shear_mid/A_shear_mid;

SF_shear_mid = SY_al/S_shear_mid;
```

```
Shear tearout Factor of safety for B1: 14.7
```

Figure 113: Analysis of Spiral Bevel Miter Gears Backlash Under Maximum Possible Torque

Failure Condition: Spiral Bevel gear at full axial load against B1 where three out of the four bolts have backed out of the bearing flange plate.

Justification: Excessive vibrations may cause the bolts to back out of the housing, and in the worse case, there would only be one bolt left to withstand the load.

Load Diagram:

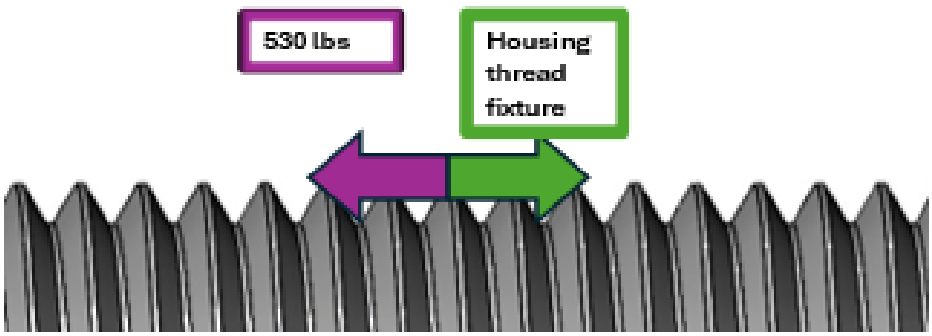

FOS: 20

Equations (If Applicable):

$$A = \pi(dr)(wi)(Tpi)$$

$$\tau = \frac{F}{A}$$

Confidence Level & Explanation

Medium confidence. Equations known to be accurate and the failure criteria is extremely unlikely.

Calculations and/or FEA:

```
% Shear stress to strip the threads
wi = 0.8;
Q20p = 1/20;

Astrip = pi*dr*wi*Q20p;

F_axial_input = (2.3553e+03)/4.4482216152605; %lbs

% Shear strength
Sys_q20 = 30000; %psi
num_threads = 20;

SF = num_threads*(Sys_q20*Astrip)/(F_axial_input);
```

```
Safety factor with only one bolt:  20.00
```

Figure 114: Analysis of Spiral Bevel Gear at Full Axial Load Against B1

4.2.2.4. Bearings

Following the approach of the 2024-2025 team, we chose to select deep groove ball bearings to eliminate the necessity of pre-load in our design. Selecting these bearings, we performed a detailed analysis of forces induced by the spiral bevel miter gears, spur gears, and the bending moment produced from the tension in the CVT belt on the input shaft. The CVT belt tension was estimated by taking the motor's torque, times the maximum CVT gear ratio, times the diameter of the CVT secondary pulley which resulted in a force of approximately 900N.

KHK's website has an incredibly useful gear force calculator to speed up this process, however the equations governing gear forces can be seen in Table 27 and Table 28, alongside Figure 159 and Figure 160. Once gear forces were solved, all bearing reaction forces could then be found via a typical mechanics approach (a sum of moments/ forces.) As with years prior, we are anticipating a sponsorship from SKF this year, so all bearings will be sourced from this vendor. Their "product select" website was utilized to spec and determine L_{10} values for all 6 bearings. These values, in hours, can be seen in Table 21.

Bearing Number	Description	Anticipated Radial Load [kN]	Anticipated Axial Load [kN]	L_{10} [h]
1	6204: Deep Groove Ball (Input Shaft)	2.32	2.36	809
2	HK1212: Needle Roller (Input Shaft)	2.11	0	692
3	6202: Deep Groove Ball (Intermediate Shaft) _	2.97	0	362
4	6004: Deep Groove Ball (Intermediate Shaft) _	3.17	0.53	558
5	61905: Deep Groove Ball (Output Shaft) _	1.93	0	871
6	61905: Deep Groove Ball (Output Shaft) _	1.93	0	871

Table 21: Bearing Numbers, Types, Loads, and L_{10} Values

4.2.2.5. Franken-Box Output Shaft

To connect the Franken-Box to the rear differential, the output shaft has a keyed slot connecting to the spur gear in the Franken-Box and a spline pattern that connects to the input pinion on the Yamaha differential. While we don't have the capabilities to machine an internal spline, we can modify one of the old U-joints with the Yamaha internal spline pattern to press fit into the end of the output shaft. Roll pins with axes parallel to the output shaft axis will be inserted between the shaft housing and the Yamaha differential. Figure 115 below shows the output shaft.

Figure 115: Output shaft with press fit internal spline and roll pin holes between the output shaft and spline pattern.

4.2.2.6. Shafts & Keys

The shaft and key dimensions were decided based on a mix of gear choices, bearing limitations, axial loading considerations, and stress analysis. There are 3 shafts going through the gearbox, the input shaft, the pinion shaft, and the output shaft. Both the input and pinion shaft are ¾" in diameter, and the output shaft is increased to 1" in diameter to account for the increased torque due to the gear reduction. In order to calculate these diameters, we used an equation that mixes Von Mises Stress and Goodman fatigue criteria in order to estimate a minimum shaft diameter based on a chosen factor of safety, in this case 1.5. We use normalized AISI 4140 Steel for its increased strength while still maintaining machinability (HRC 32), which allows us to help support loading cases such as our cantilevered CVT secondary on our input shaft.

$$d = \left\{ \frac{32N_f}{\pi} \left[\frac{\sqrt{\left(K_f M_a\right)^2 + \frac{3}{4}\left(K_{fs} T_a\right)^2}}{S_f} + \frac{\sqrt{\left(K_{fm} M_m\right)^2 + \frac{3}{4}\left(K_{fsm} T_m\right)^2}}{S_{ut}} \right] \right\}^{\frac{1}{3}}$$

Figure 116 – Equations used to solve for shaft diameter

```
Assuming normalized AISI 4140 with an Ultimate Tensile Strength of 1020 MPa
Minimum Shaft Diameter (in) calculations for a Factor of Safety of 1.5
Input shaft minimum diameter (in): 0.71546
Pinion shaft minimum diameter (in): 0.62744
Output shaft minimum diameter (in): 0.75481
```

Figure 117 - Estimated Minimum Shaft Diameters

These shafts also include a variety of steps and threads in order to enforce gear mating distances and gearbox stability, along with key slots for the keys used for our CVT, gears, and driveshaft. Besides the CVT key slot which uses a 0.25” x 0.25” key, all keys used inside the Transfer Case are 7mm x 7mm in width and height, with the length varying based on each gear’s specific geometry and clearance. Our key Factor of Safety used was 1.5, and all keys meet or exceed this in terms of both shear and bearing stress experienced. Included below are the equations used to solve for the stresses:

$$\tau_{xy} = \frac{F}{A_{shear}} \qquad \sigma_x = \frac{F}{A_{bearing}}$$

Figure 118 – Equations for Average Shear and Bearing Stress for keys

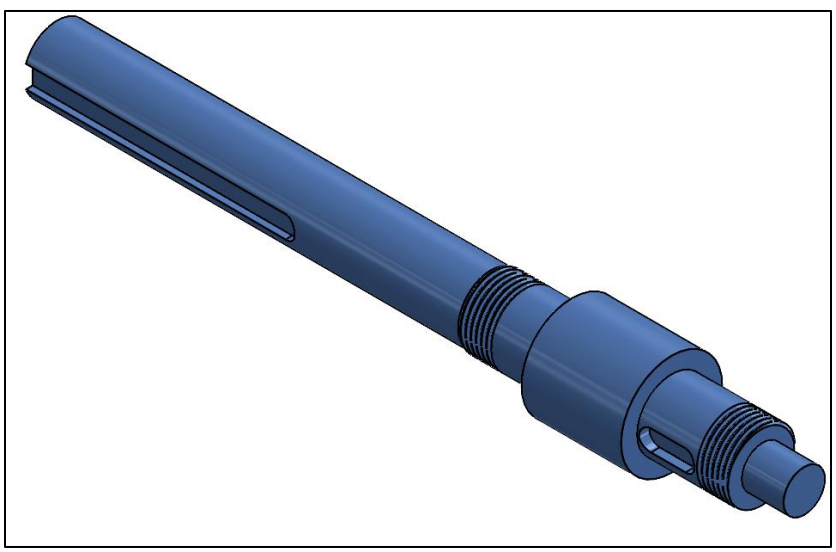

Figure 119 – Transfer Case Input Shaft

```
Material Properties for 1045 Steel with Brinell B87 Hardness
Ultimate Shear Strength: 329 MPa
Yield Strength: 450 MPa
Ultimate Tensile Strength: 570 MPa
Minimum Factor of Safety Goal for Keys: 1.5
----------------------------------------
Key #1: Input Shaft Spiral Bevel Gear Key
Shear stress: 142.3873 MPa                      about a 2.3106 FOS
Crush stress: 284.7745 MPa                       about a 1.5802 FOS
----------------------------------------
Key#2_1: Pinion Shaft Spiral Bevel Gear Key
Shear stress: 149.9813 MPa                      about a 2.1936 FOS
Crush stress: 299.9625 MPa                       about a 1.5002 FOS
----------------------------------------
Key#2_2: Pinion Shaft Spur Gear Key
Shear stress: 124.9844 MPa                      about a 2.6323 FOS
Crush stress: 249.9688 MPa                      about a 1.8002 FOS
----------------------------------------
Key#3: Output Shaft Spur Gear Key
Shear stress: 141.7146 MPa                      about a 2.3216 FOS
Crush stress: 283.4291 MPa                      about a 1.5877 FOS
```

Figure 120 - Key Stress Calculations Results

4.2.2.6.1. Strength Calculations for Shaft and Keys

Failure Condition: Input shaft experiences yielding due to bending moments and torques greater than the yield strength of our material, normalized AISI 4140 Steel.

Justification: The major loads that would cause failure on this shaft are the bending moment and torque caused by the Secondary CVT, cantilevered against the bearings. Von Mises and Goodman fatigue are well recognized methods for calculating shaft failure.

Load Diagram:

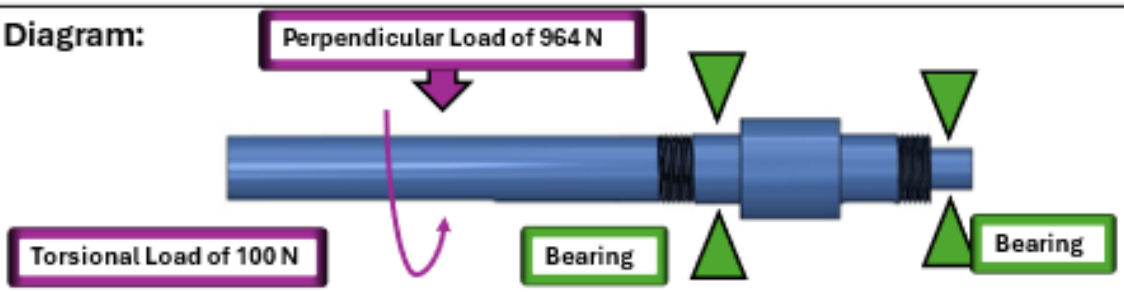

FOS: 1.5

Equations (If Applicable):

$$d = \left\{ \frac{32N_f}{\pi} \left[\frac{\sqrt{(K_f M_a)^2 + \frac{3}{4}(K_{fs} T_a)^2}}{S_f} + \frac{\sqrt{(K_{fm} M_m)^2 + \frac{3}{4}(K_{fsm} T_m)^2}}{S_{ut}} \right] \right\}^{\frac{1}{3}}$$

$$S_f = C_{load}\, C_{size}\, C_{surf}\, C_{temp}\, C_{reliab}\, S_f'$$

Confidence Level & Explanation: Medium-High: Given that our shaft diameters are all larger than our minimum calculated diameter, and assuming a certain level of heat treatment, this should perform well.

Variable	Notes	Value
K_f	Fatigue stress concentration factor	1
K_{fm}	Mean stress fatigue concentration factor	1
K_{fs}	Shear stress concentration factor	1
K_{fsm}	Mean stress fatigue concentration factor	1
M_a	Moment amplitude,	73417 Nmm

Variable	Notes	
T_a	Alternating torque	5000 Nmm
T_m	Mean torque	100000 Nmm
S_f	Fatigue limit, found through correction factors	276.8344 Mpa
S_{ut}	Ultimate tensile strength of material	1020 Mpa
N_f	Safety factor	1.5
S_f'	Uncorrected fatigue limit	510 MPa

Figure 121 - Input shaft failure calculation

Failure Condition: The keys will yield if they experience too much bearing or shear stress, binding up in the shaft and causing failure.

Justification: Bearing and shear stress are the two different ways keys can fail, with the forces coming from the torque of the shaft and gears.

Load Diagram:

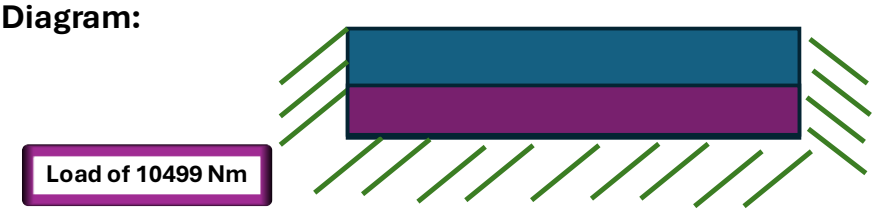

FOS: Minimum of 1.5

Equations (If Applicable):

$$\sigma_x = \frac{F}{A_{bearing}} \qquad \tau_{xy} = \frac{F}{A_{shear}}$$

Confidence Level & Explanation:
High: According to calculations, every key is greater than our minimum factor of safety.

Calculations and/or FEA:

$$\sigma_x = \frac{2T}{(H - depth) * l * D} * \frac{1}{10^6} = 284.8\ MPa(2.3\ FoS)$$

$$\tau_{xy} = \frac{2T}{W * l * D} * \frac{1}{10^6} = 142.4\ MPa(1.6\ FoS)$$

Variable	Notes	Value
W and H	Width and height of key	7 mm
D	Shaft Diameter	0.75 in
T	Torque (worse case)	100 Nm
L	Key length	10 mm
depth	Key slot depth	3.5 mm

Figure 122 - Key failure calculation

4.2.3. Differentials

4.2.5.1. Discussion of Selection Reasoning and CAD Model:

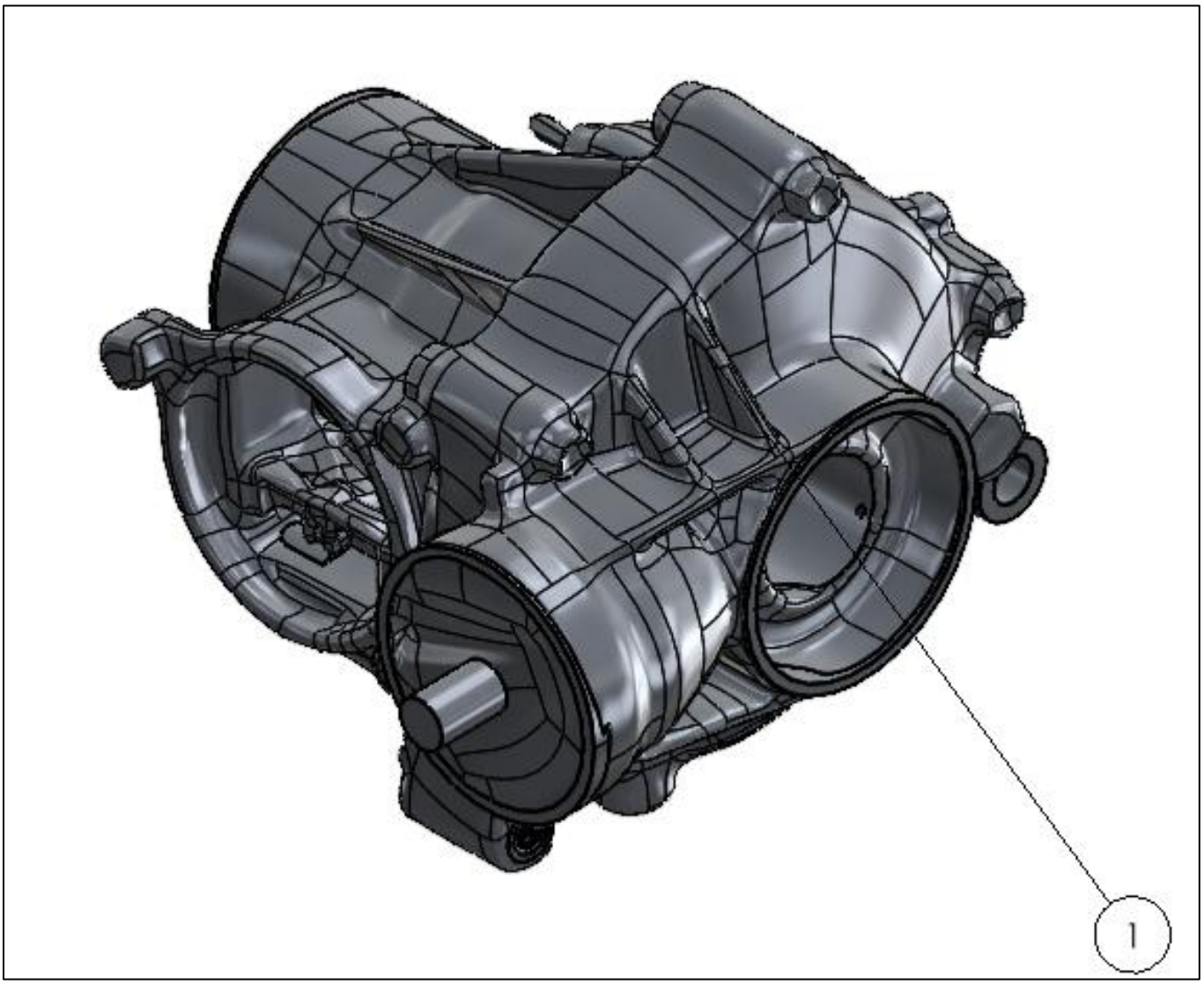

We decided to reuse the same differentials from last year since they proved to be reliable. Initially we had considered replacing the rear differential with a custom-made locked differential, as we did not see a reason to unlock the rear wheels. This switch initially seemed beneficial since we could design the locked rear differential to be smaller and lighter than the Yamaha differential. However, selecting gears for this proved to be more difficult than expected and the locked diff ended up being heavier and larger than the Yamaha. This prompted us to switch back since the Yamaha since it had an easily engageable locked setting that had already proved itself at competition. Furthermore, the ability to toggle between locked, unlocked, and limited slip will help us achieve our sub team goals of improving acceleration. With the ability to toggle the front differential to fully open and undriven, we can effectively turn out vehicle into 100% rear wheel drive which will help improve the acceleration and handling.

BOM Part #	Description	Qty:	Source (Hyperlink to Part)	Cost:	Weight/1Pc [lbs]
1	Yamaha differential	2	On Hand	0	16.5

Table 22: Differential BOM

4.2.4. CV Axles

4.2.4.1. Discussion of Design Reasoning:

Following the guidance of past Baja teams, we will be using OE Yamaha CV axle shafts alongside a custom sized center shaft to match the geometry of the car. This center shaft will be concentrically welded to the inboard and outboard CV shafts, which will allow for complete adjustability of length.

4.2.4.2. CV Axel CAD Model:

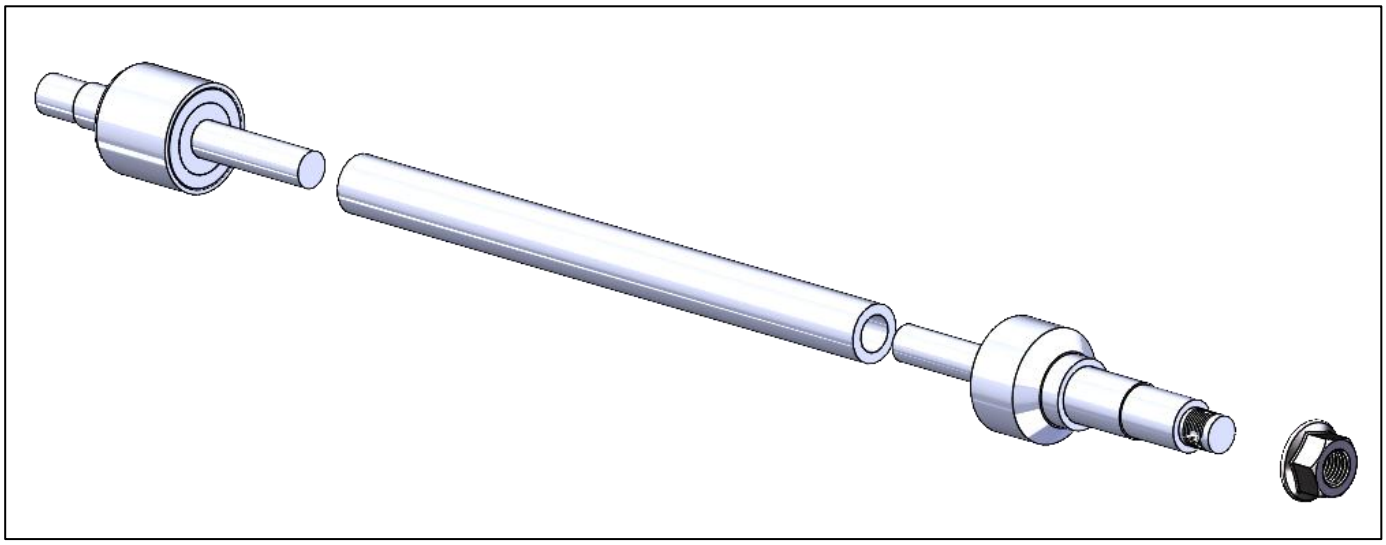

Figure 123: CV Axle Assembly

4.2.4.3. CV Analysis:

Failure Condition: The applied torque on the CV Shafts is too large for the given size and material.

Justification: The 2024-2024 team used a similar wall thickness and material for their shafts.

Load Diagram:

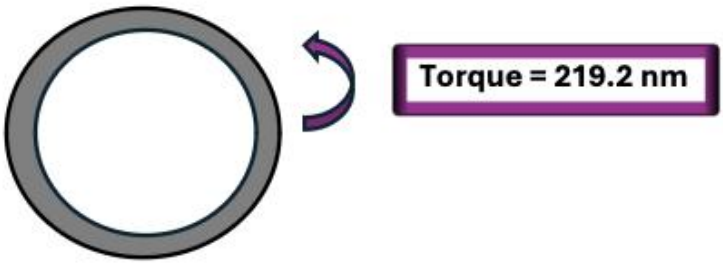

FOS: 10.67

Equations (If Applicable): See Below

Confidence Level & Explanation: Medium high- A large safety factor combined with a known "worst case scenario" gives high confidence.

Calculations and/or FEA:

Torque (in lbf)	applied torque	1940.033333
OD (in)	outer diameter	1.25
Thickness (in)	wall thickness	0.25
Shear Strength (ksi)	4130 tube	62
ID (in)	OD - 2*t	0.75
c (in)	OD/2	0.625
J (in^4)	polar moment	0.208621387
Shear Stress (ksi)	T*c/(J/1000)	5.812063901
Modulus of Rigidity (GPa)	Found on MatWeb	80
Length (in)	Length of shaft from CAD	25
Angle of Twist (degrees)	TL/GJ	1.148000297
FOS	Shear strength/shear stress	10.66746702

Figure 124: Analysis of CVT Center Shaft in Torsion

4.2.5. Driveshaft

4.2.5.1. Driveshaft CAD Model:

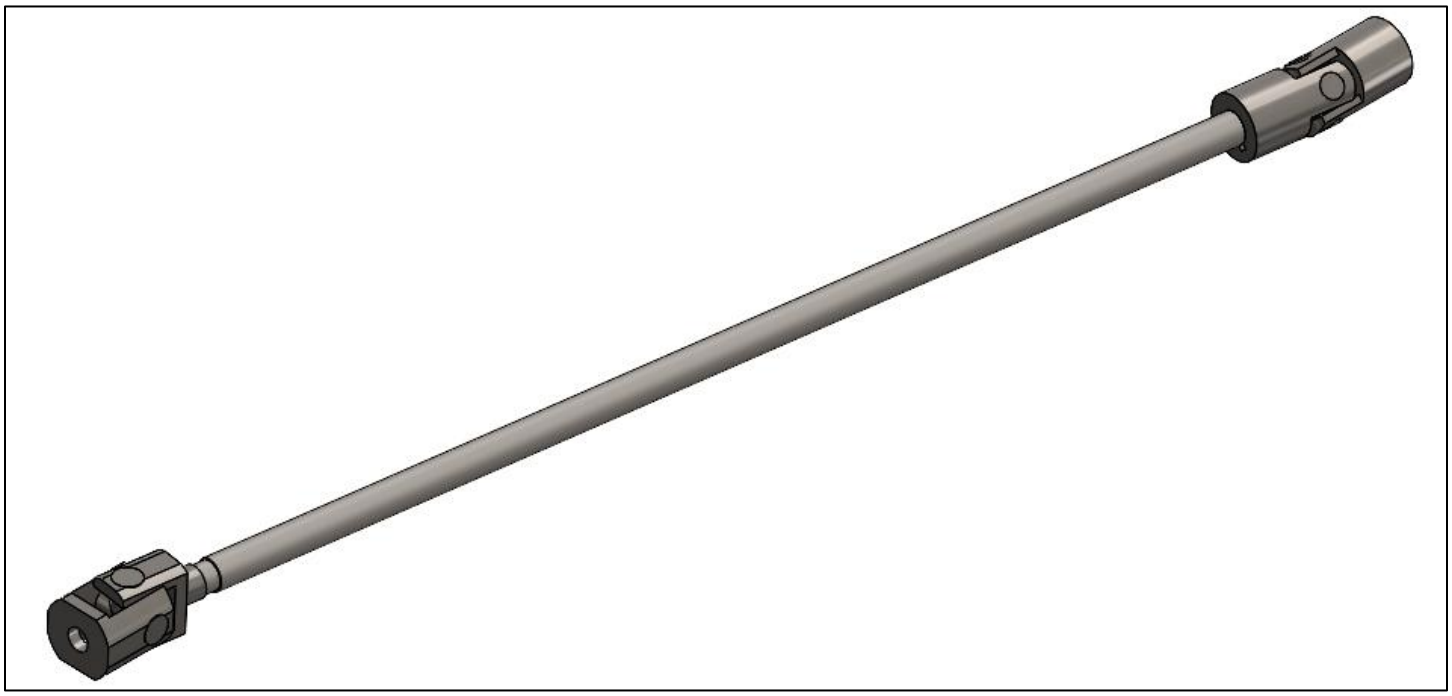

Figure 125: Driveshaft CAD Model

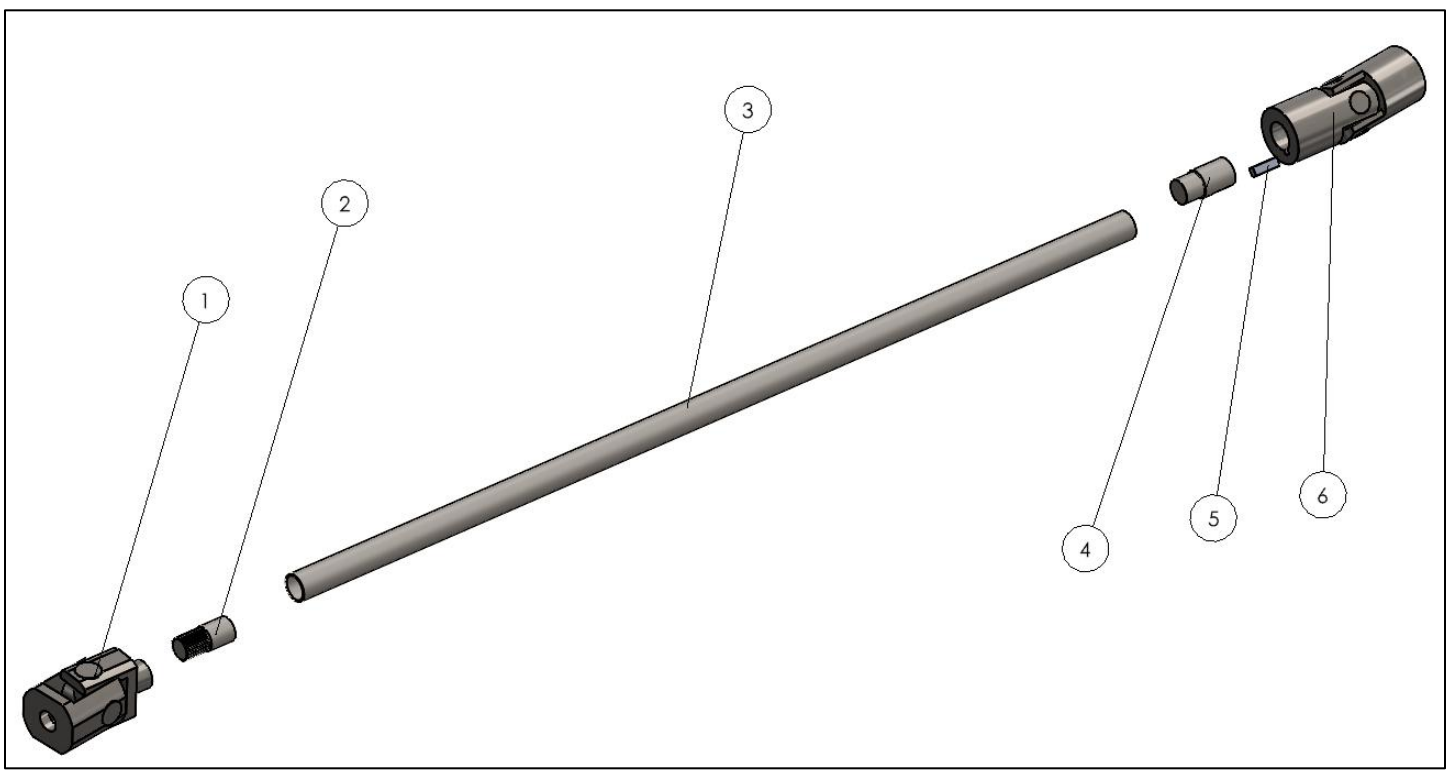

Figure 126: Exploded Driveshaft Model

4.2.5.2. Drive Shaft BOM:

BOM Part #	Description	Qty:	Source (Hyperlink to Part)	Cost:	Weight/1Pc [lbs]
1	Yamaha U Joint	1	On Hand	0	2.5
2	Yamaha Spline Adapter	1	On Hand	0	0.3
3	Driveshaft	1	(Stock) On Hand	0	1.75
4	Belden Joint Adapter	1	Metal Supermarkets	30	0.4
5	Adapter Key	1	(Stock) On Hand	0	0.02
6	Belden U Joint	1	Ebay	150	3.3
Total				180	

Table 23: Driveshaft BOM

4.2.5.3. Drive Shaft Analysis:

Failure Condition: The maximum CVT ratio causes too much torque for the driveshaft to withstand.

Justification: the maximum torque condition comes from calculating the torque on the driveshaft after the transfer case reduction and maximum possible CVT ratio, making it the highest torque we can possibly achieve.

Load Diagram:

Constraints:

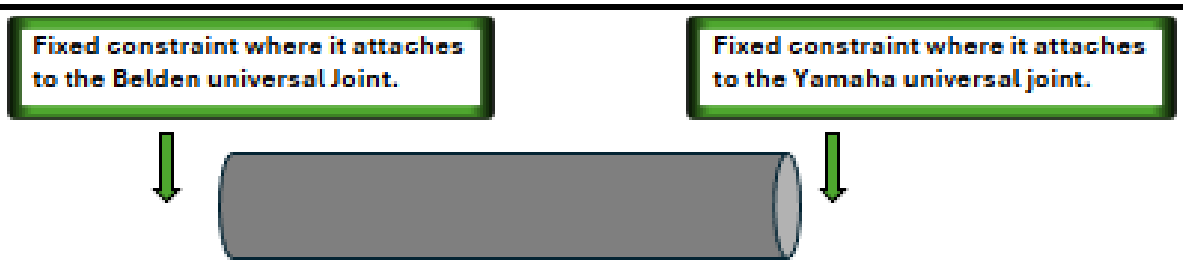

FOS: 2

Equations (If Applicable): See Below

Confidence Level & Explanation: Medium- Since factor of safety is calculated at the highest possible calculated torque but there is not real world measured torque values.

Calculations and/or FEA:

Driveshaft Torque	Input/Output	Equations	Calculation
4130 Alloy Normalized	OD (in)	outer diameter	1
	Thickness (in)	wall thickness	0.049
	G (ksi)	Shear Modulus	11600
	J(in^4)	Polar moment of inertia	0.03319
	T (lb-ft)	Applied torque	175
	Y (Ksi)	Yield strength	63.1

Figure 127: Driveshaft Torsional Failure Analysis

The driveshaft was designed to have a smaller outer diameter than last years for improved drivetrain packaging. In order to achieve this, we increased the outer diameter of the driveshaft to 1 inch, and set the wall thickness to 0.048 inches. We decided to keep the driveshaft material as 4130 steel because it offered better strength at smaller outer diameters than aluminum did. This geometry and material ensure the driveshaft has an acceptable factor of safety, and a reasonable angle of deflection under our max

torque load. Another reason 4130 is preferred is so we can weld in the two shaft adapters on the end of the driveshaft so it can interface with the universal joints. The front adapter utilizes the same method as last year, where we cut the male spline off a Yamaha driveshaft and weld it into an adapter that interfaces with the driveshaft as shown in figure .

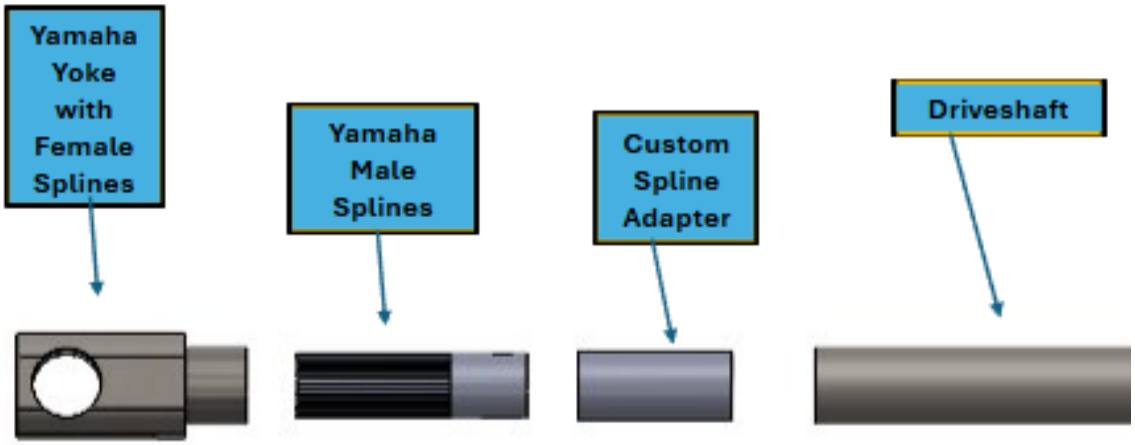

This allows us to take advantage of the female splines on the Yamaha universal joint. For the other shaft connection, we are machining a shaft adapter with a keyway that interfaces with the Belden universal joint keyway. This allows us to have removable connections on both ends of the driveshaft, which will help with serviceability. The stock Yamaha universal joint is being kept due to its easy interfacing capability with the front Yamaha differential. The rear universal joint that interfaces with the transfer case, and is a smaller outer diameter than last year by 0.4 inches to improve driveline packaging and slightly lower engine height.

4.2.5.4. Drive Shaft Critical Component:

Figure 128: Driveshaft U-joint

The critical component pictured above in figure 128 is the Belden universal joint that will be used to connect the driveshaft to the transfer case. The universal joints in the driveline need to in phase with each other so the sinusoidal power output they create is canceled out. We achieved phasing by keeping the output face of the transfer case parallel to the face of the front differential as shown in figure. This ensures that we do not introduce unwanted vibrations into the drivetrain.

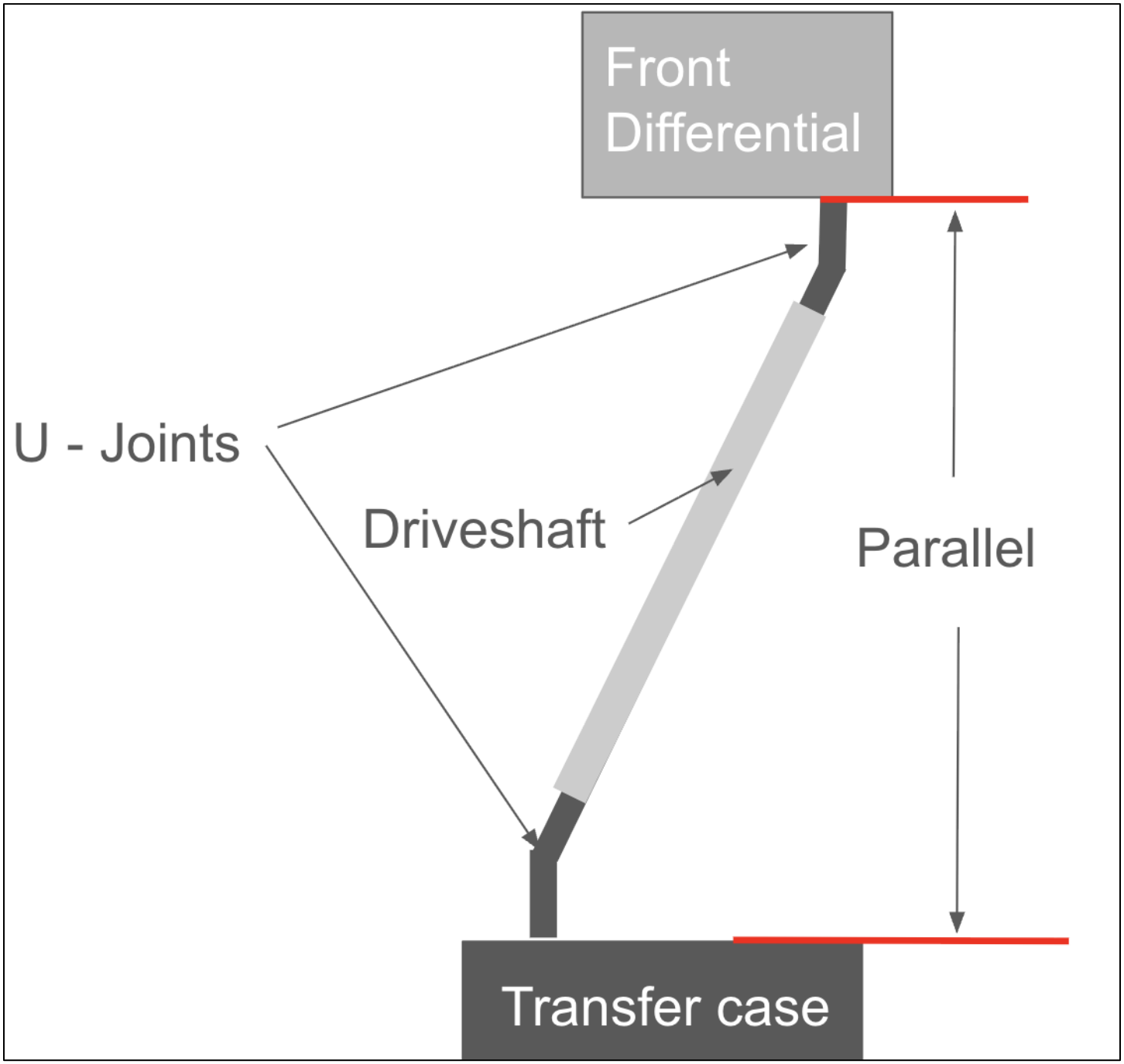

Figure 129: Driveshaft U-joint Phasing Diagram

The universal joint will experience high rpm at the minimum CVT ratio, and high torque at the maximum CVT ratio, so it had to be carefully chosen to withstand the loads at these conditions. Since we are aiming to increase the maximum speed of the vehicle, the joint needs to be capable of running at a higher rpm than last year. In addition to this, we wanted to decrease the overall diameter of the joint to help improve drivetrain packaging. The initial transmissible torque numbers were analyzed using plots published in the Belden Universal Joints and Drive Shafts catalogue. The figures published in this document specified that the universal joints transmissible torque was heavily dependent on the angle of operation multiplied by the rpm. The initial transmissible toque numbers seemed very low, so last year's universal joints were analyzed using this plot, and were found to be well within failure territory. Based on this and the fact the universal joints from last year's car showed no obvious signs of failure, we assumed Belden was factoring in long cycle lifetimes that are much higher than the run time of our vehicle into their curves. To develop a

more accurate plot, last year's universal joints were inspected, and the maximum toque curves were adjusted to the toques they experienced. This yielded an approximated torque curve factor of safety of approximately 2.3 on Belden's plots. The resulting transmissible torque curve for our 2-inch diameter joint using this new factor of safety is shown in figure 130. The blue dot represents the torque on the universal joint at our minimum shaft rpm and current driveshaft angle. The red dot represents the torque on the universal joint at our maximum shaft rpm and current driveshaft angle. The black line indicates the maximum possible transmittable torque for a 2-inch outer diameter driveshaft at a specific angle and rpm. Both dots lie well below the torque curve, meaning they should hold up to the torque we will be applying to them.

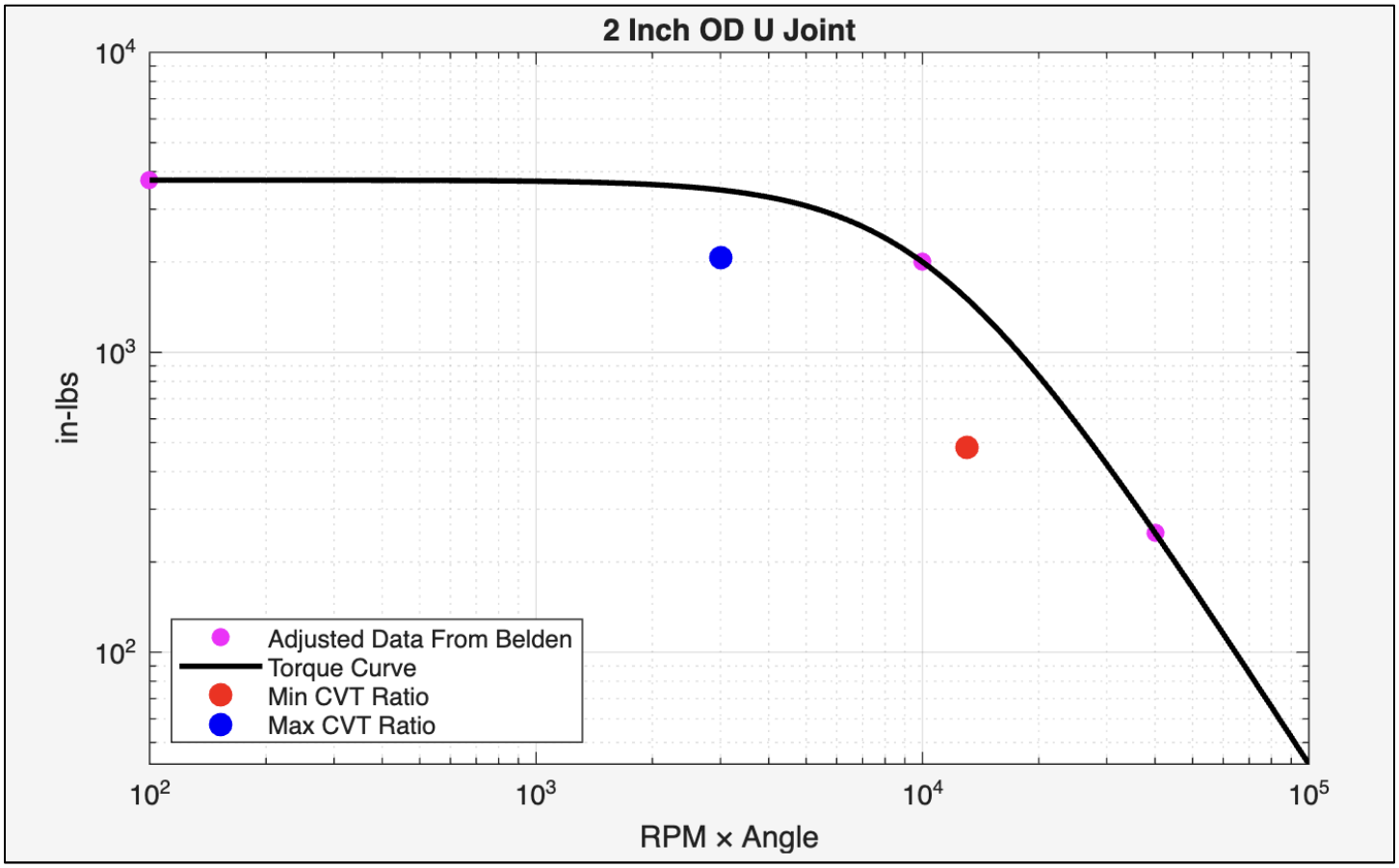

Figure 130: Graph of U-joint angle vs. RPM and Transmittable Torque

4.2.5.5. HROE and PPAE Guards

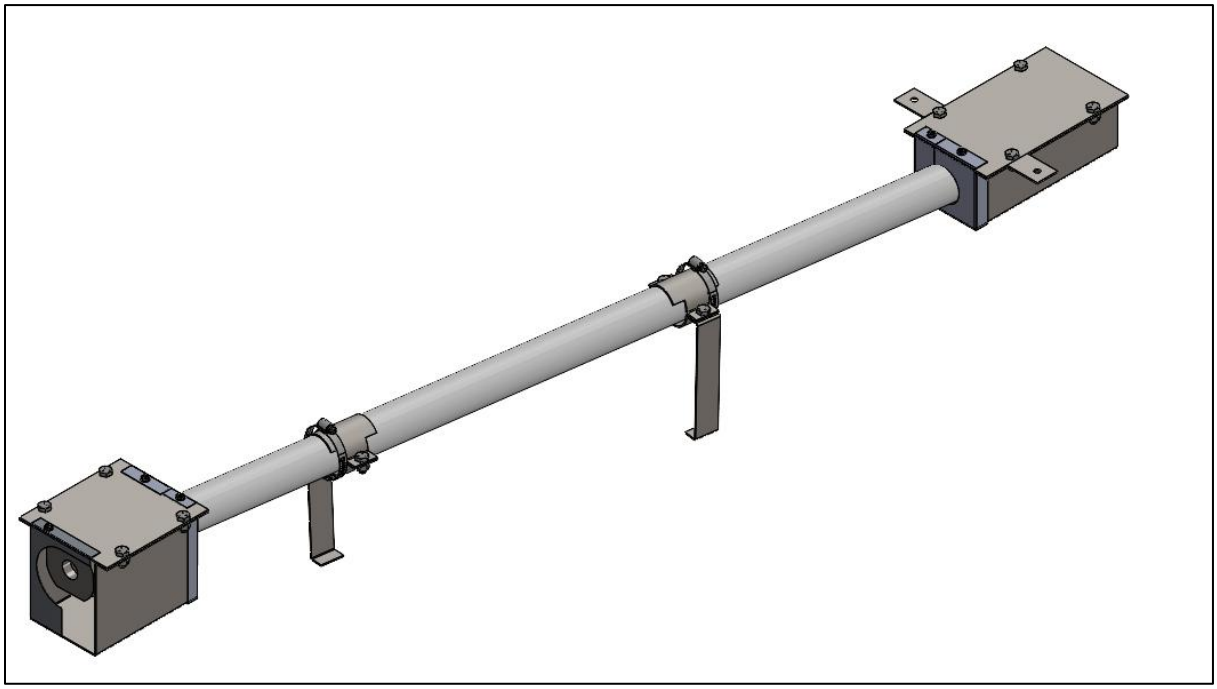

Figure 131: Driveshaft with HROE and PPAE Guards

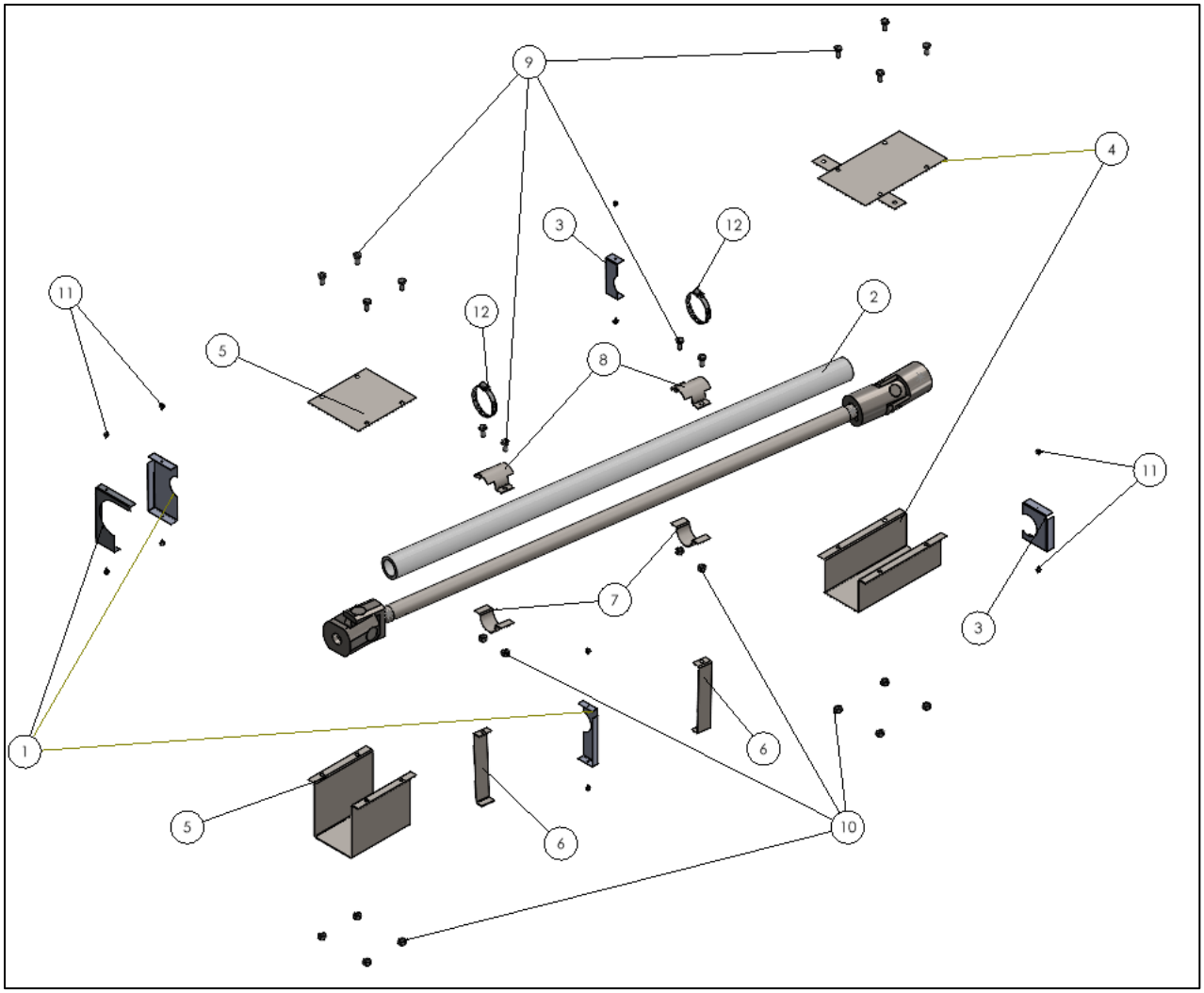

Figure 132: Exploded Assembly of Driveshaft with HROE and PPAE Guards

4.2.5.6. HROE and PPAE BOM:

BOM Part #	Description	Qty:	Source (Hyperlink to Part)	Cost:	Weight/1Pc [lbs]
1	Yamaha PPAE Cover	4	Metal Supermarkets	23	0.0015
2	Driveshaft PPAE Cover	1	Home Depot	10	1.34
3	Belden PPAE Cover	1	Metal Supermarkets	22	0.0125
4	Belden HROE Cover	2	Metal Supermarkets	12	0.75
5	Yamaha Joint HROE Cover	2	Metal Supermarkets	13	0.8
6	Safety Hoop Support	2	Metal Supermarkets	1.5	0.1
7	Driveshaft Safety Hoop Bottom	2	Metal Supermarkets	1	0.06
8	Driveshaft Safety Hoop Top	2	Metal Supermarkets	1.5	0.1
9	Grade 8, 1/4-20 Hex Head Bolt	12	McMaster-Carr	16	0.01
10	Grade 8, 1/4-20 Nylon-Insert Lock Nut	12	McMaster-Carr	5	0.01
11	Philips Head Drilling Screws	12	McMaster-Carr	11	0.003
12	Hose Clamp	2	McMaster-Carr	15	0.021
			Total	596	

Table 24: Driveshaft HROE and PPAE BOM

The main goal with the HROE covers was to improve their removability to help improve the removability of other drivetrain components in order to achieve our 10-minute custom component removability goal. This year we designed the covers to be a two piece cover that bolt together with threaded fasteners. This allows them to be removable quickly so we can access the universal joints underneath them easily. HROE covers will be manufactured out of AISI 1010 sheet metal, which will be bent into the desired shapes. We kept the profiles of the covers square so we don't have to attempt to roll the sheet metal into a certain radius, this will hopefully reduce manufacturing time of the covers. Additionally, the safety hoops for the driveshaft are a two-piece design that is bolted together. This allows the top half of the safety hoop to be removable so the driveshaft can be more easily removable.

5. Chassis

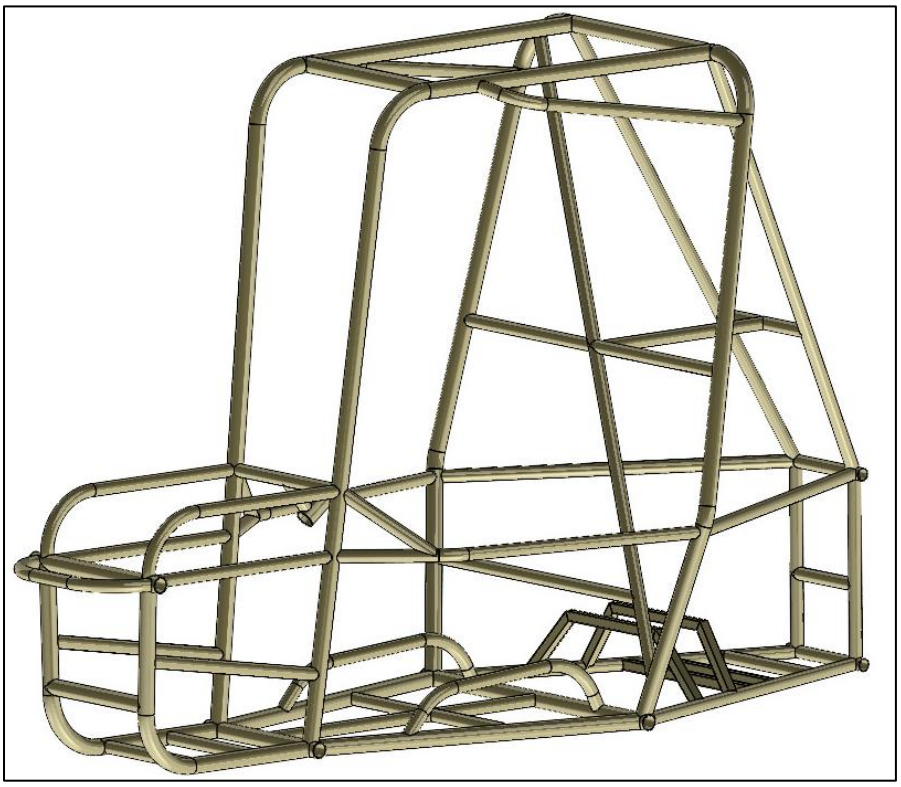

Figure 133: Overall Chassis View

5.2. System Level Breakdown

5.2.1. Design Choices

We choose to use a rear supported design, which aligns with our goals of a lighter and shorter chassis. We reduced the length of the chassis by 9” compared to last year’s vehicle, while maintaining a similar height and width. We also reduced the amount of tubing aft of the firewall.

We choose to use 4130 Chromoly Steel tubing for its light weight and strength surpassing the minimum requirements specified in the rules. We selected our primary tubing to be 1.25” x .063, secondary tubing to be 1” x .049, and tertiary tubing to be .75” SQR x .049. We determined our primary selection to be suitable for our loading conditions while surpassing the minimum strength and thickness, while our secondary and tertiary tubing are the minimum diameter and thickness we can weld to the primary tubing.

Spec	This Year	Last Year
Weight	66.8 lbs	83.7 lbs
Length	75.9 in	84.8 in
Width	33.6 in	33.3 in
Height	50.6 in	51.6 in

Table 25: Comparison of chassis dimensions and weight

5.2.2. Critical Rules

Chassis must follow a large array of rules from sections: A.5.3, B.1, B.3, B.4, B.8, B.11, B.12, B.13.

5.2.3. Integration Overview

“Chassis typically stays in a state of 80% done in CAD as others update things from PDR through manufacturing” -Peter

Chassis team acts as a base for all the other teams, and has the hard balance of moving forward with our own work and moving backward to accommodate other sub teams. While chassis has stayed with a rear supported design the entire time, everything else has changed. As of writing, the chassis is on revision D.30, indicating 4 major changes and encompassing nearly 100 revisions.

The largest change since PDR is changing to an under-seat driveshaft rather than offset driveshaft. This caused sweeping changes through the chassis to ensure that the seat template has adequate clearance to all bars. While the chassis was forced to grow from PDR, we are still smaller than last year, which is in line with our goals.

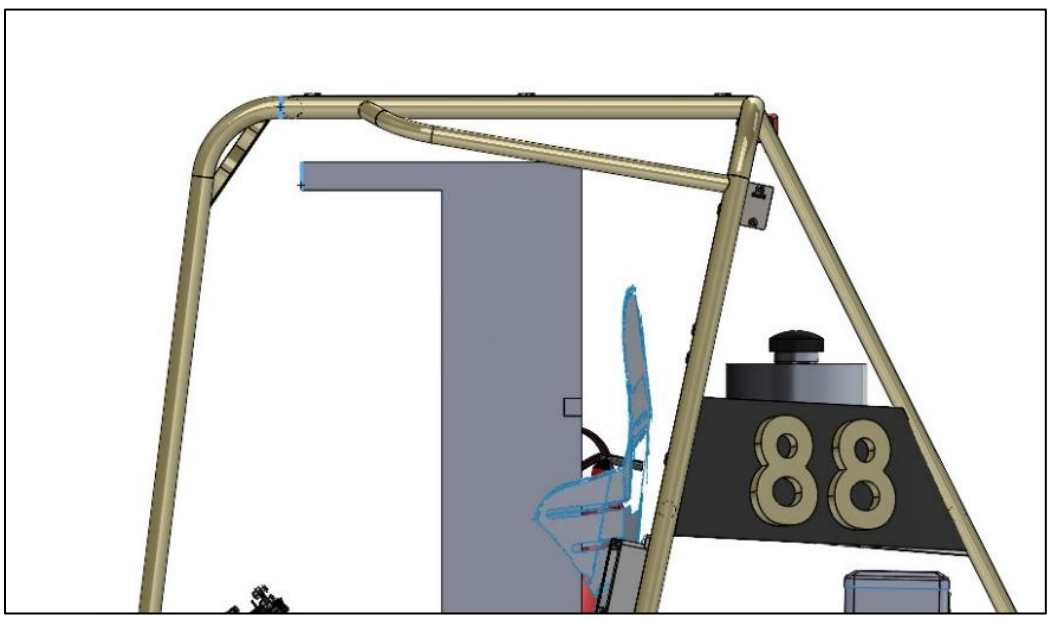

Figure 134: Seat Clearance Template, resting on 3D seat scan

We also did our best to test for potential clearance issues and rules compliance, using a human model, helmet model, and clearance bubbles around the head and hands. This helped influence our gusset geometry, which should help us prevent last year’s triple gusset situation.

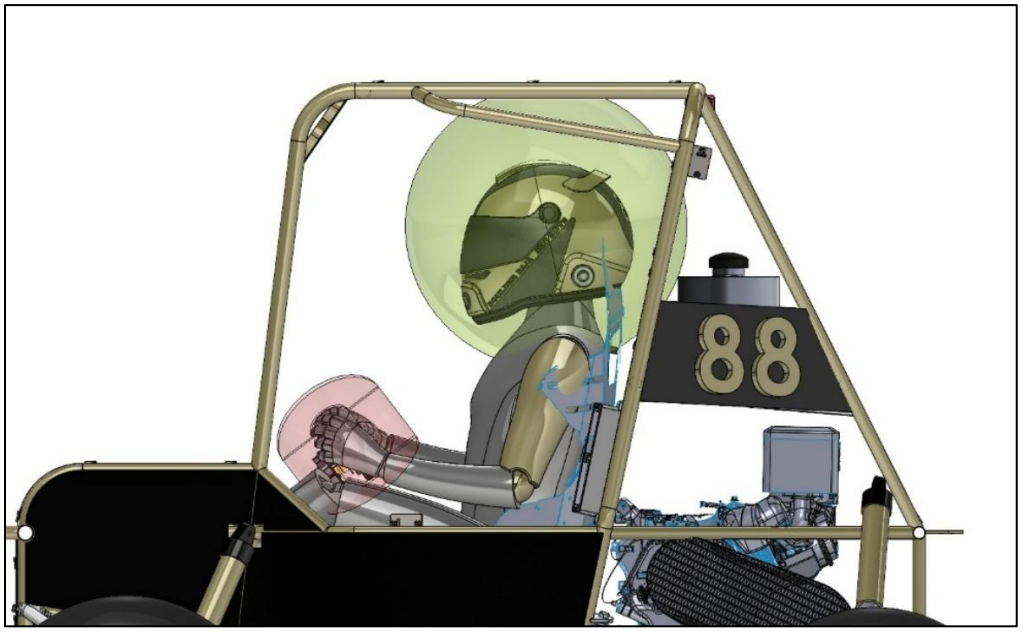

Figure 135: 6-inch helmet bubble, 3-inch hand bubble

When working with such a large team this year, it was quite common to go back and forth with new ideas and new problems. Front suspension decided to tilt back 10 degrees, controls needed more room for foot clearance and pedals, drivetrain and suspension had to compromise on diff locations, engine mounting was always changing, etc. etc.

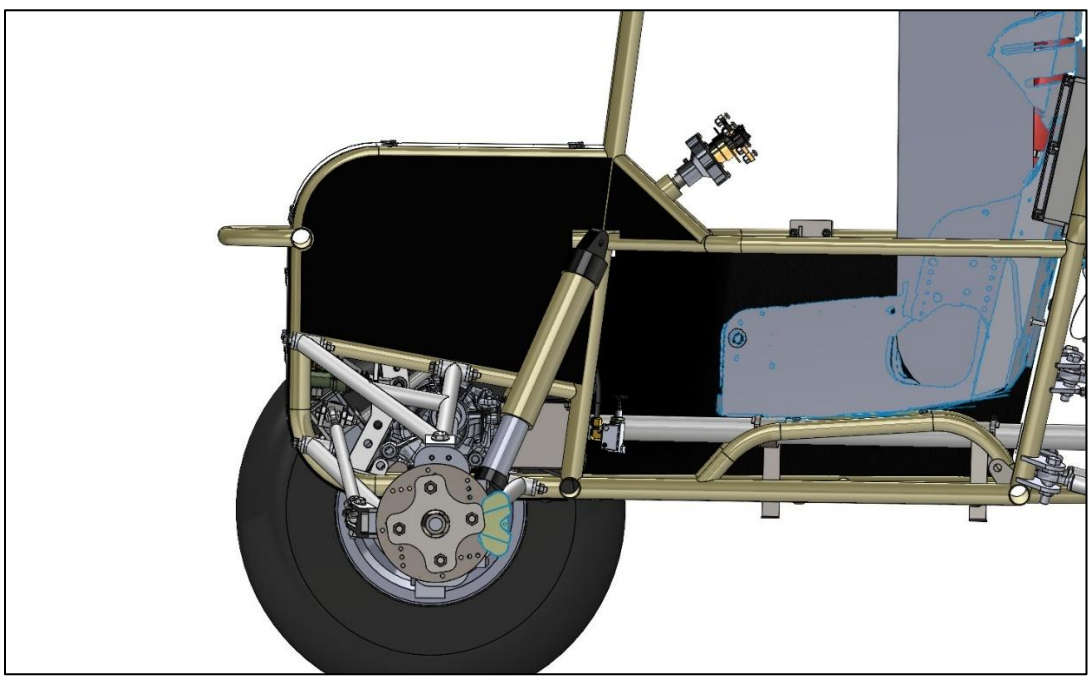

Figure 136: Tilted front suspension member removed other mounting bars for controls and PPAE

5.3. Part Level Breakdown

5.3.1. Frame Tubes

The chassis will be constructed of 1.25” x 0.063” primary and 1.0” x .049” secondary round chromoly tubing, just like years before us. This is the best material selection due to meeting the required bending stiffness rules, while being lighter than alternatives due to the thin walls. Tertiary tubing will be ¾” square

x .049” wall for engine and transfer case mounting, simply to work with their flat mounting plates better. We plan to use automotive gold paint to stand out from previous black frames.

Primary	**1.25” x .063**
Secondary	**1” x .049**
Tertiary	**.75” SQR x .049**
Steering Column Support	**1.5” x .049**

Table 26: Color-coded legend of tubing sizes

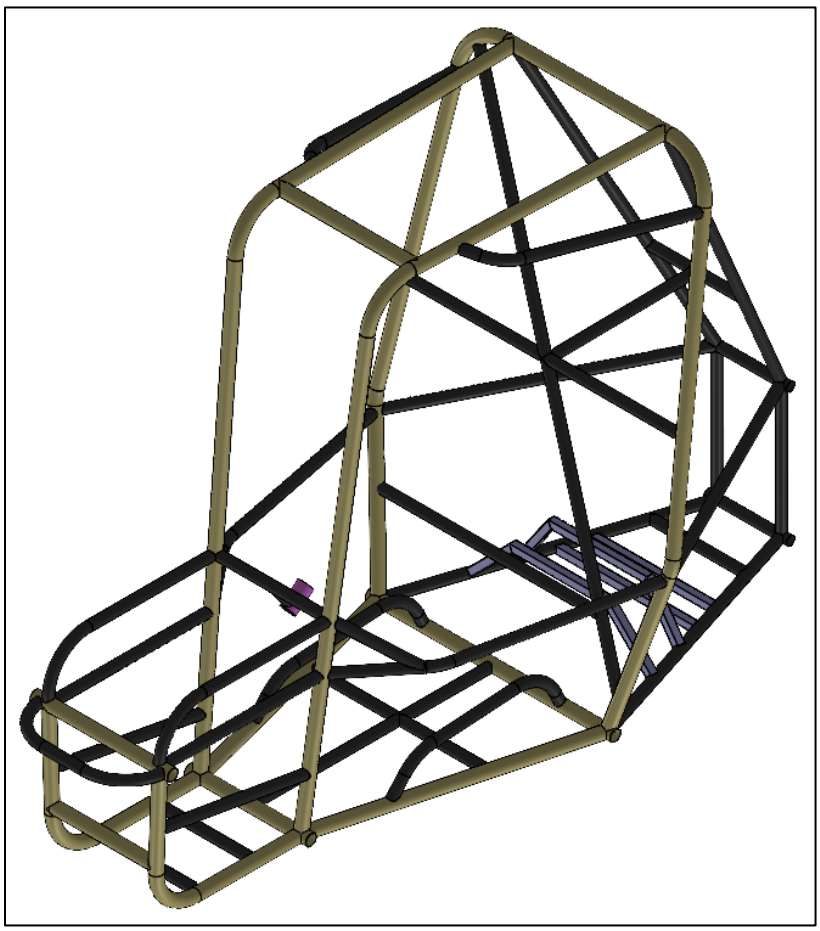

Figure 137: Chassis Schematic, separated by color

5.3.2. Body Panels and Numbers

Body panels will be made of ABS sheet like last year. We chose this material for its easy formability and ability to be cut with simple scissors. It’s rigid enough to comply with rules, while being light and strong enough to mount easily. We will retain the ¼ turn D-zus style fasteners for body panels, but stay cautious of alignment issues that made last year’s panels difficult to install.

As for numbers, we will be 3D printing them to be rules compliant with font, size, and contrast requirements. They will be fastened to ABS backer plates with ¼-20 bolts, and the panels will use P-clips around the frame.

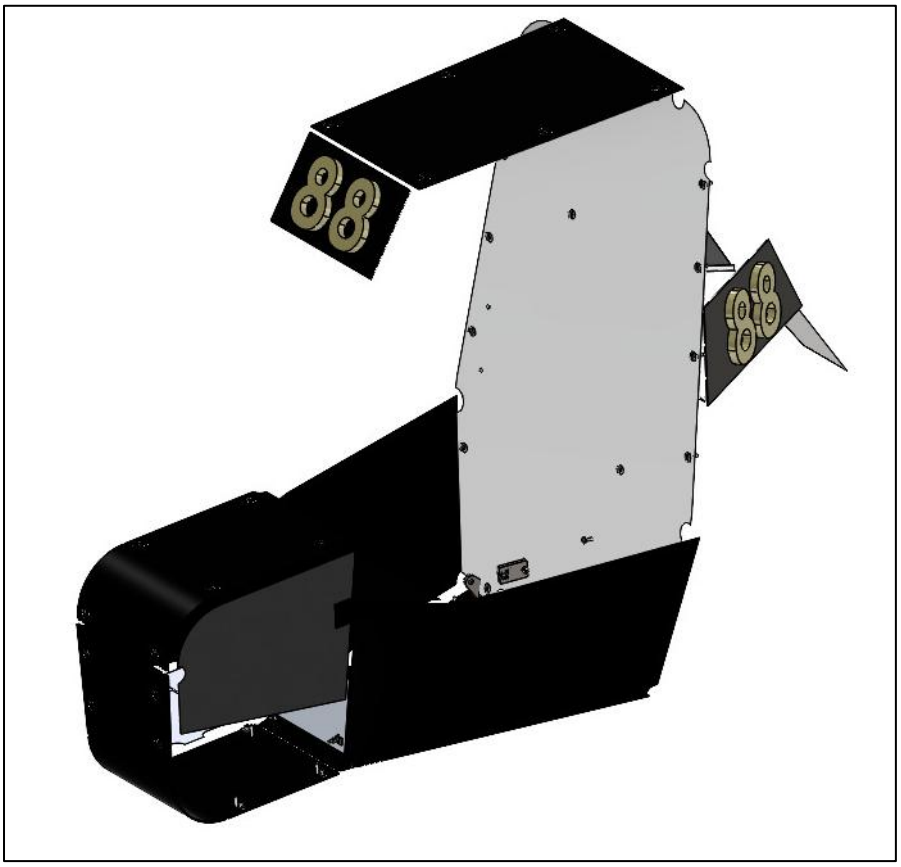

Figure 138: Panels, Numbers, and Plates

5.3.3. Firewall and Splash Guard

The firewall is the same design as last year: fore of the RRH centerline, .02” aluminum sheet, fastened with ultrawide ¼-20 screws. The only difference will be the nut side, which are planned to be RivNuts. These will allow quicker fabrication, but more importantly should increase serviceability. We noticed quite a few issues with the previous car came from trying to reach both sides of fasteners, and this should eliminate that.

The splash guard will follow suit. One important note: the rules specify that the exhaust axis and drip tray axis cannot be the same. Exhaust must be redirected out the side to not impinge on the rear-most member of the frame, so the drip tray must go out the back.

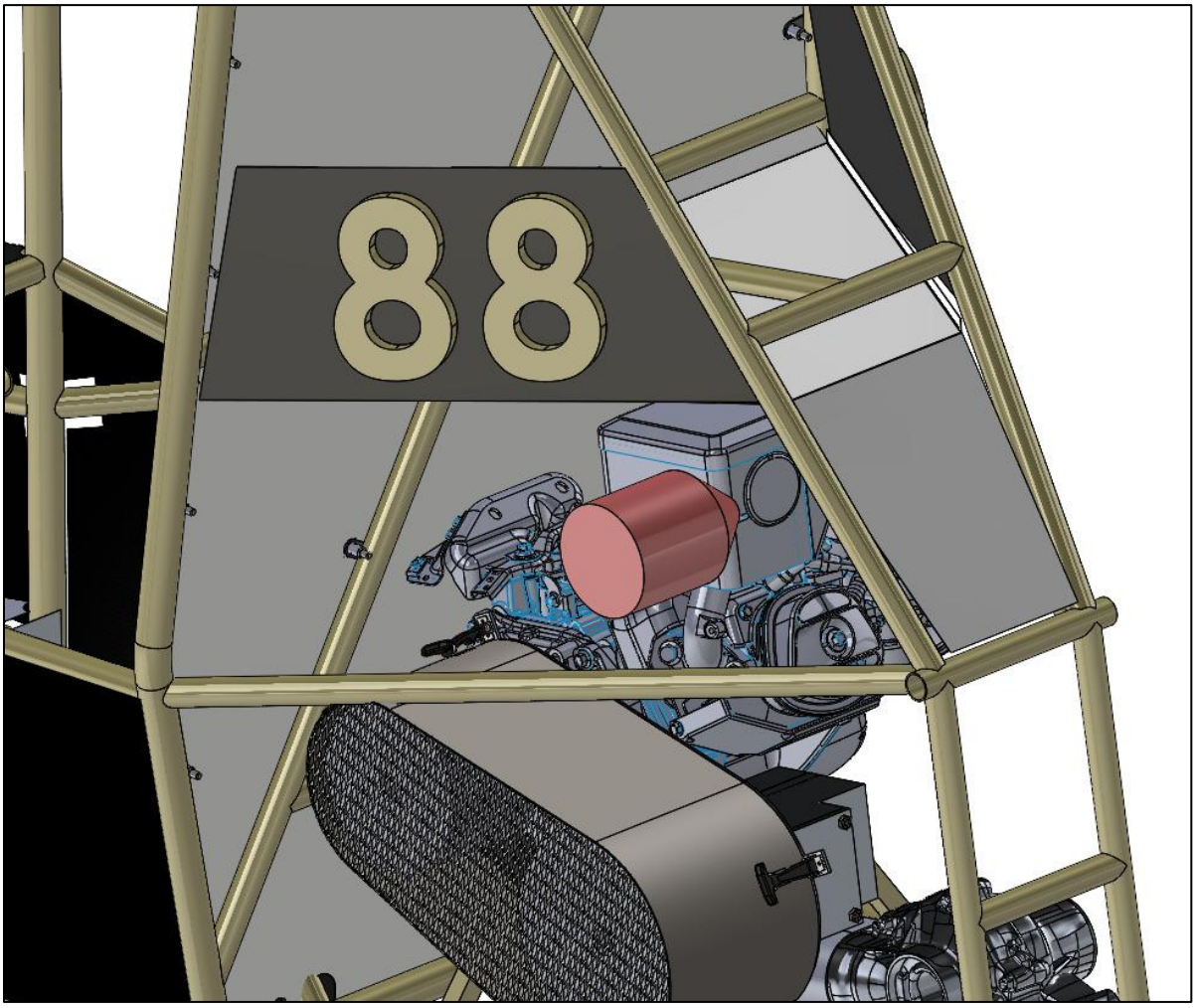

Figure 139: Red exhaust cone redirected out the left side, and drip tray out the back

5.3.4. Skid plates

Because the competition this year is at the notorious Washougal MX Park, extra time and weight have been allocated to skid plates this year. We anticipate a fair amount of rock and log skidding along the center of the car, especially at the front. Because of this, we have selected a minimum .100” steel front skid plate, and developed the curved nose further. We expect the steel to slide better, and withstand repeated deformations better. We will perform testing on the cockpit skid plate, and see if aluminum skids or grabs into sharp objects.

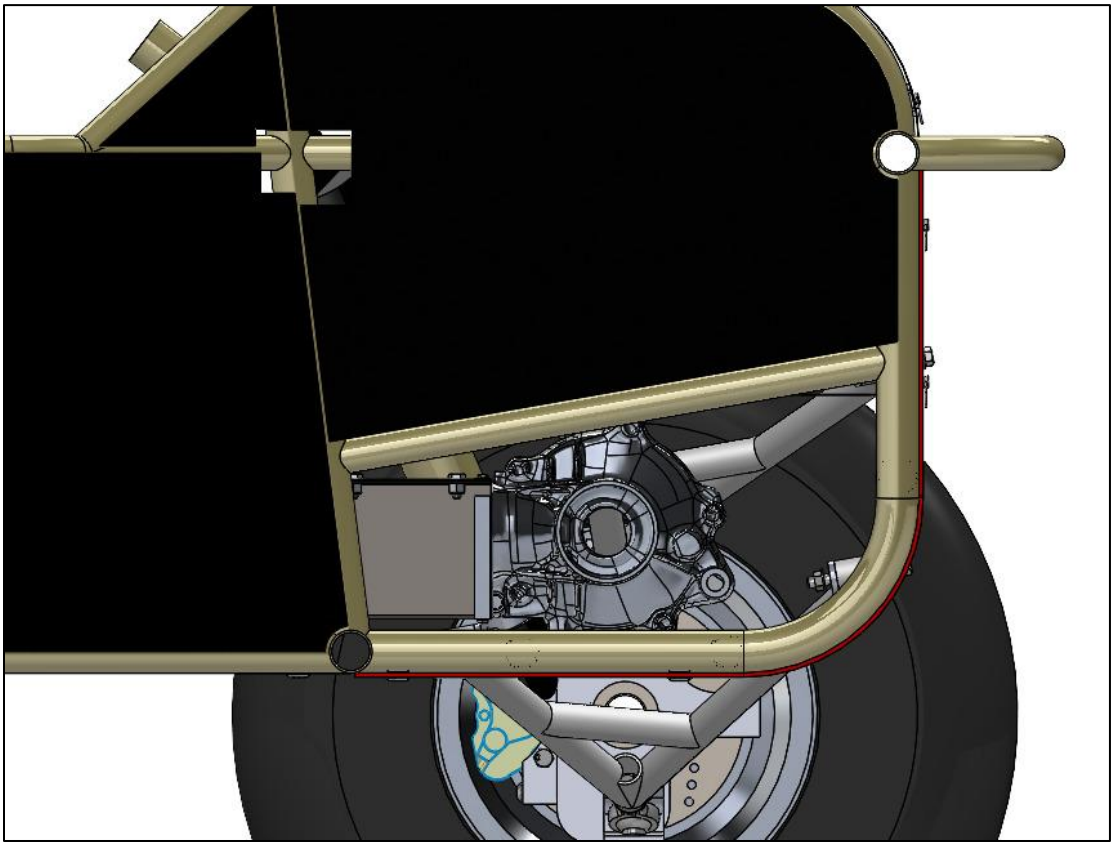

Figure 140: Curved front nose, with thick skid plate (in red)

We are also aware of the relatively small amount of front stick-out. While we tried to optimize this, compromises had to be made to allow controls to mount their steering box and suspension to have mounting points.

5.3.5. Stress Analysis

Failure Condition: Rollover (Direct Down)
Material: Alloy Steel 4130; 1.25" x .065 Primary, 1.0" x .049 Secondary

Justification: Rollover is semi-common at competition due to obstacle geometry and short wheelbase.

Load Diagram & Constraints:

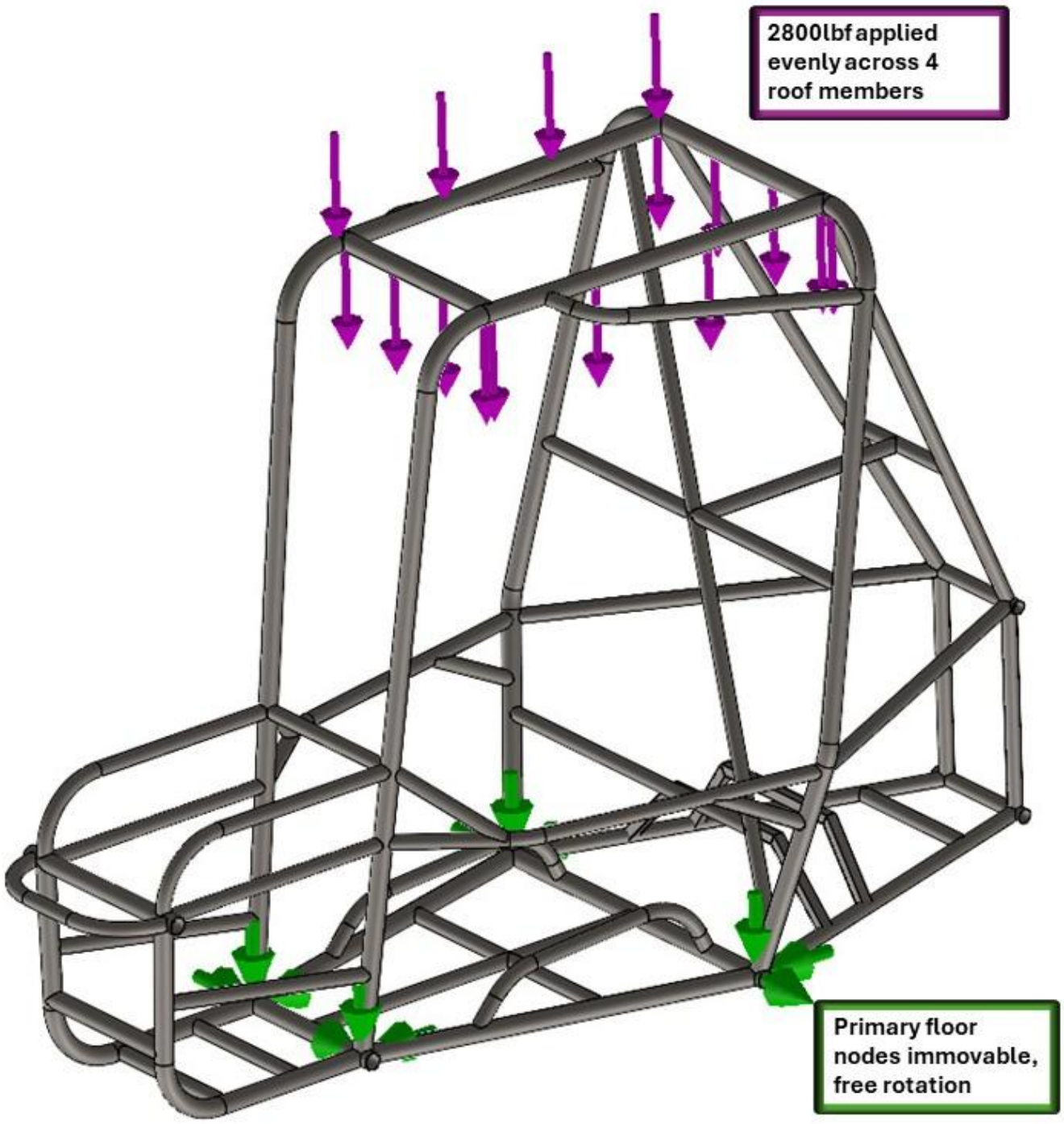

Figure 141: Rollover Load Case

FOS: 1.42	**Confidence Level & Explanation:** Medium. Loads are not well known, but are 4x the loaded vehicle weight, and chassis is a proven design. Mesh based off ANSYS mesh convergence, using 0.35in segments. Similar results achieved when running as a solid body.

FEA:

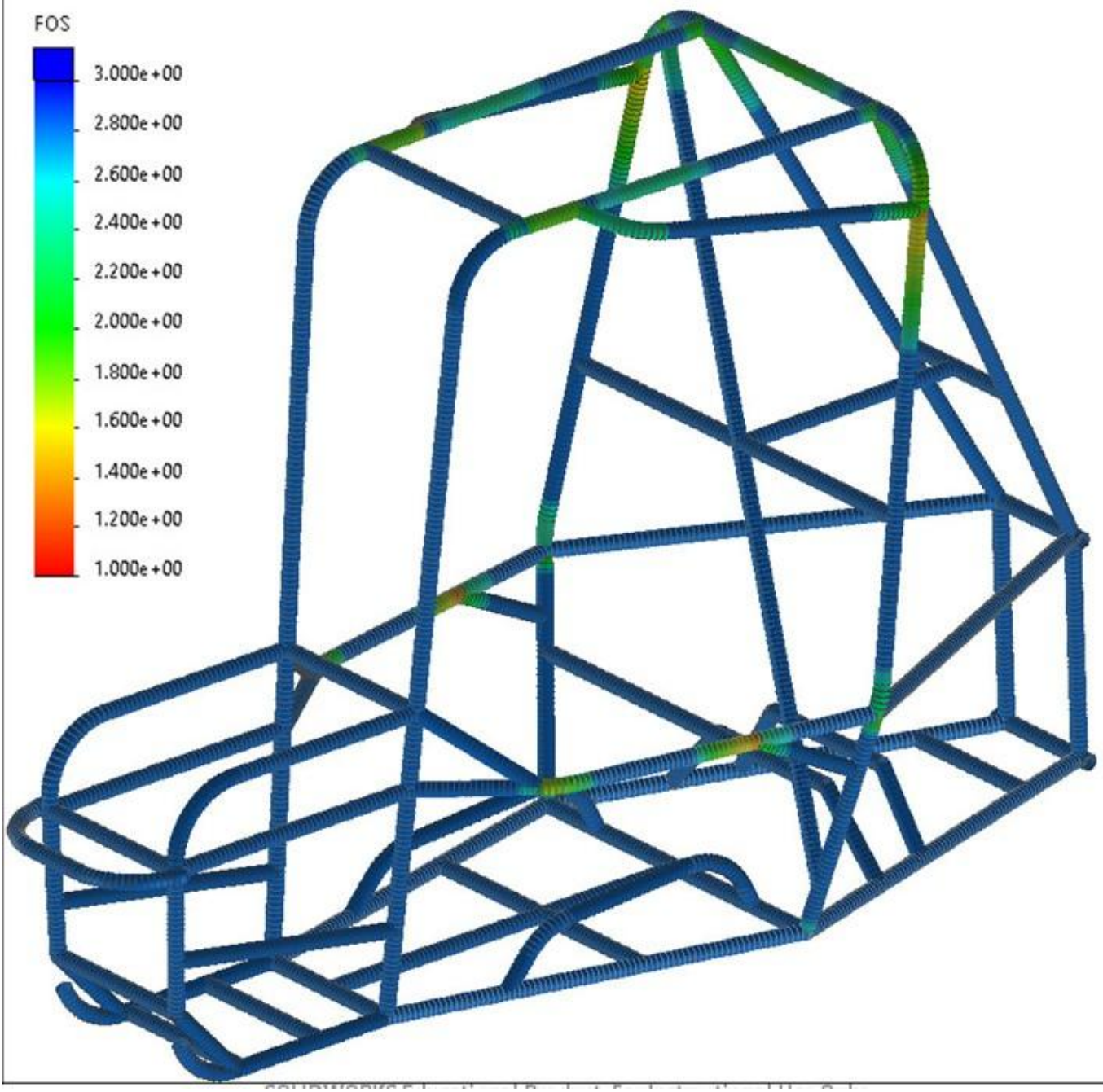

Figure 142: Rollover FOS

Failure Condition: Rollover (Frontal)
Material: Alloy Steel 4130; 1.25” x .065 Primary, 1.0” x .049 Secondary

Justification: Frontal rollover is the primary load case when rolling, and provides greater stress farther from the roll hoop

Load Diagram & Constraints:

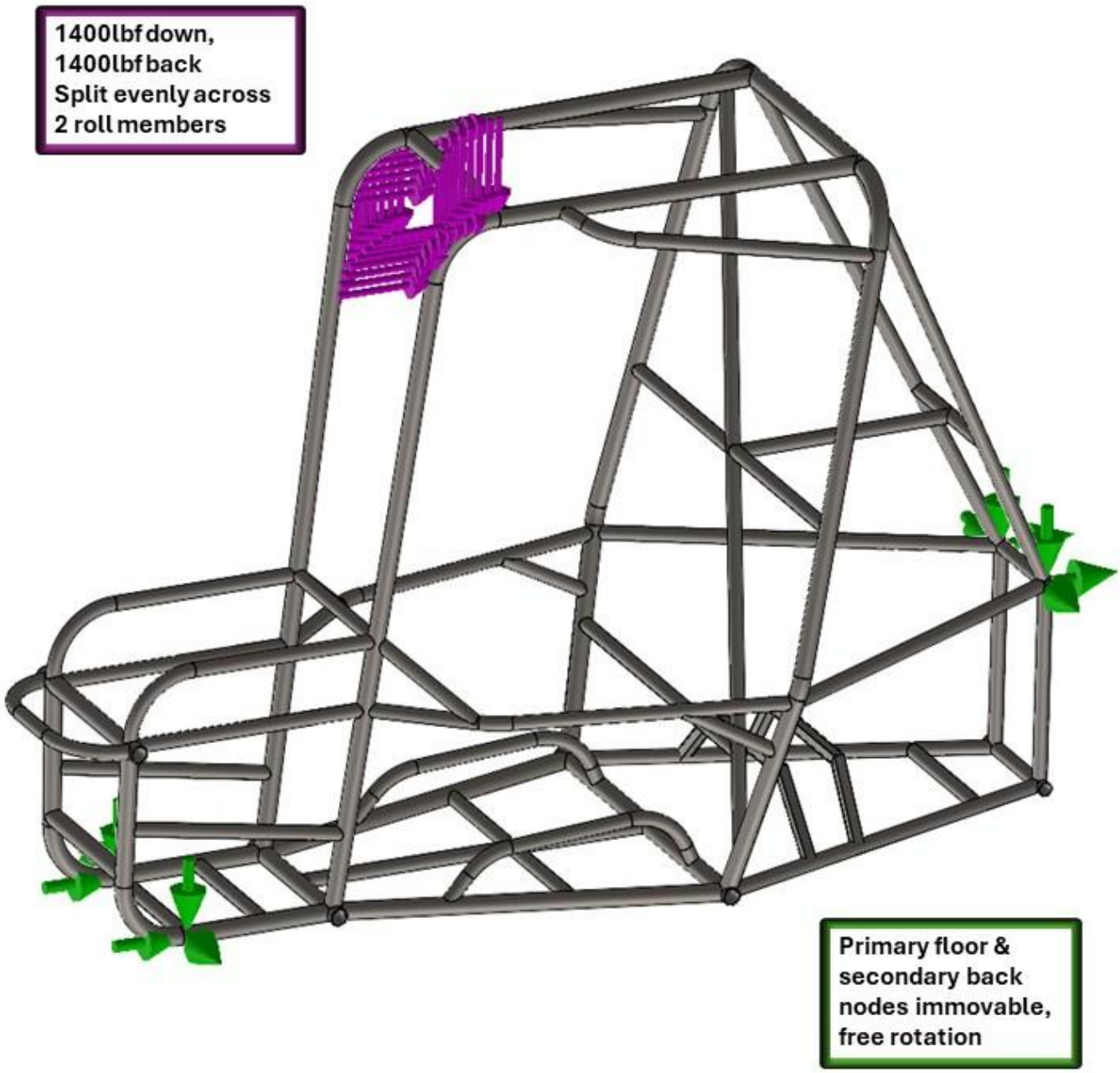

Figure 143: End over end Loads

FOS: 1.34	**Confidence Level & Explanation:** Medium-Low. Similar load scenario to top rollover, but with stress concentrations highest in side impact member instead of rear roll hoop (secondary instead of primary tube)

FEA:

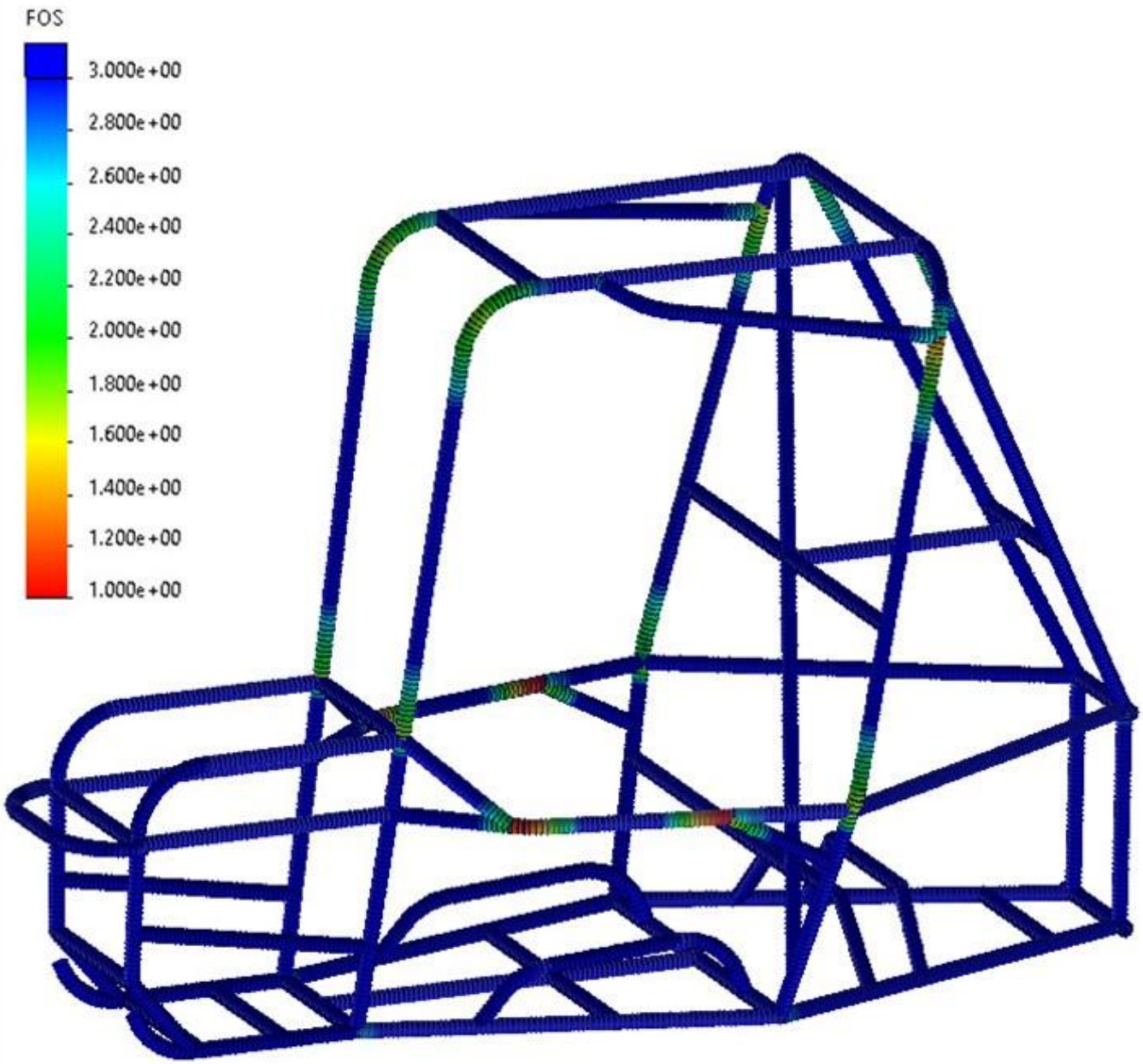

Figure 144: End over end FOS

Failure Condition: Front Impact
Material: Alloy Steel 4130; 1.25” x .065 Primary, 1.0” x .049 Secondary

Justification: There is a good chance that the chassis experiences a head on collision during testing or competition, either with a tree, rock, or other solid object

Load Diagram & Constraints:

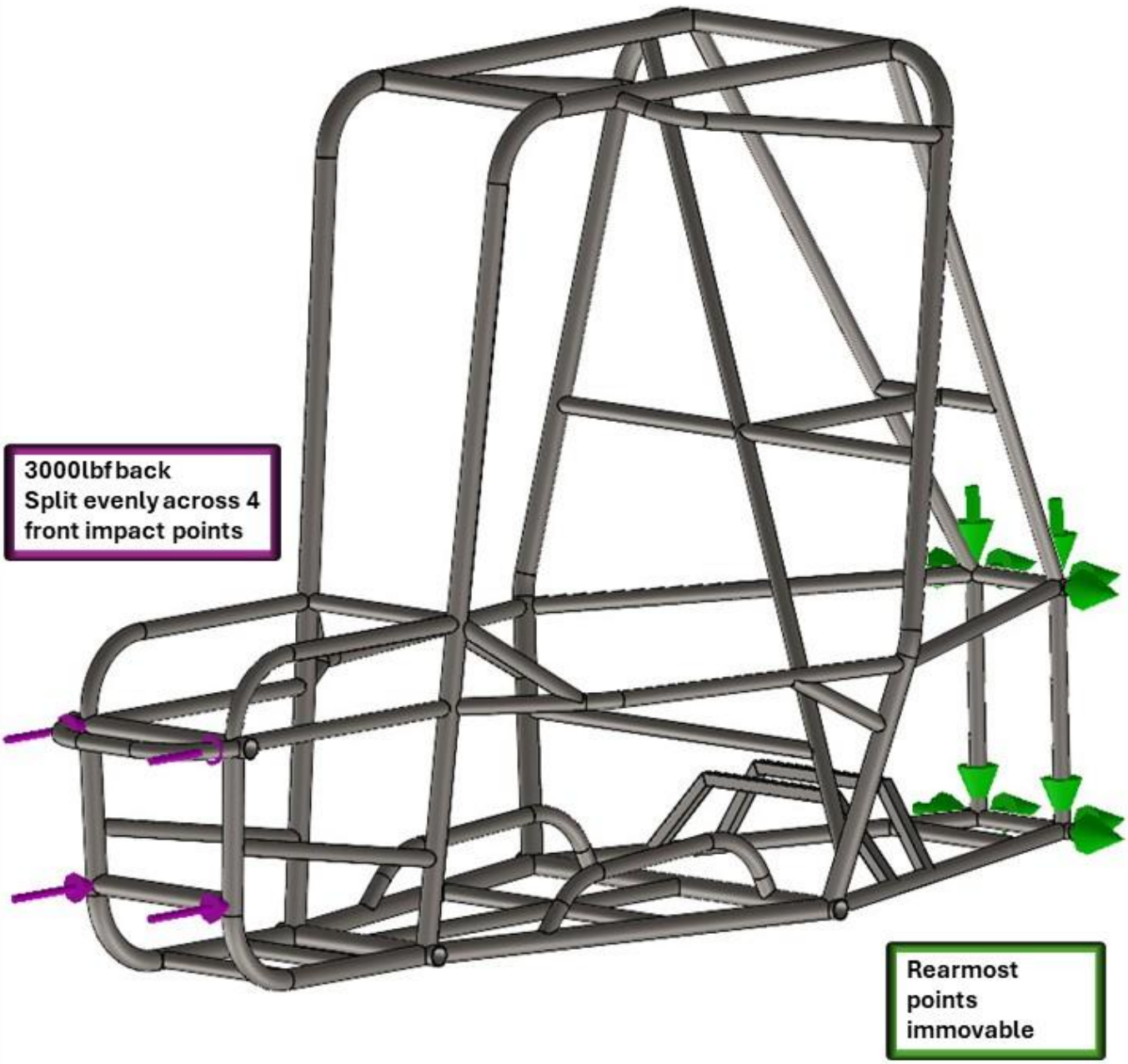

Figure 145: Front Impact Loads

FOS: 1.29	**Confidence Level & Explanation:** Medium. Loads derived from suspension impulse and common car crash accelerations. Hotspot at roll hoop diagonal brace due to fixture constraints, lower stresses through SIM.

FEA:

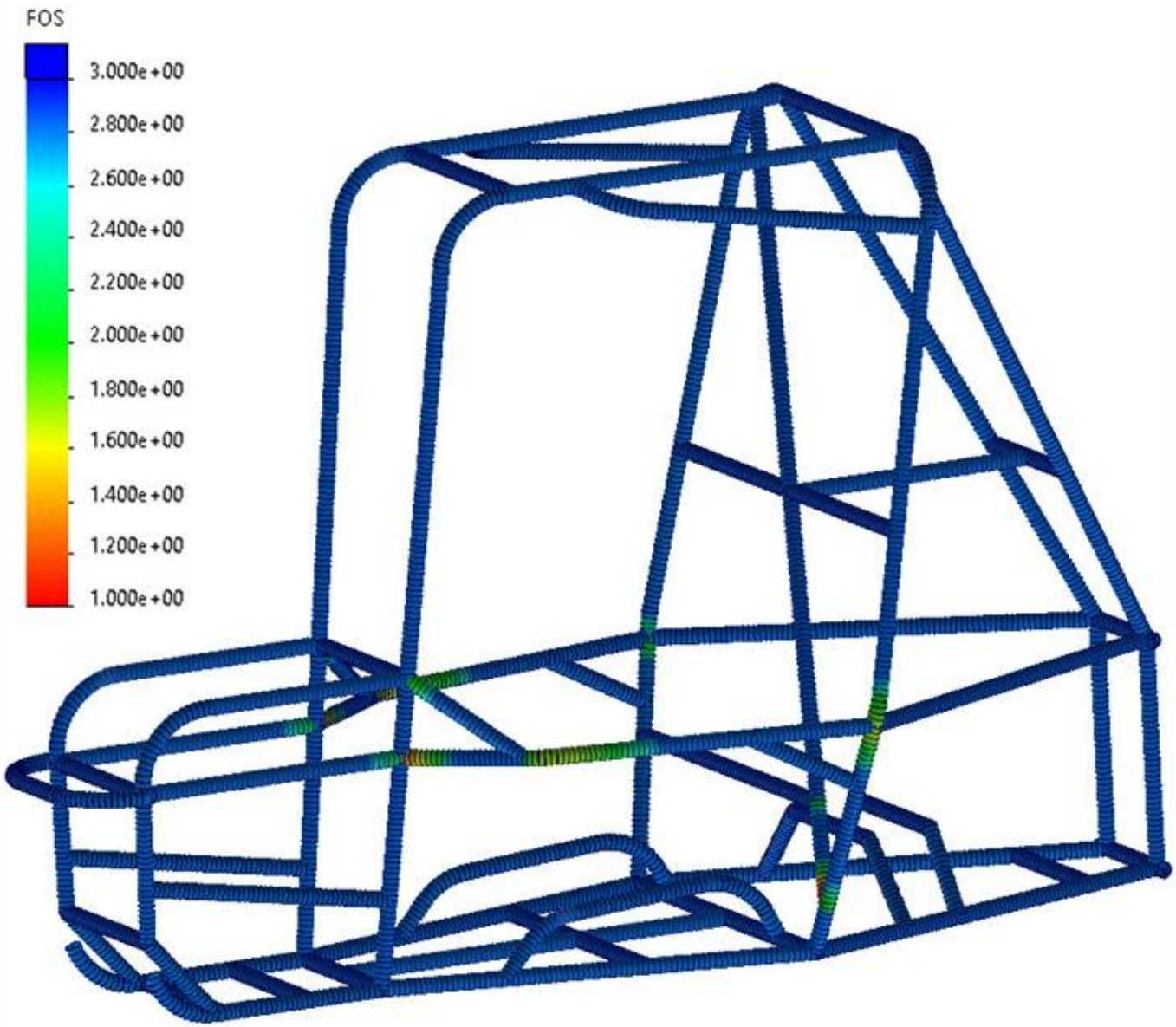

Figure 146: Front Impact FOS

Failure Condition: Side Rollover (Byron)
Material: Alloy Steel 4130; 1.25" x .065 Primary, 1.0" x .049 Secondary

Justification: Byron pointed out that the weakest point of our frame would be sideways deflection, due to being rear supported, and only having a single "upright" member at the front.

Load Diagram & Constraints:

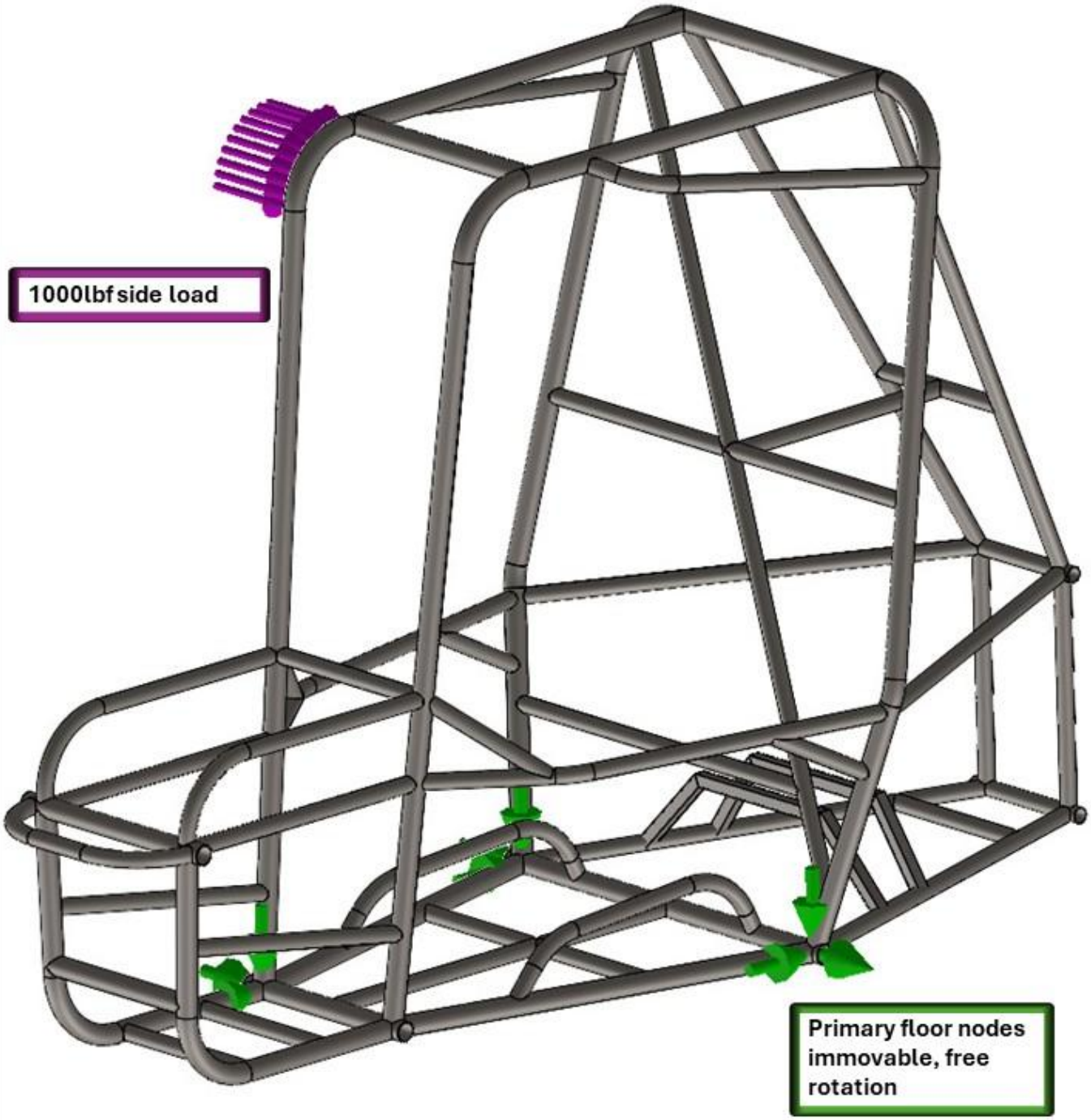

Figure 147: Byron-Case Loads

FOS: .99	**Confidence Level & Explanation:** Low. Can't accurately constrain chassis to simulate a side rollover without tire impact points. Effectively just testing deflection of the long beam elements (1 in max movement, which seems high). True load unknown.

FEA:

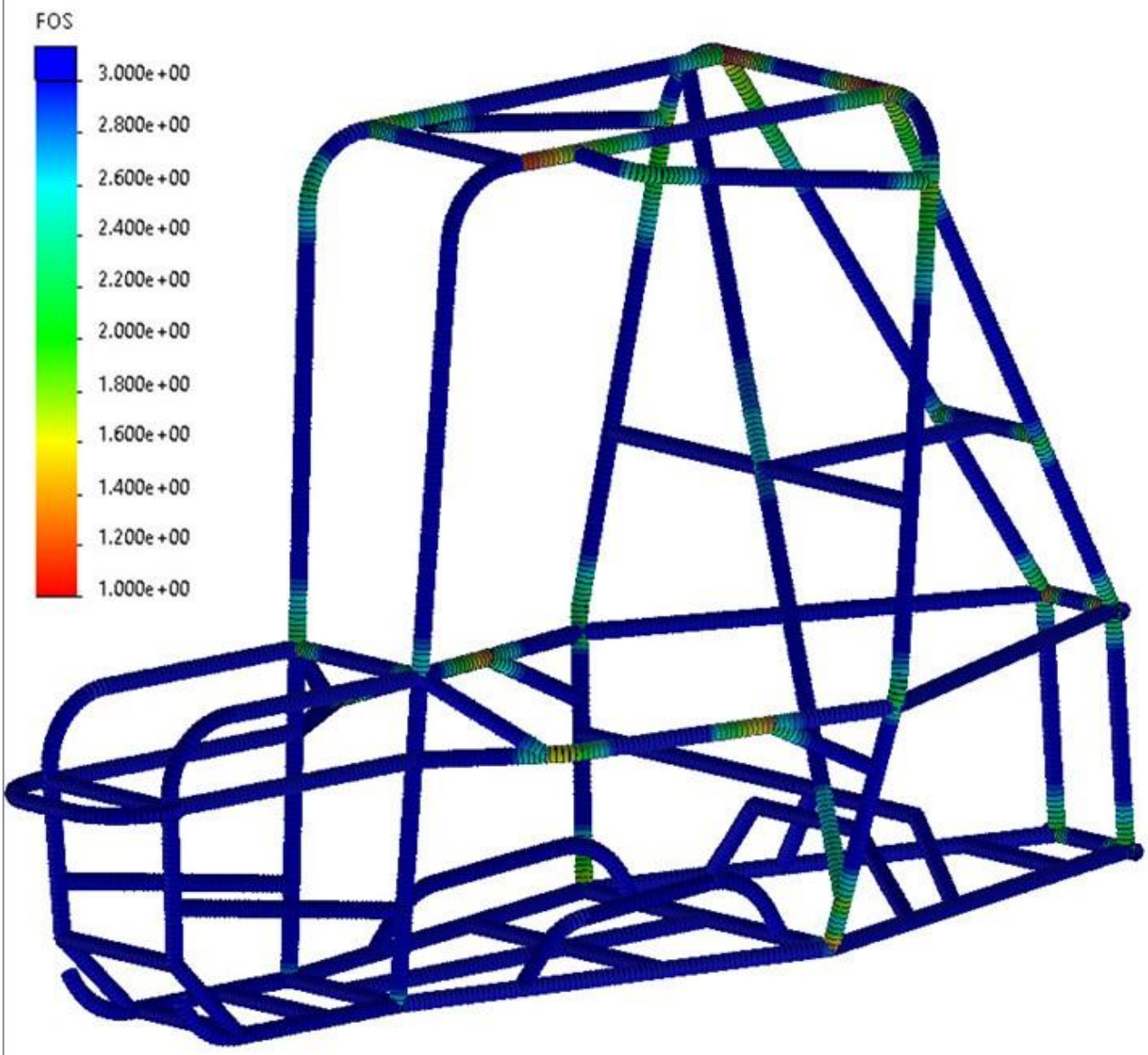

Figure 148: Byron-Case FOS

Failure Condition: Front Suspension Max Combined Loading
Material: Alloy Steel 4130; 1.25" x .065 Primary, 1.0" x .049 Secondary

Justification: Using the worst possible case for any suspension load to ensure wall thicknesses and mounting points are adequate. Full bump and max shock pressure.

Load Diagram & Constraints:

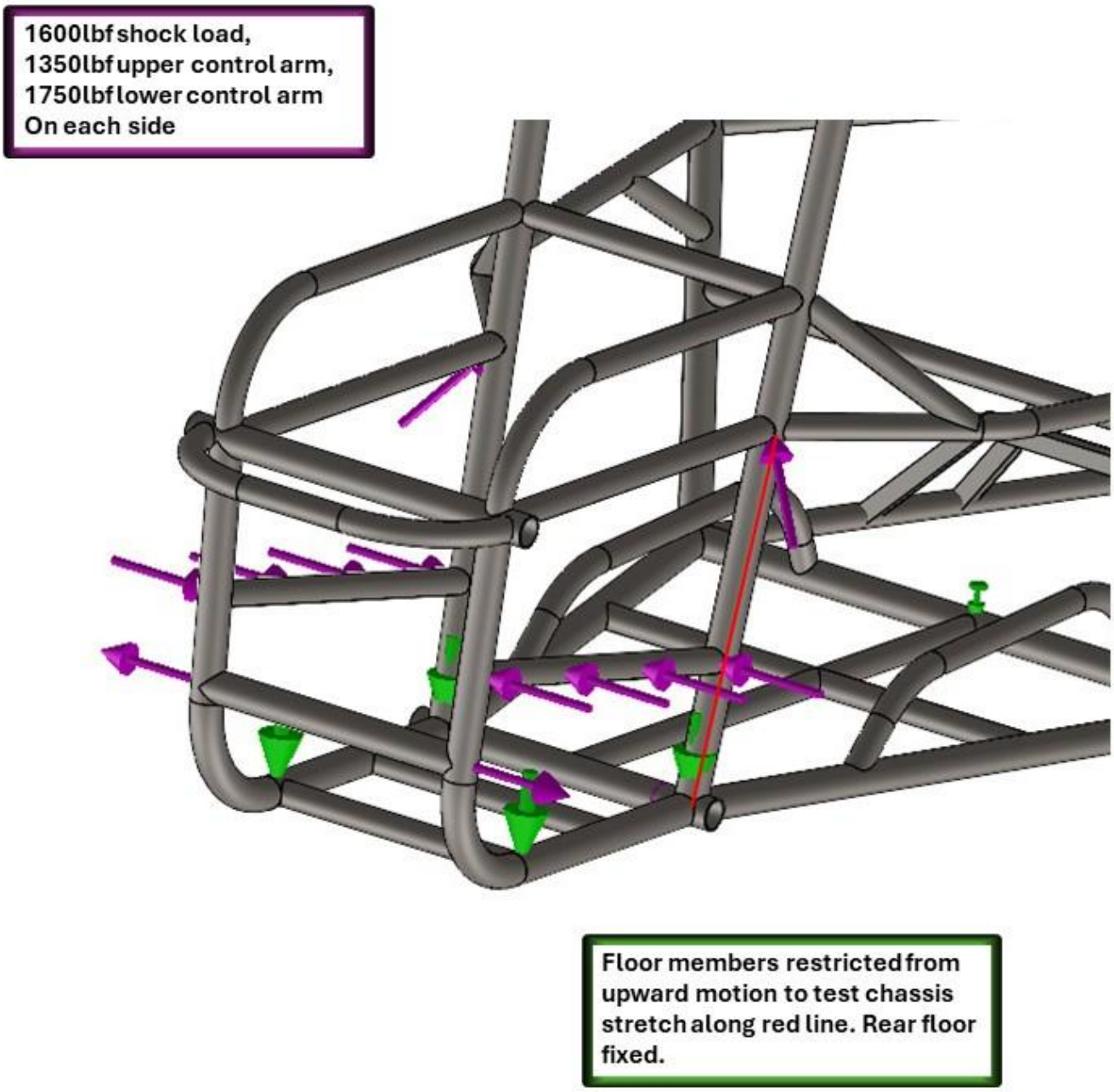

Figure 149: Front Combined Loads

FOS: 1.11	**Confidence Level & Explanation:** Medium-High. Exaggerated maximum loads applied at the same time. Individual loads also tested (ensure no accidental cancelling), all with higher FOS. Combined load is the lowest FOS.

FEA:

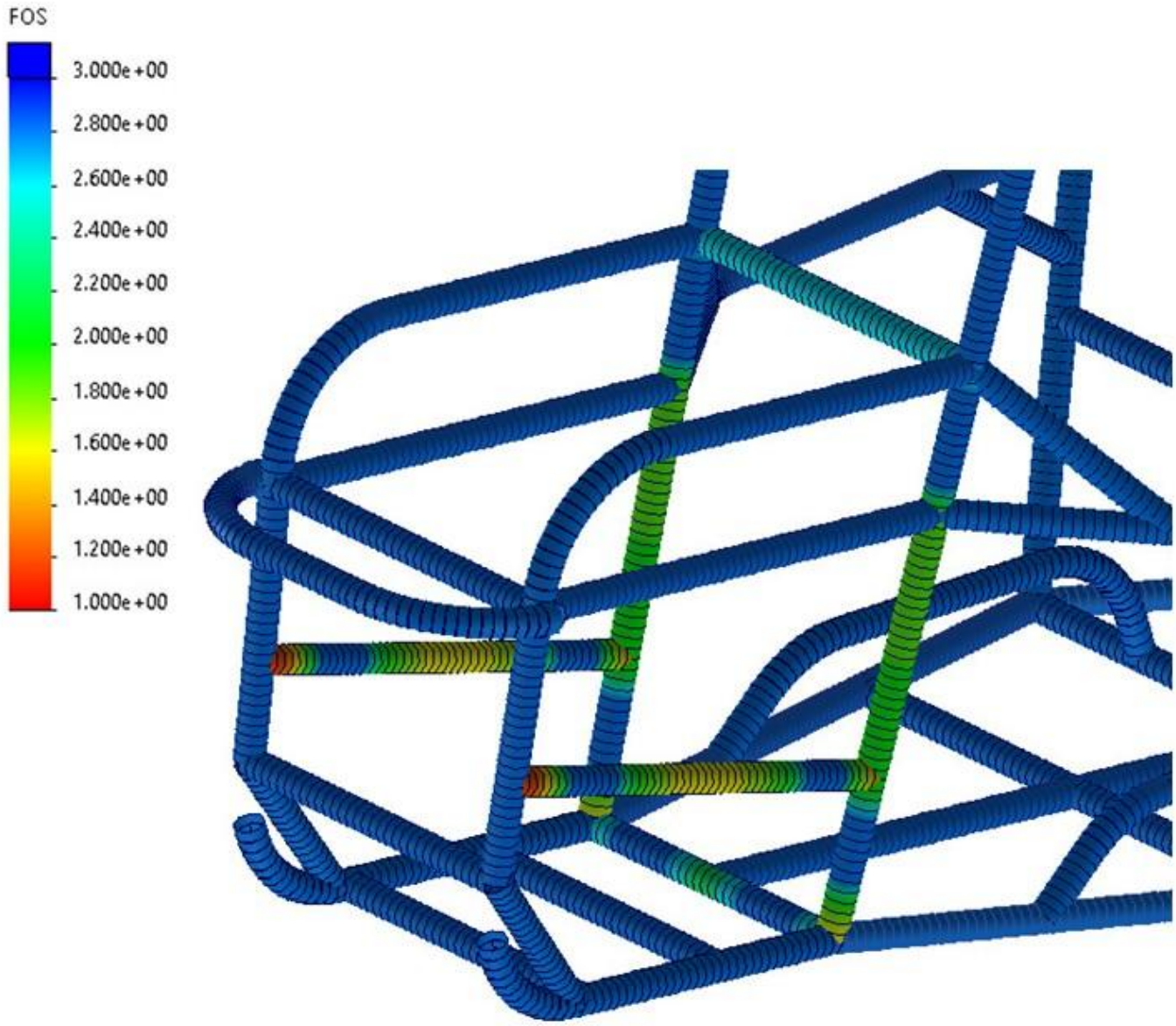

Figure 150: Front Combined FOS

Failure Condition: Rear Suspension Max Combined Loading
Material: Alloy Steel 4130; 1.25" x .065 Primary, 1.0" x .049 Secondary

Justification: Using the worst possible case for any suspension load to ensure wall thicknesses and mounting points are adequate. Full bump and max shock pressure. Upper control arm bar (yellow) added after initial FEA to pass.

Load Diagram & Constraints:

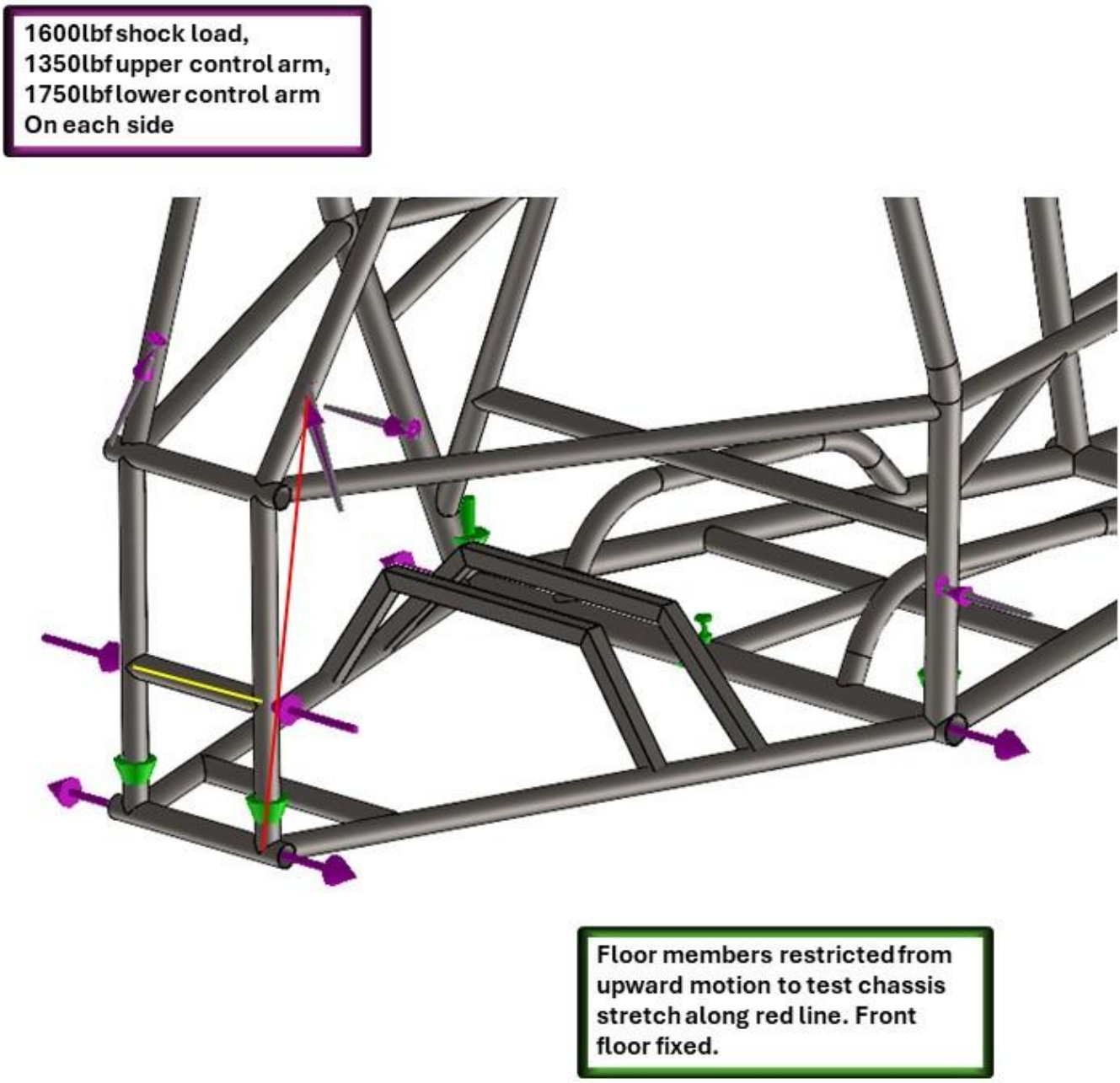

Figure 151: Rear Combined Loads

FOS: 1.15	**Confidence Level & Explanation:** Medium. Exaggerated maximum loads applied at the same time. Individual loads also tested (ensure no accidental cancelling), all with higher FOS. Combined load is the lowest FOS. Slightly lower confidence due to shock mount on secondary instead of primary member.

FEA:

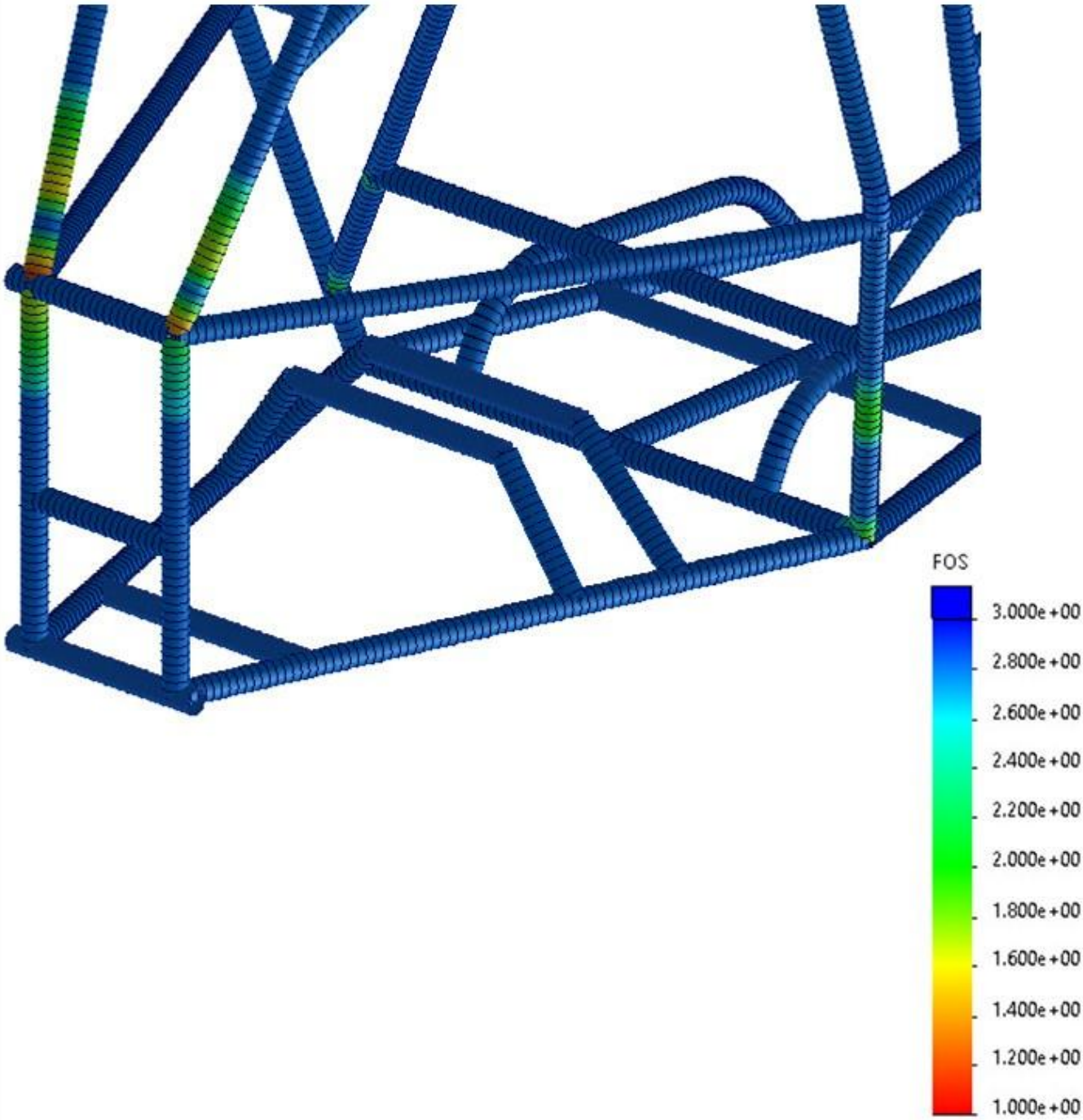

Figure 152: Rear Combined FOS

5.3.6. Supporting Calculations

The following hand calculations were done for our primary material to check they meet the minimum specifications per rule B.3.2.16 - Roll Cage Material. These calculations confirm that our material selection is within rules spec.

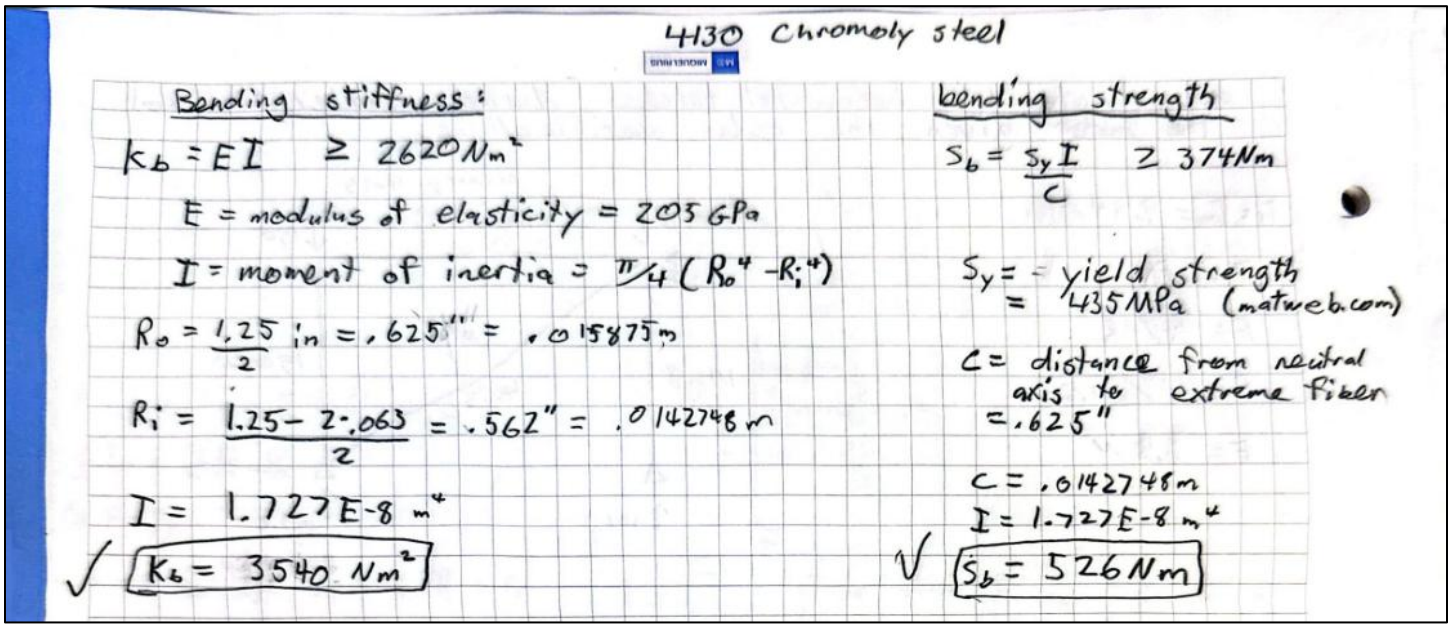

Figure 153: Hand Calculations to Validate the Strength of Frame Material

5.3.7. Bill of Materials

BOM Part #	Description	Length	Qty:	Vendor	Estimated Cost per Unit:
1	4130 Steel Tube 1 OD x 0.049 Wall	12ft	6	EMJ Metals	$300
2	4130 Steel Tube 1.25 OD x 0.063 Wall	12ft	4	EMJ Metals	$300
3	4130 Steel Tube 1.5 OD x 0.094 Wall	1ft	1	EMJ Metals	$25
4	4130 Steel Tube 0.75 SQR x 0.049 WALL	12ft	1	EMJ Metals	$225
Total					$2,650.00

Figure 154: Chassis Tubing BOM

6. Electronics

6.2. Differential PCB

6.2.1.2. Discussion of Design Reasoning

We will be reusing last year's differentials, so we ultimately decided to reuse last year's PBC as it is extremely capable and saves us cost. The PCB consists of eight relays; two control power while the other six work with the switches to semi-lock, lock, and open the differentials.

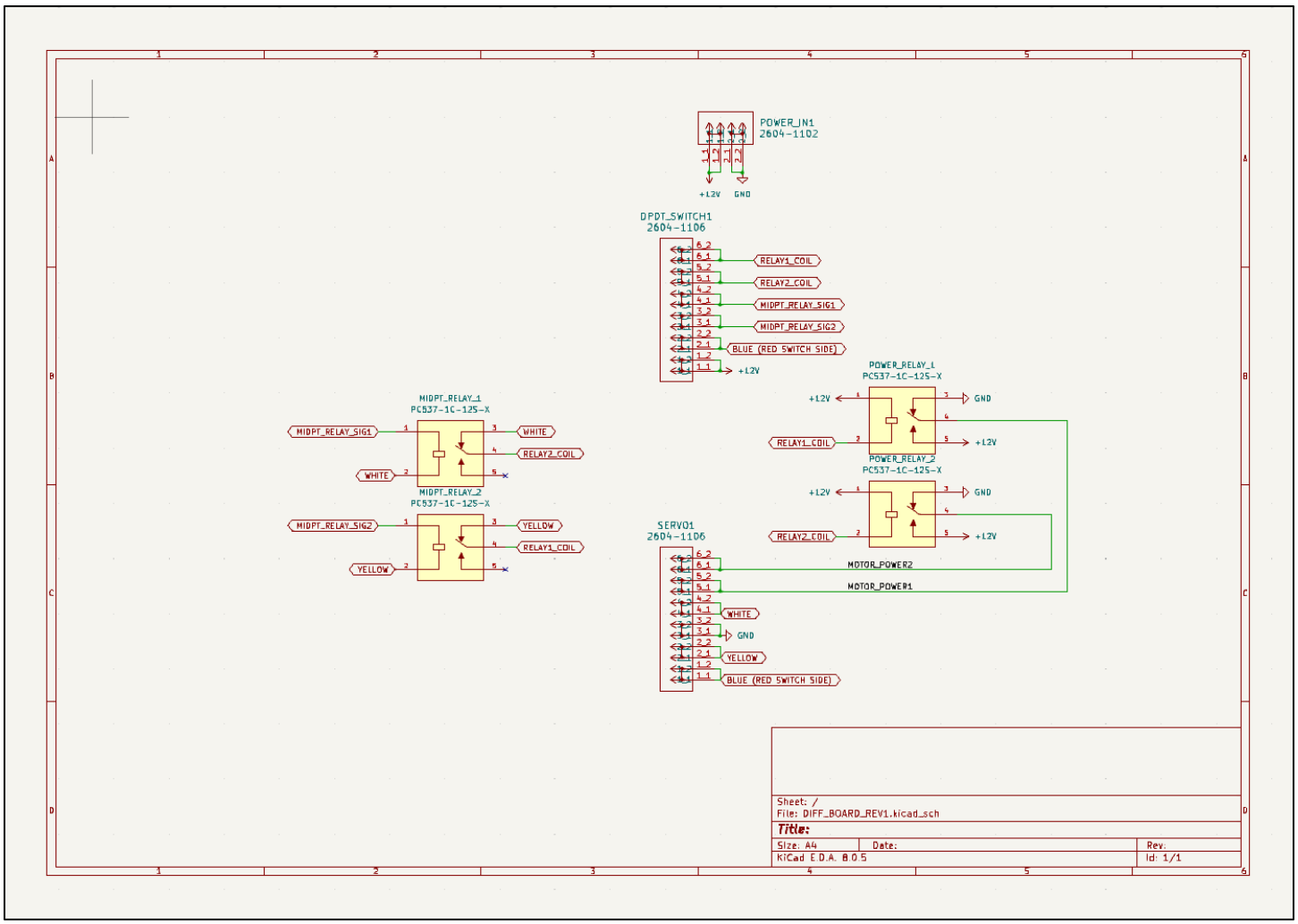

Figure 155: Wiring Diagram

6.3. Differential Switches

6.3.1.2. Discussion of Design Reasoning – Mounting

The differential switches will be mounted directly onto the steering wheel to optimize driver focus, where the right switch is the front, and the left switch is the rear differential. This is because most of our drivers are right-handed, and the differential that will be switched on more often will be the front. Previously, the switches were mounted to the right of the steering column support, which placed the switches in front of the steering wheel. This required the driver to take their hand off the steering wheel to operate the

switches. The access wiring will be wrapped around the steering column in a way similar to a clock spring to prevent unwanted tension and potentially interfering with steering or the accidental disconnection of wiring.

6.3.1.3. Powering the Switches

The differential switches will be powered by two 12-volt, 5-amp hour DeWalt drill batteries. The power supplied by the batteries then goes into a power relay, which then goes into another three relays. These control what position the differential is in.

6.4. Brake Light

6.4.1.2. Discussion of Design Reasoning – Mounting, Signal, Part

The brake light will be positioned such that it will be over 39.4 inches from the ground and will not be angled up. To be rules compliant we will be purchasing the Polaris Part # 2411092-432 brake light. There are two pressure sensors in parallel. One sensor detects brake pressure in the front, while the other detects pressure from the rear. Since the sensors are in parallel, if one fails the circuit will still function and we will still have a brake light.

6.4.1.3. Powering the Brake Light

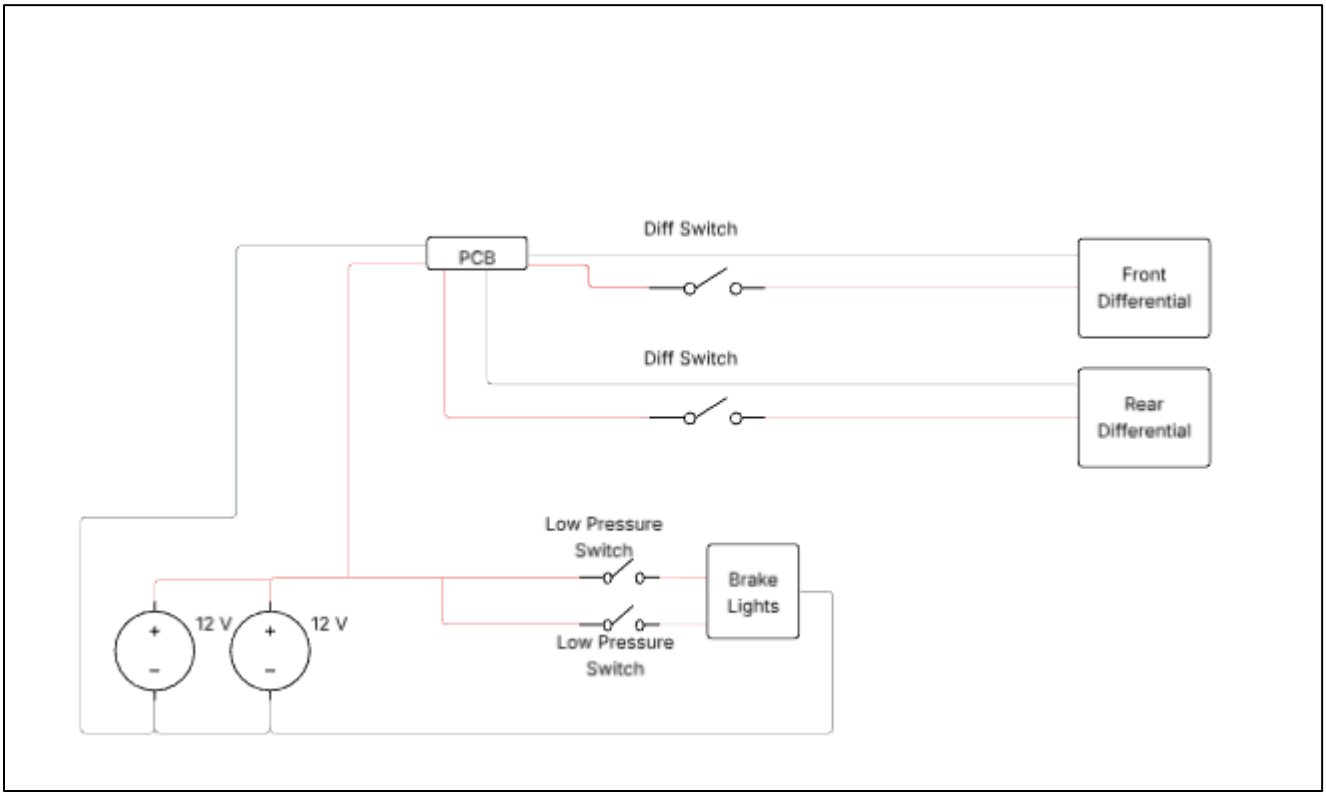

Figure 156: Brake Light and Diff Power Circuit

Similar to our differential switches, the brake light will be powered by our two 12-volt, 5-amp hour DeWalt drill batteries. While we don't know the exact power draw from the brake light, most Polaris RZR brake lights are 1.45 to 2.1 Amps, meaning the batteries would last between 6.9 to 4.8 consecutive hours of run time. Furthermore, last year's team used these batteries and a different Polaris brake light and ran into no issues. The brake light will be operable regardless of kill switch setting. See Figure 156.

6.5. Kill Switches

6.5.1.2. Discussion of Design Reasoning – Mounting

There will be two kill switches located on the vehicle. One kill switch must be located inside the cockpit and accessible to the driver. There will be no wiring modification of the kill switches, as per the rules. The kill switches are to ground the vehicle's ignition. The external kill switch shall be located within easy access to track workers on the right side of the vehicle. Both kill switches will be rigidly mounted to the frame with unobstructed access and will be mechanically fastened while meeting the requirements in Article 12 – Fasteners.

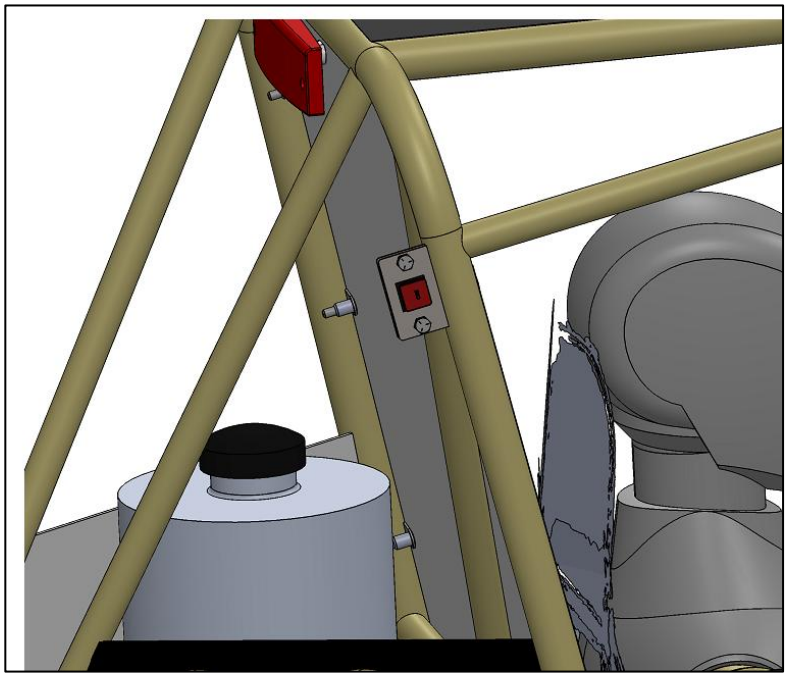

Figure 157: External Kill Switch Location

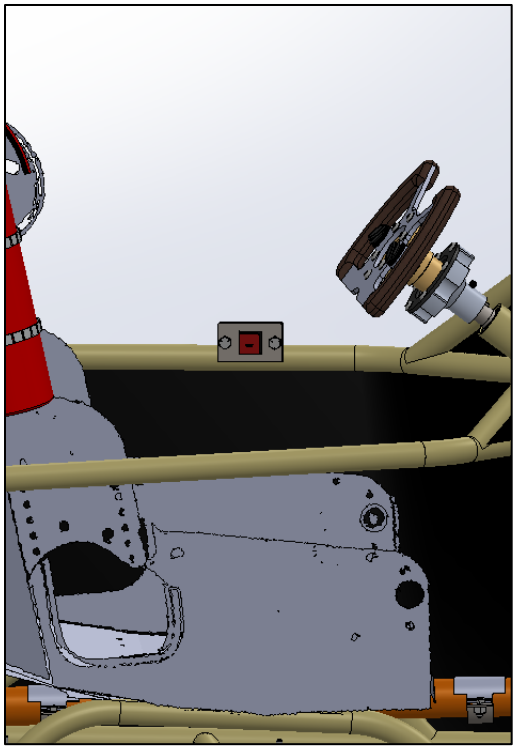

Figure 158: Driver Kill Switch Location

7. Appendix

7.2. Supplemental Hand Calculations and Code

7.2.1. Suspension Calculations

7.1.1.1 Front Suspension Calculations

7.1.1.1.1 Hand Calculations for Front Upright

Al bracket calc

```
clear all; clc; % tear out
A = 2*0.17*.625; % calc based on min distance and a total thickness of the
bracket arms
F = 3000/2; % 3000 lbs on the knuckle, 1/2 for 2 brackets
Stress = F/A; % Pa
Fs_tear = 35*10^3 / Stress; % 421 is yeild strenght found for 6061 t6 on
www.engineeringtoolbox.com

%bending
b = 1.75; %width of bracket
h = .625; %thickness
c = h/2;
LShock  = 6.5; %[in] moment arm from frame out for shock
LArm = 15.25; %[in] moment arm of lower control arm
FShock = 1600; % gather from past year white pappers for max shock force
FonBracket = FShock.*LShock./LArm;
FonBacket  = FonBracket.* cos(18*2*pi);
L = 1.65;
I = b*h^3 / 12;
M = FonBacket.*L;
BendingStress = M.*c./I;
Fs_bending = 35*10^3 ./ BendingStress;

fprintf('--- Aluminum Bracket Calculations ---\n');
fprintf('Tear-Out Area:                %.4f in^2\n', A);
fprintf('Force per Bracket:       %.2f lb\n', F);
fprintf('Tear-Out Stress:              %.2f psi\n', Stress);
fprintf('Safety Factor (Tear-Out):     %.2f\n\n', Fs_tear);
fprintf('--- Aluminum Bracket Calculations ---\n');
fprintf('Moment of Inertia (I):        %.6f in^4\n', I);
fprintf('Applied Moment:               %.2f lb·in\n', M);
fprintf('Bending Stress:               %.2f psi\n', BendingStress);
fprintf('Safety Factor (Bending):      %.2f\n', Fs_bending);
```

```
--- Aluminum Bracket Calculations ---
Tear-Out Area:                0.2125 in^2
Force per Bracket:       1500.00 lb
Tear-Out Stress:              7058.82 psi
Safety Factor (Tear-Out):     4.96

--- Aluminum Bracket Calculations ---
Moment of Inertia (I):        0.035604 in^4
Applied Moment:               1125.25 lb·in
```

```
Bending Stress:                9876.44 psi
Safety Factor (Bending):       3.54
```

Thread tear out calc

```
clear; clc;
D_major = 0.250;          % Major diameter (in) for 1/4"-20
D_minor = 0.1887;           % Minor diameter (in)
threads_per_inch = 20;     % TPI for UNF thread
L = 0.59;                 % Thread engagement length (in)
tau_allow = 24000;         % Allowable shear stress (psi) for 6061-T6 aluminum
                           % Adjust as needed for your material
D_avg = (D_major + D_minor) / 2;
A_shear = pi * D_avg * L;
F_tearout = tau_allow * A_shear;

fprintf('THREAD TEAR-OUT CALCULATION RESULTS:\n');
fprintf('-----------------------------------\n');
fprintf('Bolt Size:           1/4"-20 UNF\n');
fprintf('Major Diameter:      %.4f in\n', D_major);
fprintf('Minor Diameter:      %.4f in\n', D_minor);
fprintf('Engagement Length:   %.3f in\n', L);
fprintf('Average Diameter:    %.4f in\n', D_avg);
fprintf('Shear Area:          %.4f in^2\n', A_shear);
fprintf('Tear-Out Strength:   %.0f lb\n', F_tearout);
```

```
THREAD TEAR-OUT CALCULATION RESULTS:
-----------------------------------
Bolt Size:           1/4"-20 UNF
Major Diameter:      0.2500 in
Minor Diameter:      0.1887 in
Engagement Length:   0.590 in
Average Diameter:    0.2193 in
Shear Area:          0.4066 in^2
Tear-Out Strength:   9758 lb
```

Bolt shear

```
%{
SAE Bolt Strength
Safe Tensile Load at 6,000 PSI Load
Safe Shear Strength at 7,500 PSI Load

Source: https://www.calfast.com/cs_wiki/wiki/981-sae-bolt-strength?
srsltid=AfmBOopAiPUUg1d3PJwTYvQimYxPOuihs92TUtQN_d3b4Ma1b9NWtsLr&show=wiki
%}
```

Published with MATLAB® R2025a

7.1.1.1.3 Hand Calculations for FUCA

7.1.1.1.4 Hand Calculations for FLCA

7.1.1.2 Rear Suspension Calculations

7.1.1.2.1 Hand Calculations for Back Upright

Al bracket calc

```
clear all; clc;
% tear out due to side impact
A = 2*0.35*.75; % calc based on min distance and a total thickness of the
bracket arms
F = 2000; % F on Bracket
LBottomBrackettoTop = 4+3; % 4in above center of upright and 3 inches below
between brackets
LbottomBrackettoWheelBottom = 11.5-3; % wheel radius - bottom bracket drop
Fonwheel = 1500*LBottomBrackettoTop/LbottomBrackettoWheelBottom; % lever
ratio
Stress = F/A; % Pa
Fs_tear = 35*10^3 / Stress; % 421 is yeild strenght found for 6061 t6 on
www.engineeringtoolbox.com


fprintf('--- Aluminum Bracket Calculations ---\n');
fprintf('Tear-Out Area:                 %.4f in^2\n', A);
fprintf('Force per Bracket Side:        %.2f lb\n', F);
fprintf('Force on Bottom Wheel:        %.2f lb\n', Fonwheel);
fprintf('Tear-Out Stress:               %.2f psi\n', Stress);
fprintf('Safety Factor (Tear-Out):      %.2f\n\n', Fs_tear);
```

```
--- Aluminum Bracket Calculations ---
Tear-Out Area:                 0.5250 in^2
Force per Bracket Side:        2000.00 lb
Force on Bottom Wheel:        1235.29 lb
Tear-Out Stress:               3809.52 psi
Safety Factor (Tear-Out):      9.19
```

tear out due to Shock

```
clear all; clc;
LShock  = 11.15; %[in] moment arm from frame out for shock
LArm = 15.3; %[in] moment arm of lower control arm
FShock = 1600; % gather from past year white pappers for max shock force
FonBracket = FShock.*LShock./LArm;
A = 0.25*0.5; % calc based on min distance and a total thickness of the
bracket arms
LBottomBrackettoTop = 4+3; % 4in above center of upright and 3 inches below
```

```
between brackets
LbottomBrackettoWheelBottom = 11.5-3; % wheel radius - bottom bracket drop
Stress = FonBracket/A; % Pa
Fs_tear = 35*10^3 / Stress; % 421 is yeild strenght found for 6061 t6 on
www.engineeringtoolbox.com

fprintf('--- Aluminum Bracket Calculations ---\n');
fprintf('Tear-Out Area:                %.4f in^2\n', A);
fprintf('Force per Bracket Side:       %.2f lb\n', FonBracket);
fprintf('Tear-Out Stress:              %.2f psi\n', Stress);
fprintf('Safety Factor (Tear-Out):     %.2f\n\n', Fs_tear);
```

```
--- Aluminum Bracket Calculations ---
Tear-Out Area:                0.1250 in^2
Force per Bracket Side:       1166.01 lb
Tear-Out Stress:              9328.10 psi
Safety Factor (Tear-Out):     3.75
```

bending

```
clear all; clc;
b = 1.75; %width of bracket
h = 0.75; %thickness
c = h/2;
Fbend = 3000; % test data for front impact
L = 1;
I = b*h^3 / 12;
M = Fbend.*L;
BendingStress = M.*c./I;
Fs_bending = 35*10^3 ./ BendingStress;

fprintf('--- Aluminum Bracket Calculations ---\n');
fprintf('Moment of Inertia (I):        %.6f in^4\n', I);
fprintf('Applied Moment:               %.2f lb·in\n', M);
fprintf('Bending Stress:               %.2f psi\n', BendingStress);
fprintf('Safety Factor (Bending):      %.2f\n', Fs_bending);
```

```
--- Aluminum Bracket Calculations ---
Moment of Inertia (I):        0.061523 in^4
Applied Moment:               3000.00 lb·in
Bending Stress:               18285.71 psi
Safety Factor (Bending):      1.91
```

Thread tear out calc

```
clear; clc;
D_major = 0.250;          % Major diameter (in) for 1/4"-20
D_minor = 0.1887;           % Minor diameter (in)
threads_per_inch = 20;    % TPI for UNF thread
L = 0.59;                 % Thread engagement length (in)
tau_allow = 24000;         % Allowable shear stress (psi) for 6061-T6 aluminum
                           % Adjust as needed for your material
```

```
D_avg = (D_major + D_minor) / 2;
A_shear = pi * D_avg * L;
F_tearout = tau_allow * A_shear;

fprintf('THREAD TEAR-OUT CALCULATION RESULTS:\n');
fprintf('-----------------------------------\n');
fprintf('Bolt Size:           1/4"-20 UNF\n');
fprintf('Major Diameter:      %.4f in\n', D_major);
fprintf('Minor Diameter:      %.4f in\n', D_minor);
fprintf('Engagement Length:   %.3f in\n', L);
fprintf('Average Diameter:    %.4f in\n', D_avg);
fprintf('Shear Area:          %.4f in^2\n', A_shear);
fprintf('Tear-Out Strength:   %.0f lb\n', F_tearout);
```

```
THREAD TEAR-OUT CALCULATION RESULTS:
-----------------------------------
Bolt Size:           1/4"-20 UNF
Major Diameter:      0.2500 in
Minor Diameter:      0.1887 in
Engagement Length:   0.590 in
Average Diameter:    0.2193 in
Shear Area:          0.4066 in^2
Tear-Out Strength:   9758 lb
```

Bolt shear

```
%{
SAE Bolt Strength
Safe Tensile Load at 6,000 PSI Load
Safe Shear Strength at 7,500 PSI Load

Source: https://www.calfast.com/cs_wiki/wiki/981-sae-bolt-strength?
srsltid=AfmBOopAiPUUg1d3PJwTYvQimYxPOuihs92TUtQN_d3b4Ma1b9NWtsLr&show=wiki
%}
```

Published with MATLAB® R2025a

7.1.1.2.2 Hand Calculations for RUCA

7.1.1.2.2.1 Front to back Hand Calculations for RUCA

```
"Upper suspension arm (with shock mount) front to back ideal beam calculations"
"known"
L_arm=26.3 [in] "length between chassis front and rear pick up points"
Shock_dist=5.02 [in] "distance of shock between front and rear pickup points on chassis"
Tube_diam_out=1 [in]
Tube_wall=.065 [in]
E=29700000[psi] "4130 chomolly"
Sigma_Yield=67000[psi]

"Assumptions"
F_Shock=1000[lbf]
Shock_angle=90[deg]
"pinned end condition"

"derived quantities"
P_y=F_shock*Sin(Shock_angle)
P_x=F_shock*Cos(Shock_angle)
L=L_arm
b=L-Shock_dist
a=Shock_dist
Tube_diam_in=Tube_diam_out-2*Tube_wall
I=PI/64*(Tube_diam_out^4 - Tube_diam_in^4) "2nd area moment of inertia"
C=Tube_diam_out/2

"equations"
R_a_y=P_y*b/L "reaction at A (chassis side)"
R_b_y=P_y*a/L "reaction at B (knuckle side)"

M_max=P_y*a*b/L "maximum internal torque"

Y_max=(P_y*a*b)/(6*L*E*I)*(L^2-a*b) "max displacement"

Sigma_max=M_max*C/I "max bending stress"

FOS=Sigma_yield/Sigma_max  "factor of safety based on tube"
```

Upper suspension arm (with shock mount) front to back ideal beam calculations

known

L_{arm} = 26.3 [in] length between chassis front and rear pick up points

$Shock_{dist}$ = 5.02 [in] distance of shock between front and rear pickup points on chassis

$Tube_{diam,out}$ = 1 [in]

$Tube_{wall}$ = 0.065 [in]

E = 2.97×10^7 [psi] 4130 chomolly

σ_{Yield} = 67000 [psi]

Assumptions

F_{Shock} = 1000 [lbf]

$Shock_{angle}$ = 90 [deg]

pinned end condition

derived quantities

$P_y = F_{Shock} \cdot \mathbf{sin}(Shock_{angle})$

$P_x = F_{Shock} \cdot \mathbf{cos}(Shock_{angle})$

$L = L_{arm}$

$b = L - Shock_{dist}$

$a = Shock_{dist}$

$Tube_{diam,in} = Tube_{diam,out} - 2 \cdot Tube_{wall}$

$I = \frac{\pi}{64} \cdot (Tube_{diam,out}^4 - Tube_{diam,in}^4)$ 2nd area moment of inertia

$C = \frac{Tube_{diam,out}}{2}$

equations

$R_{a,y} = P_y \cdot \frac{b}{L}$ reaction at A (chassis side)

$R_{b,y} = P_y \cdot \frac{a}{L}$ reaction at B (knuckle side)

$M_{max} = P_y \cdot a \cdot \frac{b}{L}$ maximum internal torque

$Y_{max} = \frac{P_y \cdot a \cdot b}{6 \cdot L \cdot E \cdot I} \cdot (L^2 - a \cdot b)$ max displacement

$\sigma_{max} = M_{max} \cdot \frac{C}{I}$ max bending stress

$FOS = \frac{\sigma_{Yield}}{\sigma_{max}}$ factor of safety based on tube

SOLUTION

Unit Settings: Eng F psia mass deg

a = 5.02 [in]	b = 21.28 [in]	C = 0.5 [in]
E = 2.970E+07 [psi]	FOS = 0.6917	F_{Shock} = 1000 [lbf]
I = 0.02097 [in^4]	L = 26.3 [in]	L_{arm} = 26.3 [in]
M_{max} = 4062 [in*lbf]	P_x = 1.897E-16 [lbf]	P_y = 1000 [lbf]

$R_{a,y}$ = 809.1 [lbf]
$Shock_{dist}$ = 5.02 [in]
$Tube_{diam,in}$ = 0.87 [in]
Y_{max} = 0.6359 [in]

$R_{b,y}$ = 190.9 [lbf]
σ_{max} = 96870 [psi]
$Tube_{diam,out}$ = 1 [in]

$Shock_{angle}$ = 90 [deg]
σ_{Yield} = 67000 [psi]
$Tube_{wall}$ = 0.065 [in]

No unit problems were detected.

KEY VARIABLES
M_{max} = 4062 [in*lbf]
σ_{max} = 96870 [psi]
Y_{max} = 0.6359 [in]
FOS = 0.6917

7.1.1.2.2.1 Side to Side Hand Calculations for RUCA

```
"Upper suspension arm (with shock mount) side to side ideal beam calculations"
"known"
L_arm=15.2 [in] "length between chassis rear pick up point and upright connection points"
Shock_dist=10.32 [in] "distance of shock between rear pickup point on chassis and upright connection point"
Tube_diam_out=1.25 [in]
Tube_wall=.095 [in]
E=29700000[psi] "4130 chomolly"
Sigma_Yield=67000[psi]

"Assumptions"
F_Shock=1000[lbf]
Shock_angle=90[deg]
"pinned end condition"

"derived quantities"
P_y=F_shock*Sin(Shock_angle)
P_x=F_shock*Cos(Shock_angle)
L=L_arm
b=L-Shock_dist
a=Shock_dist
Tube_diam_in=Tube_diam_out-2*Tube_wall
I=PI/64*(Tube_diam_out^4 - Tube_diam_in^4) "2nd area moment of inertia"
C=Tube_diam_out/2

"equations"
R_a_y=P_y*b/L "reaction at A (chassis side)"
R_b_y=P_y*a/L "reaction at B (knuckle side)"

M_max=P_y*a*b/L "maximum internal torque"

Y_max=(P_y*a*b)/(6*L*E*I)*(L^2-a*b) "max displacement"

Sigma_max=M_max*C/I "max bending stress"

FOS=Sigma_yield/Sigma_max "factor of safety based on tube"
```

Upper suspension arm (with shock mount) side to side ideal beam calculations

known

$L_{arm} = 15.2$ [in] length between chassis rear pick up point and upright connection points

$Shock_{dist} = 10.32$ [in]

distance of shock between rear pickup point on chassis and upright connection point

$Tube_{diam,out} = 1.25$ [in]

$Tube_{wall} = 0.095$ [in]

$E = 2.97 \times 10^{7}$ [psi] 4130 chomolly

$\sigma_{Yield} = 67000$ [psi]

Assumptions

$F_{Shock} = 1000$ [lbf]

$Shock_{angle} = 90$ [deg]

pinned end condition

derived quantities

$P_y = F_{Shock} \cdot \mathbf{sin}(Shock_{angle})$

$P_x = F_{Shock} \cdot \mathbf{cos}(Shock_{angle})$

$L = L_{arm}$

$b = L - Shock_{dist}$

$a = Shock_{dist}$

$Tube_{diam,in} = Tube_{diam,out} - 2 \cdot Tube_{wall}$

$I = \frac{\pi}{64} \cdot (Tube_{diam,out}^4 - Tube_{diam,in}^4)$ 2nd area moment of inertia

$C = \frac{Tube_{diam,out}}{2}$

equations

$R_{a,y} = P_y \cdot \frac{b}{L}$ reaction at A (chassis side)

$R_{b,y} = P_y \cdot \frac{a}{L}$ reaction at B (knuckle side)

$M_{max} = P_y \cdot a \cdot \frac{b}{L}$ maximum internal torque

$Y_{max} = \frac{P_y \cdot a \cdot b}{6 \cdot L \cdot E \cdot I} \cdot (L^2 - a \cdot b)$ max displacement

$\sigma_{max} = M_{max} \cdot \frac{C}{I}$ max bending stress

$FOS = \frac{\sigma_{Yield}}{\sigma_{max}}$ factor of safety based on tube

SOLUTION

Unit Settings: Eng F psia mass deg

a = 10.32 [in]	b = 4.88 [in]	C = 0.625 [in]
E = 2.970E+07 [psi]	FOS = 1.872	F_{Shock} = 1000 [lbf]

$I = 0.05787$ [in^4]
$M_{max} = 3313$ [in*lbf]
$R_{a,y} = 321.1$ [lbf]
$Shock_{dist} = 10.32$ [in]
$Tube_{diam,in} = 1.06$ [in]
$Y_{max} = 0.05805$ [in]

$L = 15.2$ [in]
$P_x = 1.897E-16$ [lbf]
$R_{b,y} = 678.9$ [lbf]
$\sigma_{max} = 35783$ [psi]
$Tube_{diam,out} = 1.25$ [in]

$L_{arm} = 15.2$ [in]
$P_y = 1000$ [lbf]
$Shock_{angle} = 90$ [deg]
$\sigma_{Yield} = 67000$ [psi]
$Tube_{wall} = 0.095$ [in]

No unit problems were detected.

KEY VARIABLES
$M_{max} = 3313$ [in*lbf]
$\sigma_{max} = 35783$ [psi]
$Y_{max} = 0.05805$ [in]
FOS = 1.872

7.2.2. Controls Calculations

7.2.2.2. Brake Force Calculations:

Assume negligible pressure differentials due to height

$F_{pedal} = 120$ [lbf] driver input force

$Length_{pedal} = 14.8$ [in] length from pedal to pivot

$Length_{master} = 6.1$ [in] length from master cylinder bolt sleeve to pivot

$A_{caliper} = 2 \cdot A_{piston}$ 1 caliper has 2 opposing pistons

$A_{piston} = R_{piston}^{2} \cdot \pi$ area calc

$$R_{piston} = \frac{1.1125}{2} \text{ [1/in]}$$

$$A_{master} = \left[\frac{Diam_{master}}{2}\right]^{2} \cdot \pi$$ area calc

$$Diam_{master} = \frac{5}{8} \text{ [1/in]}$$

$M_{baja} = 700$ [lbf] mass of car

friction coefficients

$\mu_{asphalt} = 0.9$ worst case scenario, .9 is a large overestimate *120lbs braking force required to lock wheels on asphalt

$\mu_{brakepad} = 0.37$

$R_{tire} = 11.5$ [in]

$R_{rotor,effective} = 3.25$ [in] the assumed radius of the rotor where the brace force is applied

force on master cylinder calc

$$F_{master} = \frac{F_{pedal} \cdot \frac{Length_{pedal}}{Length_{master}}}{2}$$ Lever Arm calc

system pressure calcs

$$P_{Master,front} = \frac{F_{master}}{A_{master}}$$ the force at the master cylinders

$P_{Master,rear} = P_{Master,front} \cdot 0.75$

$F_{caliper,front} = P_{Master,front} \cdot A_{caliper} \cdot 2$

$F_{caliper,rear} = P_{Master,rear} \cdot A_{caliper} \cdot 2$

wheel stopping calcs

assuming unequal force on all 4 wheels

$Force_{normal,frontwheel} = M_{baja} \cdot 0.3$

$Force_{normal,rearwheel} = M_{baja} \cdot 0.2$

$F_{Friction,Tirefront} = Force_{normal,frontwheel} \cdot \mu_{asphalt}$ The force of static friction between the tire and road

$F_{Friction,Tirerear} = Force_{normal,rearwheel} \cdot \mu_{asphalt}$ The force of static friction between the tire and road

$Torque_{road,frictionfront} = F_{Friction,Tirefront} \cdot R_{tire}$ the torque the front wheels apply to the axle

$Torque_{road,frictionrear} = F_{Friction,Tirerear} \cdot R_{tire}$ the torque the rear wheels apply to the axle

$Torque_{braking,front} = F_{caliper,front} \cdot \mu_{brakepad} \cdot R_{rotor,effective}$ the torque the brake force from one caliper applies back to the axle

$Torque_{braking,rear} = F_{caliper,rear} \cdot \mu_{brakepad} \cdot R_{rotor,effective}$ the torque the brake force from one caliper applies back to the axle

SOLUTION

Unit Settings: Eng F psia mass deg

$A_{caliper} = 1.944$ [in*in]
$Diam_{master} = 0.625$ [in]
$F_{caliper,front} = 1845$ [lbf]
$F_{Friction,Tirerear} = 126$ [lbf]
$Length_{master} = 6.1$ [in]
$\mu_{brakepad} = 0.37$
$P_{Master,rear} = 355.9$ [psi]
$R_{tire} = 11.5$ [in]
$Torque_{road,frictionfront} = 2174$ [in*lbf]

$A_{master} = 0.3068$ [in*in]
$Force_{normal,frontwheel} = 210$ [lbf]
$F_{caliper,rear} = 1384$ [lbf]
$F_{master} = 145.6$ [lbf]
$Length_{pedal} = 14.8$ [in]
$M_{baja} = 700$ [lbf]
$R_{piston} = 0.5563$ [in]
$Torque_{braking,front} = 2219$ [in*lbf]
$Torque_{road,frictionrear} = 1449$ [in*lbf]

$A_{piston} = 0.9721$ [in*in]
$Force_{normal,rearwheel} = 140$ [lbf]
$F_{Friction,Tirefront} = 189$ [lbf]
$F_{pedal} = 120$ [lbf]
$\mu_{asphalt} = 0.9$
$P_{Master,front} = 474.5$ [psi]
$R_{rotor,effective} = 3.25$ [in]
$Torque_{braking,rear} = 1664$ [in*lbf]

No unit problems were detected.

KEY VARIABLES

$Torque_{braking,rear} = 1664$ [in*lbf]
$Torque_{braking,front} = 2219$ [in*lbf]
$Torque_{road,frictionfront} = 2174$ [in*lbf]
$Torque_{road,frictionrear} = 1449$ [in*lbf]

7.2.3. Drivetrain Calculations

7.2.3.2. Gearbox Calculations:

7.2.3.2.1. Bearing Calculations:

Governing Equations for Spiral Bevel Gear Forces

Variables	Equation	Value
Number of Teeth (z_1 & z_2)	-	20
Transverse Module (m)	-	4 [mm]
Pressure Angle (α_n)	-	20º
Helix Angle (β_m)	-	35º
CVT Max Gear Ratio (Gr_{CVT})	-	3.9
Maximum Motor Torque (T_m)	-	25.08 [N]
Reference Diameter (d_m)	zm	80 [mm]
Reference Cone Angle (δ)	$\tan^{-1}\left(\frac{z_1}{z_2}\right)$	45º
Shaft Torque (T)	$T_m \cdot Gr_{CVT}$	97.82 [Nm]
Force Type	**Equation**	**Value [N]**
Tangential (F_{t1}) [N]	$\frac{2000T}{d_m}$	2,908.26
Axial (F_{x1}) [N]	$\frac{F_t}{\cos\beta_m}\left(\tan\alpha_n \sin\delta + \sin\beta_m \cos\delta\right)$	-2,353.67
Radial (F_{r1}) [N]	$\frac{F_t}{\cos\beta_m}\left(\tan\alpha_n \cos\delta - \sin\beta_m \sin\delta\right)$	526.21
Axial (F_{x2})	F_{r1}	526.21

[N]		
Radial (F_{r2}) [N]	F_{x1}	-2,353.67
Tangential (F_{t2}) [N]	F_{t1}	2,908.26

Table 27: Spiral Bevel Gear Force Calculations

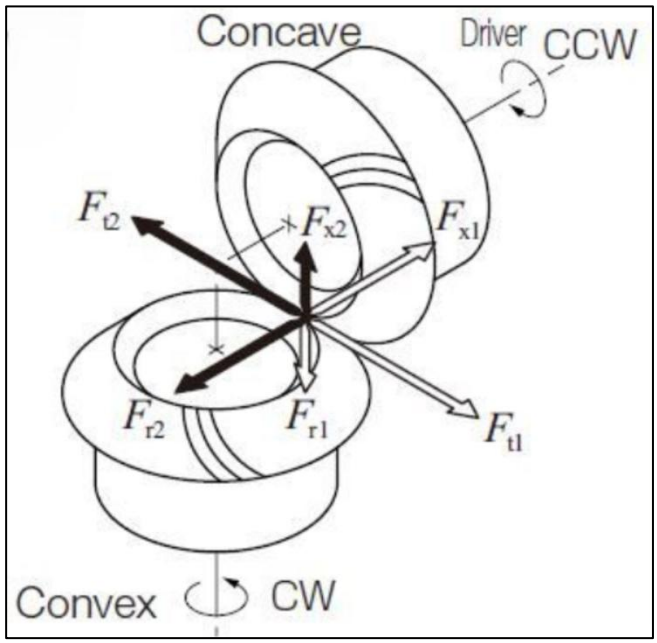

Figure 159: Spiral Bevel Gear Force Reference Directions

Governing Equations for Spur Gear Forces

Variables	Equation	Value
Driving Spur Teeth Number (z_1)	-	18
Driven Spur Teeth Number (z_2)	-	44
Transverse Modules (m)	-	3 [mm]
Pressure Angles (α_n)	-	20º
Spur Gear Ratio (Gr_{Spur})	$\frac{z_2}{z_1}$	2.444
Reference Diameter (d)	zm	54 [mm]
Shaft Torque (T)	$T_m \cdot Gr_{CVT} \cdot Gr_{Spur}$	239.12 [Nm]

Force Type	Equation	Value [N]
Tangential (F_{t1}) [N]	$\frac{2000T}{d}$	3,623.05
Radial (F_{r1}) [N]	$F_t \cdot \tan\alpha_n$	1,318.05
Axial (F_{x1}) [N]	-	0
Tangential (F_{t2}) [N]	F_{t1} (Equal and Opposite)	3,623.05
Radial (F_{r2}) [N]	F_{r1} (Equal and Opposite)	1,318.05
Axial (F_{x2}) [N]	-	0

Table 28: Spur Gear Force Calculations

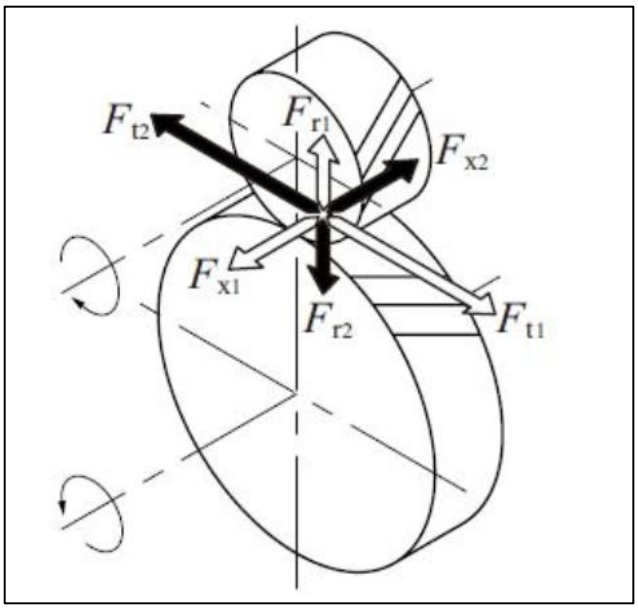

Figure 160: Spur Gear Force Reference Directions

Transfer Case Key Stresses:

```
clc;
clear all;
%Assuming 1045 Steel, Brinell B87
ShearStrength = 219; %MPa, corrected with 1.5 FoS
UncorShearStrength = 329; %MPa, corrected with 1.5 FoS
YieldStrength = 380; %MPa, corrected with 1.5 FoS
UncorYieldStrength = 570; %MPa, no safety factor


disp(['Material Properties for 1045 Steel with Brinell B87 Hardness'])
disp(['Ultimate Shear Strength: ', num2str(UncorShearStrength), ' MPa'])
disp(['Yield Strength: ', num2str(UncorYieldStrength), ' MPa'])
disp(['Minimum Factor of Safety Goal for Keys: 1.5'])
disp(['----------------------------------------'])

%key1
T = 100; %Nm
w = 6/1000; %mm to m
h = 6/1000; %mm to m
depth = .125*.0254; %in to m
D = .79*0.0254; %m
% l = .37*.0254; %m
l = 10/1000; %mm to m


disp('Key #1: Input Shaft Spiral Bevel Gear Key')
ShearStress1 = 2*T/(w*l*D)/10^6; %MPa
CrushStress1 = 2*T/((h-depth)*l*D)/10^6; %MPa
disp(['Shear stress: ', num2str(ShearStress1), ' MPa
about a ' num2str(UncorShearStrength/ShearStress1), ' FOS'])
disp(['Crush stress: ', num2str(CrushStress1), ' MPa
about a ' num2str(UncorYieldStrength/CrushStress1), ' FOS'])
disp(['----------------------------------------'])

%key2-1
T = 100; %Nm
w = 6/1000; %mm to m
h = 6/1000; %mm to m
depth = .125*.0254; %in to m
D = .75*0.0254; %m
lOld = (.69-.13)*.0254; %m
l = 10/1000; %mm to m


disp('Key#2_1: Pinion Shaft Spiral Bevel Gear Key')
ShearStress2_1 = 2*T/(w*l*D)/10^6; %MPa
CrushStress2_1 = 2*T/((h-depth)*l*D)/10^6; %MPa
```

```
disp(['Shear stress: ', num2str(ShearStress2_1), ' MPa
about a ' num2str(UncorShearStrength/ShearStress2_1), ' FOS'])
disp(['Crush stress: ', num2str(CrushStress2_1), ' MPa
about a ' num2str(UncorYieldStrength/CrushStress2_1), ' FOS'])
disp(['----------------------------------------'])

%key2-2
T = 100; %Nm
w = 6/1000; %mm to m
h = 6/1000; %mm to m
depth = .125*.0254; %in to m
D = .75*0.0254; %m
% l = (0.75-.13-.04)*.0254; %m
l = 12/1000; %mm to m


disp('Key#2_2: Pinion Shaft Spur Gear Key')
ShearStress2_2 = 2*T/(w*l*D)/10^6; %MPa
CrushStress2_2 = 2*T/((h-depth)*l*D)/10^6; %MPa
disp(['Shear stress: ', num2str(ShearStress2_2), ' MPa
about a ' num2str(UncorShearStrength/ShearStress2_2), ' FOS'])
disp(['Crush stress: ', num2str(CrushStress2_2), ' MPa
about a ' num2str(UncorYieldStrength/CrushStress2_2), ' FOS'])
disp(['----------------------------------------'])
%key3

T = 240; %Nm
w = 6/1000; %mm to m
h = 6/1000; %mm to m
depth = .125*.0254; %in to m
D = 1*0.0254; %m
l = .75*.0254; %in to m

disp('Key#3: Output Shaft Spur Gear Key')
ShearStress3 = 2*T/(w*l*D)/10^6; %MPa
CrushStress3 = 2*T/((h-depth)*l*D)/10^6; %MPa
disp(['Shear stress: ', num2str(ShearStress3), ' MPa
about a ' num2str(UncorShearStrength/ShearStress3), ' FOS'])
disp(['Crush stress: ', num2str(CrushStress3), ' MPa
about a ' num2str(UncorYieldStrength/CrushStress3), ' FOS'])
```

```
Material Properties for 1045 Steel with Brinell B87 Hardness
Ultimate Shear Strength: 329 MPa
Yield Strength: 570 MPa
Minimum Factor of Safety Goal for Keys: 1.5
----------------------------------------
Key #1: Input Shaft Spiral Bevel Gear Key
Shear stress: 166.1185 MPa                    about a 1.9805 FOS
Crush stress: 352.818 MPa                     about a 1.6156 FOS
----------------------------------------
Key#2_1: Pinion Shaft Spiral Bevel Gear Key
Shear stress: 174.9781 MPa                    about a 1.8802 FOS
Crush stress: 371.635 MPa                     about a 1.5338 FOS
----------------------------------------
```

```
Key#2_2: Pinion Shaft Spur Gear Key
Shear stress: 145.8151 MPa                    about a 2.2563 FOS
Crush stress: 309.6958 MPa                    about a 1.8405 FOS
----------------------------------------
Key#3: Output Shaft Spur Gear Key
Shear stress: 165.3337 MPa                    about a 1.9899 FOS
Crush stress: 351.1511 MPa                    about a 1.6232 FOS
```

Published with MATLAB® R2025a

Transfer Case Calculations

Table of Contents

Gear ratio calculations for Baja 2025-2026. 1

Gear ratio calculations for Baja 2025-2026.

```
close all
clc

% Assuming power limited acceleration.

% Assuming 40% effciency, car + rider weight of 700 lbs, and a 10%
improvement over
% last years car.

% The torque from the engine goes through the gear ratio to the wheels,
% where the inertias of the rotating drivetrain components needs to be
% accounted for. The inertia of each component is affected by the gear
% ratios ahead of that component in the drivetrain.

% Using english units
g = 32.2*12;

% Physical car parameters.
P_engine = 10; %Hp
W_car = 700; %lbm
T_engine = 18.5*12; %in-lbs
R_wheel = 22.5/2; % in
Wheel_Weight = 19; %lbm


% Resistance forces
C_rr = 0.23;
F_rr= W_car*C_rr;

% Inertias
Wheel_Izz = 4*2/3*Wheel_Weight*(R_wheel^2);

% Acceleration, improve 10% from last year
imp = 10/100;
a = ((9-4)*17.6)/(1.5*(1-imp)); %in/s^2
a_real = 0.9*a;

% Efficiency
n_eff = 0.6;

% Calculating GR after the CVT
Ntf = ((((W_car + Wheel_Izz/R_wheel^2)*(a/g)) + F_rr)*(R_wheel/
(T_engine*n_eff)))/2.7;

% Finding the efficiency


Wheel_RPM = 112;
T_Wheel = R_wheel*(F_rr + (W_car*a_real/32.2))/12;
P_real = T_Wheel*Wheel_RPM/5252;

N_disp = sprintf('\n \t Gear Ratio: %0.2f',Ntf);
disp(N_disp);
```

```
Gear Ratio: 9.00
```

Table of Contents

2025-2026 Franken Love Box Shaft Stresses. 1
Physical prameters. 1
Gear Geometry 1
Gear Backlash calculations 2
Forces and Torques 2
Spur Gear Bending tooth stresses 3
Spiral Bevel Miters Bending tooth strength 4
Bearing Reaction Forces 6
Input Inner shaft diameter 8
Midshaft Inner shaft diameter 8
Tearout stress on the bearing bore step 8

2025-2026 Franken Love Box Shaft Stresses.

```
clear
close all
clc
```

Physical prameters.

```
% motor torque, maximum torque for worst case senario.
Tm = 25.1; %Nm

% CVT Gear ratios and Info
GCVT_GR_Min = 3.9;
GCVT_GR_Max = 0.9;
GCVT_Secondary_Max_Diam = 8*0.0254; %m

% angle of the CVT driveshaft, degrees
a_CVT = 25;
```

Gear Geometry

A bunch of these factors ended up not being used since I was going to deep.

```
S_module = 3;
S_addendum_coeff = 1; %mm
S_deddedum_coeff = 1.25;
S_pressure_angle = 20; %deg

S_face_width = 19.05; %mm
S_addendum = S_addendum_coeff*S_module;
S_deddedum = S_deddedum_coeff*S_module;

SBM_tooth = 20;
SBM_module = 4;
SBM_pitch_diam = SBM_tooth*SBM_module; %mm
```

```
SBM_pressure_angle = 20; %deg
SBM_helical_angle = 35; %deg
SBM_face_width = 18; %mm
SBM_cone_angle = 45; %deg
SBM_pitch_angle = 45; %deg
SBM_tooth_thickness = pi()*SBM_module/2;
SBM_base_diameter = SBM_pitch_diam*cosd(SBM_pressure_angle);
SBM_cone_distance = SBM_base_diameter/(2*sind(SBM_cone_angle));

SP_tooth = 18;
SP_pitch_diam = SP_tooth*S_module; %mm
SP_tip_diam = SP_pitch_diam + 2*S_addendum;

SG_tooth = 44;
SG_pitch_diam = SG_tooth*S_module;
SG_tip_diam = SG_pitch_diam + 2*S_addendum;

Center_distance = SP_pitch_diam/2 + SG_pitch_diam/2; %mm
S_TCR = (sqrt((SP_tip_diam/2)^2 - (SP_pitch_diam/2)^2) + sqrt((SG_tip_diam/
2)^2 - (SG_pitch_diam/2)^2) - (Center_distance*sind(S_pressure_angle)))/
(pi()*S_module*cosd(S_pressure_angle));
SP_ttha = (90/SP_tooth);
% SP_Chordal_height = (SP_tooth*S_module*(1-cosd(SP_ttha))/2 + S_addendum);
SP_Chordal_height = 2*S_addendum;
SP_tip_radius = 0.5; %mm

% Shaft lengths and moment arms (ma), [m]

% Input shaft
GCVT_mab1 = 3.125*0.0254;
GCVT_mab2 = 5.775*0.0254;
SBML_mab1 = 1.9*0.0254;
SBML_mab2 = 0.75*0.0254;
b1_mab2 = 2.65*0.0254;
```

Gear Backlash calculations

```
jns = 0.0655;
jts = jns/(cosd(S_pressure_angle));
jasp = 360*jts/(pi()*SP_pitch_diam);
jasg = 360*jts/(pi()*SG_pitch_diam);
jrs = jns/(2*sind(S_pressure_angle));

% Sprial bevel gears backlash
jnsb = 0.01062992;
jasb = jnsb/(2*sind(SBM_pressure_angle)*sind(SBM_pitch_angle));
```

Forces and Torques

```
% CVT Forces [N]
F_GCVT = 900;
F_GCVT_x = cosd(a_CVT)*F_GCVT;
F_GCVT_y = sind(a_CVT)*F_GCVT;
```

```
% Gear forces [N], from khk gear calculator, make sure to understand inputs
SBML_r = 2355.30341;
SBML_x = -526.5724;
SBML_t = 2910.27133;

SBMR_r = -526.5724;
SBMR_x = 2355.30341;
SBMR_t = 2910.27133;

S_t = 2000*Tm*GCVT_GR_Min/SP_pitch_diam;
S_r = S_t*tand(S_pressure_angle);
```

Spur Gear Bending tooth stresses

Defining the Bending tooth stress limit

```
Ob_tlim = 340; %Mpa

% Defining the length of action for the contact ratio
Z = sqrt((SP_pitch_diam/2 + S_addendum)^2 -
(SP_pitch_diam*cosd(S_pressure_angle)/2)^2) + sqrt((SG_pitch_diam/2
+ S_addendum)^2 - (SG_pitch_diam*cosd(S_pressure_angle)/2)^2) -
Center_distance*sind(S_pressure_angle);

% Finding the base pitch, doesn't matter if pinion or gear is used.
pb = pi()*SP_pitch_diam/SP_tooth;

% Finding the contact ratio
mp = Z/pb;


% Finding the bending tooth stress factors, using ISO_6336-3

%Yf
% First finding the value of theta for the bendng moment arm height,
% chordal root normal thickness. The line of action is assumed to be
% colinear with the line definined by the pressure angle
% Assuming theta = pi/6 rad
% theta = pi()/6; %rad
% SP_G = (SP_tip_radius/S_module) - (SP_Chordal_height/S_module);
% SP_sfn = S_module*((SP_tooth*sin((pi()/3)- theta)) + (sqrt(3)*((SP_G/
cos(theta)) - (SP_tip_radius/S_module))));
%
% SP_dan = SP_pitch_diam + S_addendum;
% SP_dbn = SP_pitch_diam*cosd(S_pressure_angle);
% SP_dena = sqrt((SP_dan/2)^2 - (SP_dbn/2)^2);
% SP_denb = pi()*SP_pitch_diam*cosd(S_pressure_angle)*(S_TCR-1)/SP_tooth;
% SP_den = 2*sqrt((Sp_dena - (SP_denb))^2 + (SP_dbn/2)^2);
% ye = 0.5*pi()/(SG_tooth);
%
% hFea = (cos(ye) - (sin(ye)*tand(S_pressure_angle)))*(SP_den/SP_tooth);
% hFeb = (SP_G/cos(theta)) - (SP_tip_radius/S_module);
```

```
% hFe = (S_module/2)*(hFea - (SP_tooth*cos((pi()/3) - theta)*(hFeb)));
%
% Yfp = 2.9;
% Yfg = 2.32;
% Ye = 1/S_TCR;
% Yb = 1;
%
%
% KL = 1;
% Kfx = 1;
% Kv = 1.5;
% Ko = 1.25;


% from engineering edge as a table
Y_lewis = 0.308;
S_t_one = S_t/mp;
Obt_lewis = S_t_one/(S_module*S_face_width*Y_lewis);
Lewis_SF = mp*Ob_tlim/Obt_lewis;
disp(Lewis_SF)
%Lewis bending strength matches
```

```
    3.8762
```

Spiral Bevel Miters Bending tooth strength

Finding the bending tooth stress, using the lewis bending formula, with geometry adjustments

```
SBM_yield = 415; %Mpa

% equivelent virtual teeth
SBM_zv = SBM_tooth/(cosd(SBM_cone_angle)*(cosd(SBM_helical_angle)^3));

% Y Factors
SB_Yf = 2.47;
SB_Ye = 1/1.293;
SB_Yb = 0.75;
SB_Yc = 1;

SB_Re = SBM_cone_distance/(SBM_cone_distance - (0.5*SBM_face_width));

% K factors
SB_Km = 1.4;
SB_Kv = 1.7;
SB_Ko = 1;
SB_Kl = 1;
SB_Kr = 1.2;
SB_Kfx = 1;

% Tooth bending strength
SBM_of = SBMR_t*((SB_Yf*SB_Ye*SB_Yb*SB_Yc*SB_Re)/
(0.85*cosd(SBM_helical_angle)*SBM_module*SBM_face_width))*((SB_Km*SB_Kv*SB_Ko
*SB_Kr)/(SB_Kl*SB_Kfx));
```

```
SBM_sf = SBM_yield/SBM_of;
SBM_sf_disp = sprintf('\n\n Safey factor under JGMA standards: \n\n\t
%0.2f',SBM_sf);

% Comparison to last years gears, using the same loading conditions
J = 0.4;
k_a = 1.5; %mod shock
k_m = 1.6; %AGMA
k_s = 1; %size factor typ 1
k_v = 1; %dynamic factor for vibrations
k_x = 1.5; %AGMA
omega = SBML_t/(SBM_face_width*J*SBM_module)*((k_a*k_m*k_s)/(k_v*k_x));
% omega = omega*10^-6;
SF_comp = SBM_yield/omega;
SF_comp_disp = sprintf(' \n\n Safety factor under last years conditions
(AGMA standard): \n\n\t %0.2f',SF_comp);
LySf_disp = sprintf('\n\n Last years safety factor under last years
conditions (AGMA standard): \n\n\t %0.2f \n\n',2.3360);

% Comparison to last years gears, under the JGMA standards
T_p = 75.25; %Nm
d_ly = 37.5/1000; %m
p_d = (9/37.5)*1000; %m^-1
f_w = 15/1000; %m

ly_ref = atan2(9,27);
ly_ref_2 = atan2(27,9);
z_ly = 9/(cos(ly_ref)*(cosd(SBM_helical_angle)^3));
R_ly = 42/(2*sin(ly_ref_2));

% Y Factors
SBp_Yf = 3.27;
SBp_Ye = 1/1.15;
SBp_Yb = 0.75;
SBp_Yc = 1;

SBp_Re = R_ly/(R_ly - (0.5*15));

% K factors
SBp_Km = 1.4;
SBp_Kv = 1.7;
SBp_Ko = 1;
SBp_Kl = 1;
SBp_Kr = 1.2;
SBp_Kfx = 1;



omega_l = 2*(T_p/d_ly)*(p_d/
(f_w))*((SBp_Yf*SBp_Ye*SBp_Yb*SBp_Yc*SBp_Re)*(SBp_Km*SBp_Kv*SBp_Ko*SBp_Kr)/
(SBp_Kl*SBp_Kfx));
omega_l = omega_l*10^-6;
yeildStr = 600; %mpa
```

```
Sf_ly_nc = yeildStr/omega_1;
Sf_ly_nc_disp = sprintf('\n\n Last years safety factor under JGMA standards:
\n\n\t %0.2f',Sf_ly_nc);
```

Bearing Reaction Forces

From sum of the moments equals 0 for worse case senario

```
Fb1x = (1/(b1_mab2))*(-SBMR_r*SBML_mab2 - F_GCVT_x*GCVT_mab2);
Fb1x_disp = sprintf('\n\tBearing 1 x: %0.2f',Fb1x);
Fb1y = (-1/b1_mab2)*(SBMR_t*SBML_mab2 + F_GCVT_y*GCVT_mab2);
Fb1y_disp = sprintf('\n\tBearing 1 y: %0.2f',Fb1y);
Fb2x = (1/b1_mab2)*(-SBMR_r*SBML_mab1 + F_GCVT_x*GCVT_mab1);
Fb2x_disp = sprintf('\n\tBearing 2 x: %0.2f',Fb2x);
Fb2y = (1/b1_mab2)*(F_GCVT_y*GCVT_mab1 - SBMR_t*SBML_mab1);
Fb2y_disp = sprintf('\n\tBearing 2 y: %0.2f',Fb2y);
SFX_check = sum(F_GCVT_x + Fb1x + Fb2x + SBMR_r);
SFX_disp = sprintf('\n\t Sum of Fx: %0.2f',SFX_check);
SFY_check = sum(F_GCVT_y + Fb1y + Fb2y + SBMR_t);
SFY_disp = sprintf('\n\t Sum of Fy: %0.2f',SFY_check);
Fb1z = -SBML_x;
Fb1z_disp = sprintf('tBearing 1 z: %0.2f',Fb1z);
Fb2z = 0;
Fb2z_disp = sprintf('Bearing 2 z: %0.2f\n\n',Fb2z);
b1r = sprintf('Bearing 1 Resultant Force: %0.2f',sqrt(Fb1x^2 + Fb1y^2));
b2r = sprintf('Bearing 2 Resultant Force: %0.2f',sqrt(Fb2x^2 + Fb2y^2));
disp('Bearing Reaction Forces [N]')
disp(b1r)
disp(b2r)
disp('Sum Of Forces Check')
disp(SFX_disp)
disp(SFY_disp)
disp(SBM_sf_disp)
disp(Sf_ly_nc_disp)
disp(SF_comp_disp)
disp(LySf_disp)


% midshaft bearing reactions

% Lengths
SBMR_mab3 = 0.625*0.0254;%L1
SBMR_maSG = 1.25*0.0254;%L2
SG_mab4 = 0.75*0.0254;%L3
L_c = SBMR_mab3 + SBMR_maSG + SG_mab4;

Fb3y = (1/L_c)*((-SBMR_t*(SBMR_maSG + SG_mab4)) - (S_r*SG_mab4));

Fb3z = (1/L_c)*((-S_t*SG_mab4) + (SBMR_r*(SBMR_maSG + SG_mab4)));

Fb4y = (1/L_c)*((-SBMR_t*SBMR_mab3) - (S_r*(SBMR_mab3 + SBMR_maSG)));

Fb4z = (1/L_c)*((SBMR_r*SBMR_mab3) - (S_t*(SBMR_mab3 + SBMR_maSG)));
```

```
% check forces
sum_mid_y = Fb3y + Fb4y + SBMR_t + S_r;
sum_mid_y_disp = sprintf('\n Sum of Midshaft Forces y: %0.2f',sum_mid_y);
sum_mid_z = -Fb3z + SBMR_r - S_t - Fb4z;
sum_mid_z_disp = sprintf('\n Sum of Midshaft Forces z: %0.2f \n',sum_mid_z);
disp(sum_mid_y_disp)
disp(sum_mid_z_disp)


Fb3_Result = sqrt(Fb3y^2 + Fb3z^2);
Fb4_Result = sqrt(Fb4y^2 + Fb4z^2);
b1a = sprintf('\n\n\nBearing 1 Axial: %0.2f',SBMR_x);
b4a = sprintf('Bearing 4 Axial: %0.2f;',-SBML_x);
disp(b1a)
disp(b4a)
disp(b1r)
disp(b2r)
disp(['Bearing 3 Resultant Force: ', num2str(Fb3_Result)])
disp(['Bearing 4 Resultant Force: ', num2str(Fb4_Result)])
```

```
Bearing Reaction Forces [N]
Bearing 1 Resultant Force: 2320.14
Bearing 2 Resultant Force: 2115.98
Sum Of Forces Check

     Sum of Fx: -0.00

     Sum of Fy: 0.00


 Safey factor under JGMA standards:

     1.45


 Last years safety factor under JGMA standards:

     1.01


 Safety factor under last years conditions (AGMA standard):

     2.57


 Last years safety factor under last years conditions (AGMA standard):

     2.34



 Sum of Midshaft Forces y: 0.00
```

```
Sum of Midshaft Forces z: 0.00


Bearing 1 Axial: 2355.30
Bearing 4 Axial: 526.57;
Bearing 1 Resultant Force: 2320.14
Bearing 2 Resultant Force: 2115.98
Bearing 3 Resultant Force: 2965.7988
Bearing 4 Resultant Force: 3169.5991
```

Input Inner shaft diameter

```
% solve for the diameter of the input shaft on the inside of the spiral
% bevel miter gear.
Sf_4140 = 166.7*10^6; %Pa
N = 1.5;
Sy = 220.5*10^6;
Svm = (Sy/N)^2;
Mx = SBML_mab2*Fb2x;
My = SBML_mab2*Fb2y;
K = 1.5;

Sx = (K*Mx*2/pi)^2;
Sy = (K*My*2/pi)^2;

d = (2/0.0254)*nthroot((Sx + Sy)/Svm,6);

% d = nthroot((32*N*K*M/(pi*Sf_4140)),3)/0.0254;
```

Midshaft Inner shaft diameter

```
Mmz = Fb3z*0.5*0.0254;
Mmy = Fb3y*0.5*0.0254;

Smz = (K*Mmz*2/(pi))^2;
Smy = (K*Mmy*2/(pi))^2;

dm = (2/0.0254)*nthroot((Smz + Smy)/Svm,6);
```

Tearout stress on the bearing bore step

Aluminum shear yield strength

```
SY_al = 30000; %psi

A_shear_mid = pi*42*0.05/25.4;
F_shear_mid = 530; %lbs

S_shear_mid = F_shear_mid/A_shear_mid;
```

```
SF_shear_mid = SY_al/S_shear_mid;


sf_s_mid_disp = sprintf('\n\n\nShear tearout Factor of safety for B1: %0.1f
\n\n\n',SF_shear_mid);
disp(sf_s_mid_disp)
```

```
Shear tearout Factor of safety for B1: 14.7
```

Table of Contents

Fastner strength for the 2025 - 2026 Baja SAE Franken-Box 1

Fastner strength for the 2025 - 2026 Baja SAE Franken-Box

```
clear
close all
clc
% Desired preload, same as force pulling apart from spiral bevel miter
% gears.
Tensile = 70*10^3; %psi
Shear_tensile = 35*10^3; %psi
Bolt_preload = 125; %lbs

% Maximum force possible, calculating the effective area
N = 20; %TPI
d = 0.25; %in
dr = d - (1.299038/N);
dp = d - (0.649519/N);

At = (pi()/4)*((dp + dr)/2)^2; %in^2

% Shear stress to strip the threads
wi = 0.8;
Q20p = 1/20;

Astrip = pi*dr*wi*Q20p;

F_axial_input = (2.3553e+03)/4.4482216152605; %lbs

% Shear strength
Sys_q20 = 30000; %psi
num_threads = 20;

SF = num_threads*(Sys_q20*Astrip)/(F_axial_input);

num_threads_input = SF*F_axial_input/(Sys_q20*Astrip);
nti_disp = sprintf('\n Safety factor with only one bolt:  %0.2f
\n',num_threads_input);
disp(nti_disp)


% Looking at the shear strength for the shoulder bolt
A_shoulder = (pi()/4)*(3/8)^2; %in^2

F_x_shear = (530)^2; %lbs
F_y_shear = (300)^2; %lbs



F = sqrt(F_x_shear + F_y_shear);

tau = F/(3*A_shoulder + 3*At);

Sf = Shear_tensile/tau;
```

```
 Safety factor with only one bolt:  20.00
```

Table of Contents

2025-2026 Franken Love Box Shaft Stresses. 1
Physical prameters. 1
Gear Backlash calculations 2
Forces and Torques 2
Spur Gear Bending tooth stresses 3
Spiral Bevel Miters Bending tooth strength 4
Bearing Reaction Forces 4
Second Bearing Reaction Forces 5
GCVT Secondary Input Shaft Stress 6

2025-2026 Franken Love Box Shaft Stresses.

```
clear
close all
clc
```

Physical prameters.

```
% motor torque, maximum torque for worst case senario.
Tm = 25.1; %Nm

% CVT Gear ratios and Info
GCVT_GR_Min = 3.9;
GCVT_GR_Max = 0.9;
GCVT_Secondary_Max_Diam = 8*0.0254; %m

% angle of the CVT driveshaft, degrees
a_CVT = 28;

% Gear Geometry
S_module = 3.175;
S_addendum_coeff = 1; %mm
S_deddedum_coeff = 1.25;
S_pressure_angle = 20; %deg

S_face_width = 13; %mm
S_addendum = S_addendum_coeff*S_module;
S_deddedum = S_deddedum_coeff*S_module;

SBM_tooth = 20;
SBM_module = 4;
SBM_pitch_diam = SBM_tooth*SBM_module; %mm
SBM_pressure_angle = 20; %deg
SBM_helical_angle = 35; %deg
SBM_face_width = 23;
SBM_tooth_thickness = pi()*SBM_module/2;

SP_tooth = 12;
```

```
SP_pitch_diam = SP_tooth*S_module; %mm
SP_tip_diam = SP_pitch_diam + 2*S_addendum;

SG_tooth = 40;
SG_pitch_diam = SG_tooth*S_module;
SG_tip_diam = SG_pitch_diam + 2*S_addendum;

Center_distance = SP_pitch_diam/2 + SG_pitch_diam/2; %mm
S_TCR = (sqrt((SP_tip_diam/2)^2 - (SP_pitch_diam/2)^2) + sqrt((SG_tip_diam/
2)^2 - (SG_pitch_diam/2)^2) - (Center_distance*sind(S_pressure_angle)))/
(pi()*S_module*cosd(S_pressure_angle));

% Shaft lengths and moment arms (ma), [m]

% Input shaft
GCVT_mab1 = 3*0.0254; %moment arm to bearing 1; length of shafts in to m
GCVT_mab2 = 5.775*0.0254;
SBMR_mab1 = 2.25*0.0254;
SBMR_mab2 = 0.75*0.0254;
b1_mab2 = 3*0.0254;

SBML_mab1 = .25*0.0254;
SBML_mab2 = .25*0.0254;
b1_2mab2 = 1.25*0.0254;


SBML_mab1 = .015875;
SBML_maS = .03175;
S_mab2 = 0.01905;
b1_2mab2 = .01905;
```

Gear Backlash calculations

```
jns = 0.0655;
jts = jns/(cosd(S_pressure_angle));
jasp = 360*jts/(pi()*SP_pitch_diam);
jasg = 360*jts/(pi()*SG_pitch_diam);
jrs = jns/(2*sind(S_pressure_angle));
```

Forces and Torques

```
% CVT Forces [N]
% F_GCVT = 900;
F_GCVT = Tm*GCVT_GR_Min/(GCVT_Secondary_Max_Diam/2);
F_GCVT_x = cosd(a_CVT)*F_GCVT;
F_GCVT_y = sind(a_CVT)*F_GCVT;
% F_GCVT_beltT = 1112.06; %N


%adjusted with new gears
% Gear forces [N], from khk gear calculator, make sure to understand inputs.
% SBML_r = -537.92257;
```

```
% SBML_x = 2406.07152;
% SBML_t = 2973.00167;
%
% SBMR_r = 2406.07152;
% SBMR_x = -537.92257;
% SBMR_t = 2973.00167;

SBML_r = -2353.67;
SBML_x = 526.21;
SBML_t = 2908.26;

SBMR_r = 526.21;
SBMR_x = -2353.67;
SBMR_t = 2908.26;

Fb3y = 1623.679598;
Fb3z = 1763.355119;
Fb4y = -2893.05;
Fb4z = -173.78;

% S_t = 2000*Tm*GCVT_GR_Min/SP_pitch_diam;
% S_r = 1348.0379;

S_t = 3623.05;
S_r = 1318.68;

B5Reaction = 1928; %N
B6Reaction = 1928; %N
```

Spur Gear Bending tooth stresses

Defining the Bending tooth stress limit

```
Ob_tlim = 200*145; %MPa

% Defining the length of action for the contact ratio
Z = sqrt((SP_pitch_diam/2 + S_addendum)^2 -
(SP_pitch_diam*cosd(S_pressure_angle)/2)^2) + sqrt((SG_pitch_diam/2
+ S_addendum)^2 - (SG_pitch_diam*cosd(S_pressure_angle)/2)^2) -
Center_distance*sind(S_pressure_angle);

% Finding the base pitch, doesn't matter if pinion or gear is used.
pb = pi()*SP_pitch_diam/SP_tooth;

% Finding the contact ratio
mp = Z/pb;

% Finding the bending tooth stress factors
Yfp = 2.9;
Yfg = 2.32;
Ye = 1/S_TCR;
Yb = 1;
```

```
KL = 1;
Kfx = 1;
Kv = 1.5;
Ko = 1.25;

% Finding the tooth bending stress
Ob_t = 145*S_t*((0.3)/(S_module*S_face_width))*((Kv*Ko)/(KL*Kfx)); % Mpa
Sf = Ob_tlim/Ob_t;
Ob_t_disp = sprintf('Bending tooth stress [psi]: %0.2f \n',Ob_t);
disp(Ob_t_disp);
Sf_disp = sprintf('Safety Factor: %0.2f\n\n',Sf);
disp(Sf_disp);
```

Bending tooth stress [psi]: 7159.42

Safety Factor: 4.05

Spiral Bevel Miters Bending tooth strength

Finding the bending tooth stress factors

```
% Axial shift factor
```

Bearing Reaction Forces

From sum of the moments equals 0 for worse case senario

```
Fb1x = (1/(b1_mab2))*(SBML_r*SBML_mab2 - F_GCVT_x*GCVT_mab2);
Fb1x_disp = sprintf('\n\tBearing 1 x: %0.2f',Fb1x);
Fb1y = (-1/b1_mab2)*(SBML_t*SBML_mab2 + F_GCVT_y*GCVT_mab2);
Fb1y_disp = sprintf('\n\tBearing 1 y: %0.2f',Fb1y);
Fb2x = (1/b1_mab2)*(SBML_r*SBML_mab1 + F_GCVT_x*GCVT_mab1);
Fb2x_disp = sprintf('\n\tBearing 2 x: %0.2f',Fb2x);
Fb2y = (1/b1_mab2)*(F_GCVT_y*GCVT_mab1 - SBML_t*SBML_mab1);
Fb2y_disp = sprintf('\n\tBearing 2 y: %0.2f',Fb2y);
SFX_check = sum(F_GCVT_x + Fb1x + Fb2x - SBML_r);
SFX_disp = sprintf('\n\t Sum of Fx: %0.2f',SFX_check);
SFY_check = sum(F_GCVT_y + Fb1y + Fb2y + SBML_t);
SFY_disp = sprintf('\n\t Sum of Fy: %0.2f',SFY_check);
Fb1z = 0;
Fb1z_disp = sprintf('\n\tBearing 1 z: %0.2f',Fb1z);
Fb2z = -SBML_x;
Fb2z_disp = sprintf('\n\tBearing 2 z: %0.2f\n\n',Fb2z);
disp('Bearing Reaction Forces [N]')
disp(Fb1x_disp)
disp(Fb1y_disp)
disp(Fb1z_disp)
disp(Fb2x_disp)
disp(Fb2y_disp)
disp(Fb2z_disp)
disp('Sum Of Forces Check')
```

```
disp(SFX_disp)
disp(SFY_disp)
```

```
Bearing Reaction Forces [N]

    Bearing 1 x: -1968.44

    Bearing 1 y: -1184.71

    Bearing 1 z: 0.00

    Bearing 2 x: 431.25

    Bearing 2 y: -115.87

    Bearing 2 z: -526.21


Sum Of Forces Check

     Sum of Fx: 1667.18

     Sum of Fy: 2060.02
```

Second Bearing Reaction Forces

From sum of the moments equals 0 for worse case senario.

```
disp('Shaft #2')
F2b1x = (1/(b1_2mab2))*(SBMR_r*SBMR_mab2);
F2b1x_disp = sprintf('\n\tBearing 1 x: %0.2f',F2b1x);
F2b1y = (-1/b1_2mab2)*(SBMR_t*SBMR_mab2);
F2b1y_disp = sprintf('\n\tBearing 1 y: %0.2f',F2b1y);
F2b2x = (1/b1_2mab2)*(SBMR_r*SBMR_mab1);
F2b2x_disp = sprintf('\n\tBearing 2 x: %0.2f',F2b2x);
F2b2y = (1/b1_2mab2)*(-SBMR_t*SBMR_mab1);
F2b2y_disp = sprintf('\n\tBearing 2 y: %0.2f',F2b2y);
SFX2_check = sum(F2b1x + F2b2x - SBMR_r);
SFX2_disp = sprintf('\n\t Sum of Fx: %0.2f',SFX2_check);
SFY2_check = sum(F2b1y + F2b2y + SBMR_t);
SFY2_disp = sprintf('\n\t Sum of Fy: %0.2f',SFY2_check);
F2b1z = -SBMR_x;
F2b1z_disp = sprintf('\n\tBearing 1 z: %0.2f',F2b1z);
F2b2z = 0;
F2b2z_disp = sprintf('\n\tBearing 2 z: %0.2f\n\n',F2b2z);
disp('Bearing Reaction Forces [N]')
disp(F2b1x_disp)
disp(F2b1y_disp)
disp(F2b1z_disp)
disp(F2b2x_disp)
disp(F2b2y_disp)
disp(F2b2z_disp)
disp('Sum Of Forces Check')
```

```
disp(SFX2_disp)
disp(SFY2_disp)
```

```
Shaft #2
Bearing Reaction Forces [N]

    Bearing 1 x: 526.21

    Bearing 1 y: -2908.26

    Bearing 1 z: 2353.67

    Bearing 2 x: 1578.63

    Bearing 2 y: -8724.78

    Bearing 2 z: 0.00


Sum Of Forces Check

     Sum of Fx: 1578.63

     Sum of Fy: -8724.78
```

GCVT Secondary Input Shaft Stress

% Breaking up the forces into x and y components for von misses stress. % Using von mises with shear and bending stress, to find the shaft % diameter.

```
N = 1.275;
% Sy = 220.5*10^6;
Sy = 415*10^6; %MPa
Svm = (Sy/N)^2;

% Bending from the Gage CVT belt tension [Pa]
S_input_x = (((4*F_GCVT_x*GCVT_mab1)/pi()) - ((4*SBML_r*1.5*0.0254)/pi()))^2;
S_input_y = (((4*F_GCVT_y*GCVT_mab1)/pi()) + ((4*SBML_t*1.5*0.0254)/pi()))^2;


% Torsion from the Gage CVT
T_input = Tm*GCVT_GR_Min;
T_input_xy = sqrt(3)*(2*T_input/pi())^2;

% Shaft Diameter
Diam_input = 2*nthroot((S_input_x + S_input_y + T_input_xy)/Svm,6); %m
Diam_input_in = Diam_input*39.37 %in

% axial stress
A_input = SBML_x/(pi*(Diam_input/2)^2) / 1000000; %MPa

% disp(Diam_input_in);
%input shaft post_gear
Diam_input2 = 2*nthroot((S_input_x + S_input_y)/Svm,6); %m
```

```
Diam_input2_in = Diam_input2*39.37 %in


%Diameter equation:

K_f = 1;
K_fs = 1;
T_a = 0;
M_m = 0;
K_fm = K_f;
K_fsm = K_fs;
M_a = 25.4*F_GCVT; % assuming 1" from CVT to first bearing
T_m = 100000; %70 Nm to Nmm

S_ut = 655; %MPa worst case 4140
S_fu = S_ut/2; %MPa, TEMP Uncorrected fatigue limit
C_size = 1.189*19.05^-.097; %assuming 1In shaft or 25.4 mm
C_load = 1; %bending is present
Temp = 54.4444; %130F in C
C_temp = 1; %T<= 450C or 840F
C_surf = 0.7; %Based off of Fig 6-26 table from comp m book assuming
machined shaft and based off of S_ut
C_reliab = 0.814; %assumes 99% reliability

S_f = C_load * C_size * C_surf * C_temp * C_reliab * S_fu;

Part1_1 = sqrt((K_f*M_a)^2 + (3/4)*(K_fs*T_a)^2)/S_f;
Part2_1 = sqrt((K_fm*M_m)^2 + (3/4)*(K_fsm*T_m)^2)/S_ut;


%shaft 1
disp('Minimum Shaft Diameter (in) calculations for a Factor of Safety of
1.5')

diam_input_fatigue_1 = (32*N/pi* (Part1_1+Part2_1))^(1/3)*0.0393701 %mm to in

%-----------------------------------------------------------------------
%shaft2

K_f_2 = 1;
K_fs_2 = 1;
T_a_2 = 0;
M_m_2 = 0;
K_fm_2 = K_f;
K_fsm_2 = K_fs;
M_a_2 = 46.7358*1000;
T_m_2 = 100000; %70 Nm to Nmm

S_ut_2 = 655; %MPa worst case 4140
S_fu_2 = S_ut_2/2; %MPa, TEMP Uncorrected fatigue limit
C_size_2 = 1.189*19.05^-.097; %assuming 1In shaft or 25.4 mm
C_load_2 = 1; %bending is present
Temp_2 = 54.4444; %130F in C
C_temp_2 = 1; %T<= 450C or 840F
```

```
C_surf_2 = 0.7; %Based off of Fig 6-26 table from comp m book assuming
machined shaft and based off of S_ut
C_reliab_2 = 0.814; %assumes 99% reliability

S_f_2 = C_load_2 * C_size_2 * C_surf_2 * C_temp_2 * C_reliab_2 * S_fu_2;


Part1_2 = sqrt((K_f_2*M_a_2)^2 + (3/4)*(K_fs_2*T_a_2)^2)/S_f_2;
Part2_2 = sqrt((K_fm_2*M_m_2)^2 + (3/4)*(K_fsm_2*T_m_2)^2)/S_ut_2;


diam_input_fatigue_2 = (32*N/pi* (Part1_2+Part2_2))^(1/3)*0.0393701 %mm to in

%-----------------------------------------
%shaft3

K_f_3 = 1;
K_fs_3 = 1;
T_a_3 = 0;
M_m_3 = 0;
K_fm_3 = K_f;
K_fsm_3 = K_fs;
M_a_3 = 65000;
T_m_3 = 240000; %240 Nm to Nmm, TEMP RATIO VALUE

S_ut_3 = 655; %MPa worst case 4140
S_fu_3 = S_ut/2; %MPa, TEMP Uncorrected fatigue limit
C_size_3 = 1.189*25.4^-.097; %assuming 1In shaft or 25.4 mm
C_load_3 = 1; %bending is present
Temp_3 = 54.4444; %130F in C
C_temp_3 = 1; %T<= 450C or 840F
C_surf_3 = 0.7; %Based off of Fig 6-26 table from comp m book assuming
machined shaft and based off of S_ut
C_reliab_3 = 0.814; %assumes 99% reliability

S_f_3 = C_load_3 * C_size_3 * C_surf_3 * C_temp_3 * C_reliab_3 * S_fu_3;


Part1_3 = sqrt((K_f_3*M_a_3)^2 + (3/4)*(K_fs_3*T_a_3)^2)/S_f_3;
Part2_3 = sqrt((K_fm_3*M_m_3)^2 + (3/4)*(K_fsm_3*T_m_3)^2)/S_ut_3;

diam_input_fatigue_3 = (32*N/pi* (Part1_3+Part2_3))^(1/3)*0.0393701 %mm to in


Diam_input_in =

    0.7993


Diam_input2_in =

    0.7882

Minimum Shaft Diameter (in) calculations for a Factor of Safety of 1.5
```

```
diam_input_fatigue_1 =

    0.6384

diam_input_fatigue_2 =

    0.7273

diam_input_fatigue_3 =

    0.8749
```

Published with MATLAB® R2025a

7.2.3.2.2. Shaft Calculations

Driveshaft calcs

driveshaftCalc.m

/MATLAB Drive/driveshaftCalc.m

```
clear; close all; clc;

format long g;
engineTorque = 18.5; % ft-lb
engineTorque_inlb = 18.5 * 12;
engineRPM = 3600; % rpm
cvtRatio = 3.9;
minCvtRatio = 0.9;
transferCaseRatio = 2.4;
yamahaDiffRatio = 3.67;

torqueOnDriveshaft = engineTorque_inlb * cvtRatio * transferCaseRatio
dshaftrpm = 3600 / (minCvtRatio * transferCaseRatio)

% Driveshaft geometry
d_o = 1; % in
wall = 0.049 % in
d_i = d_o - 2 * wall; % in
r_o = d_o / 2; % outer radius
r_i = d_i / 2; % inner radius

J = (pi * (d_o^4 - d_i^4)) / 32 % in^4 (polar moment of area)
L = 36 % in
G_4130 = 116 * 10.^5 % psi

ang_deflect = (torqueOnDriveshaft * L) / (J * G_4130) * (180/pi) % deg
Torzion = torqueOnDriveshaft * (d_o / 2) / J; % psi
YeildStrengh_4130 = 63100; % psi
FOS_4130 = YeildStrengh_4130 / Torzion

wheelDia = 22.5; % in
wheelCirc = pi * wheelDia; % in
OverallGearRatio = (minCvtRatio) * (transferCaseRatio) * (yamahaDiffRatio);
wheelRPM = engineRPM * (1 / OverallGearRatio);
```

2025-2026 CU Boulder Baja SAE